



Piezoelectric systems for precise and high dynamic positioning: design, modeling, estimation and control

Micky Rakotondrabe

► To cite this version:

Micky Rakotondrabe. Piezoelectric systems for precise and high dynamic positioning: design, modeling, estimation and control. Engineering Sciences [physics]. University of Franche-Comté - FEMTO-ST, 2014. tel-01229629

HAL Id: tel-01229629

<https://hal.science/tel-01229629>

Submitted on 17 Nov 2015

HAL is a multi-disciplinary open access archive for the deposit and dissemination of scientific research documents, whether they are published or not. The documents may come from teaching and research institutions in France or abroad, or from public or private research centers.

L'archive ouverte pluridisciplinaire **HAL**, est destinée au dépôt et à la diffusion de documents scientifiques de niveau recherche, publiés ou non, émanant des établissements d'enseignement et de recherche français ou étrangers, des laboratoires publics ou privés.

Année : 2014

Habilitation à Diriger des Recherches

**U.F.R. DES SCIENCES ET TECHNIQUES
DE L'UNIVERSITÉ DE FRANCHE-COMTÉ (UFC) à Besançon**

(Doctoral School: Sciences Physiques pour l'Ingénieur et Microtechniques)

Piezoelectric systems for precise and high dynamic positioning
design, modeling, estimation and control

par

Micky RAKOTONDRABE

Dissertation date: December 10, 2014

COMMITTEE:

President of the jury:

Nacim RAMDANI

Full Professor, University of Orléans, Orléans France

Reviewers:

Gildas BESANÇON

Full Professor, INPG, Grenoble France

Eric BIDEAUX

Full Professor, INSA, Lyon France

Ian R. PETERSEN

Full Professor, University of NSW / ADFA, Canberra Australia

Examiners:

Reza MOHEIMANI

Full Professor, University of Newcastle, Newcastle Australia

Dan POPA

Associate Professor, University of Texas at Arlington, Texas USA

Nicolas CHAILLET

Full Professor, University of Franche-Comté, Besançon France

Philippe LUTZ

Full Professor, University of Franche-Comté, Besançon France

Preface

The works reported in this thesis have been carried out at the Laboratoire d'Automatique de Besançon, which became the department of Automatic Control and MicroMechatronic Systems (AS2M) of FEMTO-ST Institute in 2008. These works have been under the guarantee of Dr Philippe Lutz, Full Professor at the University of Franche-Comté, who gave me a high autonomy and his full trust to explore the field. I would like to sincerely acknowledge him.

I would like to thank Dr Nicolas Chaillet, Full Professor at the University of Franche-Comté - director of the AS2M departement between 2007 and 2011 - and since, director of FEMTO-ST, for allowing me work in good conditions at the department and for the occasional but fruitful discussions in the fields of piezoelectric systems. My thanks also go to Professor Nouredine Zerhouni (director of the AS2M departement between 2011 and 2012) and to Dr Michaël Gauthier (deputy director between 2011 and 2012, and director of the departement since 2012) for allowing me have good works conditions. The works reported here are within the CODE team of the AS2M department and I thank Yann Le Gorrec, team responsable, for its management.

My full gratitude goes to Dr Ian R. Petersen, Full Professor at the University of New South Wales - the Australian Defence Force Academy (UNSW-ADFA), to Dr Gildas Besançon, Full Professor at the National Polytechnic Institute (INPG) Grenoble, and to Dr Eric Bideaux, Full Professor at the National Institute of Applied Sciences (INSA) Lyon, for having accepted to review this thesis. Also I would like to thank Dr Nacim Ramdani, Full Professor at the University of Orléans, for having accepted to chair the jury, and to Dr Reza Moheimani, Full Professor at the University of Newcastle NSW Australia, and Dr Dan Popa, Associate Professor at the University of Texas at Arlington (TX USA), for having accepted to be examiners of the thesis. In particular, many thanks to Dr Reza Moheimani for welcoming me at the Laboratory for Dynamics and Control of NanoSystems (LDCN) of the University of Newcastle during three months in 2012. My stay there was a unique experience, both in the scientific aspect and in the human aspect. I will definitely do it again.

The progress of many of the works reported here have also been possible thanks to national and international discussions, exchanges and collaborations. I am particularly thankful to Dr Mohammad Al Janaideh, Associate Professor at the University of Jordan, to Dr Mathieu Grossard, researcher at the CEA Paris, to Dr Stéphane Régnier, Full Professor at the UPMC Paris, to Dr Reza Moheimani and to his postdoctoral and PhD fellowships at the University

of Newcastle Australia, and to Dr Dan Popa, Associate Professor at the University of Texas at Arlington (UTA), and to his postdoctoral and PhD fellowships. My gratitude to Dr Dan Popa for welcoming me at the NexGen lab of the UTA during one month in 2011. My gratitude also goes to PERCIPIO-ROBOTICS company with which two important projects (MIM-HAC and MYMESYS) have resulted in interesting results reported in this thesis.

I thank all my colleagues at the AS2M departement. In particular, my full thanks to those with whom I had close collaborations to succeed in many of the works reported here: Cédric Clévy, Joël Agnus, Joël Abadie, Patrick Rougeot, Kanty Rabenorosoa, Yassine Haddab, Philippe Lutz, Nicolas Andreff, Nicolas Chaillet and Yann Le Gorrec. Particular thanks to Cédric Clévy for his perpetual support during these years in both the research and the teaching aspects. Thank you Patrick for the proofread and for the full support during the thesis writing.

Being lecturer at the University, I would like to thank the members of the GAP¹ teaching team. In particular, thanks to Dr Maryvonne Dulmet, team-responsible, for its management. Many thanks also to Maurice Lab, secretary, to Patricia Hirtz, technician, to Christophe Perrard, lecturer and Associate Professor, and to Dr Arnaud Hubert, ex-lecturer, ex-Associate Professor and ex-lab manager at the GAP team. A thought to my past and present students.

Of courses, all my acknowledgements go:

- i) to Dr Ioan Alexandru Ivan, Dr Juan-Antonio Escareno, Dr Alex Bienaimé, Dr Eakkachai Ton Pengwang, Dr Vincent Chalvet, and Dr Omar Al Janaideh, all postdoctoral fellowships,
 - ii) to Dr Sofiane Khadraoui, Sergio Lescano, Didace Habineza, and Yasser Al Hamidi, all PhD fellowships,
 - iii) and to all internships
- without whom many of the works reported in this thesis would not have been possible.

My full gratitude to Isabelle Gabet, Martine Azema and Sandrine Franchi, who fully helped and assisted in the administrative aspects. My gratitude to all the colleagues of FEMTO-ST, in particular: Thomas Baron and Ausrine Bartaszyte for the different fruitful exchanges.

Last but not the least, the very deep thought and thanks to my family: Bianca and David, Rory, Maholy - Nathan and Titi, mum and dad, for their full and endless support. Thanks to my friends who supported me during the hard work of this thesis writing, in particular: Mathieu, Sarah, Francis and his family, Bertrand, Nancia, Elise, Pauline, Antoine, Perle, Laurence, fr. Vincent and fr. Raphaël.

Micky

"Un voyage de mille lieues commence toujours par un premier pas."

"A journey of a thousand miles begins with a single step."

Lao-Tseu, [360].

¹GAP: Groupe Automatique et Productique is the team that rassembles the lecturers on Control, Robotics and Industrial Processes at the University of Franche-Comté at Besançon.

Contents

List of figures	1
List of tables	4
1 Introduction and context	7
1.1 Context: precise and high dynamics positioning	8
1.2 Piezoelectric materials based positioning systems	11
1.3 Challenges posed in precise and high dynamics positioning with piezoelectric systems	13
1.4 PhD works (2003 - 2006)	16
1.4.1 Context and results	16
1.4.2 PhD general information	17
1.4.3 Publications related to the PhD works	18
1.5 Post-PhD works (2006 onwards)	18
1.5.1 Fundamental themes	18
1.5.2 Applications	19
1.5.3 Supervised works	20
1.5.4 Projects and fundings	21
1.5.5 From research to teaching	23
1.5.6 Collaborative context	25
1.6 Timeline of the research since 2006	25
1.7 Organization of this thesis	27
2 Design, development and modeling	29
2.1 Introduction	30
2.2 Multimorph piezoelectric cantilevers as basic actuators	31
2.2.1 Principles	31
2.2.2 Ballas linear modeling	32
2.2.3 Extension to nonlinear modeling	34
2.3 Hybrid thermopiezoelectric actuator	36
2.3.1 Principle	37
2.3.2 Modeling	38
2.3.3 Other leads to represent the behavior of hybrid actuators	41
2.3.4 Acknowledgments	42

2.4	Parallel kinematic piezoelectric microrobot for laser phonomicrosurgery	42
2.4.1	Context	42
2.4.2	A high resolution, high bandwidth, and high range 2-DOF microrobot	43
2.4.3	A macro version of the robot	46
2.4.4	Perspectives	47
2.4.5	Acknowledgments	48
2.5	Cartesian piezoelectric microstructure	48
2.5.1	Microfabrication of PZT materials	48
2.5.2	The designed and microfabricated microstructure	50
2.5.3	Perspectives	51
2.5.4	Acknowledgments	51
2.6	Design methodology for piezoelectric cantilever systems using interval tools	51
2.6.1	Redesign of piezoelectric actuators	53
2.6.2	Design of piezoelectric actuators with the performances inclusion theorem	55
2.6.3	Perspectives	56
2.6.4	Acknowledgments	56
2.7	Conclusions and perspectives	57
3	Feedback control	59
3.1	Introduction	60
3.2	Classical robust control	62
3.2.1	Displacement modeling and control	63
3.2.2	Force modeling and control	66
3.2.3	Displacement and force control of piezoelectric microgrippers	68
3.2.4	Multivariable control of multi-axes piezoelectric actuators	69
3.2.5	Acknowledgements	71
3.3	Interval techniques combined with classical control theory	71
3.3.1	The Performances Inclusion Theorem (PIT)	72
3.3.2	Controllers design by using the PIT	73
3.3.3	H_∞ interval controllers synthesis	75
3.3.4	Robust performances analysis with interval techniques	77
3.3.5	General remarks	79
3.3.6	Acknowledgments	79
3.4	Feedforward-feedback control schemes	79
3.5	Control of hybrid thermopiezoelectric microgrippers	81
3.6	Conclusions and perspectives	83
4	Feedforward control	85
4.1	Introduction	86
4.2	Creep modeling and control	87
4.2.1	Overview	87
4.2.2	Creep modeling	88
4.2.3	Feedforward control by using the inverse multiplicative structure	89
4.2.4	Multivariable creep modeling and control	90

4.3	Hysteresis modeling and control	92
4.3.1	Overview	93
4.3.2	Inverse multiplicative structure combined with monovariable and rate-independent cases	96
4.3.3	Inverse multiplicative structure combined with multivariable and rate-independent hysteresis	98
4.3.4	Other ongoing works and perspectives	103
4.3.5	Acknowledgements	104
4.4	Badly damped vibration modeling and control	104
4.5	Complete feedforward control	106
4.6	Conclusion and perspectives	107
5	Signals measurement and estimation	109
5.1	Introduction	110
5.2	Development of force measurement platform for micromanipulation and microassembly tasks	111
5.3	Observers as complementary tools for signal measurements	113
5.4	Self-sensing techniques in piezoelectric actuators	115
5.4.1	Overview	115
5.4.2	Modeling the electrical circuit and the actuator	117
5.4.3	Static self-sensing	118
5.4.4	Dynamic self-sensing	119
5.4.5	Towards multivariable self-sensing	120
5.4.6	Acknowledgements	121
5.5	Conclusions and perspectives	121
6	General conclusions and perspectives	123
6.1	General conclusions	123
6.2	General perspectives	126
6.2.1	Going further in the miniaturization of high performances and high dexterity piezoelectric systems	127
6.2.2	Towards highly autonomous and smart miniaturized systems	129
6.2.3	From MEMS harvesters to matters harvesters	135
7	Appendix	137
A	<i>Curriculum Vitae</i>	139
A.1	Personal track	
A.1.1	Positions	
A.1.2	Education and diploma	
A.1.3	Research activities: summary	
A.1.4	Teaching activities: summary	
A.1.5	Prizes, awards and distinctions	
A.1.6	Misc	

A.2	Research activities	
A.2.1	Journals editorial activities	
A.2.2	Editorial and organization responsibilities in conferences	
A.2.3	Supervising: post-doc, PhD, BSc, MSc	
A.2.4	Projects responsibilities	
A.2.5	Projects participation	
A.2.6	Other responsibilities	
A.2.7	Workshops/tutorials organization	
A.2.8	PhD Committee member	
A.2.9	Reviewing	
A.2.10	Societies and group memberships	
A.3	Teaching activities	
A.3.1	Pedagogic and administrative responsibilities	
A.3.2	Teaching for undergrads (BSc), UFC University	
A.3.3	Teaching for MSc UFC University and <i>écoles d'ingénieurs</i> at Besançon	
A.3.4	Invited lecture	
B	Personal publications (accepted or published) and invited talks/seminars	147
B.1	Book and edited books	
B.2	Book chapters	
B.3	Patents	
B.4	Journal papers	
B.5	International conferences	
B.6	Workshops	
B.7	Invited talks and seminars	
B.7.1	Invited talks in organized workshops and tutorials	
B.7.2	Invited seminars in research institutes and universities	
C	Ballas linear model of multimorph piezoelectric cantilevers	159
C.1	Introduction	
C.2	Model of multimorph piezoelectric cantilevers	
C.2.1	Static behavior	
C.2.2	Dynamic behavior	
C.3	Usual cases	
C.3.1	Unimorph actuators	
C.3.2	Bimorph actuators	
D	Basics on intervals and on related techniques	165
D.1	Definitions	
D.2	Operations on intervals	
D.3	A set inversion problem	
D.4	Interval systems	
D.4.1	Definition	
D.4.2	Kharitonov vertex polynomials	

D.4.3	Stability of interval systems	
D.4.4	H_∞ -norm of interval systems	
E	Approximation schemes for nonlinear dynamical systems	171
E.1	Hammerstein-Wiener scheme	
E.2	Hammerstein scheme	
E.3	Wiener scheme	
References		173

List of Figures

1.1	A precisely guided microrobot for ophthalmic surgery [12] (<i>ETH Zurich, Switzerland</i>).	8
1.2	An atomic force microscopy with integrated positioner and a MEMS nanopositioner [26] (<i>University of Newcastle, Australia</i>).	9
1.3	A MEMS based data storage [36] (<i>IBM Zurich, Switzerland</i>).	9
1.4	An assembled optical bench [47] (<i>AS2M department Besançon, France and ARRI Institute/UTA Arlington, TX USA</i>).	10
1.5	Replacement of a classical polyarticulated arm by a bulk smart material.	12
1.6	Piezoelectric microgrippers developed at the AS2M department. (a): the first version of piezoelectric microgripper at the AS2M department [59; 60]. (b) and (c): a 4-DOF microgripper on chip [61; 62]. (d): a hybrid thermopiezoelectric microgripper [PT1][J14]. (e): a microgripper with optimized sensing and actuation capability [64–66]. (f)[C11], (g) [61], and (h) [63]: utilization of the microgrippers for micromanipulation or microassembly tasks.	13
1.7	Example of hysteresis obtained from a piezoelectric cantilevered actuator [BC5].	14
1.8	Example of creep in a piezoelectric cantilever [J7].	14
1.9	Step response (the transient part) of a piezoelectric actuator [J7].	15
1.10	A TRING-module: a very high resolute 2-DOF microrobot with angular and linear motion capabilities.	16
1.11	Links between the context and motivation, fundamental themes and applications.	19
1.12	General repartition (in months number) of the supervised works.	21
1.13	General repartition that links projects with supervised works (in months).	23
1.14	Timeline of the research since 2006.	26
2.1	Principle of a piezoelectric microgripper.	30
2.2	A piezoelectric cantilever.	31
2.3	A step response of a multimorph piezoelectric actuator.	34
2.4	(a) Unimorph piezoelectric cantilever. (b) Piezoelectric actuation. (c) Thermal actuation.	37
2.5	Hybrid thermopiezoelectric actuator. (a): CAD drawing (b): photography of the prototype.	37
2.6	Scheme of the hybrid thermopiezoelectric actuator with the TEC-device.	38
2.7	Thermal network of the whole hybrid thermopiezoelectric actuator.	40
2.8	Objective of the μ -RALP project [6].	43

2.9	Principle of the μ PIBOT. (a): CAD-design. (b): the upper part (c): the lower part.	45
2.10	The μ PIBOT. (a): CAD-design. (b): the components of the lower part. (c): the arms of the lower parts. (d): the lower part. (e): the unfolded upper part. .	46
2.11	The macro version of the μ PIBOT.	47
2.12	Three approaches for treating PZT materials.	50
2.13	(a): CAD-design of the cartesian microstructure. (b): fabricated piezoelectric cantilevers with the "thick film" approach. (c): fabricated cartesian microstructure.	51
2.14	Redesign of a unimorph piezoelectric actuator.	53
2.15	Numerical results of the problem in 2.19.	54
3.1	Schematic of the feedback.	63
3.2	(a): the quadrilateral approximation. (b): the equivalent block-diagram.	64
3.3	(a): block-diagram for the synthesis. (b): the standard scheme.	65
3.4	The force actuator manipulating an object.	66
3.5	Closed-loop force control.	67
3.6	(a): force/displacement control of a piezoelectric microgripper. (b): experimental results [C11].	69
3.7	(a): a photo of the piezoelectric duo-multimorph actuator. (b) and (c): bi-variable system.	70
3.8	A closed-loop transfer $[H_d]$	73
3.9	(a): solution set Θ for a PI controller. (b): closed-loop frequency response of two piezoelectric actuators with two controllers $C_1(s)$ $C_2(s)$. (c): step responses. .	75
3.10	(a): block-diagram for the synthesis. (b): the standard scheme.	76
3.11	A standard scheme.	78
3.12	Feedforward-feedback control architectures in piezoelectric actuators control. . .	80
3.13	A hybrid thermopiezoelectric microgripper.	81
3.14	A hybrid control law for a hybrid thermopiezoelectric actuator.	81
3.15	Position/force control of the hybrid thermopiezoelectric microgripper. (a): implementation scheme. (b) and (c): experimental results.	83
4.1	Feedforward control of a system.	86
4.2	Step response of a piezoelectric actuator for creep parameters identification and for dynamics parameters identification.	89
4.3	(a): implementation of the creep compensator. (b): experimental results.	90
4.4	Feedforward control of a 2-DOF piezoelectric actuator.	103
4.5	Principle of the input shaping technique: a shaper with two impulses.	105
4.6	Experimental results of input shaping control of a piezoelectric cantilevered actuator.	106
4.7	Full (or complete) compensation of the hysteresis, creep and badly damped vibration.	107

5.1	Instrumented platform. (a): a view. (b): the estimator. (c): example of force estimation.	113
5.2	(a): scheme of the observer and of the piezoelectric system. (b): measured output displacement $\delta(t)$ and its estimate $\hat{\delta}(t)$. (c): measured force $F_m(t) = -F(t)$ and estimate force $\hat{F}_m(t) = -\hat{F}(t)$	116
5.3	(a): principle scheme of a self-sensing. (b): the electrical circuit.	117
5.4	Diagram of a dynamic self-sensing in a piezoelectric actuator.	119
5.5	(a): estimation of the displacement with the static self-sensing. (b): estimation of the displacement with the dynamic self-sensing.	120
6.1	Towards autonomous and smart miniaturized devices.	129
6.2	MEMS in automotive (Precision Engineering, by V.C. Venkatesh, Sudin Izman).	133
6.3	An active tracking device to track livestock, developed and industrialized by <i>Tekvet</i> and <i>IBM</i> [357; 358].	134
6.4	High autonomy and smart miniaturized systems as basic element of high autonomy and smart matter.	135
C.1	A multilayered piezoelectric cantilever.	160
C.2	A unimorph piezoelectric actuator.	162
C.3	A bimorph piezoelectric actuator.	163
E.1	A nonlinear system.	171
E.2	The Hammerstein-Wiener scheme.	172
E.3	The Hammerstein scheme.	172
E.4	The Wiener scheme.	172

List of Tables

1.1	<i>Information summary regarding my PhD works.</i>	17
1.2	<i>Effective months and themes for the advised fellowships and internships.</i>	20
1.3	<i>List of projects and supervised works for each project.</i>	22
2.1	Numerical values of $(k_m L)$ for the m^{th} mode.	33
C.1	Numerical values of $k_m L$ for the m^{th} mode.	162
D.1	The SIVIA algorithm [171] .	167

Chapter 1

Introduction and context

The aim of this chapter is to remind the context of my research and the scientific themes carried out so far. This includes my PhD works (2003 - 2006) and my post-PhD works (2006 onwards) all effectuated at the department of Automatic Control and MicroMechatronic Systems (AS2M) of FEMTO-ST Institute. After presenting the context, a brief presentation of the PhD works is first given. Then, we give an overview of the post-PhD research works. This encompasses the supervised works, the transfer of the research results to teaching and the works within (external) collaborative context.

Contents

1.1	Context: precise and high dynamics positioning	8
1.2	Piezoelectric materials based positioning systems	11
1.3	Challenges posed in precise and high dynamics positioning with piezoelectric systems	13
1.4	PhD works (2003 - 2006)	16
1.4.1	Context and results	16
1.4.2	PhD general information	17
1.4.3	Publications related to the PhD works	18
1.5	Post-PhD works (2006 onwards)	18
1.5.1	Fundamental themes	18
1.5.2	Applications	19
1.5.3	Supervised works	20
1.5.4	Projects and fundings	21
1.5.5	From research to teaching	23
1.5.6	Collaborative context	25
1.6	Timeline of the research since 2006	25
1.7	Organization of this thesis	27

1.1 Context: precise and high dynamics positioning

Precise positioning deals with the positioning that requires micrometric or submicrometric accuracy. Actuated miniaturized systems, microsystems or even MEMS¹ are considered as the best candidates to perform precise positioning if the travel distances are not large [1]. They can provide very high resolution of positioning (the range of nanometer is possible) and thus very high accuracy if controlled. Furthermore, since the sizes of the system are reduced, the energy consumption is lessened. Finally, the price of the operation and of the positioner systems could be much less than if we used classically sized positioning systems. When employing all these miniaturized systems, the task is called micropositioning or nanopositioning according to the resolution and to the accuracy played into role. The rest of this thesis deals with precise positioning in this spirit.

The applications of precise positioning (micropositioning or nanopositioning) are numerous, among which the following are widely studied or are emerging.

Medical surgery applications

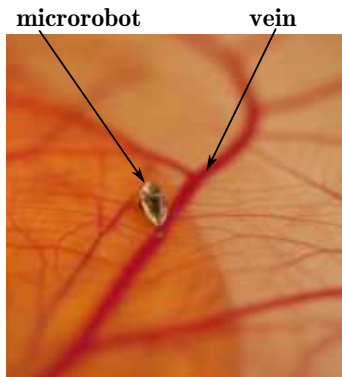


Figure 1.1: A precisely guided microrobot for ophthalmic surgery [12] (*ETH Zurich, Switzerland*).

An emerging medical application is the laser surgery [2–8][C55][C46][C45]. An endoscopic element is brought inside the human body to drop laser fibers and cameras from the external. At the extremity of the endoscope are placed actuated microstructures or microrobots which permit to precisely reflect and orient the laser beams towards the cells to be treated. The capability of the positioners to perform precise and fast orientation of the laser beams is fundamental in this application in order to avoid the destruction of alive cells and to avoid side effects from the surgery. Another surgery application of precise positioning consists in inserting microrobots in the eye for ophthalmic surgery [9–12], for instance to enable sutureless and

precise ophthalmic procedures which require a precise movement of the microrobots, see Fig. 1.1.

Microscopes and surfaces scanning

In scanning probe microscopes (SPM) which includes atomic force microscopes, scanning tunnelling microscopes, electronic force microscopes,..., a tip is used to raster scan over a

¹MEMS: MicroElectroMechanical Systems.

surface to be sampled [13–18]. A data is created from each discrete point of the raster scan. For instance, in atomic force microscopes, the data corresponds to the deflection of the tip caused by atomic level attraction forces between this and the surface. These attraction forces become important when the distance between the tip and the surface is small. Thus the set of data after the scanning provides a map of the scanned surface at micrometric or nanometric level. The scan rate depends on the bandwidth of the actuator and on its control. Piezoelectric actuators with tubular structure (piezotube scanners or PTS) are widely employed to precisely position the tip during the scanning. These last years, the development of additional positioners to increase the performances of the scanning has been raising. These positioners serve as complementary scanners to the piezotubes scanners and bring more precision, more resolution, more range or more scan rate [19–28]. Fig. 1.2 pictures an example of commercial AFM collaborating with a third precise MEMS positioner that holds the surface sample [26].

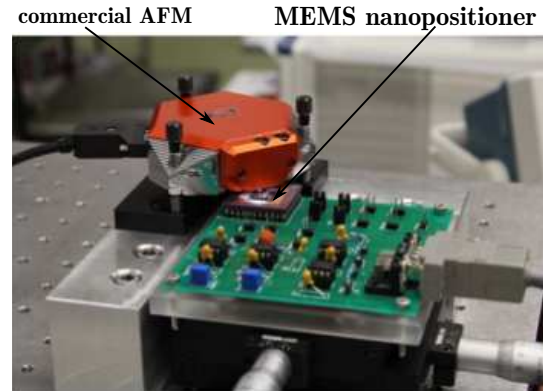


Figure 1.2: An atomic force microscopy with integrated positioner and a MEMS nanopositioner [26] (*University of Newcastle, Australia*).

Data storage

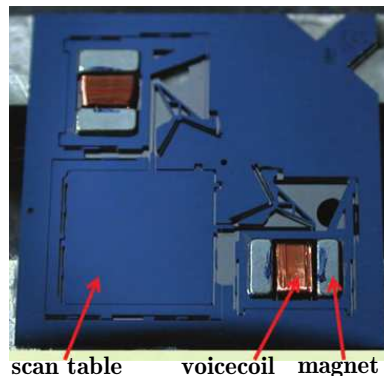


Figure 1.3: A MEMS based data storage [36] (*IBM Zurich, Switzerland*).

The development of ultra-high storage densities devices based on MEMS precise positioners is raising these last years. The principle is taken from scanning probe microscopes (SPM): nanometer sharp tips are employed to interrogate matter down to the atomic scale [29–37]. The presence or the absence of indentation on the matter (in general thin polymer films) indicates the logical state (one or zero). Each tip is actuated individually to create or to verify the indentation making the writing or reading possible. One of the particularity of these novel data storage technologies is that all the tips are fixed in a single scanner and can be moved in parallel which permit to maintain competitive data rates relative to the classical data storage devices. Their main feature is the high storage density offered. Fig. 1.3 pictures a MEMS based data storage where the scan table, moved along axis x and axis y by the magnets and voicecoils, precisely positions a set of tips on

storage medium for the reading or writing [36].

Micromanipulation and microassembly

Micromanipulation deals with the precise manipulation of small objects, and microassembly deals with their precise assembly to produce more complex small structures. Microrobots and actuated precise positioners and manipulators are widely employed to execute the tasks in order to benefit from their high resolution [38–42][J29]. There are several usages of micromanipulation and microassembly. One of the emerging is the precise assembly of optical components to obtain optical benches [43–49; 51–53][C21]. In Fig. 1.4-a is pictured an example of assembled optical bench [47]. The bench is composed of a rail in which are placed holders of lenses. The challenge consisted in inserting and guiding the holders in the rail and then performing a very precise positioning to maintain a well defined distance between them. Placing the lenses in the holders poses an additional challenge. After packaging, this optical bench has been used for gas characterization by spectrometry [49]. Fig. 1.4-b depicts the smallest cow assembled in the world. Called "Maghi"², the micro-cow has been developed by microassembly task at the AS2M department and was prized "micron d'or" during the 2008 Micronora congress held in Besançon [50]. Micromanipulation has also been extensively employed to manipulate and to characterize biological cells [54–57]. Since more than a decade, we also assist to the emergence of nanomanipulation, where the sizes of the manipulated objects downscale and where the resolution and accuracy required are more severe than in micromanipulation [58].

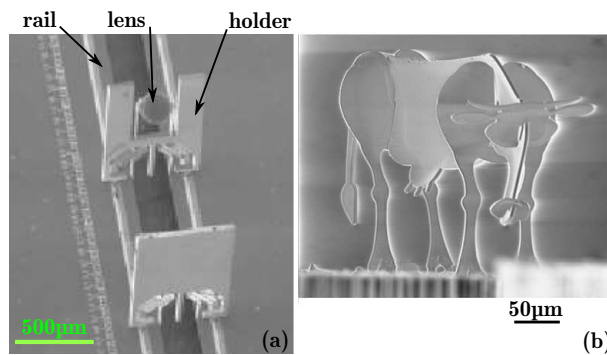


Figure 1.4: An assembled optical bench [47] (AS2M department Besançon, France and ARRI Institute/UTA Arlington, TX USA).

A common characteristic of precise positioning based on miniaturized systems is that, generally, high bandwidth can be achieved. In fact, due to the small sizes of the systems, the inertia is weak and thus the capability of the structure to move quickly is increased. This large bandwidth is congruent with the requirement of many of the targeted applications such as laser surgery applications, high cadence microassembly and micromanipulation, data-storage...

The department of Automatic control and MicroMechatronics Systems (AS2M) of FEMTO-ST Institute deals with the development of precise positioning systems (microactuators, actuated microsystems, and microrobots) since 1995. The main targeted applications of these systems have been being multiple: micromanipulation and characterization of biological cells, micromanipulation and characterization of artificial objects (nonbiological objects), microassem-

²Maghi: MicroAssembly with Gripper Handling (*in english*), Micro-AssemblaGe d'HerbIvores (*in french*)

bly of artificial objects such as optical components, measurement and characterization of forces at the microscale, and since a couple of years the precise laser phonomicrosurgery. Though, micromanipulation and microassembly of artificial objects are particularly the principal core. These developments and these applications have been carried out within different national, european and international projects and collaborations and made the department well ranked in the field at the international level. When I arrived at the AS2M department³ in november 2003 as a PhD student with a ministerial scholarship grant, I was given the opportunity to design, develop and control novel microassembly stations capable of automatic or semi-automatic manipulation or assembly of small objects. The subject, very exciting and multidisciplinary, was part of an european project dealing with the development of modular microfactories, a new concept of factories of the future with reconfigurability property and for the production of micro-products at low cost. The PhD works comprised the design and development of a piezoelectric microrobot, its modeling and control, and the automation of the whole microassembly station based on this microrobot.

1.2 Piezoelectric materials based positioning systems

The design and development of miniaturized systems for precise and high dynamics positioning are very different from the design and development of classically sized positioning systems like robots, arms, conveyors. For these latters, the actuators used (DC motors, pneumatic actuators, magnetic actuators,...) are composed of several subcomponents such as stator, rotor, movable parts, and of other elements that permit to attach them (screws, nuts,...). These actuators are afterwards integrated with other mechanical components and hinges to transform the movement from rotation into translation (or conversely), to amplify the strokes or the torques, to transmit them, or to increase/decrease the speed. At the end, the positioning systems are made up of many components. For miniaturized precise positioning systems, such method of design and development will not work. First, as the sizes downscale, it is difficult or even impossible to fabricate the subcomponents. Second, assembling too many small subcomponents is a very challenging task. Finally, the mechanical plays and backlashes found in the assembled subcomponents as well as the frictions between them are not favourable for the obtention of high resolution of positioning. New methods of design and of development have therefore been raised by engineers and researchers. The main idea is that, instead of using several assembled components (actuators and articulations), one employs smart materials and deformable structures. These materials and structures react and generate motion and torques subjected to external excitation like electrical voltages and fields, magnetic fields, temperature,... The most used in precise positioning comprise: thermally and electrothermally movable or deformable structures, shape memory and magnetic shape memory alloys, electroactive and magnetoactive polymers, magnetostrictive materials, electrostatically driven structures, and last but not least piezoelectric materials.

³At this time, the AS2M department name was LAB (Laboratoire d'Automatique de Besançon). The actual name (AS2M) was given in january 2008 when the department becomes a department of FEMTO-ST Institute.

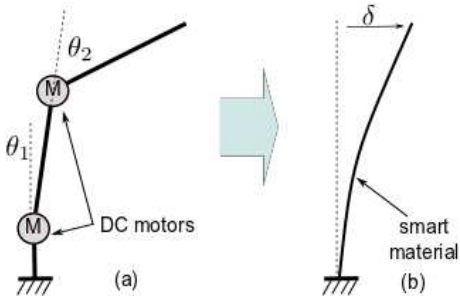


Figure 1.5: Replacement of a classical polyarticulated arm by a bulk smart material.

By using them, the set of subcomponents are replaced by one bulk material which can perform the same functionalities. To show the principle, Fig. 1.5 depicts the replacement of a polyarticulated arm by a bulk smart material. Both systems can provide a displacement at their extremities. With the smart material, the absence of mechanical plays, of clearances and of friction makes possible a positioning with a very high resolution.

Piezoelectric materials are very well recognized in the development of precise and high dynamics positioning systems. This recognition is thanks to the high resolution (up to nanometric level), the high bandwidth (tens of kiloHertz) and the high stiffness that many of them can offer. These properties render them well adapted to high resolution and high speed actuation. Furthermore, the fact that their excitation is electrical eases their integration and utilization. Finally, they can be used as sensors or as actuators and thus opens their range of applications broader. At the AS2M department, piezoelectric materials, mainly lead-zirconate-titanate (PZT) ceramics, are extensively employed to develop microgrippers for microassembly and micromanipulation aims. PZT piezoceramics exhibit a large stiffness and a high coupling factor and are widely available in commerces at low costs. These piezoelectric microgrippers are most of the time made up of two piezoelectric cantilevers with rectangular section which, when driven by independent voltages, are able to pick, transport and place or to assemble small objects with a very high positioning resolution. The development and the utilization of these microgrippers raised several PhD thesis works and patents from the AS2M department [59–66]⁴. Fig. 1.6-a, b, c, d and e depict different versions of the developed microgrippers at the department and Fig. 1.6-f, g and h some examples of their utilization to manipulate or to assemble small gears.

The works reported in this thesis deal with the design and development of piezoelectric cantilevered structures systems, their modeling, control and signal estimation. The systems are devoted to precise and high dynamics positioning. The development comprises microgrippers, more complex structured systems (for example: with more degrees of freedom) or more performant systems (for example with higher range). It is shown that simple piezoelectric cantilever structures can be exploited to develop dexterous and highly performant systems with other capabilities than simple bending. We will also demonstrate that control theory tools (modeling, robustness, control, estimation,...) bring additional possibilities, or are even necessary, to reach these targets. In the control side, an important aim is that the controllers should satisfy the severe performances required in precise and high dynamics positioning (settling time less than tens of milliseconds, no-overshoot and no-vibrations from the actuators during the tasks,

⁴The references do not include my works as they will be cited as contribution in the rest of the thesis.

micrometric accuracy) with a worry about their simplicity to match with real-time implementation and with the actual available real-times machines (limited in computing powers and memories).

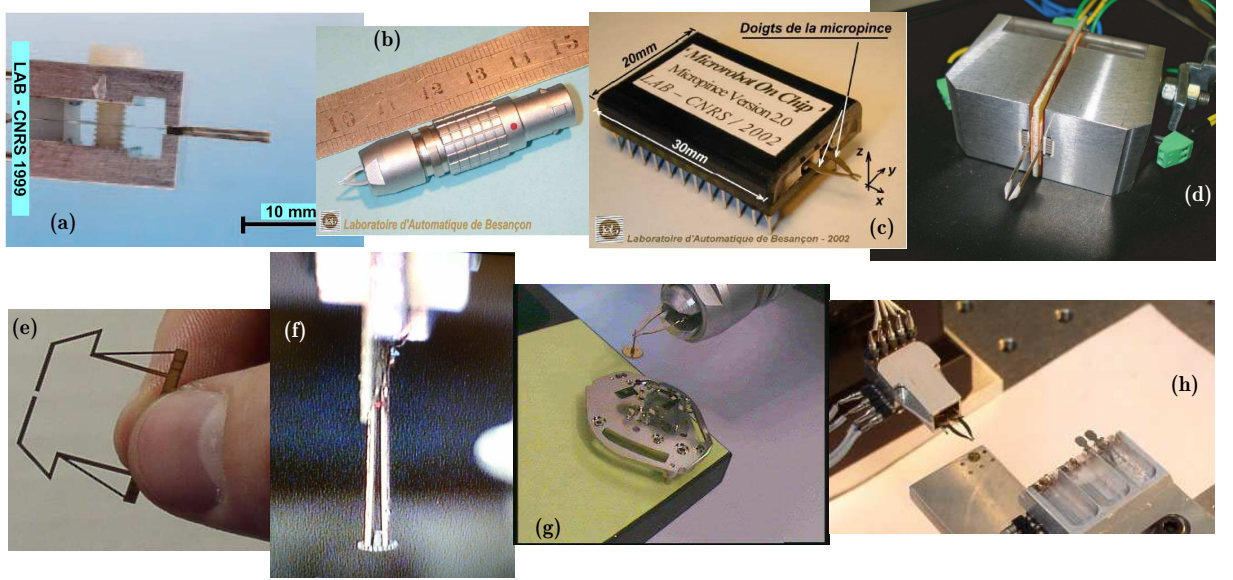


Figure 1.6: Piezoelectric microgrippers developed at the AS2M department. (a): the first version of piezoelectric microgripper at the AS2M department [59; 60]. (b) and (c): a 4-DOF microgripper on chip [61; 62]. (d): a hybrid thermopiezoelectric microgripper [PT1][J14]. (e): a microgripper with optimized sensing and actuation capability [64–66]. (f)[C11], (g) [61], and (h) [63]: utilization of the microgrippers for micromanipulation or microassembly tasks.

1.3 Challenges posed in precise and high dynamics positioning with piezoelectric systems

Piezoelectric cantilevers based positioning systems possess very high resolution, high bandwidth and high stiffness and are relatively easy to develop. However they exhibit strong nonlinearities which are the hysteresis and the creep, and are typified by badly damped vibrations. Furthermore they are very sensitive to the environment (temperature, surrounding vibrations). The nonlinearities lead to a loss of performances (mainly the final precision) of the micromanipulation and microassembly tasks and the vibrations strongly compromise their stability. In a closed-loop scheme, both the nonlinearities and the vibrations affect the stability if not well accounted for. These properties should definitely be considered by control techniques to reach the performances required in micromanipulation and microassembly tasks. Additionally to these properties, other characteristics that are found in microsystems and miniaturized systems in general also pose challenges. They are all quickly reminded below.

Hysteresis phenomenon

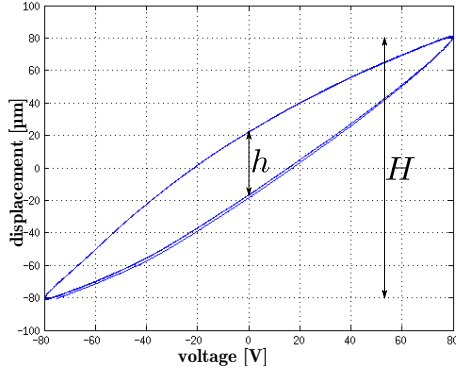


Figure 1.7: Example of hysteresis obtained from a piezoelectric cantilevered actuator [BC5].

piezoelectric positioning systems more complex. Fig. 1.7 depicts an example of hysteresis of a piezoelectric cantilever structured actuator [BC5]. The amplitude of the hysteresis is of $\frac{40\mu m}{160\mu m} = 25\%$ which is very important.

Creep phenomenon

The creep phenomenon is defined as the progressive time-dependent inelastic deformation of a material under constant load and temperature. The shape of the creep and the duration of the creep stages depend strongly on the stress and temperature values [72][B4]. In an analogous way, the creep in piezoelectric materials is defined as the drift in deformation after applying a constant electric field, the evaluation being made at constant temperature.

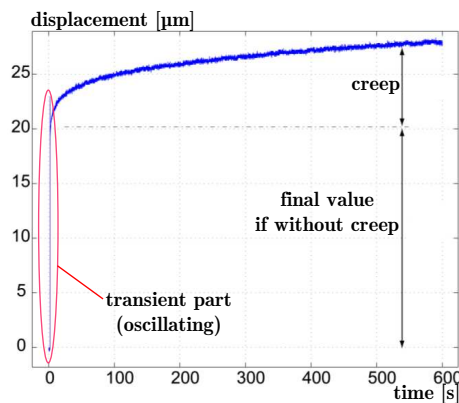


Figure 1.8: Example of creep in a piezoelectric cantilever [J7].

The hysteresis in piezoelectric systems are a nonlinear phenomenon in which forth and back displacement paths are different [70; 71] and thus cause an important positioning error. To characterize the hysteresis, a sine driving voltage signal with a fixed frequency is applied to the piezoelectric actuator. Then the output displacement is recorded. The amplitude of the hysteresis $\frac{h}{H} \times 100\%$ (see Fig. 1.7) is therefore calculated from the input-output map [B4]. The hysteresis in piezoelectric systems are known to be rate-dependent (or dynamic): the shape of the hysteresis varies according to the frequency or to the rate of the driving voltage signal. This renders the dynamic control of the piezoelectric

positioning systems more complex. The creep, similarly to the hysteresis, is due to a complex phenomenon inside the material. It depends on the internal structure and properties of the material such as the domains walls, impurities and vacancies. The creep is more important when the temperature is high. Furthermore, the creep due to an electrical excitation is more important than that the creep due to a mechanical stress in piezoelectric materials. The observation of the creep is made by applying a step voltage to the piezoelectric system. The phenomenon is taken as the low rate drift that occurs just after the transient part, see Fig. 1.8. The settling time of the transient part is very quick and does not exceed hundreds of milliseconds

while the settling time of the drift can be many hours. As an example, Fig. 1.8 depicts the step response of a piezoelectric cantilevered actuator with $20\text{mm} \times 2\text{mm} \times 0.3\text{mm}$ sizes and based on lead zirconate titanate (PZT) and copper materials. The response has been recorded for a long period. The settling time of the transient part is calculated as about 82ms whilst the drift is still evolving even after 10min of observation [J7].

Badly damped vibrations

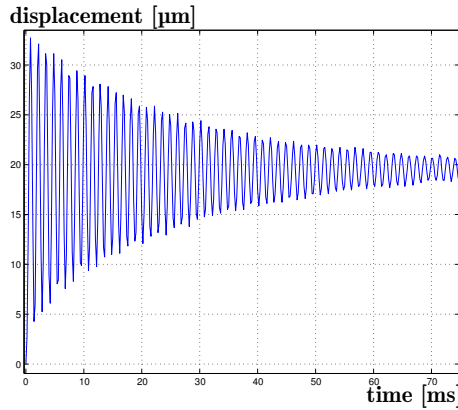


Figure 1.9: Step response (the transient part) of a piezoelectric actuator [J7].

in Fig. 1.8. This figure corresponds to the transient part before the creep starts. A quick identification shows that the actuator exhibits a damping ratio of $\xi = 0.01$ at the natural frequency of 4713rad/s [J7].

High noise-to-signal ratio

The ranges of the useful signals⁵ involved in precise positioning systems are weak and the accuracy required in the tasks are severe (micrometric or submicrometric). Any noise introduced by the sensors or caused by the environment (thermal noise, mechanical vibrations,...) will drown the signals [74–76][BC7]. It results in a high noise-to-signal ratio that conditions the success of the micromanipulation or microassembly tasks.

High sensitivity to environmental disturbances

As the sizes of the matter downscale, forces imperceptible at the classical sizes become predominant face to volume forces (weights). Called surface forces, they include the electrostatic force, the van der Waals forces and the capillary force [77–79]. When the sizes of the manipulated objects or of the positioning systems are too small, these forces inevitably affect

⁵Range of useful signals: range of positioning or range of force.

the tasks. Last, miniaturized positioning systems are very sensitive to the environmental conditions like the temperature or surrounding vibrations [80]. A small amount of temperature variation that is classically irrelevant can greatly impact the precision of miniaturized systems.

Difficulty to sense and to measure

When working with small sized systems, a characteristic is the difficulty to sense. Thus, camera and microscopes are often utilized to follow the micromanipulation and microassembly tasks. Meanwhile, this is not always realisable if the space available for the visualisation is restricted. Finally, measuring the movement and the forces in precise and high dynamics positioning systems is still limited nowadays. As we will discuss in Chapter 4 and in Chapter 5, sensors that have the required performances to track these signals are bulky, not integrable and very expensive (examples: optical sensors with triangulation principle) whilst sensors that are embeddable are not convenient for certain applications due to their limited performances (limited ranges and precision).

1.4 PhD works (2003 - 2006)

1.4.1 Context and results

My PhD works were carried out at the AS2M department between november 2003 and november 2006. They dealt with the design, development and control of a microassembly station and were under the guidance of Philippe Lutz and Yassine Haddab. The works are part of an european project (EUPASS project) that aimed to develop reconfigurable microfactories [80]. The microfactories are miniaturized factories capable of producing miniaturized products at low costs.

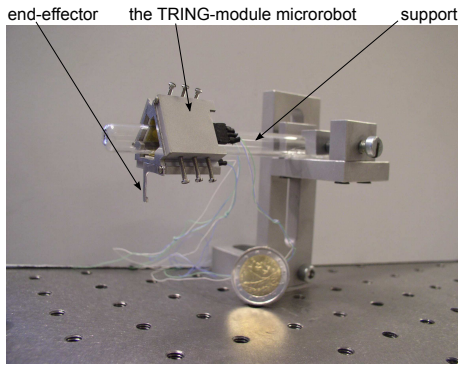


Figure 1.10: A TRING-module: a very high resolute 2-DOF microrobot with angular and linear motion capabilities.

ters are possible.

One of the important outcomes of the PhD works was the development of new microrobots (called TRING-module) capable of performing very precise angular and linear motions (2-DOF) [BC1][J3][C5][C4][C2], see Fig. 1.10. Based on the stick-slip motion principle and on piezoelectric actuators, one TRING-module can move with a step between $70nm$ and $200nm$. Its linear velocity can be in excess of $2mm/s$ and the angular velocity is about 1 round per $18s$. When working in sub-step, the resolution of the movement is nanometric (better than $10nm$). Additionally to the very high resolution, another advantage from the TRING-modules is the very high range: several tens of centimeters are possible.

The PhD works also include the development of a whole station based on one or several TRING-modules [C3][C1], and the modeling and control of all the modules within the station. A novel control technique for stepper microrobots has been proposed [BC1][J1][C8][C6]. Called voltage/frequency proportional control, the technique encompasses the existing ones and is more general. A main advantage of this technique is that the two modes of movement, i.e. the step-by-step motion for the coarse positioning and the substep for the fine positioning, are automatically switched by the controller. We have also demonstrated that the Lyapunov stability is guaranteed by the novel control technique for any stick-slip microrobot. Finally, another principal result of the PhD works is the modeling and control of piezoelectric cantilevers used as active end-effector for the microrobots [J2][C10][C9][C7]. My works regarding the piezoelectric cantilevered structures with rectangular sections started with this result.

1.4.2 PhD general information

Table 1.4.2 summarizes the administrative information relative to my PhD and to its defense.

lightgray GENERAL INFORMATION	
Starting date	November 3, 2003
Date of defense	November 30, 2006
University	University of Franche-Comté (UFC) at Besançon
Laboratory	Automatic Control and MicroMechatronic Systems (AS2M), FEMTO-ST Institute CNRS UMR6174 / UFC / ENSMM / UTBM
Speciality	Control Systems
Title	Développement et commande modulaire d'une station de microassemblage
lightgray COMMITTEE MEMBERS	
Reviewers	- Henri BOURLÈS, Full Professor CNAM Paris France - Hervé-Tanneguy REDARCE, Full Professor INSA Lyon France
Examiners	- Jean-Marc BREGUET, Director of Group EPFL Lausanne Switzerland - Nicolas CHAILLET, Full Professor UFC Besançon France - François PIERROT, Director of Research LIRMM Montpellier France - Stéphane RÉGNIER, Full Professor UPMC Paris France
Advisors	- Philippe LUTZ, Full Professor UFC Besançon France - Yassine HADDAB, Associate Professor ENSMM Besançon France
lightgray HIGHLIGHTS	
Ministerial scholarship award	
UFC best PhD thesis finalist	
IEEE ICARCV-2006 best paper award finalist (4 papers selected among 580 papers)	

Table 1.1: *Information summary regarding my PhD works.*

1.4.3 Publications related to the PhD works

The list of publications related to the PhD works are listed in [Appendix B](#) and are clarified by the "*(related to my PhD works)*" statement. They include one book⁶, one book chapter, three journals, ten international conferences or workshops papers and four national and regional workshops.

1.5 Post-PhD works (2006 onwards)

1.5.1 Fundamental themes

My works since 2006 can be splitted into three fundamental themes: 1) the design and the development of piezoelectric based precise and high dynamics positioning systems, 2) their control, 3) and the study of measurement techniques for them.

Design and development of piezoelectric systems

This theme is related to the design and development of precise and high dynamics positioning systems based on piezoelectric materials. Cantilever structures with rectangular section are principally the basis. It is shown that these simple structures of piezoelectric actuators can be utilized to yield more complex or more performant systems. For examples, they have been employed for the design of a new high range and high resolution hybrid actuator (see [Section 2.3](#)), of a high rate scanner in phonosurgery (see [Section 2.4](#)), or of cartesian MEMS with three DOF capabilities (see [Section 2.5](#)). Finally, control theory tools (interval techniques and modeling) have also been proposed to make design of these systems with guaranteed performances.

Control of piezoelectric systems

The objective of this theme is the control of piezoelectric based positioning systems. Both open-loop (feedforward) and closed-loop (feedback) schemes are studied. Feedforward scheme have been proposed to satisfy the lack of convenient sensors. In feedback scheme, robustness face to the disturbances and to the model uncertainties and simplicity of the controllers (low orders) are the main criteria for the synthesis. In both schemes, modeling the behavior of the piezoelectric systems constitutes an important part and success of the controllers synthesis. The properties previously listed, in particular the nonlinearities, the vibrations, and the sensitivity to the environment (manipulated objects, ambient temperature), are conveniently considered in the modeling and in the controllers synthesis.

Measurement techniques

The main limitation to utilize feedback control techniques in the studied piezoelectric systems is the actual lack of embeddable and performant sensors. Regarding the feedforward

⁶In fact the PhD itself has been published by the *Editions Universitaires Européennes* as a book later on.

techniques, the main limitation is the lack of robustness relative to models uncertainties and relative to external disturbances. Thus, we also studied the development of measurement techniques devoted to piezoelectric systems. Self-sensing measurement techniques are among them. We also show that combining control theory tools (observers) with the existing or developed instruments can help to go further in the measurement capabilities. Observers are very interesting complementary tools for the existing sensing technologies to execute measurement during micromanipulation and microassembly tasks and for precise and high dynamics positioning in general.

1.5.2 Applications

Fig. 1.11 summarizes the links between the context, the fundamental themes and the applications of my works. Precise and high dynamics positioning is the principal context and motivation. The three fundamental themes are to reach the objectives in this context. The applications are mainly the micromanipulation and microassembly tasks as well as the phonosurgery by microrobots. These applications are all treated at the AS2M department since many years. My contribution to them is related to the piezoelectric materials based systems to execute the tasks.

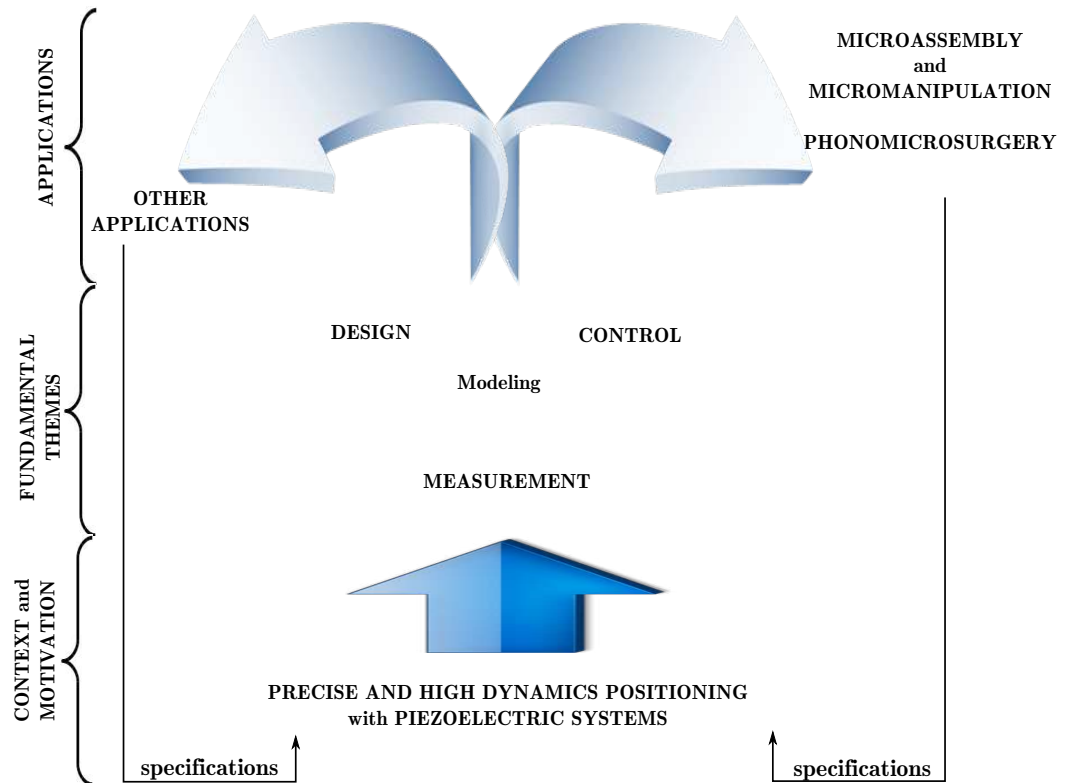


Figure 1.11: Links between the context and motivation, fundamental themes and applications.

1.5.3 Supervised works

Since 2006, I was advisor or co-advisor of six post-doc fellows, four PhD students and MSc, BSc or Engineers students. Table 1.5.3 presents the repartition of their works according to the theme. The numbers of months consecrated to each theme are approximative. M_{tot} is the total number of months of recruitment. There are 85 months of post-doc fellowships, 144 months for PhD fellowships, and 58 months for internships.

lightgray Post-DOC				
FELLOW OR STUDENT	Design	Control	Measurem.	Total (M_{tot})
Omar AL JANAIDEH	0	3.5	3.5	7
Vincent CHALVET	6	3	0	9
Ton Pengwang EAKKACHAI	12	0	0	12
Ioan Alexandru IVAN	0	0	6	6
Alex BIENAIMÉ	12	0	0	12
Juan Antonio ESCARENO	0	15	0	15
Ioan Alexandru IVAN	9.6	2.4	12	24
yellow Total (months)	yellow 39.6	yellow 23.9	yellow 21.5	yellow = 85
lightgray PHD				
Yasser AL HAMIDI	0	36	0	36
Didace HABINEZA	3.6	32.4	0	36
Sergio LESCANO	27	9	0	36
Sofiane KHADRAOUI	5.4	30.6	0	36
yellow Total (months)	yellow 36	yellow 108	yellow 0	yellow = 144
lightgray INTERNSHIPS (MSc, BSc, ENGINEERS)				
Fadwa HOUSSALI	5	0	0	5
Vincent TRENCHANT	0	3.5	3.5	7
Erwann DUPONT	3.5	3.5	0	7
Ismaël Ahmed ISMAËL	5	0	0	5
Yasser AL HAMIDI	0	2	0	2
Adiasa ADIASA	5	0	0	5
Quentin ASSAILLY	5	0	0	5
Mohamed Lamine BERRANDJIA	0	0	2	2
Paul Michaël MOORE	1	0	1	2
Qihong ZHOU	0	2	0	2
Kamel NCIR	3	0	3	3
Elodie HAVET	6	0	0	6
Mamadou Cissé DIOUF	0	4	0	4
yellow Total (months)	yellow 33.5	yellow 15	yellow 9.5	yellow = 58

Table 1.2: *Effective months and themes for the advised fellowships and internships.*

Finally, Figure 1.12-a is a sector view of the above repartition, the total months number being 287. As we can see, the control theme presents the highest volume of investigation (in excess of 51%). Figure 1.12-b summarizes the repartition of the themes according if they were affected to post-doc, PhD or internships. We can conclude that design is equitably affected to the three types of fellowships, control is principally affected to PhD students and measurement theme has been mostly carried out by post-doc and internships.

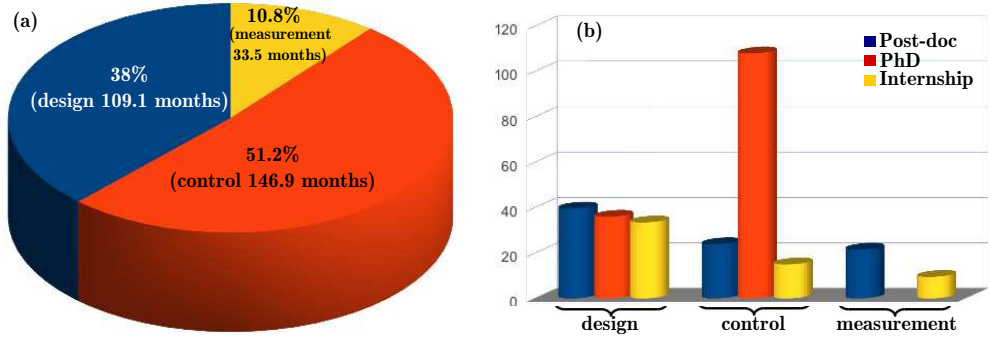


Figure 1.12: General repartition (in months number) of the supervised works.

1.5.4 Projects and fundings

Table 1.5.4 lists the past and the ongoing projects that I have coordinated or to which I have contributed. Complementary information on these projects are also given in Appendix A.2.4 and in Appendix A.2.5. Regarding the coordinated projects, the amount of fundings and grants given to the department are also displayed in the table. The total amount in these coordinated projects is 827k€. There are one european (μ PADS) and two national coordinated projects (C-MUMS and MYMESYS), one of which is a young investigator award. Self-funding means that there is no allowance. This case concerns a PhD student (Yasser Al Hamidi) and an internship (Mohamed Lamine Berrandjia) came with their own fundings.

In order to have an idea of the investigated theme in each project, the number of months effectuated by the all supervised fellowships without distinction (post-doc, PhD and internships) has also been put in the table. They are indicated by m_d (number of months devoted to the design theme), m_c (for the control theme) and m_m (for the measurement theme). The total months number of supervised works in each project is: $M_{tot} = m_d + m_c + m_m$. It is worth to notice that other concerns like equipments costs are not assessed and are not considered in the themes repartition.

lightgray DURATION (IN MONTHS) OF FELLOWSHIPS FOR EACH PROJECT.				
PROJECT/FUNDING	Design (m_d)	Control (m_c)	Measurem. (m_m)	Total (M_{tot})
COORDINATED PROJECTS AND FUNDINGS				
μ PADS (2008-2010, 171k€)	9.6	2.4	12	24
ANR C-MUMS (2012-2016, 177k€)	3.6	32.4	0	36
ANR MYMESYS (2012-2014, 300k€)	23	6.5	9.5	39
UFC post-doc fellowship (2014, 21k€)	0	3.5	3.5	7
UFC post-doc fellowship (2013, 27k€)	9	0	0	9
BQR UFC (2012-2013, 16k€)	5	0	0	5
CGD funding (2009-2012, 90k€)	5.4	30.6	0	36
BQR ENSMM (2010-2011, 14k€)	4	0	0	4
BQR UFC (2010-2011, 5k€)	0	0	0	0
OSEO-ANVAR (2007, 6k€)	0	4	0	4
self-funding	0	40	0	40
CONTRIBUTED PROJECTS				
μ RALP (2012-2015)	43.5	12.5	0	56
NET4M (2011-2014)	0	0	0	0
MIM-HAC (2012-2014)	0	15	0	15
NANOROL (2008-2012)	0	0	0	0
Maturation Bourgogne-FC (2012)	0	0	0	0
MicroFactory-2 (2010-2012)	0	0	0	0
MicroFactory (2007-2009)	6	0	0	6
yellow Total months for all fellowships	yellow 109.1	yellow 146.9	yellow 31	yellow = 287

Table 1.3: *List of projects and supervised works for each project.*

Based on this repartition, a synthesis diagram is given in [Figure 1.13](#). The diagram permits to quickly see the notable effort consecrated on design during the μ RALP project. This project consists in developing parallel microrobots devoted to orient laser beams for phonomicrosurgery. The high challenge raised by this development (severe performances, very compact sizes, novel microfabrication technologies) had made this task require more energy and time. The national ANR MYMESYS project also exhibits a non-negligeable months number consecrated to design. Finally, notable efforts have been given to the control theme within three projects which correspond to PhD fundings.

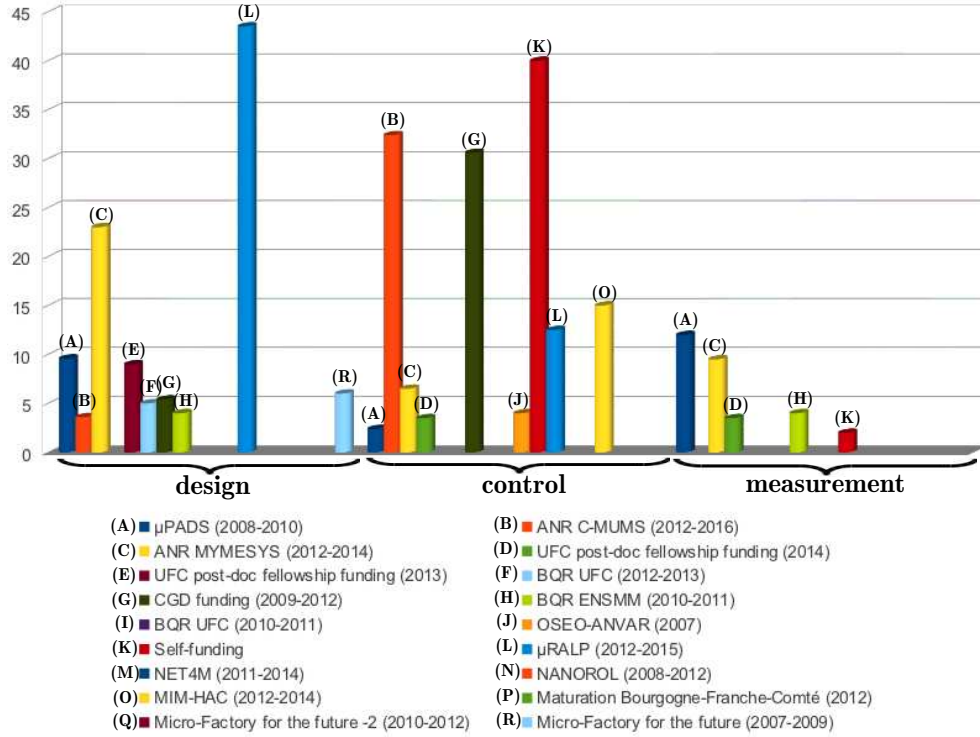


Figure 1.13: General repartition that links projects with supervised works (in months).

1.5.5 From research to teaching

Teaching

I teach CONTROL SYSTEMS, ROBOTICS and MICROMECHATRONICS at the University of Franche-Comté at Besançon. My courses are principally for junior undergrad students⁷ on Electrical Engineering (EEA: Electrotechnique, Electronique, Automatique), for professional bachelor⁸ and for postgrad students in preparation of their master's degree on Mechatronics. Complementary information on teaching are given in [Appendix A.3](#).

CONTROL SYSTEMS modules include continuous and digital linear systems (modeling and control), Kalman filtering, state-space modeling and control, and multivariable robust control (H_∞ and its derivatives). For Bachelor students, the objectives are to provide sufficient knowledge to face the modeling and the controllers synthesis in industrial and industrialized processes. After graduation, they will be able to characterize and to model these systems and to synthesize and to tune classical controllers (PID, bang-bang, ...). For Master students,

⁷Junior undergrad students: 3rd in the preparation of the bachelor, Licence 3^{ème} année.

⁸Professional bachelor: Licence Professionnelle

advanced notions of control theory are given such that they can be able to go further on the modeling and controllers synthesis and thus to face complex processes (aerospace, medical, ...). For instance, the consideration of the uncertainties and of the noise is given in depth during these advanced courses. The courses given to Master students also permit to progressively enter on the PhD program for those who think to pursue in this direction. Still in this spirit, I give courses on modeling and feedforward control of hysteresis, creep and badly damped vibrations with applications to piezoelectric systems. The objective here is to propose "exotic" control techniques and to transfer the research to teaching.

Transfer of research to teaching

Connection between the research results and the teaching: an essential point to which I attach a great importance is the transfer of research to teaching. I always endeavor to connect the teaching for Master students with research in general or with the research carried out at the department of AS2M. Many exercises, projects or tutorials examples during the CONTROL SYSTEMS modules and the MICROMECHATRONICS module are based on the research results. They comprise the feedforward control of nonlinearities and of vibrations, the robust H_∞ control of hysteretic systems,...

Importance of videos: during the lectures on ROBOTICS or on CONTROL SYSTEMS, it is important to show exciting videos of controlled complex systems. Most of the time, I take these videos during international conferences (IEEE ICRA, IEEE IROS, ACC...), from the internet or from the AS2M department. The videos are presented at the beginning of the modules and greatly influence the motivation of the students and their interest to the fields. They show the variety of applications and are complementary to the benchmarks that the students will see during the labs.

Development of labs based on research: these last years, we have duplicated experimental setups used in research works to create similar benchmarks for teaching labs. They are principally based on piezoelectric cantilever actuators and piezotubes scanners. They are devoted, but not limited, to: 1) introduction to nonlinearities and vibrations in piezoelectric systems, 2) modeling and feedforward control of hysteresis, creep and vibrations, 3) robust H_∞ control, 4) and self-sensing measurement techniques in piezoelectricity. Self-sensing which will be presented in [Section 5.4](#) consists in employing the piezoelectric actuators as sensors at the same time *via* the direct and the converse piezoelectric effects. It is evident that the students in micromechatronics should have seen such novel and very integrated technologies of sensing.

Invited lectures

When I was visitor at the University of Texas at Arlington (UTA) in USA in november 2011, I have been given the opportunity to give a one hour lecture to BSc, MSc and PhD students of the department of Electrical Engineering. I therefore gave an introduction to the modeling, the identification and the feedforward control of hysteresis in smart materials based actuated systems. The lecture was taught in a way that, after some preliminaries and

definitions, the students follow an illustrative example (Prandtl-Ishlinskii technique applied to piezoelectric materials) from the initial hysteresis characterization to its final control. The title of the lecture was: "*Hysteresis modeling, identification and feedforward control for piezoelectric based Microsystems and microrobots*".

1.5.6 Collaborative context

Besides the collaborative projects to which I participate or I coordinate, below are listed researchers with whom I have direct and active collaborations (technical, visiting, organization of sessions and focused sections, ...):

- ⇒ Prof. S.O. Reza MOHEIMANI, University of Newcastle, LCDN and CDSC, Newcastle Australia
- ⇒ Prof. Gloria WIENS, University of Florida in Gainesville, FL USA
- ⇒ Prof. Dan POPA, University of Texas at Arlington, TX USA
- ⇒ Prof. John T. WEN, Rensselaer Polytechnic Institute, NY USA
- ⇒ Prof. Hamid PARSAEI, Texas A&M University at Qatar, Doha Qatar
- ⇒ Dr Andrew J. FLEMING, University of Newcastle, Precision Mechatronics Lab and CDSC, Newcastle Australia
- ⇒ Dr Mohammad Al JANAIDEH, University of Jordan, Amman Jordan
- ⇒ Dr Qingsong XU, University of Macau, Macau
- ⇒ Dr. Yuenkuan YONG, University of Newcastle, LCDN and CDSC, Newcastle Australia
- ⇒ Prof. Xiaobo TAN, University of Michigan, Ann Arbor, MI USA
- ⇒ Prof. Juan Antonio ESCARENO, Polytechnic Superior Institute on Aerospace (IPSA), Paris France

The above list is not exhaustive if we consider co-authoring point of view. Furthermore, the list does not include partners with whom future projects are expected.

Regarding the industrial context, the AS2M department is in strong collaboration with the PERCIPIO-ROBOTICS company [82]. This company, located in Besançon, is specialized in the precise and high cadence positioning with robotic tools. I have been involved in a project to reach this objective where my contribution deals with the control of piezoelectric devices.

1.6 Timeline of the research since 2006

Figure 1.14 presents a timeline of the research since 2006. The figure presents the major projects, with in parenthesis my contributions, and the scientific subjects dealt. Temporally, the works carried out are in a continual evolution. We started with simple piezoelectric multimorph, i.e. monovariable systems. Their modeling and control have been extensively investigated and led to important results recognized at the international level. Over the time, the need of convenient measurement techniques to make feedback control architecture possible led us to also investigate in this direction. In parallel, the feedforward control architecture

has been investigated as alternative way to enhance the performances when there is a lack of sensors. The different contributions have been being gradually extended to multivariable due to the raise of multi- DOF piezoelectric systems. Finally, these last years, we have started to investigate on even more miniaturized, highly performant, highly dexterous and low costs piezoelectric MEMS.

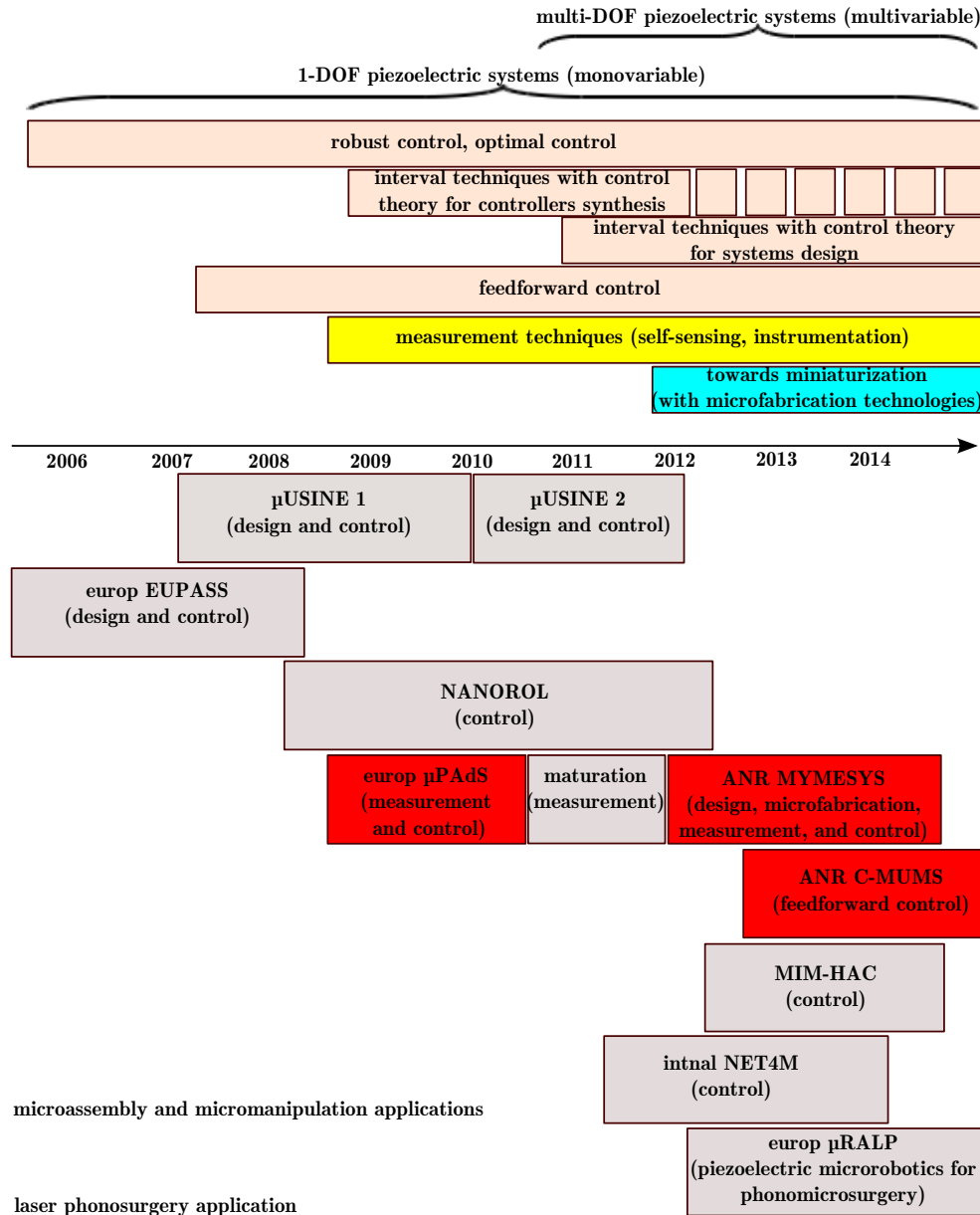


Figure 1.14: Timeline of the research since 2006.

1.7 Organization of this thesis

The remainder of this thesis provides a synthesis of my works on precise and high dynamics positioning systems based on piezoelectric materials. The organization of the thesis is as follows. [Chapter 2](#) is devoted to the design, the development and the modeling aspects. In [Chapter 3](#), the different feedback control techniques for these systems and studied so far are presented. [Chapter 4](#) deals with their feedforward control. Finally, all investigated measurement development and techniques are presented in [Chapter 5](#).

In [Chapter 6](#), after providing the conclusions, I will give the perspectives. The details of my *Curriculum Vitæ* are in [Appendix A](#) and the list of my publications in [Appendix B](#). All along the thesis, the citations related to my works are referred to this list (example [\[J1\]](#)).

Chapter 2

Design, development and modeling

This chapter deals with the design and development of piezoelectric positioning systems and their modeling. A particular attention is given to piezoelectric actuators that have cantilever structure with rectangular section. They are the basis of the development of more performant or more complex systems. For that, the chapter is splitted into three classes. The first class deals with cantilever structured only piezoelectric systems and are given in [Section. 2.2](#) and [Section. 2.3](#). In the second class, we present more complex structured systems. This will be in [Section. 2.4](#) and [Section. 2.5](#). The last class deals with a new methodology to design piezoelectric systems. The methodology is based on interval techniques and will be presented in [Section. 2.6](#).

Contents

2.1	Introduction	30
2.2	Multimorph piezoelectric cantilevers as basic actuators	31
2.2.1	Principles	31
2.2.2	Ballas linear modeling	32
2.2.3	Extension to nonlinear modeling	34
2.3	Hybrid thermopiezoelectric actuator	36
2.3.1	Principle	37
2.3.2	Modeling	38
2.3.3	Other leads to represent the behavior of hybrid actuators	41
2.3.4	Acknowledgments	42
2.4	Parallel kinematic piezoelectric microrobot for laser phonomicrosurgery	42
2.4.1	Context	42
2.4.2	A high resolution, high bandwidth, and high range 2-DOF microrobot	43
2.4.3	A macro version of the robot	46
2.4.4	Perspectives	47
2.4.5	Acknowledgments	48
2.5	Cartesian piezoelectric microstructure	48
2.5.1	Microfabrication of PZT materials	48

2.5.2	The designed and microfabricated microstructure	50
2.5.3	Perspectives	51
2.5.4	Acknowledgments	51
2.6	Design methodology for piezoelectric cantilever systems using interval tools	51
2.6.1	Redesign of piezoelectric actuators	53
2.6.2	Design of piezoelectric actuators with the performances inclusion theorem	55
2.6.3	Perspectives	56
2.6.4	Acknowledgments	56
2.7	Conclusions and perspectives	57

2.1 Introduction

Piezoelectric cantilever structure with rectangular section is one the most used structures in piezoelectrically actuated systems. They can be employed to realize devices for various applications such as microgrippers [59–67; 83–86][PT1][J14][C11], switches [87–89], micro-valves [90], micro-air-vehicles [91–95], tips in atomic force microscopes [96], or orientable platforms [97–100].

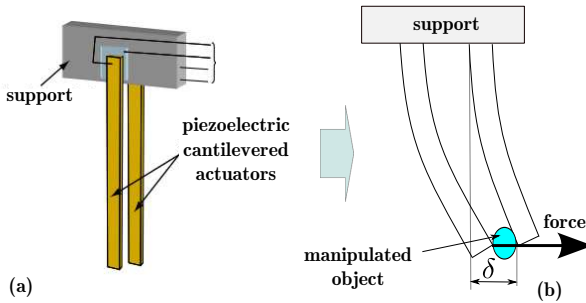


Figure 2.1: Principle of a piezoelectric micro-gripper.

With regards to piezoelectric microgrippers which are extensively employed to execute micromanipulation and microassembly tasks, there are often two piezoelectric actuators, see Figure 2.1-a. By driving the bendings of the two actuators, it is possible to perform a pick-transport and place of small objects with a very high resolution as figured in Figure 2.1-b. Since the two cantilever actuators are independent, one of them can be driven to perform the positioning while the other one to maintain the object with a desired manipulation force.

It is worth to notice that in cantilever structure, there are also the piezoelectric tube scanners (piezotubes) which have circular section. They are widely employed in scanning probe microscopy applications. Finally, piezostacks are made of the superposition of several elements piled up. Contrary to piezoelectric cantilevers with rectangular section and to piezotubes which both can bend, piezostacks only expand/contract. We will alternately employ the terms multimorph, multilayered, or piezoelectric cantilever in the remainder to state the same meaning: piezoelectric cantilever actuators with rectangular section.

The first part of this chapter is devoted to the modeling of multimorph actuators which are widely used in piezoelectric positioning systems. The relation between the bending (displacement) of the actuator, the driving voltage, any external force and the thermal excitation is derived. This will be in [Section. 2.2](#). These multimorph actuators have high resolution and high bandwidth but limited in range. Thus, in [Section. 2.3](#), we present a novel hybrid thermopiezoelectric actuator which typifies a high range of displacement. [Section. 2.4](#) and [Section. 2.5](#) are devoted to the development of more complex structured piezoelectric systems, though based on cantilevers. Finally, we present in [Section. 2.6](#) a design methodology with guaranteed performances for piezoelectric systems, based on interval tools. An illustrative example is given, it concerns the design of piezoelectric cantilever actuators. The methodology can be applied to other kinds of systems, actuated or non-actuated.

2.2 Multimorph piezoelectric cantilevers as basic actuators

After having presented the principle of bending of multimorph actuators, we present the Ballas linear model. This model is general and widely employed when the applied electrical field is relatively weak. However, this does not account for the hysteresis and the creep which are notable when the electrical field applied to the actuator becomes higher than 15% of the maximal strength [\[101\]](#). We therefore propose an extension that comprises in a single model the nonlinearities and the dynamics. Furthermore, the proposed extension also accounts for the thermal effect and for the external force applied. This extended model will be extensively employed in the rest of the thesis: modeling of newer hybrid thermopiezoelectric systems, feedback control, feedforward control, measurement techniques.

2.2.1 Principles

Consider [Fig. 2.2-a](#) which presents a piezoelectric cantilever (multimorph or multilayered actuator) that has a rectangular section and which contains n layers. At least one of the layer is piezoelectric (piezolayer). The nonpiezolayers are called passive layers. Each piezolayer has its poling direction in the vertical axis (z axis). Let h_i be the thickness of the i^{th} layer ($i = 1 \dots n$) and \bar{z} be the distance between the neutral axis and the bottom surface of the cantilever.

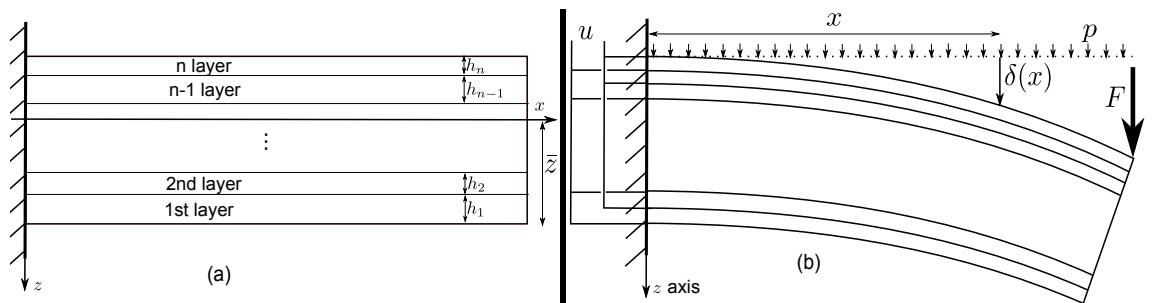


Figure 2.2: A piezoelectric cantilever.

When an electrical field is applied to each of the piezolayers thanks to the voltage u , they contract or expand along the x -axis thanks to the d_{31} coefficient¹. Due to the interfaces connection between all the layers, these contractions or expansions will result in a deflection δ of the whole cantilever Fig. 2.2-b. This bending is much larger than the contraction or expansion which is therefore the advantage of cantilever structure. Commonly utilized actuators are the unimorph and the bimorph. Unimorph has two layers in which one is piezoelectric and the other one passive. In bimorph, both the two layers are piezoelectric. Section. C.3 gives more details on them.

2.2.2 Ballas linear modeling

The linear modeling of multimorph piezoelectric cantilevers has raised several studies. The models which are utilizable in a wide range of applications are physical, i.e. they are *versus* the geometrical parameters of the cantilever and the physical properties of the materials. Their derivation is based on the linear model of a parallelepiped piezoelectric material described in the IEEE/ANSI Standards on Piezoelectricity [102]. Many of the works deal with bilayered or trilayered structures [103–108]. For n -layersss cantilevers, DeVoe and Pisano [109] derived a model of the deflection at the tip versus the applied voltage by employing the Timoschenko's bimetallic beam theory. Later on, Weinberg proposed an alternate fashion to derive a model [110] with similar performances. Finally, in [73], Ballas published the generalized model of multimorph piezoelectric cantilevers. The model, which will be reminded below, is said generalized because of the following properties.

- The model is valuable for any n number of layers.
- The model describes all possible outputs (deflection, bending angle, volume displacement, charge appearing on the electrodes surfaces) *versus* all possible input excitations (bending moment, force, pressure load, electrical voltage).
- The outputs (deflection, bending angle, volume displacement, charge appearing on the electrodes surfaces) are formulated at any point x along the longitudinal axis of cantilever. For example, the deflection $\delta(x)$ is formulated at the distance x from the clamp as pictured in Fig. 2.2-b.
- Both the static behavior and the harmonic behavior of the multimorph are given. In the harmonic behavior, the responses of the cantilever subjected to harmonic excitations are described. The resonant frequencies of the piezoelectric cantilever are also formulated.

Reconsider the clamped-free n -layersss cantilever of Fig. 2.2. Taking the voltage u and the force F at the tip as excitations, the deflection $\delta(x)$ of the actuator at a distance x from the clamp is:

$$\delta(x) = d_p(x)u + s_p(x)F \quad (2.1)$$

¹The d_{31} coefficient permits to obtain a displacement along the local axis-1 (roughly x axis) when applying an electrical field along the local axis-3 (roughly z axis).

where $d_p(x)$ is called piezoelectric coefficient of the cantilever and $s_p(x)$ its mechanical compliance. They are given as:

$$\begin{cases} d_p(x) = \frac{m_{piezo}L^2}{2C} \left(\frac{x}{L}\right)^2 \\ s_p(x) = \frac{L^3}{6C} \left[3\left(\frac{x}{L}\right)^2 - \left(\frac{x}{L}\right)^3\right] \end{cases} \quad (2.2)$$

with

$$\begin{cases} m_{piezo} = \frac{1}{2} \sum_{i=1}^n \frac{wd_{31,i}}{s_{11,i}h_i} \left[2\bar{z}h_i - 2h_i \sum_{j=1}^i h_j + h_i^2\right] \\ C = \frac{1}{3} \sum_{i=1}^n \frac{w}{s_{11,i}} \left[3h_i \left(\bar{z} - \sum_{j=1}^i h_j\right) \left(\bar{z} - \sum_{j=1}^{i-1} h_j\right) + h_i^3\right] \end{cases} \quad (2.3)$$

in which $d_{31,i}$ is the transversal piezoelectric coefficient of the i^{th} material and $s_{11,i}$ its longitudinal compliance. If the material is passive, we have: $d_{31,i} = 0$. In the equations, \bar{z} is the distance between the neutral axis and the bottom surface: $\bar{z} = -\frac{\sum_{i=1}^n \frac{w}{s_{11,i}} h_i^2 - 2 \sum_{i=1}^n \frac{w}{s_{11,i}} h_i \sum_{j=1}^i h_j}{2 \sum_{i=1}^n \frac{w}{s_{11,i}} h_i}$.

The deflection δ at the tip is easily calculated from the above model by using $x = L$.

The model in [Eq. \(2.1\)](#) is static. Ballas completed this with the resonant frequency at the mode m . The m^{th} resonant frequency of the clamped-free n -layers piezoelectric cantilever of [Fig. 2.2](#) is:

$$f_m = \frac{(k_m L)}{2\pi L^2} \sqrt{\frac{C}{\mu}} \quad (2.4)$$

where $\mu = \frac{m_c}{L} = \sum_{i=1}^n \rho_i h_i w$ is the total mass related to the actuator's length, m_c is the mass of the whole cantilever and ρ_i is the density of the i^{th} layer. The multiplication $(k_m L)$ is given in [Table C.1](#).

m	1	2	3	4	5	...
$k_m L$	1.8751	4.6941	7.8548	10.9955	14.137	...

Table 2.1: Numerical values of $(k_m L)$ for the m^{th} mode.

[Appendix. C](#) reports more description on the Ballas model. In order to have a single dynamic model that encompasses the static behavior in [Eq. \(2.1\)](#) and the dynamic behavior of the cantilever, a knowledge on the damping ratio of each mode is required. However, there is no analytical formulation of these damping ratios. In general they are characterized by experiments. Having them, transfer functions or state-space representation of the behavior of the multimorph can be yielded.

2.2.3 Extension to nonlinear modeling

The Ballas model is general and has been employed in various applications such as design, control and measurement. However this model is linear and cannot track the hysteresis and creep nonlinearities that typify piezoelectric actuators. In this section, we will extend the model in order to account for these nonlinearities. In addition, we will also include the effect of the temperature. The extension proposed here is successively described and published in [B4][J9][J7][J2][C13]. Many models have been proposed or employed to track the hysteresis and the creep in piezoelectric actuators. In fact, we aim to give here a general structure of nonlinear model. This general structure will be extensively employed in the rest of the thesis and its refinement will be presented over it.

Inspired from the Ballas linear model in Eq. (2.1), let us assume that the electrical contribution and the mechanical contribution are additive. Thus, the general form of the nonlinear dynamical model of the piezoelectric cantilever depicted in Fig. 2.2 is [B4]:

$$\delta(s) = \Gamma_d^u(u(s), s) + \Gamma_d^F(F(s), s) \quad (2.5)$$

where

- s is the LAPLACE variable,
- Γ_d^u is a dynamical nonlinear operator that encompasses the hysteresis, the creep and the dynamics of the piezoelectric cantilever,
- and Γ_d^F is a dynamical nonlinear operator related to the mechanical contribution. In small deformation, this operator comes back to a linear term as described in Eq. (2.1). For large deformation, it can be plastic (with hysteresis) or hyperelastic (nonlinear elastic) according to the materials that compose the cantilever. In this thesis, we assume that the mechanical contribution is linear. Almost all experimented multimorph piezoelectric actuators at the department exhibit such property.

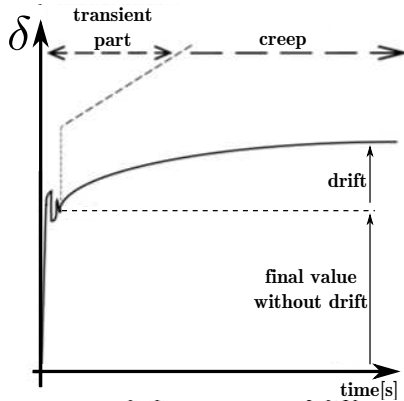


Figure 2.3: A step response of a multimorph piezoelectric actuator.

Let us now focus on the operator $\Gamma_d^u(u(s), s)$ that encompasses the piezoelectric hysteresis, creep and dynamics. If we apply a step input voltage u to the actuator, we obtain the output displacement δ as roughly pictured in Fig. 2.3. An experimental example of the step response is given in Fig. 1.8. From this response, the deflection $\delta(t)$ can be interpreted as the summation of the deflection between $t = 0$ to the end of the transient part that we denote $\delta_{transient}(t)$ and the drift evolution that we denote $\delta_{creep}(t)$. The drift is the creep itself. As the drift starts after the transient part which has a settling time t_r , the output

$\delta(t)$ is: $\delta(t) = \delta_{transient}(t) + \delta_{creep}(t - t_r)$.

However the transient part is very quick ($t_r \leq 200ms$ in many cases) and is highly negligible face to the constant time of the creep (several tens of minutes, or even in excess a hour). Therefore, we can set $t_r = 0$. Considering this additivity of the creep within $\Gamma_d^u(u(s), s)$ and the linearity of the mechanical contribution², [Eq. \(2.5\)](#) becomes:

$$\delta(s) = \Gamma_d(u(s), s) + C_{creep}(u(s), s) + s_p D(s) F(s) \quad (2.6)$$

where

- $\Gamma_d(u(s), s)$ is a nonlinear dynamical operator that contains the hysteresis and the dynamics. This is often called rate-dependent or dynamical hysteresis,
- $C_{creep}(u(s), s)$ is a nonlinear dynamical operator that represents the creep,
- s_p is the compliance of the cantilever as already seen in the Ballas model,
- and $D(s)$ is the dynamics in the mechanical contribution. It corresponds to the dynamics of the mechanical structure. Because the static gain of the mechanical contribution is s_p , $d(s)$ is normalized: $D(s=0) = 1$.

Let us now introduce the thermal effect when there is a temperature variation T applied to the multimorph actuator. Similarly to the mechanical and electrical contribution which are additive, we can assume that the same property also applies for the thermal contribution [\[B4\]\[J9\]\[C13\]](#). Consider a general case where the related thermomechanical behavior is nonlinear. Therefore, the model in [Eq. \(2.6\)](#) becomes:

$$\delta(s) = \Gamma_d(u(s), s) + C_{creep}(u(s), s) + s_p D(s) F(s) + \Gamma_{TD}(T(s), s) \quad (2.7)$$

where $\Gamma_{TD}(T(s), s)$ is the thermal contribution. It is nonlinear and dynamical.

Assuming that the Hammerstein³ scheme applies for $\Gamma_{TD}(T(s), s)$ and for $\Gamma_d(u(s), s)$ [\[B4\]](#), the final general model is yielded:

$$\delta(s) = \Gamma_d(u(s)) D(s) + C_{creep}(u(s), s) + s_p D(s) F(s) + \Gamma_T(T(s)) D_T(s) \quad (2.8)$$

where $D_T(s)$ (such that $D_T(s=0) = 1$) is the thermomechanical dynamics and $\Gamma_T(T(s))$ is the nonlinear thermomechanical gain, $\Gamma(u(s))$ is a rate-independent or statical hysteresis and $D(s)$ is the dynamics of the structure. As we can observe, the mechanical contribution and the piezoelectric contribution have the same dynamics [\[59\]\[B4\]\[J2\]](#). In the thesis, we may sometimes use the rate-dependent hysteresis instead of this rate-independent term. In such situation, we re-use $\Gamma_d(u(s), s)$ instead of $\Gamma_d(u(s)) D(s)$.

Regarding the thermomechanical contribution, the proposed formulation is general. A particular case of this is the model derived by Smits and Choi [\[104\]](#). They derived a linear

²The mechanical contribution can still be reset as nonlinear if required.

³Hammerstein scheme: see [Appendix. E](#).

thermomechanical contribution for bilayered cantilevered actuator.

The proposed general model [Eq. \(2.8\)](#) is very useful and will be the basis of many works in the rest of this thesis: design, modeling, feedback control, feedforward control, measurement and observers. The nonlinear operators $\Gamma(u(s))$, $C_{creep}(u(s), s)$ and $\Gamma_T(T(s))$ are still general and superficial. Their refinement will be presented over the thesis according to the need. The rate dependent hysteresis model $\Gamma_d(u(s), s)$ and the rate-independent hysteresis $\Gamma(u(s))$ will be treated in [Section. 3.2.1](#) and [Section. 4.3](#). The creep model $C_{creep}(u(s), s)$ will be treated in [Section. 4.2](#), and the thermal contribution $\Gamma_T(T(s))$ will be discussed in [Section. 2.3](#).

2.3 Hybrid thermopiezoelectric actuator

Comparatively to other types of actuators like thermal ones, the displacements obtained from piezoelectric actuators are weak. Thermal actuators present larger range of displacements but exhibit lower resolution, lower accuracy and lower bandwidth [\[1\]\[J9\]](#). This low accuracy is due to their high sensitivity to the thermal noise and to the varying ambient temperature. One of the most employed designs in thermal actuation is the thermal bimorph cantilever principle, which is made up of two different metallic layers [\[2; 4; 112; 113\]](#). When submitted to a temperature variation, the difference in thermal expansions of the two layers will result in a bending of the cantilever.

In applications that use piezoelectric actuators and systems, the thermal effect has been considered as unwanted disturbances [\[80; 114; 115\]\[C13\]\[C12\]](#). This is due to the fact that many of the piezoelectric systems are highly sensitive to the environment and result in an inaccuracy in the tasks to be executed. In this section, instead of considering the thermal effect as bad side, we propose to exploit and to combine this with the piezoelectric effect. The deal is to create a hybrid thermopiezoelectric actuator and to benefit from the high resolution and high bandwidth of the piezoelectric actuation and from the high range of the thermal actuation. In fact, hybridization of piezoelectricity with other types of actuation has already been investigated with success: with magnetic effect [\[116\]\[C26\]](#), with electrostatic actuation [\[C55\]\[C46\]](#) (ongoing works with promising results).

First we present the principle of the novel hybrid thermopiezoelectric actuator, which has been patented in [\[PT1\]](#). Then, we present its modeling by combining the model [Eq. \(2.8\)](#) with the thermal network theory, more detailed in [\[J9\]\[C19\]](#).

2.3.1 Principle

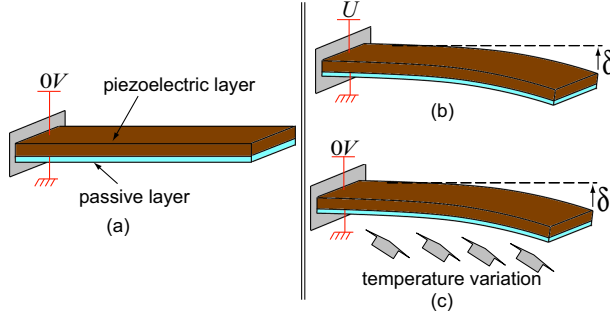


Figure 2.4: (a) Unimorph piezoelectric cantilever. (b) Piezoelectric actuation. (c) Thermal actuation.

The principal actuator is a unimorph piezoelectric cantilever which is made up of one PZT-layer (lead zirconate titanate piezoceramic) and one passive layer (copper) (Fig. 2.4-a). When an electrical voltage is applied, the PZT-layer expands/contracts resulting in a bending δ of the whole cantilever (Fig. 2.4-b). Furthermore, when a temperature variation is applied, the two layers expands/contracts at different amounts because of their different thermal expansion coefficients. A bending is also obtained (Fig. 2.4-c). The hybrid thermopiezoelectric actuator utilizes both the voltage and the temperature variation as driving inputs.

To generate the temperature variation, a Peltier module, also called Thermo-Electric-Cooler device (TEC-device), is proposed. It transforms an electrical current into a heat flux and therefore a temperature change at its surface. Its main advantage is the ease of control: electrical signal is employed to heat or to cool. By generating either positive or negative current, we can obtain a bending (displacement) of the actuator in the positive or in the negative direction. Fig. 2.5-a pictures the CAD drawing of the novel hybrid thermopiezoelectric actuator and Fig. 2.5-b pictures the fabricated prototype. The piezoelectric cantilever is glued on the upper face (called heat face) of the TEC-device. The lower face (called cooling face) of this latter device is embedded on a cooling block used for the heat evacuation.

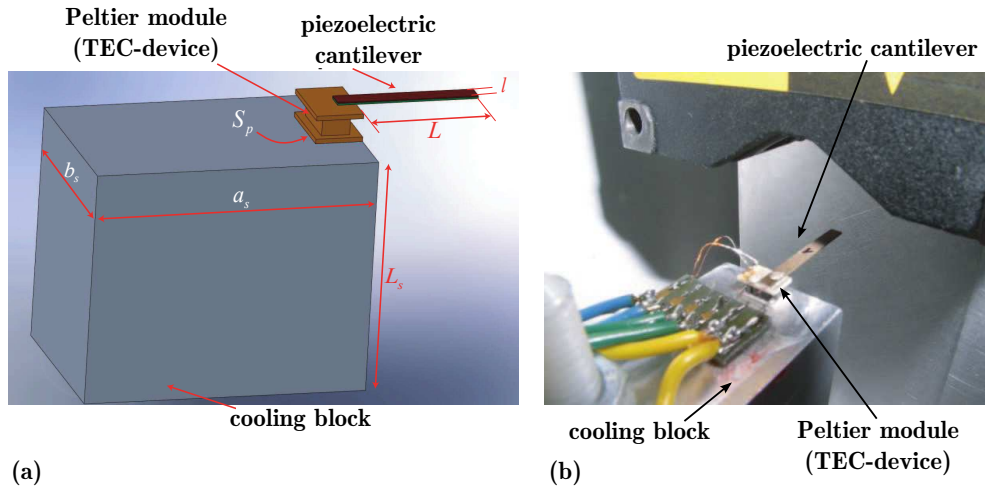


Figure 2.5: Hybrid thermopiezoelectric actuator. (a): CAD drawing (b): photograph of the prototype.

2.3.2 Modeling

Interesting applications of a model of the hybrid thermopiezoelectric actuator include the optimization of its structure for better performances and the controllers synthesis. This latter subject is treated in [Section. 3.5](#). We present in this part the modeling of the novel actuator.

General model

The actuator has two driving inputs: the voltage u and the temperature variation T . Without losing the generality, let us consider that there is no external force applied. The general model of the actuator, taken from [Eq. \(2.8\)](#), is therefore:

$$\delta(s) = \Gamma(u(s)) D(s) + C_{creep}(u(s), s) + \Gamma_T(T(s)) D_T(s) \quad (2.9)$$

Since the piezoelectric part $\Gamma(u(s)) D(s) + C_{creep}(u(s), s)$ are extensively treated in [Chapter. 3](#) and [Chapter. 4](#), we only deal here with the modeling of the thermal contribution $\Gamma_T(T(s)) D_T(s)$.

Let T_{acto} be the temperature at the interface between the actuator and the TEC-device, i.e. the temperature at the clamped end $x = 0$ of the cantilever. This corresponds to the temperature applied by the device to the actuator. It has been shown that the thermal gradient within the actuator is weak [\[J9\]\[C19\]](#). Thus, the temperature in the whole cantilever denoted with T can be considered uniform, except nearby the interface with the TEC-device. Having said that, we now need to express the relation between the excitation temperature T_{acto} and the actuator temperature T . This is a thermal modeling. In addition, we need to know the relation between the driving electrical current i applied to the TEC-device and the resulting temperature T_{acto} , which is an electrothermal modeling. [Fig. 2.6](#) depicts the scheme of the hybrid thermopiezoelectric actuator with the TEC-device. The new inputs of the system are the current i and the voltage u . The thermal model that links T_{acto} and T is strongly dependent on the thermal flux exchanged with the surrounding environment: the cooling block and the air. This thermal modeling can be rapidly a tedious task if the mechanical shapes and structures and the connection between them are not standard. In addition, the modeling complexity is increased if the interconnected systems are non-homogeneous. Deriving the model with heat equations and laws would therefore be fastidious in this case [\[117\]](#). Another fashion to observe the thermal behavior of the actuator is to employ finite element methods [\[118\]](#). These methods can rapidly provide a solution (numerically) for any given input. However they cannot provide an analytical model that can be exploited for instance in control design. A last and very interesting fashion to yield thermal models is the thermal network. Thermal network is a relatively simple

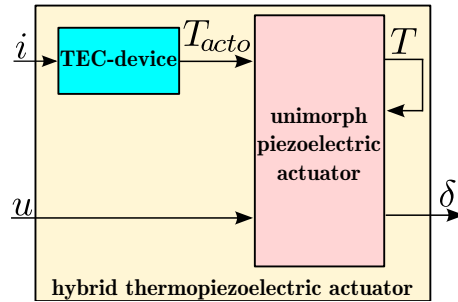


Figure 2.6: Scheme of the hybrid thermopiezoelectric actuator with the TEC-device.

but powerful tool for describing thermal and interconnected systems [119]. We will use this to track the thermal behavior between T_{acto} and T . In addition, the electrothermal behavior between the applied current i and the actuation temperature T_{acto} can also be tackled by thermal network.

Thermal network dynamic modeling

Thermal network modeling is based on the analogy between thermal and electrical models [119]. It is a simple and an efficient way to model several interconnected subsystems. A heat flow Q is equivalent to an electrical current, a temperature difference to a voltage, and a thermal resistance to an electrical resistance. From this, the thermal behavior of the cooling block and of the unimorph actuator which is composed of two layers can be schemated with an equivalent electrical circuit called thermal network. Regarding the TEC-device, Selliger et al. [120] proposed a related thermal network. This is composed of a flow source and a Joule effect which are both function of the electrical current i . Connecting the elementary networks of the different components (cooling block and its support, TEC-device, unimorph piezoelectric cantilever), the thermal network of the hybrid thermopiezoelectric actuator is depicted in Fig. 2.7. In the figure, the different parameters are defined below.

For the cooling block:

$$\begin{aligned} R_{vs} &= \frac{2}{h_{air}P_sL_s}, & R_{vsf} &= \frac{2}{h_{air}(b_s a_s - S_p)} \\ R_s &= \frac{L_s}{k_s S_s}, & R_c &= \frac{L_c}{k_s S_p}, & C_s &= \frac{\rho_s C_{ps} S_s L_s}{2} \\ R_{vs//f} &= \frac{R_{vs} R_{vf}}{(R_{vs} + R_{vf})} \end{aligned} \quad (2.10)$$

where k_s is the thermal conductivity, C_s is heat capacity and ρ_s is the density of aluminum. $S_s = a_s b_s$ is the section and $P_s = 2(a_s + b_s)$ is the perimeter of the block and h_{air} is the heat transfer coefficient. The dimensions are defined in Fig. 2.5-a. Q_r is the heat flow that traverses the thin film between the TEC-device and the cooling block.

For the TEC-device: $P_s = \alpha T_c i$ is the flow source, $P_{J/2} = \frac{R_p}{2} i^2$ is the Joule effect and $R_{th} = \frac{1}{k_p}$ is a thermal resistance term. α is the Peltier coefficient, k_p is the device thermal conductivity, R_p is the internal electrical resistance of the TEC-device, T_c and T_h are the temperature values of the two respective faces, and Q_c and Q_h are the heat flows at the cooler face and actuator face respectively.

For the unimorph actuator: we have

$$\begin{aligned} R_{pzt} &= \frac{L}{k_{pzt} S_{pzt}}, & R_{np} &= \frac{L}{k_{np} S_{np}}, & R_{va1} &= \frac{2}{h_{air} P_{act} L} \\ R_{va2} &= \frac{2}{h_{air} S_{act}}, & \rho_{pzt} C_{ppzt} S_{pzt} L, & C_{np} &= \frac{\rho_{np} C_{pcop} S_{np} L}{2} \\ R_{va1//2} &= \frac{R_{va1} R_{va2}}{(R_{va1} + R_{va2})}, & C_{act} &= C_{pzt} + C_{np} \end{aligned} \quad (2.11)$$

where k_{pzt} and k_{np} are the thermal conductivities, C_{ppzt} and C_{np} the heat capacities, ρ_{pzt} and ρ_{np} the densities of piezoelectric material and of the passive material respectively. On

the other hand, $S_{pzt} = e_{pzt}l$ and $S_{np} = e_{np}l$ are the sections of the piezolayer and the passive layer respectively. Finally, $P_{act} = 2(l + e)$ and $S_{act} = S_{pzt} + S_{np} = el$ are the perimeter and cross-section of the actuator. The thickness of the piezolayer is given by e_{pzt} and that of the passive layer by e_{np} . The total thickness is $e = e_{pzt} + e_{np}$. l and L are the width and the length of the actuator.

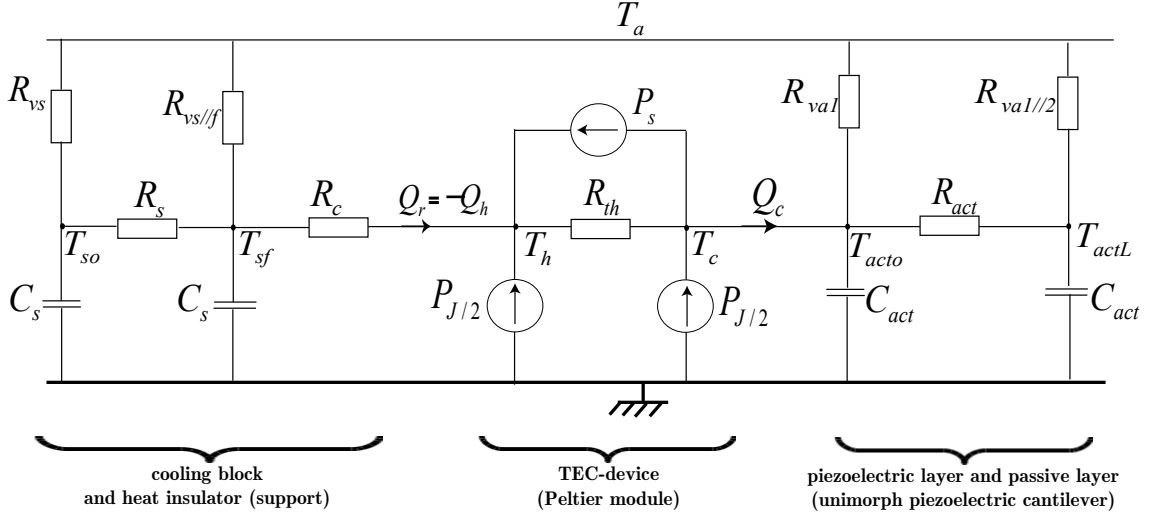


Figure 2.7: Thermal network of the whole hybrid thermopiezoelectric actuator.

Applying Kirchhoff laws to the network of Fig. 2.7, we obtain four governing equations that provide the evolution of the temperature T versus the applied input control current i . Regarding the thermomechanical relation $\Gamma_T(T(s))$, it is shown that a polynomial expression is precise enough for this actuator: $\Gamma_T(T(s)) = \sum_{i=1}^{n_{pt}} a_i(T(s))^i$, where a_i are parameters identified by least square optimization and n_{pt} is the degree of the polynomial. Concerning the thermomechanical dynamic part $D_T(s)$ in Eq. (2.9), it is not easy to characterize and to identify. Also it is very rapid compared with the electrothermal dynamics described by the four governing equations. Thus, $D_T(s)$ can be neglected ($D_T(s) = 1, \forall s$) in the model. Accounting these different remarks, we yield the whole model of the hybrid thermopiezoelectric actuator:

$$\left\{ \begin{array}{l} \frac{dT_{so}}{dt} = \frac{1}{\tau_s} T_{sf} - \frac{b_{so}}{\tau_s} T_{so} + \frac{1}{\tau_{vs}} T_a \\ \frac{dT_{sf}}{dt} = \frac{1}{\tau_s} T_{so} - \frac{c_{sf}}{\tau_{vs//f}} T_{sf} - \frac{c_{acto}}{\tau_{vs//f}} T_{acto} - \frac{c_{ps}}{\tau_{vs//f}} T_{acto} i - \frac{c_{j/2}}{\tau_{vs//f}} i^2 + \frac{1}{\tau_{vs//f}} T_a \\ \frac{dT_{acto}}{dt} = \frac{1}{\tau_{act}} T - \frac{d_{acto}}{\tau_{rva1}} T_{acto} + \frac{d_{sf}}{\tau_{rva1}} T_{sf} - \frac{d_{ps}}{\tau_{rva1}} T_{acto} i + \frac{d_{j/2}}{\tau_{rva1}} i^2 + \frac{1}{\tau_{rva1}} T_a \\ \frac{dT}{dt} = \frac{1}{\tau_{act}} T_{act0} - \frac{e}{\tau_{rva1//2}} T + \frac{1}{\tau_{rva1//2}} T_a \\ \delta(s) = \Gamma(u(s)) D(s) + C_{creep}(u(s), s) + \sum_{i=1}^{n_{pt}} a_i (T(s))^i \end{array} \right. \quad (2.12)$$

with, for the first equation

$$\tau_s = R_s C_s, \quad \tau_{vs} = R_{vs} C_s, \quad b_{so} = \frac{(R_{vs} + R_s)}{R_{vs}} \quad (2.13)$$

for the second equation

$$\begin{aligned} \tau_{vs//f} &= R_{vs//f} C_s \\ c_{sf} &= \left(\frac{R_{vs//f}}{(R_{th} + R_c)} + \frac{R_{vs//f}}{R_s} + 1 \right) \\ c_{acto} &= \left(\frac{R_{vs//f} R_c}{R_{th}(R_{th} + R_c)} - \frac{R_{vs//f}}{R_{th}} \right) \\ c_{ps} &= \alpha \left(\frac{R_{vs//f} R_c}{(R_{th} + R_c)} - R_{vs//f} \right) \\ c_{pj/2} &= \frac{R_p}{2} \left(\frac{R_{vs//f} R_c}{(R_{th} + R_c)} - R_{vs//f} \right) \end{aligned} \quad (2.14)$$

for the third equation

$$\begin{aligned} \tau_{act} &= R_{act} C_{act}, \quad \tau_{rva1} = R_{rva1} C_{act} \\ d_{acto} &= \left(\frac{R_{rva1}}{R_{act}} + \frac{R_{rva1}}{R_{th}} - \frac{R_{rva1} R_c}{R_{th}(R_{th} + R_c)} + 1 \right) \\ d_{sf} &= \frac{R_{rva1}}{(R_{th} + R_c)}, \quad d_{ps} = \alpha \left(R_{rva1} - \frac{R_{rva1} R_c}{(R_{th} + R_c)} \right) \\ d_{pj/2} &= \frac{R_p}{2} \left(R_{rva1} + \frac{R_{rva1} R_c}{(R_{th} + R_c)} \right) \end{aligned} \quad (2.15)$$

and for the fourth equation

$$\tau_{rva1//2} = R_{rva1//2} C_{act}, \quad e_{actL} = \left(1 + \frac{R_{rva1//2}}{R_{act}} \right) \quad (2.16)$$

2.3.3 Other leads to represent the behavior of hybrid actuators

More and more studies focus on the hybridization of two or several types of actuation to develop more and more performant miniaturized positioners. Their advantage is the performances gained from the combination of the different actuation types and which would not be possible if they were used individually. If the number of interconnected structures and the number of energy types for the actuation increase, the modeling may also increase in complexity.

An efficient way to tackle interconnected and multi-energy systems is the Bond-Graph tool [121]. This is an energetic approach to represent these systems in a graphical way and has been widely used for modeling, inverse design, structural analysis, or controller design in mechatronic systems [122–131]. Yet, this approach has been employed to represent the behavior of piezoelectric tube scanners [132]. The application of Bond-Graph to more complex and multi-energy miniaturized systems like hybrid precise positioners will bring simplicity in the representation of their behaviors, to perform structural analysis, or to synthesize controllers.

2.3.4 Acknowledgments

The works carried out here were during the postdoctoral fellowship of Dr. Ioan Alexandru Ivan without whom these results would not be possible.

2.4 Parallel kinematic piezoelectric microrobot for laser phonomicrosurgery

In this section, we exploit the simple structure of piezoelectric cantilevers to develop a complex positioning system devoted to a medical application.

2.4.1 Context

Within the μ -RALP project [6], the redesign of the laser phonosurgery - i.e. surgery of the vocal folds with laser treatment (nowadays performed with the Da Vinci robot [133]) - is aimed in order to create an advanced augmented and ergonomic microsurgical system through research and development of real-time cancer tissue imaging, surgeon-machine interfaces, assistive teleoperation, intelligent (cognitive) safety systems, and augmented-reality. The research and development encompass new endoscopic tools and precision microrobotic end effectors which will allow relocating the laser actuator closer to the surgical site. The outcomes of the project will be improved quality, safety, and effectiveness in laser phonomicrosurgery, enabling total tumor removal with minimal damage to healthy tissue. Technologically, the principle of the system to be developed is represented in Fig. 2.8. A flexible endoscopy with laser fibers drops the laser beam from the external to in front of the larynx tissue (Fig. 2.8-a). A microrobot placed at the extremity of the endoscopy precisely orients the laser beam towards the vocal folds to be treated (Fig. 2.8-b). The endoscopy brings wirings and fibers for powering the microrobots, for the cameras that permit to see the surgery tasks and for the laser beams. The project rassembles several research institutes, universities and hospitals over Europe: IIT Genoa Italy, FEMTO-ST institute and University of Franche-Comté (UFC) at Besançon France, Leibniz Universität Hannover (LUH) Germany, University Hospital of Besançon (UHB) France and Università degli Studi di Genova (UNIGE) Italy. The contribution of the AS2M department of FEMTO-ST institute is double: 1) the development and the control of the microrobot for the laser orientation, 2) and the visual servoing control and the (semi)automation of the laser phonomicrosurgery. My involvement is related to the first contribution.

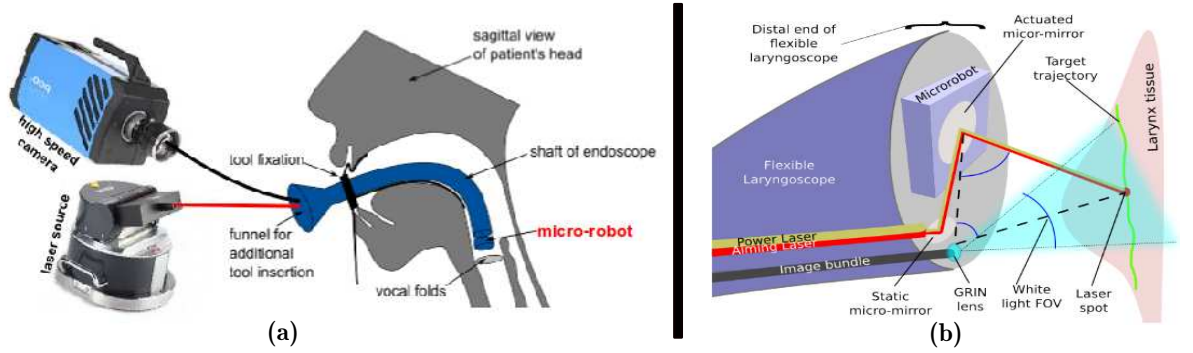


Figure 2.8: Objective of the μ -RALP project [6].

2.4.2 A high resolution, high bandwidth, and high range 2-DOF microrobot

Laser surgery is a delicate task that requires high safety. Different exchanges between the medical doctors and the partners of the μ -RALP project lead to the conclusion that for the phonosurgery aimed, the microrobot that will be employed to precisely orient the laser beams should meet at least the following performances.

- ⇒ A minimum number of two degrees of freedom (2-DOF) is required: orientation about two axes.
- ⇒ For an ergonomic point of view and due to the space constraint, the maximal dimensions allowed for the microrobot is $10\text{mm} \times 10\text{mm} \times 10\text{mm}$.
- ⇒ The resolution of the laser scanning at the surface of the larynx tissue should be better than $100\mu\text{m}$. Since the microrobot is placed at 20mm distance from the tissue, the resolution required from the microrobot is better than 5mrad (0.28°).
- ⇒ To cover the surfaces to be treated, the required minimal scanning angle from the microrobot is $\pm 13^\circ$ for each angle θ_1 and θ_2 .
- ⇒ Finally, to ensure a high safety of the laser treatment and a convenient time of scanning, the specified minimal bandwidth of the microrobot is of 200Hz .

The development of miniaturized structures with 2-DOF angular motions capabilities have raised many research. Their expected end-uses include projectors, imaging technologies like optical coherence tomography (OCT) and scanning in medical applications. Sometimes called microscanners, different actuation principles have been investigated for them: electrostatic [134–137], magnetic [138], electrothermal [2–4; 139–142], and piezoelectric [98–100; 143–146]. A more thorough state of the art on MEMS scanners has been submitted and is under review⁴. These realised technologies permitted to attain high range (mostly the electrostatic and the electrothermal based scanners) or high bandwidth (mostly piezoelectric based scanners) at a very miniaturized volume, but not both performances simultaneously and thus cannot be

⁴"A review on MEMS scanners: Eakkachai Ton Pengwang, Kanty Rabenorosoa, Micky Rakotondrabe, Nicolas Andreff, "Scanning micromirror platform based on MEMS technology for medical applications", submitted at IEEE Journal of MEMS, under review since june 2014.

employed for the phonomicrosurgery [IT6]. The challenge posed in the development of the microrobot here is that all performances must be satisfied in order to ensure the requirements of the phonomicrosurgery: high range, high bandwidth high resolution and compact sizes.

To reach the sever specifications, we have proposed a smart combination of five technologies [WT14]:

- 1) employing a set of piezoelectric cantilever actuators to generate high resolution and high bandwidth movements,
- 2) exploiting the levers principle to amplify the movements of the actuators and thus to generate a high range of displacements,
- 3) utilizing the parallel kinematic scheme to get a compact size of the structure and to maintain the high bandwidth from the actuators,
- 4) adapting the agile-eye kinematics to transform the linear motions of the actuators into 2-DOF angular motion. The agile-eye kinematics, developed by Gosselin et al. [147–149], has been developed for classically sized systems and different versions of structures have been realised. The objective of this kinematics is to create several angular motions (tilt and ball-joint) in a compact version and to permit a high speed scanning. These two advantages of the kinematics are very well suited to our need,
- 5) and finally applying the SCM (smart composites microstructures) technology to fabricate the whole structure. The SCM technology [150; 151] is a technology of fabrication of small structures developed at Harvard (Robert J. Wood) for the fabrication of bio-inspired and flying microrobots. It consists in piezoelectric materials to actuate, carbon fibers to rigidify and polyethylene terephthalate (PET) polymers to create joints in the miniaturized structures. An advantage of the technology is the relatively ease of fabrication: the structure is first micromachined in planar, and then folded to get the final 3-DOF shape.

The proposed design is composed of two parts:

The upper part is composed of an orientable platform for the laser beams reflection, one fixed leg attached to the basis (support) and two movable legs (Fig. 2.9-a). This orientable platform is an adaptation of the agile-eye kinematics. The orientation of the platform about the axis u or about the axis v is obtained thanks to the vertical movement of the two legs. To avoid the blocking of the mechanism, different ball joints have been added in the upper part.

The lower part is composed of two actuated arms (Fig. 2.9-b). The vertical movement at the extremity of each arm is employed to actuate the upper part. Each arm is composed of three redundant piezoelectric cantilever actuators. In addition, a lever-mechanism is introduced in the structure to amplify the actuators movements. Therefore, for each arm, the final vertical motion transmitted to the leg is a superposition of the amplified movements from the three actuators.

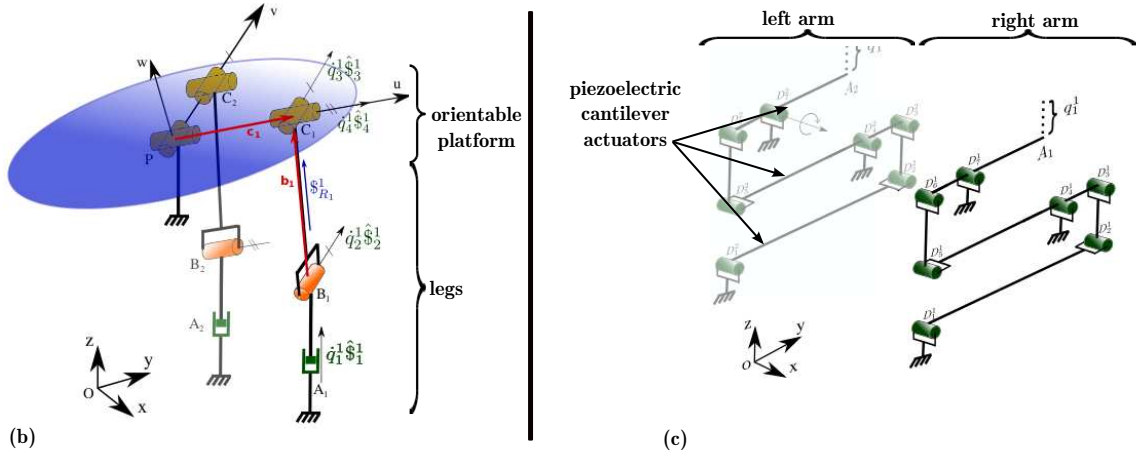


Figure 2.9: Principle of the μ PIBOT. (a): CAD-design. (b): the upper part (c): the lower part.

Fig. 2.10-a figures the CAD-design of the proposed high resolution, high range and high bandwidth 2-DOF piezoelectric microrobot, called μ PIBOT. Fig. 2.10-b shows the different elements of the lower parts: the piezoelectric cantilevers actuators, the levers and the support. Fig. 2.10-c shows the arms (piezoelectric actuator - lever base). The assembled lower part is shown in Fig. 2.10-d whilst the upper part is shown in Fig. 2.10-e.

The kinematics and the performances of the developed microrobot are unique. Sergio Lescano, who is the advised PhD student working on this novel development, expects to found a company devoted to the development of high performances scanners. The expected applications are wider than the medical domain. The submission of a patent is now under preparation and a *maturation*-project is expected to be launched in 2015 in order to prepare the company creation.

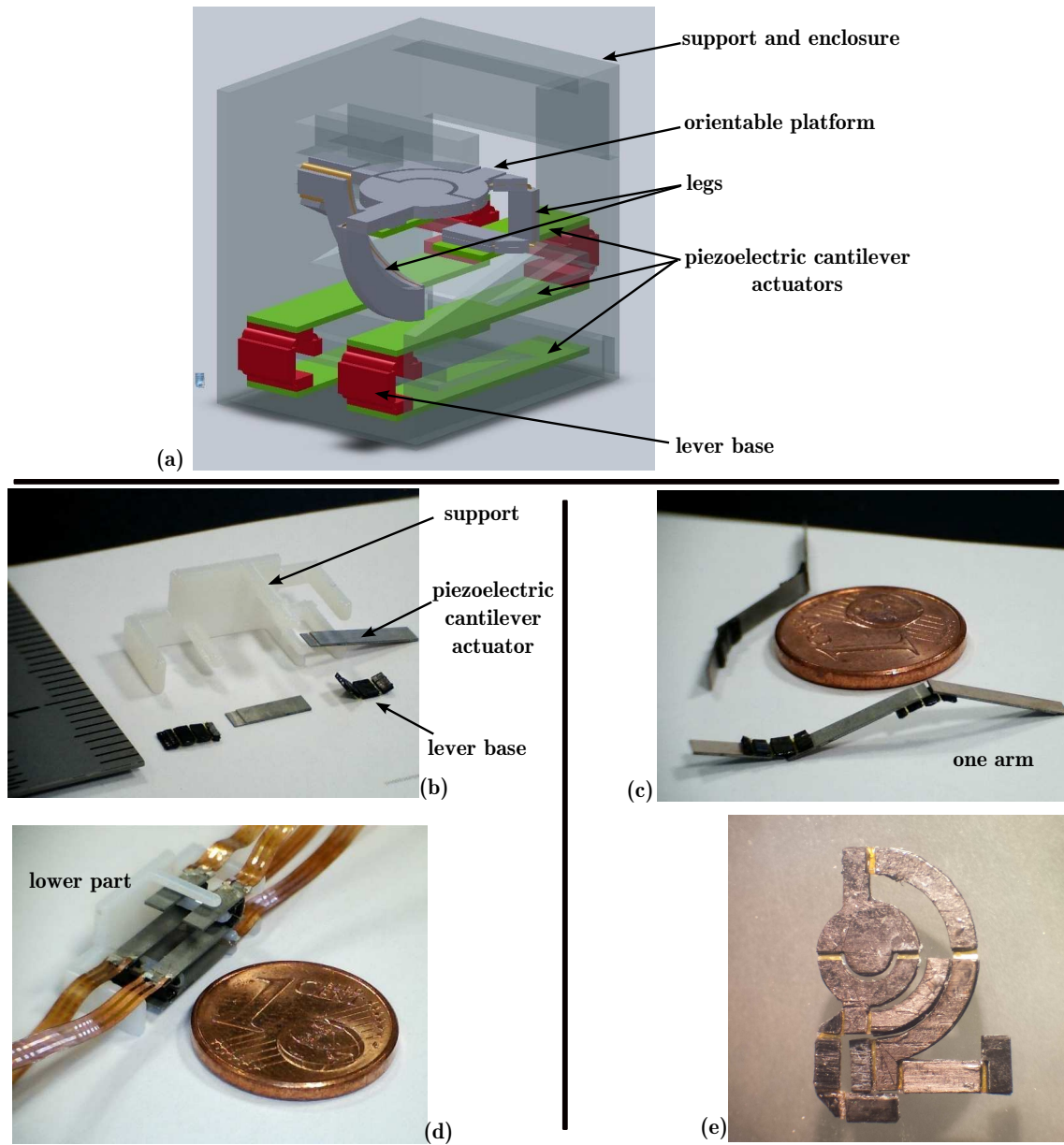


Figure 2.10: The μ PIBOT. (a): CAD-design. (b): the components of the lower part. (c): the arms of the lower parts. (d): the lower part. (e): the unfolded upper part.

2.4.3 A macro version of the robot

For the following reasons, we decided to develop a larger version of the 2-DOF microrobot:

- to duplicate the novel kinematics in large sizes for a more visual effect,

- to study the modeling and the control of the novel kinematics,
- and to further create a benchmark for teaching labs.

Ten times larger than the μ PIBOT, the macro version is based on piezoelectric stack actuators which possess high stiffness and high actuation forces. Based on aluminum material, the structure of the robot was machined with electro discharge technique. Fig. 2.11 pictures the fabricated robot. Preliminary experimental characterization demonstrates the efficiency of the kinematics and the efficiency of the amplification mechanism.

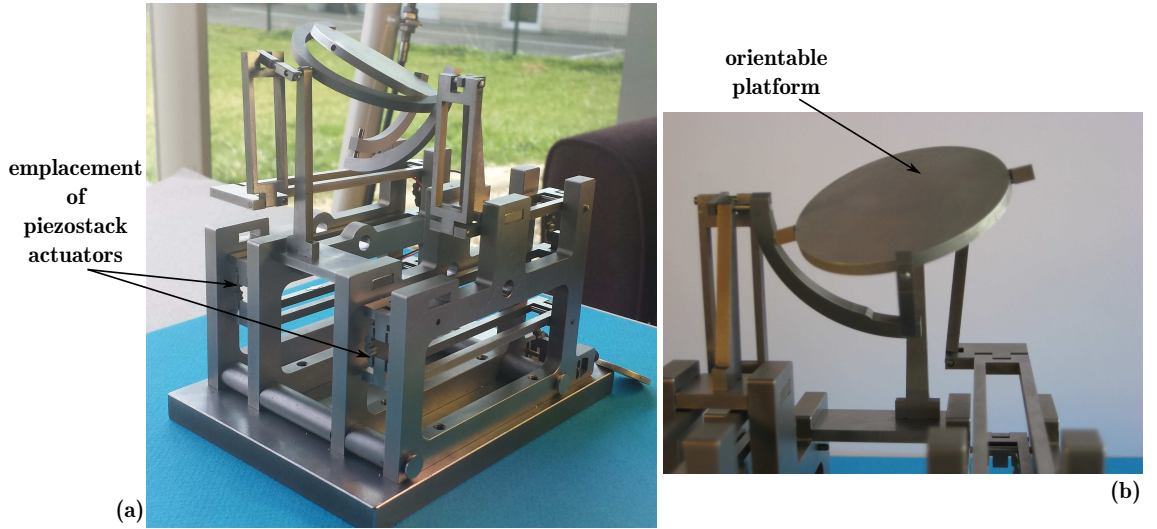


Figure 2.11: The macro version of the μ PIBOT.

2.4.4 Perspectives

A kinematic model of the microrobot has been developed in [C45]. Combined with the interval analysis, the kinematic model permitted to estimate the error of orientation at the platform *versus* the eventual error quantified in the arms and in the joints due to the microfabrication limitation⁵. Due to the intention to file a patent and to create a company, several developed studies relative to the novel microrobot have not been published nor submitted. With regards to the control, we have proposed a technique based on the standard H_∞ method. We show that this technique can reduce the lightly damped vibrations of the structure caused by the piezoelectric cantilever actuators, permits to reach an accuracy of scanning and to be robust enough face to unmodeled dynamics of the microrobot.

Another important perspective in designing microrobots is the materials themselves. PZT piezoelectric materials, utilized in our case, possess lead which is not generally desired in med-

⁵Error quantization via interval tools: submitted at IEEE ICRA conference 2015, S. Lescano, M. Rakoton-drabe, N. Andreff, "Precision Prediction Using Interval Exponential Mapping of a Parallel Kinematic Smart Composite Microstructure".

ical applications. In the μ RALP project, it is expected that the microrobot is well sheltered to avoid the exposure of the lead to the in-vivo environment. Though, studying other piezoelectric materials for the development of the microrobots should also be investigated. Competitive materials to which we expect to focus are lithium niobate. Commercially available at accessible prices, they can provide high deformation and high stiffness that can compete those of PZT if well treated.

2.4.5 Acknowledgments

The development, modeling and control of the microrobot and of its macro version are within the PhD works of Sergio Lescano and the internships of Erwann Dupont and Ismaël Ahmed Ismaël. A creation of a company related to these works is expected after the PhD of Sergio. Fully supported by the AS2M department and by I myself, Sergio is the leader of this company.

2.5 Cartesian piezoelectric microstructure

In the previous section, we show that simple piezoelectric cantilever actuators can be exploited to develop more complex structures. In this section, we still exploit piezoelectric cantilever actuators to develop complex positioning systems but with more reduced sizes (towards MEMS). A cartesian structure from which we expect to have xyz displacements is developed. The widely available and low costs PZT piezoelectric materials are still used for the actuation. Additionally to the challenge posed by the kinematics to be studied in order to have large range of displacement, another challenge is the fabrication itself. The whole structure, including the support, should be less than $10mm \times 10mm$ in surface. With such dimensions, microfabrication (in clean room) technology should be utilized. However, though many microfabrication processes are usual and well settled in the literature and at the MIMENTO center⁶ of the FEMTO-ST Institute, but the processes of microfabrication of bulk PZT materials is relatively new.

2.5.1 Microfabrication of PZT materials

Two fashions exist to fabricate PZT based systems: 1) the systems are fabricated with PZT bulk materials, 2) and the systems are based on PZT thin films.

PZT bulk materials are commercially available at low prices. They have a high coupling factor and can offer a high resolution, a high bandwidth and a high stiffness making them well adapted to actuation. The available thicknesses range between $100\mu m$ to several hundreds of micrometers. They are widely utilized to fabricate structures and systems without thinning their thicknesses. The main fabrication steps are: bonding the PZT bulk with passive materials (nickel, chrome, copper, ...) and dicing with saws. The fabrication is not in clean room. A main limitation of this technology is the minimal thickness possible which cannot go under $100\mu m$. The large thicknesses of the actuators are such that high voltages are required to

⁶MIMENTO is the center of microfabrication of FEMTO-ST Institute. It is one of the six great centers of technologies in France.

obtain a convenient electrical field and thus a convenient displacement. To maximize the displacements, the length of the actuator is often increased resulting in quite bulky devices (tens of mm long cantilevers). Examples of cantilevers structures based on PZT bulks materials are the scanners in atomic force microscopes [13–18], and the microgrippers in micromanipulation and microassembly [59–67; 83–86][PT1][J14][C11].

In thin films approach, the principle is based on the deposition of thin layers of piezoelectric materials with thicknesses less than $100nm$. The deposition step is repeated until the obtention of the specified and final thickness which does not generally exceed $10\mu m$. This approach enables the fabrication of very small actuators (often much smaller than a mm). In PZT materials, only PZT sol-gel have been employed [21; 22]. Other than PZT, aluminum nitride (AlN) piezoelectric material is the most employed [98–100; 143–146]. Because the thicknesses are very small, high electrical fields are obtained for the same range of driving voltages as in bulk. Consequently, the fabricated actuators can provide very large displacements (hundreds of μm) with low voltages. Nevertheless, the stiffness obtained with this approach is low making it not efficient for actuation that requires high torque. Furthermore, the dynamics of the structures are low (typically less than a kHz).

These two main approaches enable the fabrication of performant actuators but with very different features [152]. There is therefore an interest to succeed in the fabrication of intermediate structures, called "thick films", in order to benefit from the advantages of both: large displacements with low voltage, small sizes, high stiffness and high dynamics. The thicknesses in this intermediate approach range between $10\mu m$ and about $100\mu m$. Fig. 2.12 summarizes the three approaches where in parenthesis are indicated the main steps of the fabrication processes. Actually, "thick films" technologies have been realised recently to develop very miniaturized PZT structures [100; 153–155]. The process of microfabrication, in clean room, is based on bonding and thinning and was performed at elevated temperature. This high temperature process may cause a reduction of the mechanical and piezoelectric properties of the PZT. In the approach we have proposed and we report here, the deal consists in processing "thick films" PZT at ambient temperature which therefore limits the reduction of the properties of the piezoelectric materials. The microfabrication is roughly composed of the following steps: i) deposition of the PZT bulk on the silicon wafer thanks to gold-bonding and pulverization technique at low temperature, ii) thinning the PZT bulk with polishing technique, iii) etching the PZT layer with DRIE STS (deep reactive ion etching - surface technology systems) technique, iv) and etching the silicon with DRIE technique.

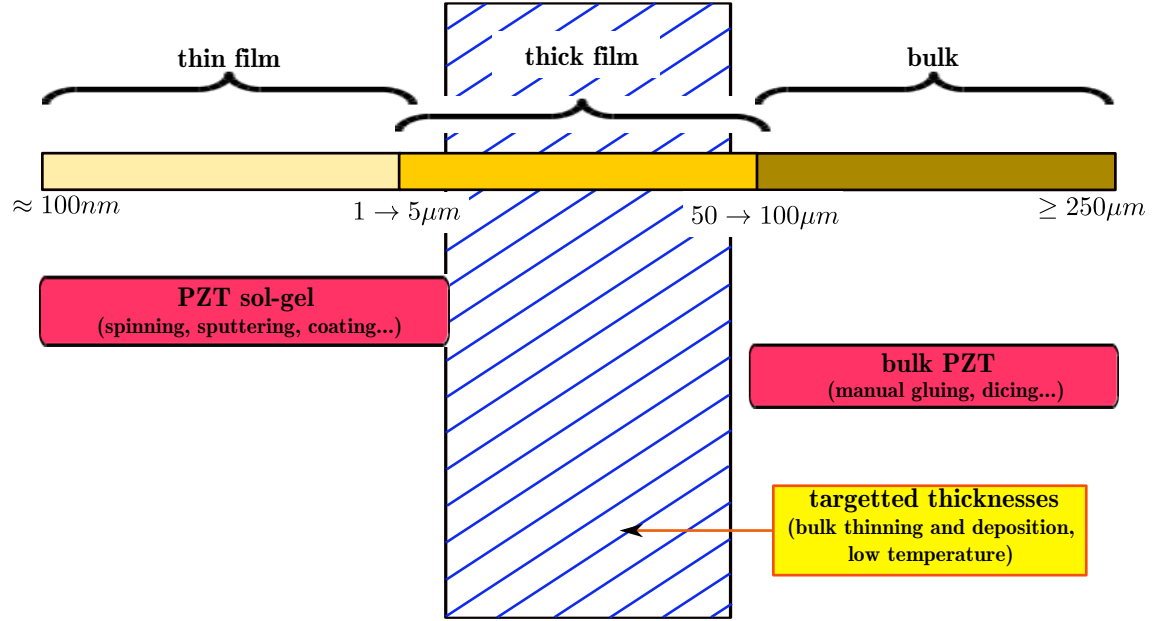


Figure 2.12: Three approaches for treating PZT materials.

2.5.2 The designed and microfabricated microstructure

Fig. 2.13-a depicts the proposed kinematics of the cartesian microstructure. It is composed of piezoelectric cantilever actuators and of the movable table which can be actuated along three directions (xyz axes). The expected range of displacement from the microstructure is of $\pm 20\mu m$ in-plane and of $\pm 30\mu m$ out-of-plane. The whole microstructure is fabricated using the "thick film" process previously presented.

The piezoelectric cantilever actuators are unimorph⁷ and can bend along two axes: in-plane and out-of-plane. The second degree of freedom (in-plane) is obtained thanks to a judicious set of electrodes on the actuator [62]. Eight of the piezoelectric actuators are spread by pair around the movable table. A spring-like cantilever connects each actuator with the table. The springs also serve as guide for the xyz movement for the minimization of the cross-couplings between the axes.

In order to validate first the process of fabrication, we have developed simple structures: unimorph piezocantilever actuators with different dimensions (length, width and thicknesses). The results are depicted in Fig. 2.13-b and the preliminary characterization shows that the performances predicted by the theoretical model were reached⁸ Finally, Fig. 2.13-c depicts a

⁷Unimorph piezoelectric cantilever actuators: see Appendix C.

⁸A paper has been submitted at the IOP Journal of Micromechanics and Microengineering in August 2014. A revision has been resubmitted. The paper presents the low-temperature microfabrication technology and the examples of realization (cantilevers).

photo of the first fabrication set of the cartesian microstructure. This first set contains many minor defects as it is from the first trial of the new process. Other fabrications are ongoing and from which experimental characterization as well as controll will be carried out.

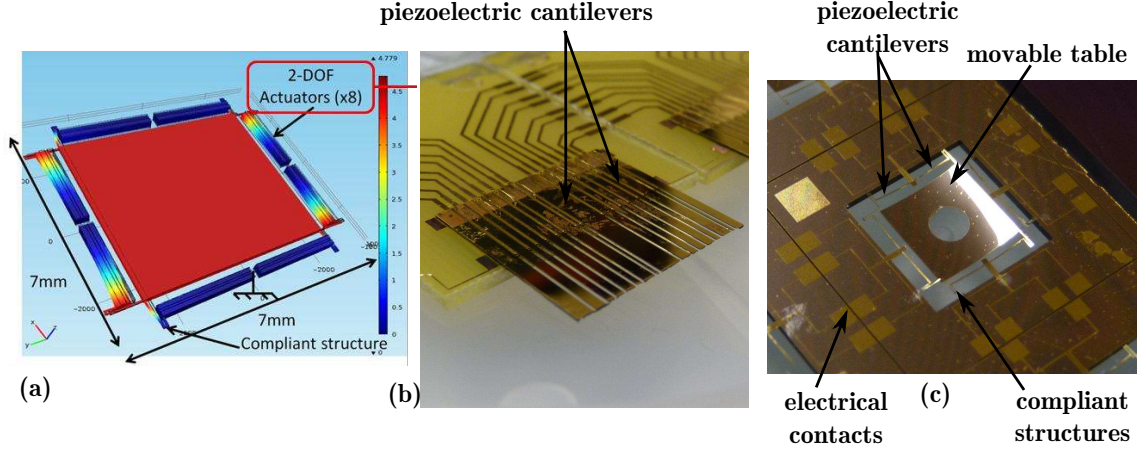


Figure 2.13: (a): CAD-design of the cartesian microstructure. (b): fabricated piezoelectric cantilevers with the "thick film" approach. (c): fabricated cartesian microstructure.

2.5.3 Perspectives

The design of smaller and smaller (towards MEMS) and complex structured PZT bulks based systems has been started through this work. PZT bulk materials are widely available at low costs and are good candidates for the development of highly performant actuators. However, microfabrication of PZT bulks were limited and did not permit to go further on the miniaturization. This technological barrier has been bypassed here which opens many possibilities in the development of highly performant actuated piezoelectric MEMS with reasonable costs.

2.5.4 Acknowledgments

The works here were carried out within the successive postdoctoral fellowships of Dr. Alex Bienaimé and Dr. Vincent Chalvet. Investigation on the miniaturization of PZT devices with sol-gel has also been started within the internships of Adiasa Adiasa and Fadwa Houssali. Finally parallel works regarding the miniaturization of PZT bulks combined with electrostatic principle have been carried within the postdoctoral fellowship of Dr. Eakkachai Ton Pengwang.

2.6 Design methodology for piezoelectric cantilever systems using interval tools

This section proposes a methodology to design actuated piezoelectric microsystems. The target is to develop the systems from *a priori* imposed desired performances and can be very

helpful to design systems for precise and high dynamics positioning.

Generally, there exist two methods to design and to develop piezoelectric systems. In the first, a sketch of the structure is yielded manually and finite element methods (FEM) are afterwards employed to verify its performances and to eventually improve or optimize it before the fabrication [60; 67; 84–91; 96–100; 140; 145; 146; 153–155][PT1][J10][J9]. This method is widely used, easy to apply and finely works with both simple and complex structures. If the structure is simple (for example cantilevers), a comparison between the FEM simulation with the theoretical model can also be effectuated. However, the method cannot be used for analytical design where desired performances are imposed *a priori* and the structure is analytically designed from them.

In the second method, the deal consists in designing the structures optimally [64–66; 156; 157]. Based on optimal control theory tools (such as observability and controllability gramians), the method can provide optimal locations of piezoelectric actuators and sensors in a wire mesh. This method is very interesting and efficient for treillis structures based on piezoelectric cantilevers.

In our works, we propose to design piezoelectric actuators by using interval tools. Interval techniques and related arithmetics have been used in several applications in the past, except for the design of mechanical systems (to our knowledge) as we intend to propose in this work. The idea of using intervals for calculation was proposed in 1924 by Burkill and in 1931 by Young. But, interval arithmetics became really popular just after the appearance of the R.E. Moore’s book in 1966 [158]. This later provided a general method and some formalization of intervals and related arithmetics. Since, there are several applications of intervals, for examples:

- robotics, see [159–165] and references herein,
- microrobotics [166; 167][C44],
- diagnosis and fault detection, see [168–170] and references herein,
- control theory which includes: uncertainties modeling, guaranteed estimation, stability analysis, performances analysis, controllers synthesis, see Section 3.3 for the survey.

By employing interval tools to design the piezoelectric actuators and systems, we benefit from two distinguished advantages:

- it is guaranteed that the designed structure will provide the desired performances if solutions exist. This advantage is inherited from the certification property in interval tools,
- and the method is not limited to piezoelectric cantilever actuators. It is applicable to any other structures and systems, subjected that the analytical models are available. A more complex model may yield however a more complex calculation.

To do so, two techniques of design are proposed: 1) the performances improvement of an existing system by redesigning this, 2) and the design of a new system by exploiting the performances inclusion theorem (PIT) developed in [C28].

2.6.1 Redesign of piezoelectric actuators

We demonstrate in this section that, by using interval techniques, it is possible to redesign an existing actuated system in order to obtain a new actuator with better performances and with more optimized structures, for instance with less dimensions. The method has been published at [J21]. As illustrative example, we present the redesign of unimorph piezoelectric cantilever actuators. The target is to calculate the dimensions of a new unimorph such that its output deflection δ_d and its first resonant frequency f_{1d} are higher than those (respectively denoted δ and f_1) of an existing unimorph actuator. The additional constraint is that the length L_d and the total thickness l_d of the desired actuator are less than the initial one, see Fig. 2.13.

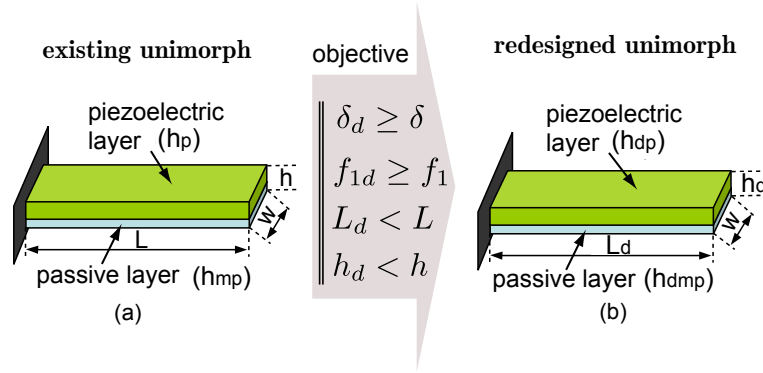


Figure 2.14: Redesign of a unimorph piezoelectric actuator.

The principle is to write the performances objectives based on the model of the desired actuator and on the model of the initial actuator. Taking the model (static and dynamic modeling) of unimorph piezocantilevers as in Section C.3), the redesign problem can be transcribed into the following mathematical problem.

Problem: Find h_{dp} and h_{dmp} such that:

$$\left\{ \begin{array}{l} \frac{m_{piezo}(h_{dp}, h_{dmp}) \left(\frac{L}{\alpha}\right)^2}{2C(h_{dp}, h_{dmp})} u \geq \frac{m_{piezo}(h_p, h_{mp}) L^2}{2C(h_p, h_{mp})} u \\ \frac{(1.8751)^2}{2\pi \left(\frac{L}{\alpha}\right)^2} \sqrt{\frac{C(h_{dp}, h_{dmp})}{w(\rho_{mp} h_{dmp} + \rho_p h_{dp})}} \geq \frac{(1.8751)^2}{2\pi L^2} \sqrt{\frac{C(h_p, h_{mp})}{w(\rho_{mp} h_{mp} + \rho_p h_p)}} \\ h_{dp} + h_{dmp} \leq h \end{array} \right. \quad (2.17)$$

which are equivalent to the following inequalities:

$$\begin{cases} \frac{m_{piezo}(h_{dp}, h_{dmp})}{\alpha^2 C(h_{dp}, h_{dmp})} \geq \frac{m_{piezo}(h_p, h_{mp})}{C(h_p, h_{mp})} \\ \alpha^4 \frac{C(h_{dp}, h_{dmp})}{w(\rho_{mp} h_{dmp} + \rho_p h_{dp})} \geq \frac{C(h_p, h_{mp})}{w(\rho_{mp} h_{mp} + \rho_p h_p)} \\ h_{dp} + h_{dmp} \leq h \end{cases} \quad (2.18)$$

where the dimensions are indicated in Fig. 2.13.

Let $[\theta] = [[h_{dp}], [h_{dmp}]]$ be a box (vector of intervals) that contains the interval parameters $[h_{dp}]$ and $[h_{dmp}]$ which are the thicknesses that satisfy the inequalities InEq. (2.18). So, the problem, when formulated with intervals, consists in finding the suitable values of $[\theta]$ such that:

$$\Theta := \{\theta \in \mathbf{D} \mid [H](\theta) \subseteq [\mathbf{Y}]\} \quad (2.19)$$

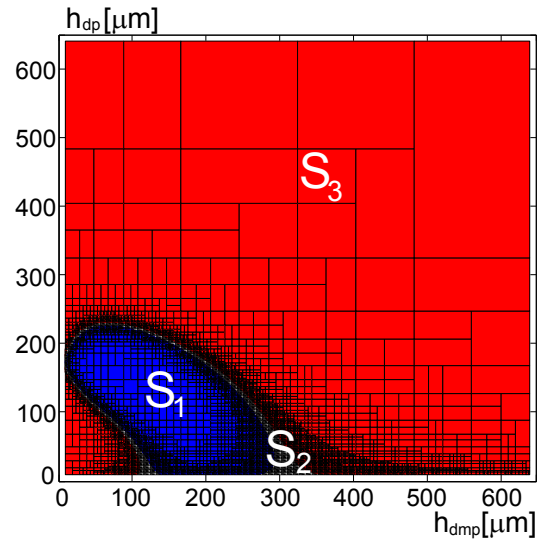
where \mathbf{D} is the domain of definition of θ . $[H](\theta)$ and $[\mathbf{Y}]$ are defined as follows:

$$[H](\theta) = \begin{pmatrix} \frac{m_{piezo}([h_{dp}], [h_{dmp}])}{\alpha^2 C([h_{dp}], [h_{dmp}])} - \frac{m_{piezo}(h_p, h_{mp})}{C(h_p, h_{mp})} \\ \frac{\alpha^4 C([h_{dp}], [h_{dmp}])}{(\rho_{mp}[h_{dmp}] + \rho_p[h_{dp}])} - \frac{C(h_p, h_{mp})}{(\rho_{mp}h_{mp} + \rho_ph_p)} \\ h - [h_{dp}] - [h_{dmp}] \end{pmatrix} \quad (2.20)$$

and

$$[\mathbf{Y}] = \begin{pmatrix} [0, +\infty] \\ [0, +\infty] \\ [0, +\infty] \end{pmatrix} \quad (2.21)$$

The problem of finding the set parameter of $[\theta]$ that ensures InEq. (2.18) is a set-inversion problem and can be solved using interval techniques. The set-inversion operation consists to compute the reciprocal image of a compact set called subpaving. For instance, the set-inversion algorithm SIVIA (Set Inversion Algorithm Via Interval Analysis [171; 172]) allows to approximate with subpavings the set solution Θ described by the Problem. (2.19). This algorithm is presented in Section D.3. For instance, having given initial values of $[0, 650\mu m] \times [0, 650\mu m]$ to the set of $[\theta]$, and having applied the SIVIA algorithm, we obtain the subpavings



of Fig. 2.15. In this, S_1 is the set of $[\theta]$ that is guaranteed to satisfy the problem Problem. (2.19) and thus the objective in InEq. (2.18), S_3 is the set that is guaranteed to not satisfy the problem. The set S_2 corresponds to uncertain results. In the situation where we can not find a solution S_1 , it is suggested to recalculate the problem solution with the following modifications: shift the initial set values, or/and relax the specifications (desired performances) because they may be too severe. Any thicknesses h_{dp} and h_{dmp} of the piezoelectric layer and of the passive layer respectively inside S_1 are guaranteed to respect the conditions in InEq. (2.18), and therefore to satisfy the wanted performances.

2.6.2 Design of piezoelectric actuators with the performances inclusion theorem

The previous technique consisted in redesigning an existing actuator with intervals techniques. Here, we completely design the actuator based on the specified performances. For that, the performances inclusion theorem [C28], described in Section 3.3.1, is utilized. Without loss of generality, the illustrative example is the design of a piezoelectric cantilever actuator. The design methodology has been published in [BC8].

Consider some desired performances specified in the time domain or in the frequency domain. For example, in the time domain, these performances can be stated as: maximal response time, maximal overshoot and minimal range of displacement. It is generally possible to transcribe these performances into transfer function, in particular interval transfer function [J15]. For instance, let us consider the following second order interval transfer function as an example of transcription of the specifications:

$$[G_d](s) = \frac{[b_o]}{[a_2]s^2 + [a_1]s + 1} \quad (2.22)$$

where $[b_o][\frac{\mu m}{V}]$ is the desired gain which is based on the desired range of displacement, and $[a_2]$ and $[a_1]$ are function of the desired dynamics (transient part, overshoot, bandwidth...).

Consider now the model of the to be designed unimorph piezoelectric actuator by using the Ballas linear model in Section C.3:

$$G(s) = \frac{y(s)}{u(s)} = \frac{K}{\left(\frac{1}{w_n}\right)^2 s^2 + \frac{2\zeta}{w_n}s + 1} \quad (2.23)$$

where the static gain $K[\frac{\mu m}{V}]$ and the natural frequency $w_n[\frac{rad}{s}]$ are dependent on the geometrical and physical properties of the unimorph. The damping ratio ζ , for lightly damped oscillating structure, is very low and is only known experimentally.

If we admit that there is a set of dimensions of the unimorph that can provide the expected performances transcribed in Eq. (2.22), thus we can utilize an interval system to represent such set of unimorph:

$$[G](s) = \frac{[K]}{\frac{1}{[w_n]^2}s^2 + \frac{2\zeta}{[w_n]}s + 1} \quad (2.24)$$

where ζ is imposed to be point instead of interval for the sake of simplicity. The problem consists therefore in finding numerically the set of geometrical properties $[K]$ and $[w_n]$ of the set of unimorph that will satisfy the specifications. The performances inclusion theorem is proposed to formulate the problem:

Problem: Find L , h_{dp} and h_{dmp} such that:

$$\left\{ \begin{array}{l} [K]([L], [h_p], [h_{mp}]) \subseteq [b_o] \\ \frac{1}{[w_n]([L], [h_p], [h_{mp}])^2} \subseteq [a_2] \\ \frac{2\zeta}{[w_n]([L], [h_p], [h_{mp}])} \subseteq [a_1] \end{array} \right\} \Rightarrow [G](s) \subseteq [G_d](s) \quad (2.25)$$

The term $[G](s) \subseteq [G_d](s)$ means that the performances in the time-domain and in the frequency domain of $[G]$ (the set of fabricated actuators) will be bounded by the performances of the specified and desired models $[G_d]$. Once again, the problem is a set inversion problem and can be solved by using interval techniques to find the set solution of the length $[L]$, the piezolayer thickness $[h_p]$ and the passive layer thickness $[h_{mp}]$. Similarly to the first design technique, an initial box of $[L]$, $[h_p]$ and $[h_{mp}]$ is required here. If there is no solution found, the same remarks than previously also hold: shift the initial set values or/and relax the specifications (desired performances) because they may be too severe.

2.6.3 Perspectives

Interval techniques were proposed here to design piezoelectric cantilever actuators. Major advantages of the proposed methodology is the guarantee aspect: if solutions exist, the designed actuators will satisfy the specified and desired performances. The methodology, which is applicable to complex structures as long as the models are available, is very interesting to design systems where both the constraint on dimensions and the specified performances need to be satisfied. This is the case for miniaturized systems devoted to precise and high dynamics positioning.

2.6.4 Acknowledgments

The works regarding the interval techniques (design and control) were within the PhD subject of Sofiane Khadraoui (nowadays researcher at Texas A&M in Qatar).

2.7 Conclusions and perspectives

This chapter presented a great part of works regarding the modeling, the design and the development of piezoelectric systems and actuators carried out. Piezoelectric cantilever structure is the main basis. We demonstrated that this simple structure could be utilized to develop performant and complex structured piezoelectric systems. Regarding the modeling, we presented first the Ballas linear model of piezoelectric cantilevers. Although this model is widely employed, it is linear and thus can track only small deformation of the piezoelectric actuators. We extended the model into nonlinear which encompasses the hysteresis and the creep nonlinearities. Furthermore, the thermal effect has also been introduced in the model. The final model, presented in [Eq. \(2.8\)](#), is extensively exploited over the thesis.

The investigation on the development of smaller and smaller multi-degrees of freedom (multi-DOF) piezoelectric systems has been started. These multi-DOF systems are highly saleable in precise positioning that requires high dexterity like microassembly of 3D microstructures, or laser scanning for medical surgery. As we will see in [Section 6](#), they can also serve as interesting base for the development of highly sensitive and highly autonomous energy harvesters.

Chapter 3

Feedback control

In [chapter. 2](#), we presented the design, development and modeling of piezoelectric systems. In this chapter, we present their feedback control. Without loss of generality, only piezoelectric cantilevered structures will be treated in order to be consistent with the works carried out. Once again, interval techniques and related tools are proposed to calculate robust controllers and present interesting results. In particular, the Performances Inclusions Theorem yet used in [section. 2.6](#) are utilized. The main interest is that these techniques combined with classical control theory can provide low order and robust controllers that are well consistent with the expectation. Classical robust control techniques based on H_∞ are also used to design controllers for piezoelectric systems. In all of them, the outputs are both the displacement and the force signals. Along the presentation, the matter of control of multi-axes piezoelectric systems and the matter of more complex structures (microgrippers) are discussed. Finally, in the last section ([section. 3.5](#)), the control of the novel hybrid thermopiezoelectric actuators and microgripper will be presented.

Contents

3.1	Introduction	60
3.2	Classical robust control	62
3.2.1	Displacement modeling and control	63
3.2.2	Force modeling and control	66
3.2.3	Displacement and force control of piezoelectric microgrippers	68
3.2.4	Multivariable control of multi-axes piezoelectric actuators	69
3.2.5	Acknowledgements	71
3.3	Interval techniques combined with classical control theory	71
3.3.1	The Performances Inclusion Theorem (PIT)	72
3.3.2	Controllers design by using the PIT	73
3.3.3	H_∞ interval controllers synthesis	75
3.3.4	Robust performances analysis with interval techniques	77
3.3.5	General remarks	79
3.3.6	Acknowledgments	79

3.4	Feedforward-feedback control schemes	79
3.5	Control of hybrid thermopiezoelectric microgrippers	81
3.6	Conclusions and perspectives	83

3.1 Introduction

Piezoelectric microsystems and actuators are well appreciated for at least their high resolution, high bandwidth and high stiffness (for PZT bulk). However, they exhibit strong nonlinearities which are the hysteresis and the creep and most of them are typified by badly damped oscillation in their response to brusque input command. These latter characteristics compromise the final performances or even the stability of the microsystems and of the actuators. Furthermore, in many applications of precise positioning, due to the small sizes of the microsystems, they are very sensitive to any disturbances that would be negligible at classical scale. Finally, the small amplitudes of the signals and the very high resolution involved in these applications make a noise to signals ratio relatively high. It is therefore essential to control the microsystems with a judicious consideration of all these characteristics.

The litterature regarding the closed-loop control of piezoelectric actuators and systems is dense due to the large variety of these latters. For instance, as variety of systems, there are: piezoelectric cantilevered systems with bending functioning, piezoelectric stack based systems, stepper piezoelectric microrobots (inch-worm or stick-slip), piezoelectric sheets for damping in flexible structures, ultrasonic piezoelectric systems... Many of these systems are modeled and controlled with more or less consideration of the above mentionned properties and can share the methods of controllers synthesis or behaviors modeling; whilst other systems (like ultrasonic systems and stepper microrobots) have very different models and require devoted control techniques that cannot be applied to other systems. In this thesis, we are in concern with piezoelectric systems for precise and high dynamics positioning and which are based on piezoelectric cantilevers with tubular or rectangular section and stacks actuators. Generally speaking, the litterature can be splitted into the following main works.

Control of piezoelectric tube scanners in microscopy - The works here deal with the control of piezoelectric tubes (piezotube scanners or PTS) utilized as actuators in scanning probe microscopes (SPM). Vibration due to the high Q-factor of the actuator, hysteresis and creep nonlinearities are the main challenge to account for during the controllers synthesis. They highly limit the precision and the throughput speed of the surface scanning [173]. Several techniques - dealing with the nonlinearities alone, with the vibrations alone or with both - have been carried out. High gain and integral control techniques¹ [174; 175] are known to well delete the hysteresis and the creep which occur at low and very low frequencies, however they exhibit low stability margin at high frequencies. Therefore they cannot be utilized at high rate scanning. In fact, it is shown [176] that the closed-loop bandwidth that can be achieved by an integral controller for a PTS is less than $2w_r\zeta$, where w_r and ζ are the resonance frequency and

¹Integral control techniques include PI, PID, and all other schemes with integral action.

the damping constant of the PTS respectively. Since the damping constant of PTS is low, usually in the order of 0.01, the closed-loop bandwidth that can be achieved by using an integral controller is less than two percent of the first resonance frequency of the PTS [176]. Although, integral control techniques are widely utilized in commercial SPM because of their simplicity and ease of implementation [177; 178]. Negative imaginary (NI) damping techniques such as positive position feedback (PPF) controllers [179; 180], integral resonant controllers (IRC) [181] and resonant controllers (RC) [182; 183] have also been designed to suppress successfully the resonant frequencies of PTS. PPF and IRC are known as low pass controllers and then may suffer from low gain and low phase margins. In counterpart, RC are high pass controllers which may amplify the noise from the sensors, even if they introduce high gain and phase margins. Recently, a mixed NI and small-gain approach has been proposed [184], which was further extended into mixed NI, passivity and small-gain approach [185]. The technique permitted to provide a large damping of the first resonant frequency with a sufficient robustness against the changes in the plant models. Since most of the SPM applications utilize periodic motion (eg. raster pattern), repetitive control techniques (RC) have also been used [186; 187]. They are efficient to track periodic reference trajectories and/or to reject periodic disturbances. Finally, [188–191] use robust control techniques (H_∞ , ...) to improve the performances of the PTS of the SPM. It is worth to notice that feedforward-feedback control schemes have also been investigated in PTS actuators [191]. In general, a feedback augmented by a feedforward permits to increase the capacity of the closed-loop scheme relative to a feedback only scheme. For instance, the size of acceptable uncertainties by still maintaining the performances robustness increases when adding a feedforward to a feedback scheme [192].

Control of piezoelectric stacks based systems - Piezoelectric stacks have been utilized to develop platform and systems that requires large stiffness. Their principles are very different from piezoelectric cantilevers (PTS or multimorph) since the longitudinal deformation of the piezoelectric layers (d_{33} coefficient) is used instead of the transversal deformation (d_{31}). Although, many control techniques for stacks actuators are exploitable for cantilevers. They include state-feedback techniques [193], adaptive techniques [194], classical robust control techniques (H_∞) [195] and sliding mode techniques [196; 197].

Control of multimorph piezoelectric based systems - The main works carried out in this thesis deal with multilayered piezoelectric cantilevers with rectangular structures (that we simply call piezoelectric cantilevers or multilayered piezoelectric cantilevers or multimorph piezoelectric cantilevers). Relative to PTS, the bending-to-length ratio ($\frac{\delta}{L}$) is high in these piezoelectric cantilevers. Approximately, we have up to $\frac{\delta}{L} = \frac{100\mu m}{15mm} = 6.67[\frac{\mu m}{mm}]$ in classical multimorph whilst $\frac{\delta}{L} = \frac{35\mu m}{30mm} = 1.17[\frac{\mu m}{mm}]$ in classical PTS when a voltage of 150V is applied. This high ratio yields larger hysteresis amplitude and creep amplitude in multimorph piezoelectric cantilevers. Furthermore, the vibrations found in these latters are more important when compared to the vibrations in piezoelectric stacks. Consequently, unless working at low electrical field, at low deformation and at slow input command, the nonlinearities and the vibrations in multimorph piezoelectric cantilevers are very strong and should definitely be considered in the modeling and in the control. Another essential point in micromanipulation and

microassembly where these actuators are widely employed is the force control, additionally to the displacement control. Controlling the force permits to avoid the destruction of the actuator itself or of the manipulated object. The literature shows however that many of the control techniques are partial: only the displacement or only the force is considered. For instance, in [83], the force control of one piezoelectric actuator of a microgripper has been investigated by utilizing strain gages sensors for the feedback and a proportional-integral as control scheme. In [59], the displacement of one unimorph piezoelectric cantilever of a microgripper has been controlled with a PID first and then with a state-feedback with integral action. In the two papers [59; 83], the integral action allowed to have a high gain at low frequency and thus to reduce the effect of the hysteresis and of the creep in the tracking precision. Recently, the simultaneous control of the force and position in a piezoelectric microgripper has been investigated [198]. While one actuator was controlled on force with a PID, the other actuator was controlled on position with a sliding mode scheme.

Comparatively to this literature, the main direction of the works reported in this thesis deals with the feedback control of (multimorph) piezoelectric cantilevers. The works focus on both force and position signals. As we shall describe in the next sections, contrary to the works in [83] [59] [198], we propose methodologies that account for the strong hysteresis and creep nonlinearities and for the badly damped vibration. Furthermore, we also account for the models uncertainties of the piezoelectric systems. These models uncertainties are due to the parameters variation during the functioning, to the difficulty to obtain precise measurement and to the high sensitivity of the systems to the environment in general (see chapter. 1). Due to these facts, robust control techniques are the most adapted.

The first part of the works deals with the robust control of piezoelectric cantilever actuators. The works include classical robust techniques (H_∞ , ...) and exotic robust techniques (based on interval techniques). Regarding these latters, one of the main theoretical results we proposed is the Performances Inclusion Theorem (PIT) [C28]. This result is utilizable to synthesis robust controllers and can also be used for systems design (see chapter. 2.6.2). The second part of the works deals with the feedforward-feedback combined schemes which are suggested when the nonlinearities or the vibrations are too strong and thus when the previous robust techniques are not anymore efficient. The general principle of feedforward-feedback here consists in reducing first the nonlinearities or the vibrations by feedforward before applying the feedback control. In the last part of the chapter, we present the case of multi-axes (or multi-DOF) piezoelectric cantilever actuators. In this case, the cross-couplings between the axes introduce new difficulty for the control, additionally to the nonlinearities and to the vibration. Finally, we present the proposed control techniques for hybrid thermopiezoelectric actuators and for thermopiezoelectric microgrippers.

3.2 Classical robust control

The aim here consists in taking into consideration the hysteresis, the creep, the dynamics and the environment effect during the modeling and during the controllers synthesis. The proposed

principle consists in delicately taking a part of these elements as model uncertainties whilst the other part as external and fictive disturbances. Uncertain and perturbed linear models are therefore derived which present a major advantage that is the utilization of existing robust control techniques.

3.2.1 Displacement modeling and control

Consider the scheme in Fig. 3.1 where $C(s)$ is the position controller to be synthesized and δ_r the reference input.

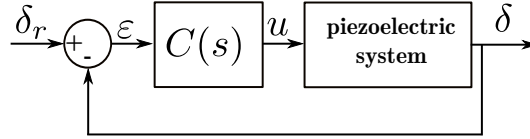


Figure 3.1: Schematic of the feedback.

Reconsider the general model in Eq. (2.8) which accounts for the hysteresis, creep, dynamics, external force and thermal variation:

$$\delta(s) = \Gamma(u(s)) D(s) + C_{creep}(u(s), s) + s_p D(s) F(s) + \Gamma_T(T(s)) D_T(s) \quad (3.1)$$

where:

- $\delta(s)$ and $u(s)$ are the output displacement and the driving voltage respectively,
- $F(s)$ and $T(s)$ are the external force applied to the actuator and the temperature variation respectively,
- $\Gamma(u(s))$ is the rate-independant (or static) hysteresis operator,
- $C_{creep}(u(s), s)$ is the creep operator,
- s_p is the compliance coefficient,
- and $D(s)$ and $D_T(s)$ are the dynamics of the structure and the thermomechanical dynamics respectively.

Regarding the operator $\Gamma(u(s))$, let us first approximate the hysteresis as a quadrilateral (see Fig. 3.2-a). From this quadrilateral, a maximal slope k_M and a minimal slope k_m among the four segments can be identified. Then, an uncertain linear model is derived as follows:

$$\Gamma(U) \cong (k + \partial) u + \delta_o \quad (3.2)$$

where δ_o is the offset (positive or negative). For a robust control synthesis case, δ_o is directly taken equal to the maximal or the minimal of the offsets possible, the one which has the highest norm. For instance, in Fig. 3.2-a, δ_o corresponds to the positive offset. The statical gain k and the uncertainty ∂ are defined as follows:

$$\begin{cases} k = \frac{k_M + k_m}{2} \\ -\frac{(k_M - k_m)}{2} \leq \partial \leq \frac{(k_M - k_m)}{2} \end{cases} \quad (3.3)$$

Introducing the quadrilateral approximation described by Eq. (3.2) and Eq. (3.3) into Eq. (3.1) yields:

$$\delta(s) = \left(1 + \frac{\partial}{k}\right) G(s)u(s) + b(s) \quad (3.4)$$

where $G(s) = kD(s)$ is the nominal model, and $b(s)$ is an (fictive) external output disturbance which rassembles the creep effect, the elastic effect (due to the force), the thermal variation effect and the offset of the hysteresis. It is defined by:

$$b(s) = C_{creep}(u(s), s) + s_p D(s)F(s) + \Gamma_T(T(s)) D_T(s) + \delta_o \quad (3.5)$$

The uncertainty of the model has a (input) direct multiplicative structure. Fig. 3.2-b depicts the new block diagram of the system with the controller to be synthesized. In the figure, the normalized uncertainty $\Delta(s)$ and the weighting $W_\Delta(s)$ are defined by:

$$\left\{ \begin{array}{l} -1 \leq \Delta \leq 1 \Rightarrow \|\Delta\|_\infty \leq 1 \\ \text{and} \\ W_\Delta = \frac{k_M - k_m}{2k} \end{array} \right. \quad (3.6)$$

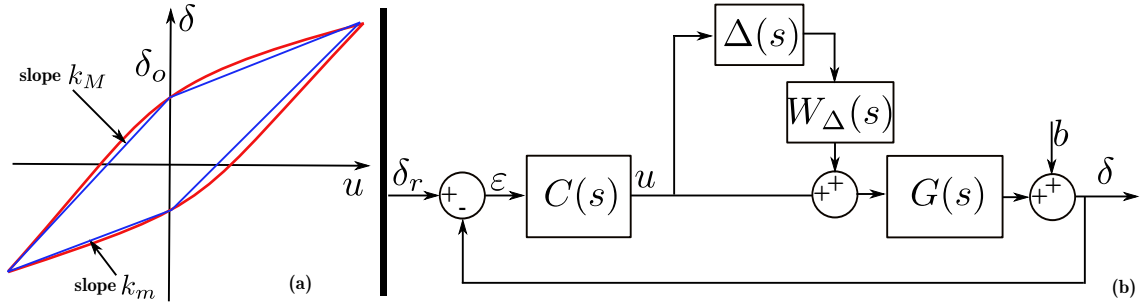


Figure 3.2: (a): the quadrilateral approximation. (b): the equivalent block-diagram.

A synthesis which is able to consider the above uncertainty, the disturbance and some specifications including the tracking performances of the piezoelectric actuator is the standard H_∞ synthesis. Let us for instance take the following specifications: tracking performances, command moderation, and disturbance rejection. With regards to the disturbance rejection, it is possible to express the related specification as a maximal permitted error ε_{max} when the worst case in disturbance b_{max} happens. In this worst case, the creep, the offset, the elastic part effect and the thermal effect are imposed to be maximal. Their values can be calculated with maximal inputs u_{max} and/or F_{max} and/or $T_{max}(s)$. All the specifications can be transcribed into the following weightings:

- $W_\varepsilon(s)$ for the tracking performances,
- $W_u(s)$ for the command moderation,
- and $W_b(s)$ for the disturbance rejection.

It is also worth to remind that the stability condition of a closed-loop in presence of a direct multiplicative structured uncertainty is $\|CSGW_\Delta\|_\infty < 1 \Leftrightarrow \|TW_\Delta\|_\infty < 1$, where $S = \frac{1}{1+CG}$ and $T = 1 - S$ are the sensitivity and the complementary sensitivity functions respectively, [199].

Considering the above weightings for the specifications and the above stability condition, the block-diagram for the controller synthesis is given by Fig. 3.3-a, which can be rearranged in order to have the standard scheme in Fig. 3.3-b. In this standard form, the augmented system $\mathcal{P}(s)$ contains the nominal system $G(s)$ and the four weightings. The (weighted) outputs are $(e_\varepsilon \ e_u \ e_\Delta)^T$ and the exogeneous inputs are $(\delta_r \ b_w)^T$.

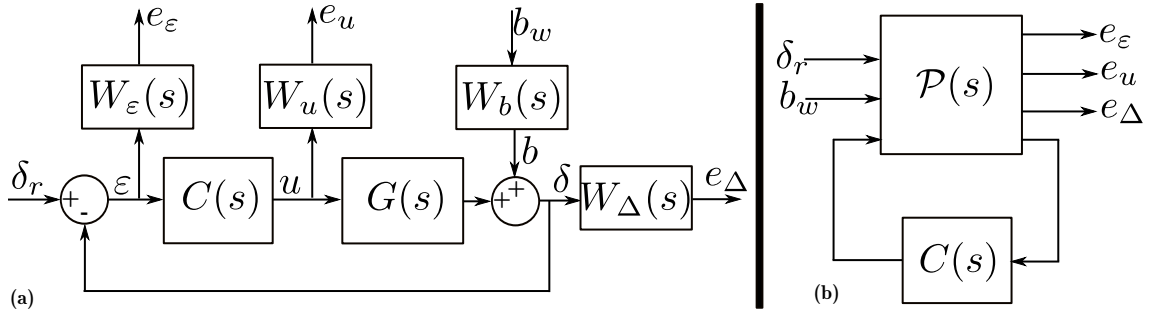


Figure 3.3: (a): block-diagram for the synthesis. (b): the standard scheme.

Applying the standard H_∞ problem [199] to the schemes in Fig. 3.3 yields:

Problem 3.2.1. Find the optimal controller $C(s)$ and the optimal value of $\gamma > 0$ (called performances level) such that the closed loop in Fig. 3.3-b is stable and:

$$\|F_l(\mathcal{P}(s), C(s))\|_\infty \leq \gamma$$

where $F_l(\mathcal{P}(s), C(s))$ is the lower fractional transformation and gives the following definition:

$$\begin{pmatrix} e_\varepsilon(s) \\ e_u(s) \\ e_\Delta(s) \end{pmatrix} = F_l(\mathcal{P}(s), C(s)) \begin{pmatrix} \delta_r(s) \\ b_w(s) \end{pmatrix} \quad (3.7)$$

After development and transformation of the above problem into magnitudes inequalities, we have the following new problem.

Problem 3.2.2. Find the optimal controller $C(s)$ and the optimal value of $\gamma > 0$ such that:

$$\begin{aligned} |S| &\leq \frac{\gamma}{W_\varepsilon} & |-S| &\leq \frac{\gamma}{W_\varepsilon W_b} \\ |CS| &\leq \frac{\gamma}{W_u} & |-CS| &\leq \frac{\gamma}{W_u W_b} \\ |CSG| &\leq \frac{\gamma}{W_\Delta} & |S| &\leq \frac{\gamma}{W_\Delta W_b} \end{aligned}$$

The above problem can be solved by using the DGKF² algorithm which is based on a state-space formulation [200; 201].

The quadrilateral approximation of a static hysteresis itself has been described in [J2]. The quadrilateral approximation is a particular and the simplest case of the plurilinear modeling of a hysteresis [C7]. In [C12], we included in the control synthesis the thermal effect rejection. These results utilized robust linear control techniques which were invariant. If the hysteresis is too strong and thus the uncertainties become too large, an LTI robust controller may not be sufficient and thus a robust adaptive scheme should be employed. This was the aim of the paper [C54] where we proposed an adaptive backstepping scheme.

3.2.2 Force modeling and control

We focus now the study when the piezoelectric actuator is used in force actuation. This is the case for the left actuator of the microgripper in Fig. 2.1-b. If we approximate the manipulated object's deformation as a spring-damper-mass system and if we consider that one of its extremity is in a contact with the actuator whilst the other one fixed in the space (see Fig. 3.4), the equations that govern the deformation of the piezoelectric actuator (taken from Eq. (2.8)) and the object deformation when they are in contact are:

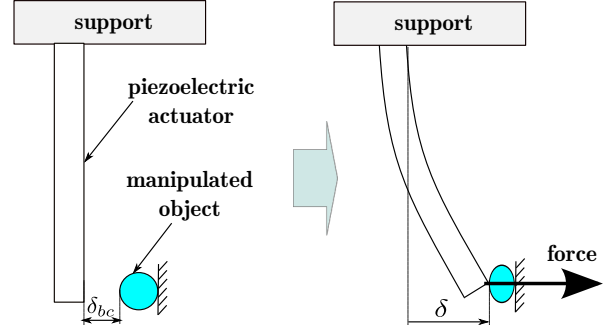


Figure 3.4: The force actuator manipulating an object.

$$\begin{cases} \delta(s) = \Gamma(u(s)) D(s) + C_{creep}(u(s), s) + s_p D(s) F(s) + \Gamma_T(T(s)) D_T(s) \\ m_o s^2 \delta(s) = -F - k_o (\delta(s) - \delta_{bc}(s)) - c_o s \delta(s) \end{cases} \quad (3.8)$$

where:

- δ_{bc} is the distance between the actuator and the object before contact (at rest),
- and m_o , c_o and k_o are the effective mass, the damping ratio and the stiffness of the object respectively.

²DGKF: Doyle, Glover, Khargonekar and Francis.

Combining the two equations in Eq. (3.8) results in the model that relates the force $F_o = -F$ applied by the actuator to the object with the driving voltage u :

$$\begin{aligned}
 F_o(s) = & (s_o + s_p) \Gamma(u(s)) D_F(s) + C_{creep}(u(s), s) \frac{1}{(s_o D_o(s) + s_p D(s))} \\
 & + \Gamma_T(T(s)) \frac{D_T(s)}{(s_o D_o(s) + s_p D(s))} - \frac{D_o(s)}{(s_o D_o(s) + s_p D(s))} \delta_{bc}(s)
 \end{aligned}
 \tag{3.9}$$

where $s_o = \frac{1}{k_o}$ is the compliance of the object and $D_o(s) = \frac{1}{\frac{m_o}{k_o} s^2 + \frac{c_o}{k_o} s + 1}$ is the normalized dynamics of its deformation. The dynamics of the actuation is $D_F(s) = \frac{D(s)}{(s_o + s_p)(s_o D_o(s) + s_p D(s))}$. As we can see from the model Eq. (3.2.2), the presence of an object strongly modifies the static behavior and the dynamics of the piezoelectric cantilever: a new normalized dynamics $D_F(s)$ is obtained whilst the new (nonlinear) static gain is $(s_o + s_p) \Gamma(u(s))$. Similar phenomenon is classical for macro robotical systems [202]. Here we have shown that this is also valuable for miniaturized systems.

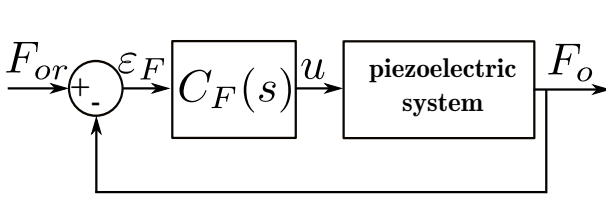


Figure 3.5: Closed-loop force control.

Having the force model of the piezoelectric actuator, assuming that the force signal is available (by measurement or by observation), the deal is now to synthesis a controller C_F (see Fig. 3.5) that will ensure some specifications related to precise and high dynamics positioning. Similarly to the displacement model, it is possible to introduce an (fictive) external disturbance which accounts for the

creep part, the thermal part, the distance between the actuator and the object at rest. Regarding the static hysteresis $\Gamma(u(s))$, the quadrilateral approximation can again be employed. All these elements lead therefore to an uncertain linear model with an external disturbance and a robust controller can be further synthesized, equivalently to the displacement controller synthesis. During a micromanipulation or microassembly task, every new manipulated object leads to new model parameters, because the model strongly depends on the object's characteristics. A way consists therefore to identify the object's parameters and manually schedule the model before synthesizing the controller. Such way may be too heavy if we are face to several types of objects or if the object characterization itself is complex. Another way consists in knowing a bound of the parameters s_o , m_o and c_o if the types of objects are known in advance, inject this bound in the model Eq. (3.2.2), and afterwards construct additional uncertainty related to the objects characteristics. However, due to the structure of the model, the related Δ -uncertainty is more complex to extract. Finally, a last possibility consists in employing the characteristics of one object only (silicon for example) in the model Eq. (3.2.2), and then synthesizing a robust controller from that model [C9]. If the actual manipulated object has properties close to these, the stability and even the specified performances will be

still maintained. If these properties are too far, an adaptive control scheme may be the most convenient. For instance, in [C23], we proposed a self-scheduled H_∞ controller that was able to maintain the specified performances for a wide types of objects.

3.2.3 Displacement and force control of piezoelectric microgrippers

The displacement control and the force control in the previous subsections deal with one piezoelectric actuator only. When a whole microgripper is working, it is possible to control the displacement and the force simultaneously. Two approaches are possible. The first approach lies in a single model and a single control for the whole microgripper. For instance a (linear or nonlinear) state-space representation can be utilized [C1] with the displacement and the force rassembled in an output vector $(\delta \ F_o)^T$ and the driving voltages of the two actuators rassembled in an input vector $(u_l \ u_r)^T$, subscript l being for left cantilever and r for right cantilever. However, this approach requires a precise knowledge of the objects characteristics and of the couplings between the object and the two actuators. The modeling in this approach is therefore complex. The alternative approach is more simple, although less precise. In this, the two cantilever actuators are modeled independantly and two monovariable models are obtained. Whilst one actuator is modeled in displacement, the other one is modeled in force. Consequently, we can apply the previous elementary modeling and robust control of displacement and of force, as pictured in Fig. 3.6-a. Fig. 3.6-b and -c depict the results obtained with this approach during a pick-and-place task performed with a piezoelectric microgripper [C11]. In this, a series of steps are applied as references to each actuator. We can observe good tracking performances by the two actuators and a convenient rejection of the couplings found in one actuator due to the movement of the other actuator.

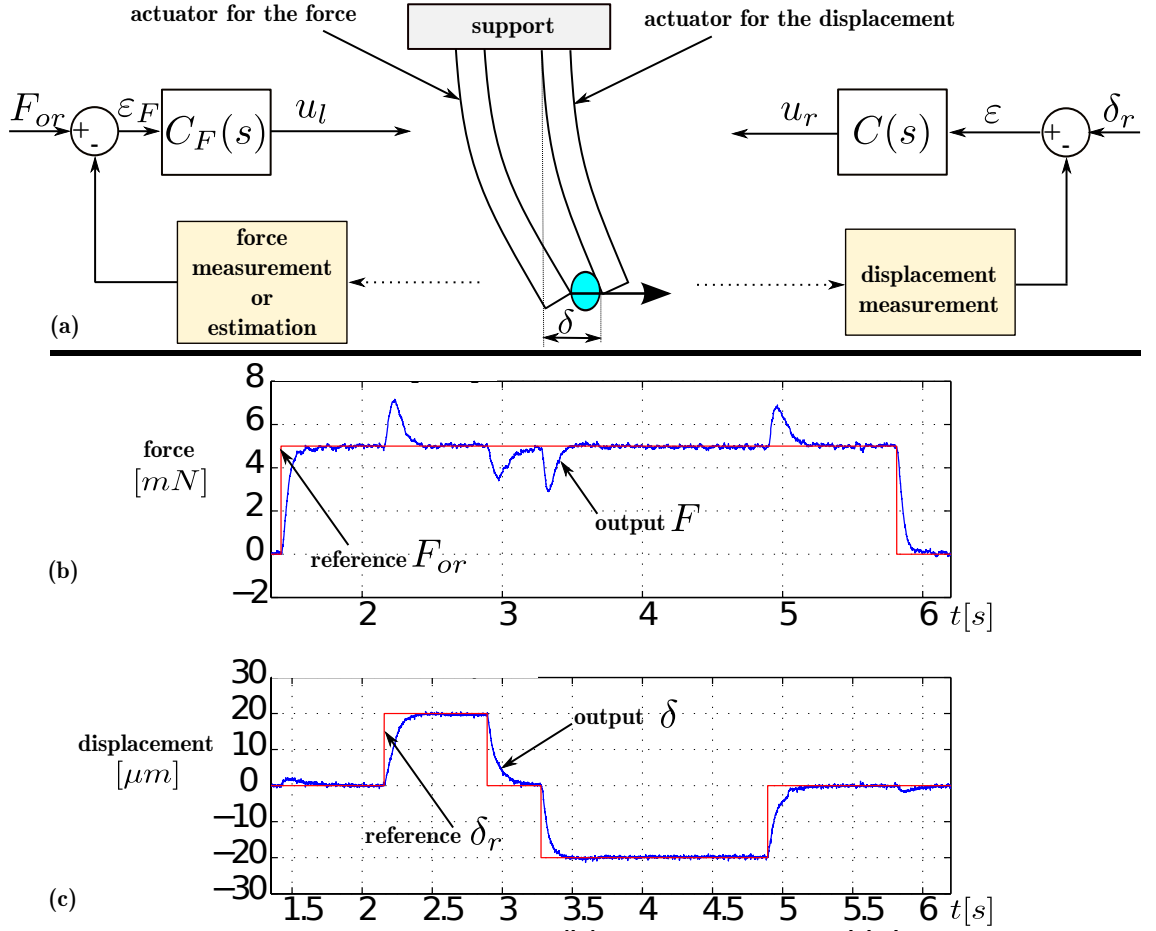


Figure 3.6: (a): force/displacement control of a piezoelectric microgripper. (b): experimental results [C11].

3.2.4 Multivariable control of multi-axes piezoelectric actuators

The modeling and control techniques so far presented were devoted to mono-axis piezoelectric systems, mainly piezoelectric cantilever actuators that bend along one axis. Some applications need however piezoelectric cantilever actuators that can provide displacements along two or three directions. In scanning probe microscopes for instance, the piezoelectric tube scanners bend along x and y axis and contract or expand along the z axis. In dexterous micromanipulation and microassembly [J19], 4-DOF piezoelectric microgrippers have been used. Each of the cantilever of the microgripper can perform a bending along two axes. Two versions of the actuators permitted such performances. The first version - designed and developed as proof-of-concept of a patent authored by the department [203] - is a bimorph cantilever which has two electrodes on the upper surface and two electrodes on the lower surface. The judicious applica-

tion of potentials on the four electrodes results in the bending along y only, along z only or in diagonal (see Fig. 3.7-a).

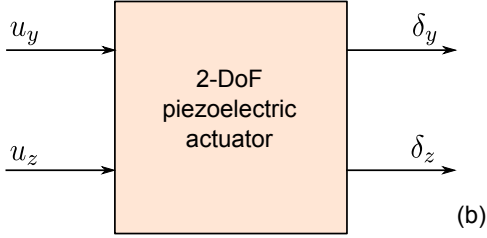
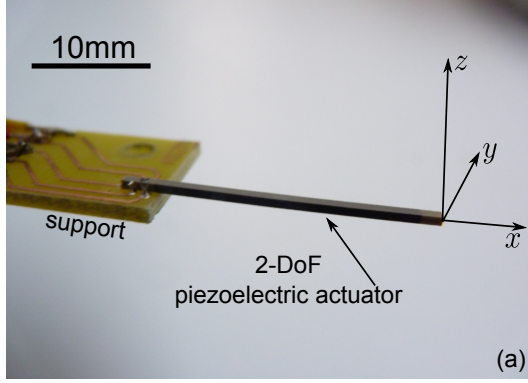


Figure 3.7: (a): a photo of the piezoelectric duo-multimorph actuator. (b) and (c): bi-variable system.

turbances. This will yield several monovariable systems with uncertainties and disturbances which account for the nonlinearities and for the cross-couplings. Applying this approach to the 2-DOF duo-multimorph actuator, with block-diagram in Fig. 3.7-b, by adding the cross-couplings to the initial model in Eq. (2.8), we have:

$$\delta_i(s) = \Gamma_i(u_i(s)) D_i(s) + C_{creep-i}(u_i(s), s) + s_{pi} D_i(s) F_i(s) + \Gamma_{Ti}(T_i(s)) D_{Ti}(s) + \Gamma_{ci}(u_j(s)) \quad (3.10)$$

where $i \in \{y, z\}$ and $j \in \{y, z\} - \{i\}$. The cross-coupling found at the output δ_i and due to the voltage u_j is denoted $\Gamma_{ci}(u_j(s))$. From here, the modeling and the controllers synthesis comes back to the case of monovariable approach, see Section 3.2.1 and Section 3.2.2 for the displacement and for the force respectively. We just add the cross-couplings $\Gamma_{ci}(u_j(s))$ in the fictive external disturbance. In [BC6], the displacement control of the duo-multimorph piezoelectric actuator with the standard H_∞ technique was developed and experimented. Two optical sensors were used for that. In [C52], the same control was applied but with two novel and embeddable magnetic sensors for the feedback. The magnetic sensors being noisy, a Kalman filtering can be added in the feedback to reduce the signal propagation [BC3].

3.2.5 Acknowledgements

The works dealing with robust adaptive control techniques were within the postdoctoral fellowship of Dr. Juan-Antonio Escareno.

3.3 Interval techniques combined with classical control theory

The classical robust control techniques (H_∞ , μ -synthesis...) often derive high order controllers: the controllers orders are higher than the systems orders. These orders can be reduced with existing techniques, however this is often accompanied by a reduction of the performances of the closed-loop controlled piezoelectric systems. Other techniques like H_∞ synthesis with orders constraint may eventually be a possibility to explore [204] but in the works carried out, we proposed to explore interval techniques combined with control theory. In fact, intervals permit to model more naturally and easily uncertain parameters by bounding them. This is very interesting when, for example, facing to objects parameters or actuator model parameters that are not precisely known, as usual in micromanipulation or microassembly. Another particularity of interval techniques is the guarantee (or certification) notion: if an algorithm finds a solution set, this latter is guaranteed to satisfy the problem. If an algorithm finds a non-solution set, it is guaranteed that this set does not contains any solution of the problem. Finally, it is possible to synthesis robust and low orders controllers with interval techniques combined with classical control theory, as we will present below.

In control theory applications, interval techniques are widely used for guaranteed estimation (state estimation and parameters estimation/identification) [171; 205–209] and for robust stability analysis [172; 210–216]. Many works also report elementary tools that may be useful to complete the robust stability: the algorithm to solve a set inversion problem in interval functions [216], the H_∞ norm [217] and the envelop of the Nyquist plots [218] all for interval systems. Regarding the synthesis of controllers with interval techniques, PID controllers structures [219], state-feedback controllers [220] and control schemes with prefilter [221] have been mainly developed. In [222], a predictive control law has been synthesized from an interval system and efficiently applied to a consumable double-electrodes gas metal arc welding process.

Our aim is to utilize intervals to model first the uncertainties in piezoelectric actuators, and afterwards to develop low order robust controllers capable to ensure robust performances. A particular attention will be paid in the structure of the system: we employ a generalized structure of interval systems. This is not the case for the works in the litterature. For example, the controller designed in [219] is only practical for second order interval systems. The main theoretical results in our works can be summarized as follows: 1) the performances inclusion theorem which is applicable in different applications (controllers synthesis, performances analysis, systems design), 2) and the combination of the classical standard H_∞ techniques with interval tools for robust controllers synthesis or for performances analysis. These results are presented below with some of the experimental applications to piezoelectric actuators. The reader is invited to read the quick remind on interval techniques provided in Chapter D if required. In the sequel, we utilize as model (including for piezoelectric actuator) the inter-

val system $[G](s)$ where the parameters are intervals. The model is linear but we give the assumption that all uncertainties due to the parameters variability, to the sensitivity to the environment, to any inexactitude from the measurement and identification, and to the nonlinearities approximation are bounded by these intervals.

3.3.1 The Performances Inclusion Theorem (PIT)

The performances inclusion theorem, that we provided and detailed in [C28], deals with the performances of two stable interval systems³. The theorem contains two properties: one property for the frequency domain performances and one property for the time domain performances.

Consider two stable interval systems having the same polynomials degrees m and n :

$$[G_1](s) = \frac{\sum_{l=0}^m [b_{1l}] \cdot s^l}{\sum_{k=0}^n [a_{1k}] \cdot s^k}, \quad [G_2](s) = \frac{\sum_{l=0}^m [b_{2l}] \cdot s^l}{\sum_{k=0}^n [a_{2k}] \cdot s^k} \quad (3.11)$$

Theorem 3.3.1. *The performances inclusion theorem.*

In the frequency domain:

$$\text{if } \left\{ \begin{array}{l} [a_{1k}] \subseteq [a_{2k}], \quad \forall k = 1 \dots n \\ \text{and} \\ [b_{1l}] \subseteq [b_{2l}], \quad \forall l = 1 \dots m \end{array} \right. \Rightarrow \left\{ \begin{array}{l} [\rho]([G_1](j\omega)) \subseteq [\rho]([G_2](j\omega)) \\ \text{and} \\ [\varphi]([G_1](j\omega)) \subseteq [\varphi]([G_2](j\omega)) \end{array} \right.$$

In the time domain:

$$\text{if } \left\{ \begin{array}{l} [a_{1k}] \subseteq [a_{2k}], \quad \forall k = 1 \dots n \\ \text{and} \\ [b_{1l}] \subseteq [b_{2l}], \quad \forall l = 1 \dots m \end{array} \right. \Rightarrow [g_1](t) \subseteq [g_2](t)$$

Proof. See [C28]. □

We should also notice the following remark:

Remark 3.3.1. $\left\{ \begin{array}{l} [a_{1k}] \subseteq [a_{2k}] \\ [b_{1l}] \subseteq [b_{2l}] \end{array} \right. \Rightarrow [G_1](s) \subseteq [G_2](s); \forall s \in \mathbb{R}^+$

The theorem says that when two transfer functions have coefficients which lie in (independent) intervals, and all coefficient intervals of one transfer are included in the coefficient intervals of the other, then the same holds for their Bode diagrams as well as for their time responses. In other words, the performances of one stable interval system are "bounded" by those of another stable interval system if the coefficients of the former are bounded by the coefficients of the latter. This result will be very useful to design robust controllers or to perform a performances analysis. In addition, this result can also be utilized for systems design (see [Section 2.6.2](#)).

³The stability of interval systems are discussed in [Section D.4.3](#))

3.3.2 Controllers design by using the PIT

Given an uncertain system $[G](s, [a], [b])$ to be controlled by a controller $[C](s)$ (Fig. 3.8). This controller must ensure some given performance for the closed-loop whatever the parameters a and b ranging in $[a]$ and $[b]$ respectively are. Let $[H_{cl}](s, [p], [q])$ denote the closed-loop transfer. On the other hand, let the system $[G](s, [a], [b])$ be re-arranged as follows:

$$[G](s, [a], [b]) = \frac{1 + \sum_{j=1}^m [b_j]s^j}{\sum_{i=0}^n [a_i]s^i} \quad (3.12)$$

such as $[a] = [[a_0], \dots, [a_n]]$ and $[b] = [[b_0], \dots, [b_m]]$, $m \leq n$ and $[b_0] = 1$.

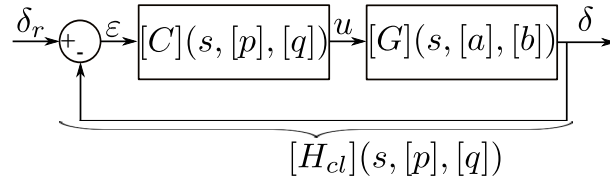


Figure 3.8: A closed-loop transfer $[H_{cl}]$.

If we impose the structure of the controller $[C](s, [\theta])$ as

$$[C](s, [\theta]) = \frac{\sum_{j=0}^l [d_j]s^j}{\sum_{i=0}^k [c_i]s^i} \quad (3.13)$$

where $\theta = [[c], [d]]$ represents the interval parameters vector (or box⁴ of parameters) of the controller and where $l \leq k$, thus the closed-loop model $[H_{cl}](s, [a], [b], [\theta])$ can be easily derived:

$$[H_{cl}](s, [p], [q]) = \frac{1 + \sum_{j=1}^e [q_j]s^j}{\sum_{i=0}^r [p_i]s^i} \quad (3.14)$$

Where $e = m + l$ and $r = n + k$ and where the boxes $[q]$ and $[p]$ are function of the boxes $[a]$, $[b]$, $[c]$ and $[d]$.

We notice that the notation of the controller is interval ($[C](s, [\theta])$) during the synthesis because the calculation will yield intervals. However, the implemented controller will be a point denoted $C(s)$ which is any point inside the solution $[C](s, [\theta])$.

⁴A box is a vector of intervals.

Let $[H](s, [w], [x])$ denote an interval transfer function, called desired closed-loop transfer, that reflects the specified closed-loop performances. This transfer function should have the same structure than the closed-loop transfer $[H_{cl}](s, [a], [b], [\theta])$, otherwise the performances inclusion theorem is not utilizable. If a first transcription of the specifications gives lower order transfer for $[H](s, [w], [x])$, we can add filter to this latter such that its final structure is similar to that of $[H_{cl}](s, [a], [b], [\theta])$. We have:

$$[H](s, [w], [x]) = \frac{1 + \sum_{j=1}^e [x_j] s^j}{\sum_{i=0}^r [w_i] s^i} \quad (3.15)$$

where boxes $[x]$ and $[w]$ have been calculated from the specified performances.

Thus, the objective consists in finding the parameters of the controller $[C](s, [\theta])$ in [Eq. \(3.13\)](#) such that the performances of the closed-loop $[H_{cl}](s, [a], [b], [\theta])$ satisfy the desired performances described by $[H](s, [w], [x])$. The problem can be stated as finding the set Θ of controller parameters vector so that:

$$\Theta := \{\theta \in [\theta] \mid [H_{cl}](s, [p], [q]) \subseteq [H](s)\} \quad (3.16)$$

From the performances inclusion theorem, the problem becomes in finding the set Θ of controller parameters vector such that:

$$\Theta := \left\{ \theta \in [\theta] \mid \begin{array}{l} [q_j](\theta) \subseteq [x_j], \forall j = 1, \dots, e \\ [p_i](\theta) \subseteq [w_i], \forall i = 0, \dots, r \end{array} \right\} \quad (3.17)$$

This problem is a set inversion problem and can be solved with an appropriate algorithm. One of the algorithms for solving a set inversion problem is the SIVIA algorithm (Set Inversion Via Interval Analysis) [\[171; 172\]](#) which is rapid and easy in implementation. [Section D.3](#) gives a remind of this algorithm. After computation, the algorithm produces a solution set Θ . As an example, [Fig. 3.9-a](#) depicts the results from the SIVIA algorithm when calculating the integral gain K_i and the proportional gain K_p of a PI controller for a piezoelectric actuator. The region denoted S_c corresponds to the parameters of a point controller $C(s) = K_p + \frac{K_i}{s}$ with which the specified performances will be guaranteed. Any gains K_p and K_i inside this region are guaranteed to ensure the performances. In contrary, the region S_{nc} corresponds to parameters with which it is guaranteed that the specifications will not be ensured. In this example, two piezoelectric actuators having (points) models within the interval model $[G](s)$ have been used for experimental test. Two controllers $C_1(s)$ and $C_2(s)$ randomly taken from the region S_c have been successively applied to each of the two actuators. [Fig. 3.9-b and c](#) show the frequency responses and the step responses respectively [\[J15\]](#). In the same figure, the specifications plotted as envelopes have also been put. These figures show that the performances of the closed-loop, for any of the piezoelectric actuators, and with any of the two point controllers are well ensured, which experimentally confirm the robustness in the technique proposed. If, after calculation, no solution is found however, it is suggested to recalculate Θ with a different initial box. If after different attempts there is still no solution, the specifications

may be too severe for the utilized uncertainties sizes. In such a case, it is suggested to relax the specifications and/or reduce the sizes of the parametric uncertainties.

The above theoretical part as well as its application to piezoelectric actuators were detailed in [J15]. Notice that one of the main advantages here is the possibility to impose the controller structure (see Eq. (3.13)). Consequently, it is possible to impose a controller order lower than the system order. If the algorithm finds a solution, we will get a low order controller which is convenient for embarked systems. In [C27], we have calculated a robust PID controller with this technique and in [J18], we have calculated a robust RST controller, in both the controllers order being lower than that of the model.

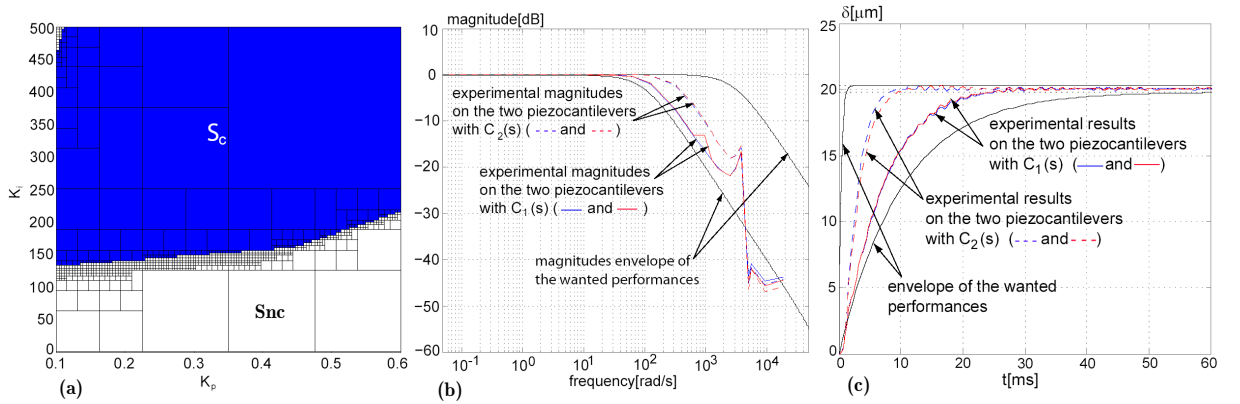


Figure 3.9: (a): solution set Θ for a PI controller. (b): closed-loop frequency response of two piezoelectric actuators with two controllers $C_1(s)$ $C_2(s)$. (c): step responses.

3.3.3 H_∞ interval controllers synthesis

We propose here to combine interval techniques with the standard H_∞ controllers synthesis. Our objective is to benefit from the natural way to model uncertainties and the low orders inherited from intervals. Both the theoretical results and the experimental sides are detailed in [C37][J16].

The system is an interval model $[G](s, [\mathbf{a}], [\mathbf{b}])$ where the parametric uncertainties (intervals) account for the nonlinearities approximation, the variability of the process behavior and the high sensitivity to the environment. Let the structure of the controller be imposed, for instance a PI or a PID controller. Again, we denote $[C](s, [\theta])$ the controller during the synthesis in which $[\theta]$ is the interval parameters vector to be calculated. Finally, we will leave the weightings for the specifications non-interval, i.e. point transfer functions similar to those used in Fig. 3.3. Since the system and the controller to be synthesized are intervals, the augmented plant is interval: $[\mathcal{P}](s)$. Thus the standard H_∞ problem, similarly to Problem. 3.2.1, can be formulated as follows.

Problem 3.3.1. Find the controller $[C](s)$ and the optimal value of $\gamma > 0$ such that:

$$\|[F_l]([\mathcal{P}](s), [C](s, [\theta]))\|_\infty \leq \gamma$$

where $[F_l]([\mathcal{P}](s), [C](s, [\theta]))$ is the lower fractional transformation between $[\mathcal{P}](s)$ and $[C](s, [\theta])$ and is an interval transfer function.

Let us take the example for which tracking performances, a command moderation and a disturbance rejection constitute the specifications that are transcribable into weightings $W_\varepsilon(s)$, $W_u(s)$ and $W_b(s)$ respectively. Following the same principle than of Fig. 3.3, we obtain the synthesis scheme in Fig. 3.10. Remark that we expressly removed from the scheme the weighting related to the uncertainties because they are already taken into account by the intervals in the system $[G](s)$. However, it is still possible to utilize both intervals (via the model $[G](s)$) and the weighting to more increase the robustness of the controller.

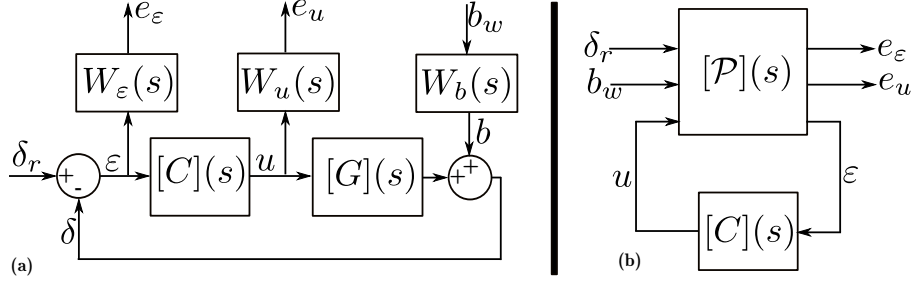


Figure 3.10: (a): block-diagram for the synthesis. (b): the standard scheme.

From Fig. 3.10, the standard H_∞ interval problem in Problem. 3.3.2 is equivalent to the following problem.

Problem 3.3.2. Find the controller $[C](s)$ and the optimal value of $\gamma > 0$ such that:

$$\begin{aligned} \|W_\varepsilon[S]\|_\infty &\leq \gamma & \| -W_\varepsilon[S]W_b \|_\infty &\leq \gamma \\ \|W_u[C][S]\|_\infty &\leq \gamma & \|W_u[C][S]W_b\|_\infty &\leq \gamma \end{aligned}$$

If $\gamma \leq 1$, the robust performances are achieved.

The problem of finding the parameters $[\theta]$ of the imposed structure controller $[C](s, [\theta])$ can therefore be formulated as the following set inversion problem.

Problem 3.3.3. Find the set Θ of parameters vector with which, for a given positive number $\gamma \leq 1$, we have:

$$\Theta := \left\{ \theta \in [\theta] \left| \begin{array}{ll} \|W_\varepsilon[S]\|_\infty \leq \gamma & \| -W_\varepsilon[S]W_b \|_\infty \leq \gamma \\ \|W_u[C][S]\|_\infty \leq \gamma & \|W_u[C][S]W_b\|_\infty \leq \gamma \end{array} \right. \right\}$$

where the interval sensitivity $[S](s)$ also depends on the controller parameters $[\theta]$.

Before solving the [Problem 3.3.3](#), γ is imposed manually, contrary to the classical standard H_∞ technique where its optimal value is found by dichotomy. Its value should be chosen to be less or equal to 1 in order to have a controller that will robustly ensure the performances. Again, this problem can be solved by using an algorithm for set inversion problem like SIVIA (see [Section D.3](#)). However, the resolution requires the computation of the H_∞ -norm of interval transfer functions. For that, we will combine the SIVIA algorithm with the techniques of computation of the H_∞ -norm of interval systems proposed in [\[223–225\]](#) and reminded in [Section D.4.4](#). Similarly to the design in [Section 3.3.2](#), if the interval techniques provides a solution set Θ , any point controller $C(s)$ with parameters θ inside this set will ensure the specifications. However, if there is no solution, it is suggested to modify the initial value of Θ . If, after different attempts, no solution is found, one can lightly increase γ or relax the specifications which might be too severe. Another attempt consists in reducing the sizes of the uncertainties which might be too large. However, increasing γ , relaxing the specifications or reducing the uncertainties sizes means that the initial expectations (i.e. initial specifications and initial uncertainties) may not be anymore obtained.

3.3.4 Robust performances analysis with interval techniques

We propose now to combine interval techniques with classical control theory to perform *a posteriori* and robust performances analysis. More than the robust stability analysis which is classical, robust performances analysis is of great interest for a given closed-loop which contains a known controller and to which we need to check if specified performances are satisfied when the system is uncertain. The proposed techniques for that are detailed in [\[J15\]\[BC4\]\[C30\]](#). There are two techniques proposed: 1) *a posteriori* performances analysis by using the performances inclusion theorem (PIT), 2) and *a posteriori* performances analysis by using the standard H_∞ technique and interval tools combined. For both, the initial problem is as follows.

Let $C(s)$ be a given (point) controller which controls an interval system $[G](s)$. Both the controller and the system are known.

Problem 3.3.4. *Does the closed-loop with sensitivity $[S](s) = \frac{1}{1+C[G]}$ satisfy the given and desired specifications (tracking performances, command moderation,...)?*

3.3.4.1 Robust performances analysis with the PIT theorem

To solve the [Problem 3.3.4](#), the closed-loop interval transfer $[T](s)$ should first be numerically calculated from the known controller $C(s)$ and the known interval system $[G](s)$. It is given as follows:

$$[T](s) = 1 - [S](s) = \frac{\sum_{j=0}^e [q_j] s^j}{\sum_{i=0}^r [p_i] s^i} \quad (3.18)$$

Then, the specifications are transcribed into interval transfer function $[H](s)$, called desired closed-loop. In many cases, tracking performances specifications are stated with maximal or minimal measures (maximal settling time, maximal statical error, maximal overshoot, minimal bandwidth,...). It is possible to put them first as inequalities and then as intervals. Finally, they can be transcribed into transfer function $[H](s)$. To apply the performances inclusion theorem, the desired transfer $[H](s)$ should have the same structure than the closed-loop $[T](s)$. If the polynomials of $[H](s)$ have lower orders than those of $[T](s)$, a filter is added in the former. In the contrary case, the filter should be added in $[T](s)$. Let the final structure of $[H](s)$ be:

$$[H](s) = \frac{\sum_{j=0}^e [x_j] s^j}{\sum_{i=0}^r [w_i] s^i} \quad (3.19)$$

Proposition 3.3.1. *if $\begin{cases} [q_j] \subseteq [x_j] & \text{for } j = 0 \dots e \\ [p_i] \subseteq [w_i] & \text{for } i = 0 \dots r \end{cases}$, thus the desired tracking performances are satisfied by the closed-loop.*

This result is very powerful and very quick to use and is for tracking performance *a posteriori* verification. For the cases of command moderation or disturbance rejection verification, similar procedure is employed by using the right transfer functions. The bad side of this approach is the fact that the condition is conservative: a small subclass only of all controllers that ensure the performances can be verified. The next proposed technique permits to effectuate a robust performances analysis with reduced conservatism. The principle is based on the combination of the standard H_∞ technique with interval techniques.

3.3.4.2 Robust performances analysis with standard H_∞ and interval techniques

We have combined the standard H_∞ technique with interval tools to synthesis low order and robust controllers in [Section 3.3.3](#). Here, we propose to utilize this combination in a robust performances analysis purpose.

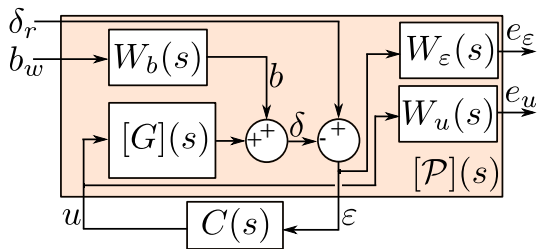


Figure 3.11: A standard scheme.

Consider a known interval system $[G](s)$. Let $C(s)$ be a known point controller that controls $[G](s)$. Let us consider as specifications the tracking performances, the command moderation and an output disturbance rejection. These specifications can be transcribed into weightings $W_\varepsilon(s)$, $W_u(s)$ and W_b respectively. A weighted closed-loop scheme as in [Fig. 3.11](#) is therefore yielded. In the figure, $[P](s)$ is the interval augmented system. We have the following proposition.

Proposition 3.3.2. *if $\|F_l([P](s), C(s))\|_\infty \leq 1$, thus the desired specifications are satisfied by the closed-loop.*

Considering the standard form of Fig. 3.11, the Proposition. 3.3.2 implies:

Proposition 3.3.3. *if $\left(\begin{array}{cc} \|W_\varepsilon[S]\|_\infty \leq 1 & \|-W_\varepsilon[S]W_b\|_\infty \leq 1 \\ \|W_uC[S]\|_\infty \leq 1 & \|W_uC[S]W_b\|_\infty \leq 1 \end{array} \right)$, thus the desired specifications are satisfied by the closed-loop.*

where $[S](s) = \frac{1}{1+C[G]}$. Once again, the calculation of the H_∞ -norm of interval systems provided by [223–225] and reminded in Section D.4.4 is required.

3.3.5 General remarks

Two techniques of robust controllers synthesis based on intervals have been presented: 1) one technique based on the performances inclusion theorem, 2) and one technique based on the combination of the standard H_∞ approach with interval tools. Other results have also been produced. For instance, in [C25][C30], we calculate robust controllers through direct synthesis, i.e. from a desired closed-loop $[H_{cl}](s)$, we directly derive the controller: $[C](s) = \frac{1}{[G](\frac{1}{[H_{cl}]} - 1)}$.

However, due to the compensation side of this technique (division $\frac{[G](s)}{[H_{cl}](s)}$), some solutions do not necessarily satisfy the initial specifications. The choice of the point controller $C(s)$ within the solution set should be verified by an *a posteriori* performances analysis.

The techniques proposed above have been employed to control the force and the displacement in a whole microgripper [J22].

Intervals are interesting to model parametric uncertainties thanks to the natural and easy way to represent them only with bounds. Combined with control theory, interval techniques permit to compute low order and robust controllers. There is a wide and interesting possibility to exploit them in controllers synthesis and in structural analysis when we are face to systems with uncertainties. The techniques proposed and presented in this thesis dealt with SISO⁵ and linear systems but future works include the case of MIMO⁶ or also nonlinear systems.

3.3.6 Acknowledgments

Many of the works regarding the interval techniques (design and control) were within the PhD subject of Sofiane Khadraoui.

3.4 Feedforward-feedback control schemes

In some situations, the feedback control scheme is augmented by one or several feedforward controllers. This permits to reach certain objectives that feedback only or feedforward only

⁵SISO: Single Input Single Output (or monovariable) systems.

⁶MIMO systems: Multi Input Multi (or multivariable) Output systems.

(see Chapter 4) could not satisfy. One scheme of combined feedforward-feedback control of piezoelectric actuators is depicted in Fig. 3.12-a. It consists of a feedback controller C , a plant-injection feedforward controller F_p (or reference anticipation) and a closed-loop-injection feedforward controller F_{cl} (or prefilter). When $F_p = 0$ is set to zero, the architecture is a feedforward closed-loop injection (FFCLI) which permits to improve the transient response as well as the tracking bandwidth [230–233]. In contrast, when F_{cl} is a unity gain and F_p is used as the feedforward controller, the architecture is a feedforward plant-injection (FFPI). In this case, F_p is often designed on the basis of the plant inverse model [234–236]. This permits to improve the transient response or to cancel the static error. In [237], both FFCLI and FFPI were utilized in the same architecture which make the feedforward-feedback control techniques account for nonminimum phase systems. In a way, FFCLI and FFPI architectures can be seen as follows: the plant is first linearized thanks to the feedback controller $C(s)$ (a high gain or an integral control is sufficient in most of the cases), then the bandwidth is enlarged (precision improvement at high frequency) thanks to the feedforward controllers F_{cl} or F_p [231; 238]. Notice that the FFCLI is sensitive to model uncertainties.

Differently from FFCLI and FFPI, another architecture of combined feedforward-feedback is depicted in Fig. 3.12-b [239–242][C13][C23][C50]. In this, a (cascade) feedforward controller Γ^c is first applied to the plant before employing the feedback. The aim of the feedforward is various. It can be a compensator for the nonlinearities (hysteresis or creep) which will yield a linearized system, or it can be a vibrations damper (vibrations compensator). In both cases, the calculation of the feedback C is rendered easier with the compensated plant.

Regarding the control of multi-DOF piezoelectric actuators, modeling the cross-couplings is complex, and thus it is common to employ several monovaryable compensators Γ^c for each axis [J13][C18][C31]. In such a way, the nonlinearities or the badly damped vibrations in the direct transfer are compensated. The non-compensated cross-couplings are considered as disturbances or model uncertainties that should be taken into account when synthesizing the closed-loop controller C .

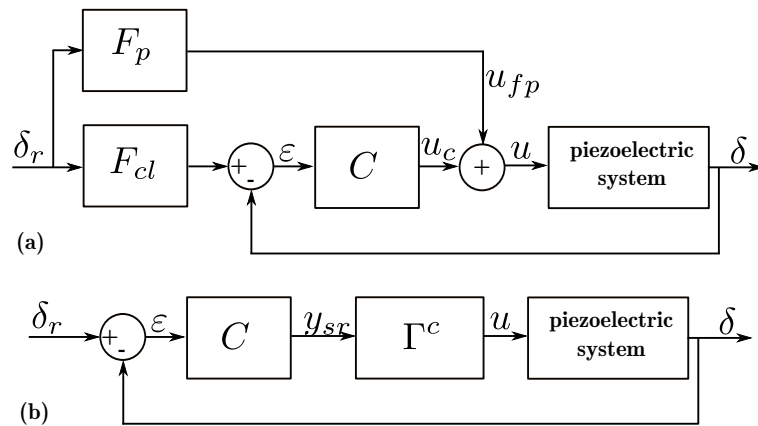


Figure 3.12: Feedforward-feedback control architectures in piezoelectric actuators control.

3.5 Control of hybrid thermopiezoelectric microgrippers

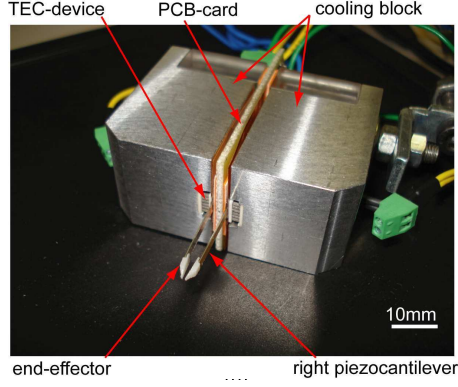


Figure 3.13: A hybrid thermopiezoelectric microgripper.

microgripper is controlled for the precise positioning (displacement control) and the other actuator controlled for the manipulation force. As the two controls are independent, they can be synthesized separately.

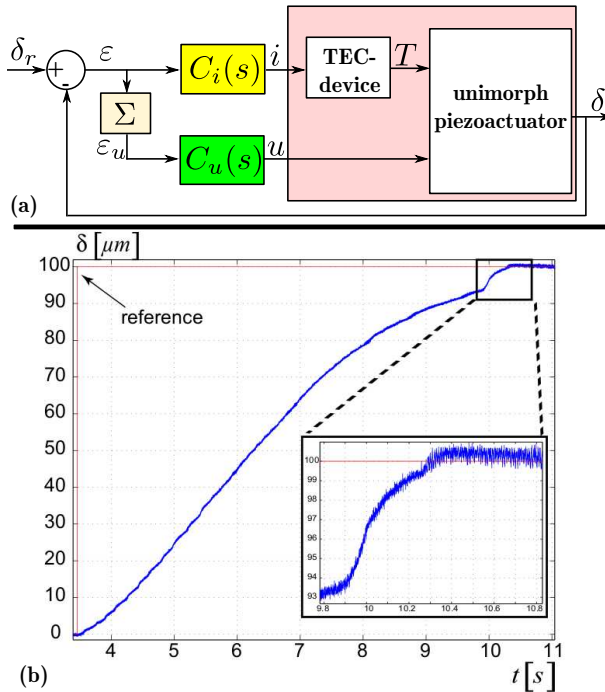


Figure 3.14: A hybrid control law for a hybrid thermopiezoelectric actuator.

Based on the hybrid thermopiezoelectric actuator presented in [Section. 2.3](#), a novel microgripper has been developed. The developed hybrid thermopiezoelectric microgripper, pictured in [Fig. 3.13](#), has two hybrid actuators and can pick or handle small objects with a high resolution thanks to the piezoelectric performances and with a large range of positioning thanks to the thermal actuation performances. The aim of this section is to report the control strategy proposed for the microgripper. The novelty in this control is evident due to the originality of the system itself. Similarly to the control of multimorph microgrippers presented in [Section. 3.2.3](#) and in [Section. 3.3.5](#), one actuator of the hybrid

First, let us regard the actuator for the displacement and its control [\[C19\]](#). The system has one output which is the displacement δ (deflection of the cantilever), and two inputs: the electrical current i that supplies the Thermo-Electric-Cooler (TEC-device) for heating or cooling, and the voltage u to actuate the piezoelectric effect. If the actuator was only thermal, we would utilize a unique cascade controller $C_i(s)$ that would furnish the input control i . In contrast, if the actuator was only piezoelectric, we would utilize a unique cascade controller $C_u(s)$ that would furnish the input control u . For a hybrid actuator, we propose to bring them together in one scheme as pictured in [Fig. 3.14-a](#). In fact, the proposition consists in activating only the controller $C_i(s)$ when the error $\varepsilon = \delta_r - \delta$ is large, to benefit from the large range of the thermal actuation. And when the error ε becomes lower than a threshold denoted δ_{max}^u , the controller $C_u(s)$ is automatically

activated. In this latter situation, the piezoelectric actuation is employed for the fine positioning thanks to its high resolution. The threshold δ_{max}^u is chosen as the maximal range of displacement obtained with the piezoelectric actuation. To manage the automatic switch, the discrete event controller Σ is defined in Eq. (3.20). The two controllers $C_i(s)$ and $C_u(s)$ are designed with standard techniques according to the specifications posed and based on the model in Eq. (2.8) or based on a more simplified model. For instance, we can benefit from the techniques detailed in the previous sections (H_∞ , Interval techniques). Fig. 3.14-b depicts an example of step response of the closed-loop controlled hybrid actuator obtained with a proportional-integral (PI) controller for the coarse positioning (i.e. $C_i(s) = PI$), and a proportional-integral-derivative (PID) controller for the fine positioning (i.e. $C_u(s) = PID$). In this, the reference input is a step of $100\mu m$. Because of the limited voltage applicable to the piezoelectric layer, the displacement furnishable by the piezoelectric actuation is very low ($\approx 10\mu m$). Thus, we choose $\delta_{max}^u = 7\mu m$ in this example. The experimental results show the thermal actuation working first until $93\mu m$, and then the piezoelectric actuation performing the fine and accurate positioning.

$$\Sigma := \begin{cases} \text{if } |\varepsilon| > \delta_{max}^u & \text{do} \\ \quad \varepsilon_u = 0 \\ \text{else} \\ \quad \varepsilon_u = \varepsilon \\ \text{end} \end{cases} \quad (3.20)$$

Let us now see the force control for the other hybrid actuator. The output of the actuator is the manipulation force which is the force applied by this to the object. Similarly to the case of multimorph piezoelectric actuators described in Section. 3.2.2, the object's characteristics strongly affect the behavior of the hybrid actuator and they need to be accounted for in the model. The additional challenge with the hybrid actuator is that we have two input control u and i , and they cannot be used haphazardly because of the limited resolution of the thermal actuation and of the limited range of the piezoelectric one. The force model of the hybrid actuator is directly defined by the generalized force model in Eq. (3.2.2). This force model includes the thermal contribution and the piezoelectric contribution. It has the same structure (two inputs and two outputs) and the same principle than in displacement. Therefore, the same controllers structures and synthesis than for displacement can be easily employed for the force.

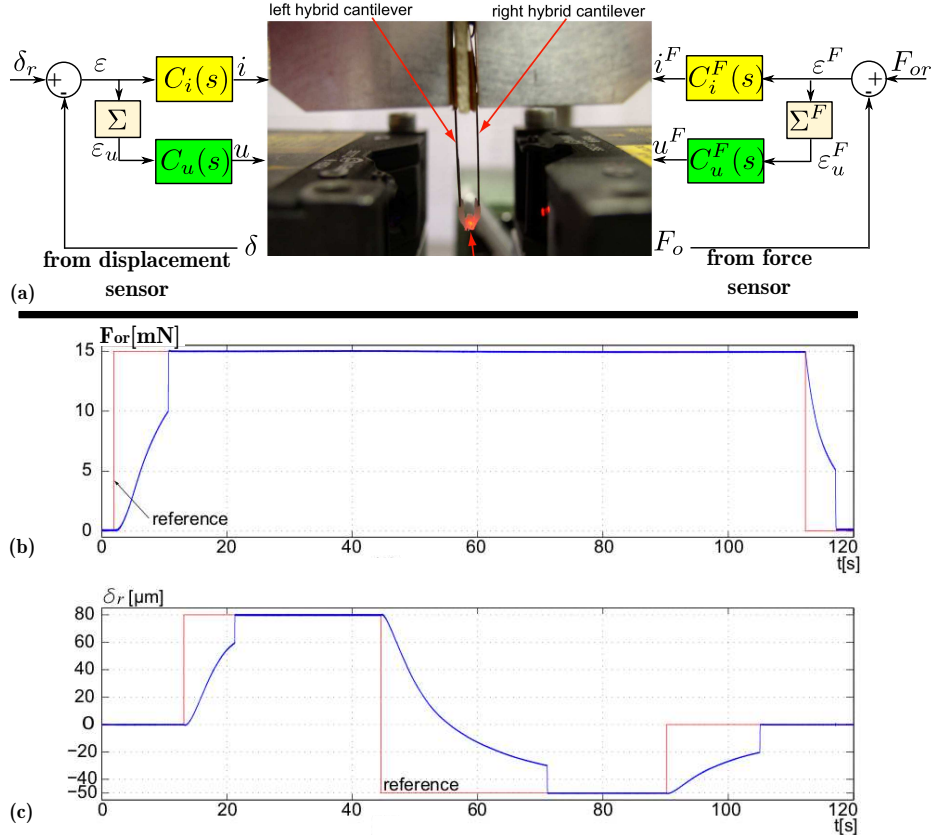


Figure 3.15: Position/force control of the hybrid thermopiezoelectric microgripper. (a): implementation scheme. (b) and (c): experimental results.

We have now the displacement controllers for one actuator and the force controllers the other actuator. They can be directly employed to fully control the hybrid microgripper as depicted in Fig. 3.15-a, [J14]. The corresponding experimental results are presented in Fig. 3.15-b and demonstrate the performances during a pick-and-place task of a small object with position/force control. In this example, the handling force was set equal to $15mN$.

Acknowledgments - The works here were within the postdoctoral fellowship of Dr. Ioan Alexandru Ivan.

3.6 Conclusions and perspectives

Among the efficient ways to enhance the performances of piezoelectric actuators are robust control techniques. A large part of this chapter describes robust control techniques devoted to such actuators in order to reach certain performances required in precise and high dynamics positioning. In a first approach, classical robust techniques (H_∞ and its derivatives) have been proposed. The literature also proposes similar synthesis but the difference of the present

works resides on how to model the actuators in order to conveniently account for the hysteresis and creep nonlinearities as well as the dynamics and the external disturbances (external force, thermal variation).

A more exotic synthesis of robust controllers proposed in this chapter consists in combining intervals and related techniques with control theory. We show that doing so presents multiple advantages: ease and natural way of modeling the uncertainties, performances robustness and guarantee of the solution, and derivation of low order controllers. Combining interval techniques with control theory are not only limited to modeling and controllers synthesis. Other important fields in control and in design can also be covered: structural analysis and *a posteriori* performances analysis, inverse design of systems (see [Section. 2.6](#)). More generally, interval techniques can bring additional degrees of freedom to control theory and related fields and there are a lot to explore in this combination. Features include the extension to nonlinear control and to multivariable control.

The last part of the chapter presents exotic control devoted to hybrid thermopiezoelectric actuators and hybrid microgrippers. Many of systems found in precise positioning are often non-classical⁷ in their functionings, principles and behaviors and are less widespread than classical sized systems. Examples include the hybrid thermopiezoelectric actuators of this chapter, stick-slip actuated systems, inch-worm actuated systems, bubble based actuators, non-contact magnetopiezoelectric actuators, and all smart material based miniaturized systems ... Generally, a new non-classical system demands a devoted control technique.

⁷Non-classical here means different from those of classically sized systems.

Chapter 4

Feedforward control

The control of piezoelectric positioning systems with feedback techniques has been detailed in [Chapter. 3](#). To make possible these feedback schemes, sensors are needed. However, integrating sensors in many micro- and nanopositioning systems is still a great challenge. On the one hand, sensors that have the required performances (accuracy, bandwidth, range of measurement...) are bulky and non-integrable in most of them and are very expensive. Examples include optical sensors based on the triangulation principle and interferometers. On the other hand, integrable sensors like strain gages have performances that are not convenient for the studied systems (noisy, limited range, ...). An emerging topics that is very interesting is the open-loop or feedforward control techniques. These techniques do not need sensors and they are therefore well appreciated for miniaturized systems, including those devoted to precise and high dynamics positioning, because of the high integration and high packaging level offered and because of the low costs. This chapter deals with the feedforward control of piezoelectric systems for precise and high dynamics positioning. The nonlinearities (hysteresis and creep) and the badly damped vibrations that typify these systems are the main challenges to be considered.

Contents

4.1	Introduction	86
4.2	Creep modeling and control	87
4.2.1	Overview	87
4.2.2	Creep modeling	88
4.2.3	Feedforward control by using the inverse multiplicative structure . .	89
4.2.4	Multivariable creep modeling and control	90
4.3	Hysteresis modeling and control	92
4.3.1	Overview	93
4.3.2	Inverse multiplicative structure combined with monovariable and rate-independent cases	96
4.3.3	Inverse multiplicative structure combined with multivariable and rate-independent hysteresis	98
4.3.4	Other ongoing works and perspectives	103
4.3.5	Acknowledgements	104

4.4	Badly damped vibration modeling and control	104
4.5	Complete feedforward control	106
4.6	Conclusion and perspectives	107

4.1 Introduction

The principle scheme of a feedforward control is depicted in Fig. 4.1. The system has a driving input u and an output δ and is controlled by the controller without sensor. The controller is also called compensator. The objective is to lead δ to be equal to the reference δ_r with or without particular specification in the transient part.

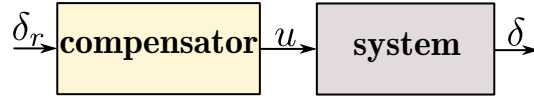


Figure 4.1: Feedforward control of a system.

Feedforward control is well known in robotics thanks to the inverse kinematic control techniques [244; 245]. The objective consists in applying as controller the inverse kinematic model such that the pose of the robot be equal to a desired pose. Based on the dimensions and on the structure of the robot, the kinematic model is seen as a "static model" and the main challenges reside in its invertibility, (sometimes) unicity of solution and the complexity of the calculation and implementation. Both closed-form and approximate inverses exist. In miniaturized systems and in microsystems, feedforward control is more than appreciated. First, due to the lack of convenient sensors for most of the systems, novel architectures of control that require a minimum number of sensors are very welcome. Second, feedforward control techniques permit a high level of packaging and integration that are consistent with the trends of miniaturized systems. Finally, since no sensors are used, they are cheaper and are interesting for the development of batch and performant systems. Regarding the feedforward control of piezoelectric systems, the challenge lies in the strong and nonclassical nonlinearities which are the hysteresis and the creep. Additionally to this, the high-Q factor of many piezoelectric structures decreases the performances of the positioning tasks (settling time augmented, large overshoots,...) and should also be controlled. The synthesis of the compensator is therefore faced to these behaviors which are new relative to the classical challenges in robotics feedforward control. This chapter deals with the feedforward control of piezoelectric systems with consideration of the creep, the hysteresis and the dynamics.

The chapter is organized as follows. First, we present the individual feedforward control of the three phenomena (creep, hysteresis and dynamics) in Section. 4.2, Section. 4.3 and Section. 4.4 respectively. Then, we give Section. 4.5 their simultaneous control. Finally, conclusions and perspectives are given in the last section.

4.2 Creep modeling and control

4.2.1 Overview

The creep is a nonlinear phenomenon mainly found in piezoelectric ceramics at very low frequency. It can be observed as the slow drift occurring when a step input electrical field is applied to these materials, see Fig. 1.8. In the literature, the modeling and the control (feedback or feedforward) of piezoelectric systems with particular attention to the creep is much less frequent than for hysteresis. However, the loss of accuracy brought by this phenomenon renders necessary to consider and to control the creep in precise positioning.

Two feedforward control classes exist for the creep: the charge control and the voltage control. In the charge control, the driving input is the charge instead of the voltage [246–250]. In fact, the behavior in the charge-strain map of a piezoelectric system is shown to exhibit very low, if not zero, nonlinearities (hysteresis and creep). The control principle consists in cascading with the piezoelectric system a well designed electrical circuit that is capable of furnishing the charge driving signal. However, this electrical circuit may introduce additional delay or may reduce the overall bandwidth. In voltage control, the driving input is the voltage. This is more convenient for dynamical control purpose and is easy to setup. However, the nonlinearities (creep and hysteresis) are strong in this and should correctly be modeled and compensated for.

Different creep models have been used in voltage control. In [251–255], a logarithmic function in the time domain is used. To compensate for the creep, an opposite logarithmic model is established for the applied voltage so that the final piezoelectric strain will remain constant. Another technique consists in using LTI¹ models [255–258]. It comes back to an exponential based function in the time-domain. Both the logarithmic function and the LTI models are phenomenological approaches. Another phenomenological approach consists in coupling the creep with the hysteresis models, for instance by using a fractional-order Maxwell resistive capacitor model [259], Prandtl-Ishlinskii models [260–262] or Preisach models [263]. Since the two phenomena are rassembled in one operator, their compensation are performed by one inverse operator. This coupled compensation is only efficient if the identification of the operator's parameters are carried out at different frequencies (very low frequencies and low frequencies). Other creep models from the view of materials have also been proposed but they are not convenient for (feedforward) control point of view [264–266].

LTI models of creep, although linear, are well appreciated because of the wide availability of tools for linear systems, whether in identification, in structural analysis, in quantitative analysis or in synthesis. Furthermore, it has been shown that LTI models were finally more appropriate for predicting creep [255]. The existing way to compensate for a creep modeled by a LTI model is the direct (or standard) inversion of the transfer function [255; 258]. This requires that the model is minimum phase². All creep models do not satisfy this condition and therefore the

¹LTI: Linear Time Invariant system.

²Minimum phase system is when the system and its inverse are stable, and causal.

method is not applicable anymore. To overcome this limitation, we proposed a new approach that does not require a direct inversion. Based on the inverse multiplicative structure, the creep compensator is yielded by re-structuring the identified model. This novel method has been developed for mono-axis piezoelectric systems [BC7][JJ] and was latter extended for multi-axes piezoelectric systems [C35]. It is worth to mention that the study of multivariable compensation of creep (with consideration of the cross-couplings) is novel and was first proposed in this latter paper.

4.2.2 Creep modeling

Reconsider the general model that we proposed in Chapter 2 and that is described by Eq. (2.8):

$$\delta(s) = \Gamma(u(s)) D(s) + C_{creep}(u(s), s) + s_p D(s) F(s) + \Gamma_T(T(s)) D_T(s) \quad (4.1)$$

where u , F and T are the driving voltage (input control), the external force applied to the actuator and the thermal variation respectively. The operator $\Gamma(u(s))$ encompasses the hysteresis nonlinearity and $C_{creep}(u(s), s)$ is the creep operator. The thermomechanical behavior of the structure is given by $\Gamma_T(T(s))$ whilst its compliance by s_p . Finally, $D(s)$ and $D_T(s)$ represent the mechanical dynamics and the thermomechanical dynamics of the structure respectively. These two dynamics are normalized: $D(s=0) = 1$ and $D_T(s=0) = 1$.

Dealing only with the creep, we assume that F and T are null and that the system is linear (no hysteresis considered). Eq. (2.8) becomes:

$$\delta(s) = d_p u(s) D(s) + C_{creep}(u(s), s) \quad (4.2)$$

where d_p is the statical gain of the actuator. It is the linear version of Γ , i.e. $\Gamma(u(s)) = d_p u(s)$. Since we deal with a LTI model of the creep, we have:

$$\delta(s) = d_p u(s) D(s) + C_{cr}(s) u(s) \quad (4.3)$$

with

$$C_r(s) = \frac{\sum_{j=0}^{m_c} b_{cj} s^j}{\sum_{i=0}^{n_c} a_{ci} s^i} \quad (4.4)$$

in which b_{cj} and a_{ci} are the parameters of the creep model to be identified, $m_c > 0$ and $n_c > 0$. For the causality, the following condition should be ensured: $n_c \geq m_c$.

The identification of the parameters of the piezoelectric side $d_p D(s)$ as well as the parameters of the creep model $C_r(s)$ is as follows. A step input voltage $u = A$ is applied to the piezoelectric actuator and the resulting displacement δ is captured for a long period of duration.

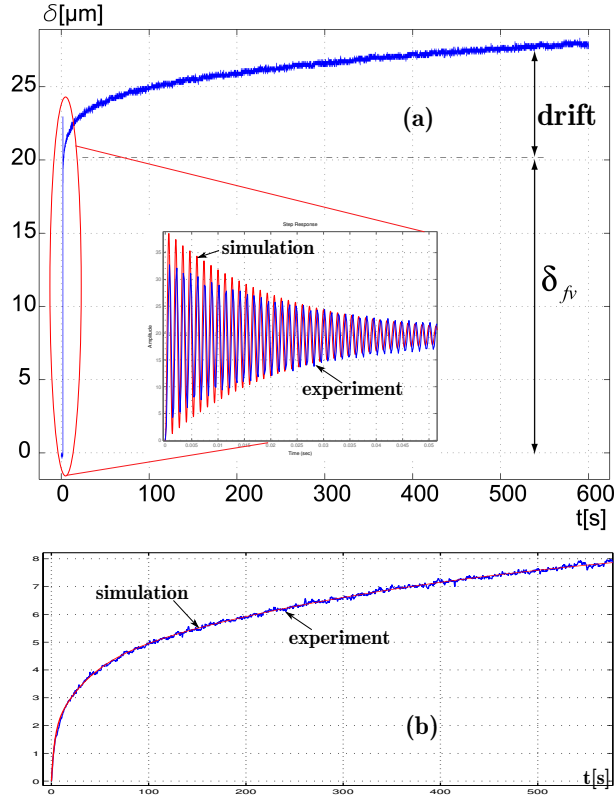


Figure 4.2: Step response of a piezoelectric actuator for creep parameters identification and for dynamics parameters identification.

For unimorph and bimorph piezoelectric actuators with sizes of $15mm \times 2mm \times 0.3mm$, the creep is still observed even beyond $10min$. The piezoelectric side $d_p D(s)$ is identified from the very quick part at the beginning of the response. LTI systems identification techniques (ARMAX, ARX, BJ, OE...) can be employed for that. This part called "transient part" is oscillating in general. Regarding the creep, the drift should be first separated from the step response. Then, once again, we can use LTI systems identification techniques to identify the transfer $C_r(s)$'s parameters. Fig. 4.2-a pictures an example of experimental step response of a piezoelectric actuator with a voltage $u = 40V$ and that will be used for the identification. In the same figure (zoom), we present the zoom of the "transient part" in which the simulation of the identified model $d_p D(s)$ is also plotted. Fig. 4.2-b pictures the experimental separated creep compared with the simulation of the identified model $C_r(s)$. The amplitude of the creep in this case is of $\frac{8\mu m}{20\mu m} = 40\%$. This creep amplitude corresponds to an analysis time of $600s$ and increases for a greater time.

Therefore, the length of the duration to capture the creep is chosen according to the expected application. For instance, in a microassembly task where a constant displacement or constant force during several tens of minutes is played into role, the creep should be characterized and identified at least during similar period of time.

4.2.3 Feedforward control by using the inverse multiplicative structure

Having identified the parameters of the model in Eq. (4.3), we can now focus on the feedforward control of the creep. Because the creep settling time is very high face to the settling time of the transient part defined by $D(s)$, we can simplify this latter as $D(s) = 1$ ($\forall s \in \mathbb{R}^+$), i.e. the transient part is quasi-static. We derive the model utilized for the creep compensation [BC7][JJ]:

$$\delta(s) = d_p u(s) + C_{cr}(s)u(s) \quad (4.5)$$

From this model, we can yield the driving voltage u that meets $\delta = \delta_r$ (δ_r being the reference):

$$u(s) = \frac{1}{d_p} (\delta_r - C_r(s)u(s)) \quad (4.6)$$

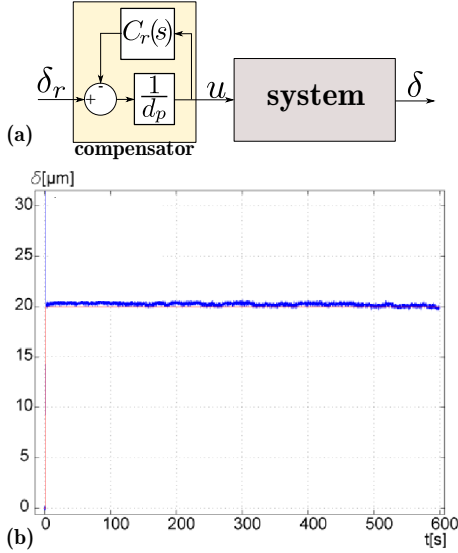


Figure 4.3: (a): implementation of the creep compensator. (b): experimental results.

The implementation scheme of this compensator is depicted in Fig. 4.3-a. As we can observe, the compensator has an inverse multiplicative structure. The main advantage is that we do not need to invert the creep model as usually done in the literature. Therefore, there is no need to satisfy some conditions on the model $C_r(s)$. Indeed, if we denote $N_{cr}(s)$ and $D_{cr}(s)$ the numerator and the denominator respectively of the creep ($C_r(s) = \frac{N_{cr}(s)}{D_{cr}(s)}$), the compensator transfer function is:

$$\frac{u(s)}{\delta_r(s)} = \frac{D_{cr}(s)}{d_p D_{cr}(s) + N_{cr}(s)} \quad (4.7)$$

which is always causal as long as the model $C_r(s)$ itself is causal. As a last remark, the compensator is a restructuring of the model. Thus, as soon as the model is known and identified, the compensator is directly known. Fig. 4.3-b pictures the experimental results obtained when applying the compensator to the actuator that has the initial creep depicted in Fig. 4.2.

It is worth to note that, not only the creep is compensated, but the accuracy is also reached since we have $\delta = \delta_r$. This accuracy was obtained thanks to the inversion of the static gain $\frac{1}{d_p}$. In the particular experimental results of Fig. 4.2 and Fig. 4.3-b, we conclude that the creep was reduced from 40% -without the compensator- to less than 2% with the proposed compensator.

4.2.4 Multivariable creep modeling and control

The results here are detailed in [C35]. The previous creep compensator was only valuable for piezoelectric actuator having one degree of freedom. In order to extend this to multivariable creep compensator, we need first to write the model of a multi-axes piezoelectric actuator with the same assumption than previously: the force and the temperature variation are null and the hysteresis is not considered. Thus, the monovariable model of Eq. (4.3) becomes a matricial equation ³:

$$\delta(s) = (d_p \circ D(s)) u(s) + C_{cr}(s) u(s) \quad (4.8)$$

where

³($A \circ B$) denotes the Hadamard product of matrices $A = [A_{ij}]_{i,j}$ and $B = [B_{ij}]_{i,j}$, *i.e.* ($A \circ B$) = $[A_{ij} B_{ij}]_{i,j}$.

$$\begin{aligned}
\delta &= \begin{pmatrix} \delta_1 \\ \delta_2 \\ \vdots \\ \delta_p \end{pmatrix} & D(s) &= \begin{pmatrix} D_{11}(s) & D_{12}(s) & \cdots & D_{1m}(s) \\ D_{21}(s) & D_{22}(s) & \cdots & \vdots \\ \vdots & \vdots & & \\ D_{p1}(s) & \cdots & & D_{pm}(s) \end{pmatrix} \\
u &= \begin{pmatrix} u_1 \\ u_2 \\ \vdots \\ u_m \end{pmatrix} & C_{cr}(s) &= \begin{pmatrix} C_{cr11}(s) & C_{cr12}(s) & \cdots & C_{cr1m}(s) \\ C_{cr21}(s) & C_{cr22}(s) & \cdots & \vdots \\ \vdots & \vdots & & \\ C_{crp1}(s) & \cdots & & C_{crpm}(s) \end{pmatrix} \\
d_p &= \begin{pmatrix} d_{p11} & d_{p12} & \cdots & d_{p1m} \\ d_{p21} & d_{p22} & \cdots & \vdots \\ \vdots & \vdots & & \\ d_{pp1} & \cdots & & d_{ppm} \end{pmatrix}
\end{aligned} \tag{4.9}$$

The piezoelectric system is fully actuated if $p = m$, underactuated if $p > m$ and overactuated if $p < m$. Again, similarly to the monovisible case, the quasi-static approximation is admitted ($D(s) = 1, \forall s \in \mathbb{R}^+$), and the multivariable model comes back to: $\delta(s) = d_p u(s) + C_{cr}(s)u(s)$. The identification of the parameters for this multivariable model is as follows.

→ First a step input voltage u_1 is applied and the remaining inputs u_j ($j = 2 \cdots m$) is left equal to zero. After capturing the resulted output δ_1 , the direct gain d_{p11} and the direct creep C_{cr11} are identified with the same method presented for the monovisible case.

→ In the meantime, the other outputs δ_i ($i = 2 \cdots p$) are also captured. Each cross-coupling gain d_{pi1} and each cross-coupling creep $C_{cri1}(s)$ are also identified from the experimental output δ_i and input u_1 .

→ Then, the input u_1 is set equal to zero, whilst a step u_j ($j \in \{2, \cdots, m\}$) is applied. For each input u_j applied, all outputs δ_i ($i = 1 \cdots p$) are reported and the gain d_{pij} and the creep C_{crij} are identified. When $i = j$, we have the direct gain and the direct creep. Otherwise, we have the cross-couplings.

The case of the under- and overactuated may require additional criterias to choose the direct transfers and the cross-couplings. This choice strongly depends on the initial design of the system and on the expected applications.

Following the same procedure than in monovisible case, the multivariable compensator is:

$$u(s) = d_p^+ (\delta_r - C_r(s)u(s)) \tag{4.10}$$

where the reference input is $\delta_r = (\delta_{r1} \ \delta_{r2} \ \cdots \ \delta_{rp})^T$ and where $d_p^+ \in \mathbb{R}^{m \times p}$ corresponds to the Moore-Penrose inverse (or pseudo-inverse)⁴ of $d_p \in \mathbb{R}^{p \times m}$ for $m \neq p$. We have $d_p^+ = d_p^{-1}$ when $m = p$.

The above multivariable compensation permits to reduce the creep in the direct transfers, to remove the cross-couplings and to increase the accuracy. That is: $\delta = \delta_r$.

4.3 Hysteresis modeling and control

This section deals with the hysteresis modeling and compensation only. From [Eq. \(2.8\)](#) (or [Eq. \(4.1\)](#)), the model is:

$$\delta(s) = \Gamma_d(u(s), s) \quad (4.11)$$

where $\Gamma_d(u(s), s)$ is the dynamic or rate-dependent hysteresis operator. For a rate-independent hysteresis, we utilize:

$$\delta(s) = \Gamma(u(s)) \quad (4.12)$$

where $\Gamma(\cdot)$ is the static or rate-independent hysteresis operator.

According to the case, we may also utilize the following time domain notations in place of [Eq. \(4.11\)](#) or [Eq. \(4.12\)](#):

$$\delta(t) = \Gamma_d(u(t), t) \quad (4.13)$$

and

$$\delta(t) = \Gamma(u(t)) \quad (4.14)$$

for a rate-dependent and for a rate-independent hysteresis operator respectively.

⁴The Moore-Penrose or pseudo-inverse [267] $D^+ \in \mathbb{R}^{m \times p}$ of a matrix $D \in \mathbb{R}^{p \times m}$ is defined by:

$$D^+ = C^T (CC^T)^{-1} (B^T B)^{-1} B^T$$

where $B \in \mathbb{R}^{p \times k}$ and $C \in \mathbb{R}^{k \times m}$ are any decomposition matrices of D such that $D = BC$. The use of this pseudo inverse guarantees that the solution has a minimum 2-norm in case of over actuated systems and minimizes the 2-norm of the error in the under actuated case. The Moore-Penrose pseudo-inverse has the following properties:

$$\begin{cases} DD^+D = D \\ D^+DD^+ = D^+ \\ (DD^+)^T = DD^+ \\ (D^+D)^T = D^+D \end{cases}$$

4.3.1 Overview

Hysteresis is one of the most discussed behaviors of piezoelectric systems and actuators in the literature. In fact, it is more studied than the creep, probably because its modeling and control require techniques different than classically used like LTI and simple (linear or nonlinear) functions,... The literature is very wide regarding the modeling of hysteresis in smart materials and many classes of techniques exist: 1) class of hysteresis models which are based on the superposition of several elementary operators called hysterons, 2) class of hysteresis models which are based on nonlinear differential equations, 3) linear approximations with uncertainties or with phasers, 4)... These models permit to predict the behaviors of the hysteretic systems or to ease the synthesis of closed-loop controllers. However, only the following approaches address both the modeling and the feedforward control: the parabolic functions based approach, the lookup tables, the Duhem approach, the Preisach approach and the Prandtl-Ishlinskii approach. The parabolic functions [268; 269], the lookup tables [270] and the Duhem [271] approaches have been used for particular cases and particular actuators. In contrary, the Preisach and the Prandtl-Ishlinskii approaches have been employed to track and to compensate for the hysteresis in a wide range of applications. This success is thanks to multiple reasons. First, they are mathematical (or phenomenological) models and thus can be employed independently from the physics of the systems. Second, each of the two approaches possesses various techniques according to the hysteresis to be modeled and to be compensated for, enlarging therefore their wide of applications. They have techniques that can track symmetrical hysteresis, asymmetrical hysteresis, rate-dependent hysteresis, rate-independent hysteresis,... Finally, both the Preisach and the Prandtl-Ishlinskii approaches are among the class based on the superposition of elementary hysteresis. This renders them very accurate subject to a high number of hysterons. In the Preisach approach, the hysteron is a nonideal relay (a delayed relay) and in the Prandtl-Ishlinskii approach, this is a play-operator (also called backlash operator). Relative to the former, the latter presents a very interesting ease of implementation for simulation or for real-time application. Nonetheless, the elegant manipulation of the hysteresis in the Preisach approach and its precedence make it have the same reputation than the Prandtl-Ishlinskii nowadays. The Preisach approach dates back to 1935 with the works of Ferencz Preisach [272] in magnetic systems and latter popularized by Mayergoyz [70], whereas the hysterons utilized in the Prandtl-Ishlinskii approach have been formally introduced in the 80s [71].

In the Preisach approach, the classical Preisach technique permits to track rate-independent or static hysteresis, symmetrical or asymmetrical and saturated or non-saturated. To be modelizable by a classical Preisach model however, the hysteresis of the plant should exhibit the wiping out property and the congruency property. This condition is described by the representation theorem [70]. The extension of the Preisach approach to model hysteresis that do not meet the representation theorem is called the nonlinear Preisach technique. Also, the extension to rate-dependent hysteresis is called the dynamic Preisach technique. Finally, the vector Preisach technique deals with hysteretic systems having two inputs and two outputs. The nonlinear, the rate-dependent and the vector Preisach techniques are called generalized Preisach techniques. The modeling of hysteresis in smart materials with the Preisach approach

is wide. However, the works that deal with the feedforward control in Preisach approach are much less. The modeling and compensation can be found in applications like: magnetic and magnetostrictive [68–70; 273–278], shape memory alloys and magnetic shape memory alloys [279–282], VO₂-coated⁵ systems [283], and piezoelectric systems [241; 257; 284–287].

There are also several techniques in the Prandtl-Ishlinskii (PI) approach. The classical PI technique permits to model and to compensate for rate-independent and symmetrical hysteresis [288; 289]. Later on, it has been extended to track asymmetrical rate-independent hysteresis [290]. The technique is called modified PI. The principle consists in cascading with the classical PI a superposition of deadzone operators that creates the asymmetry. An alternative way to account for the asymmetry was developed in [291]. Called the generalized PI, it utilizes a more generalized hysteron than a backlash, such as hyperbolic tangent function or polynomials for the ascending or for the descending curves instead of straights. [292] proposed the singularity free PI model and compensator in order to track ill-conditioned hysteresis. Ill-conditioned hysteresis are typified by a negative gradient around the turning point and cannot be tracked by the previous techniques. In [293; 294], the rate-dependent PI technique has been developed. In this, the thresholds of the backlashes are dependent on the derivative of the input signal. Another rate-dependent PI model consisted in posing the slopes (or weights) of the backlashes to be rate-dependent [295], instead of the thresholds. Finally, in a recent study [296], a called integrated PI technique was developed. This technique permits to account for rate-dependent and asymmetrical hysteresis by combining the above modified PI with the rate-dependent PI. Apart from the integrated PI technique due its recent development, all the other PI techniques have been efficiently applied for modeling and for feedforward control of piezoelectric systems [239; 256; 297–301][J4][J7][J13][C13][C14][C16][C23][C31][C51].

The above compensation techniques are voltage control. Similarly to creep, there also exists the charge control in hysteresis. In general the same electrical circuit than for creep is employed for the hysteresis [246–250].

The direction I have taken for the works reported in this thesis is multiple. In the first time, it consisted in improving the performances of multimorph piezoelectric actuators devoted to micromanipulation and microassembly context by using the existing techniques [J4][J7][J13][C13][C14][C16][C23][C31][C51]. The objective was to confront the limitation posed by the existing sensors to develop high performant, highly packaged, low cost precise and high dynamics piezoelectric positioners. Over the time, the objective have been evolving. Face to the development of multi-axes piezoelectric systems at the department (ANR C-MUMS, ANR MYMESYS projects,...), and to the raise of multi-axes actuated microsystems these last years in the litterature, it was necessary to propose novel approaches to model and to feedforward control multivariable hysteresis. This because all the above mentionned hysteresis approaches are monovariable and cannot track and compensate for hysteresis in multi-axes (multi-DOF) asystems.

⁵VO₂: vanadium dioxide is a thermally induced solid-to-solid phase transition material.

As far as we know, the only formulation of multivariable hysteresis model is based on the vector Preisach hysteresis developed by Mayergoyz [70]. The principle consists in extending a Preisach model into bi-variable hysteresis. In this, a vector hysteresis is based on the projection of a scalar hysteresis $\Gamma(u(t))$ along two directions x and y to yield vector components with a constraint parameter $\phi(t)$: $\Gamma_x(u(t)) = \Gamma(u(t)) \cos(\phi(t))$ and $\Gamma_y(u(t)) = \Gamma(u(t)) \sin(\phi(t))$. Further, the concept of vector hysteresis initially developed for a Preisach approach has been transposed to the play/stop-operators based hysteresis model [302; 303]. Because of the circular constraint with the parameter $\phi(t)$, vector models are well adapted to formulate the hysteresis in rotative magnetic systems [277; 278]. They cannot however track the hysteresis in multiple degrees of freedom where the cross-couplings are independent.

When dealing with multivariable hysteresis, several challenges are posed. Cross-couplings exist and should be modeled and compensated for. The identification procedure is more complex than for monovisible cases. The number of the model and compensator parameters substantially increases with the number of degrees of freedom, but the compensator should not be complex and not expensive in calculation and in implementation. The system itself can be square or rectangular. In this latter case, the compensation calculation becomes delicate. A novel method of modeling and compensation which handles these challenges is therefore proposed in our works. Regarding the compensation, the inverse multiplicative structure, which was already employed for the creep compensation, is again very useful here. As we will see, this structure will greatly ease the compensator calculation. The proposed compensation structure itself is valuable for any hysteresis approaches (Prandtl-Ishlinskii, Preisach, ...) under the condition that the model is rewritable as:

$$\delta(t) = \Gamma_d(u(t), t) = \rho_d u(t) + \Gamma_d^o(u(t), t) \quad (4.15)$$

for a rate-dependent hysteresis, and

$$\delta(t) = \Gamma(u(t)) = \rho u(t) + \Gamma^o(u(t)) \quad (4.16)$$

for a rate-independent hysteresis. In the two equations, ρ_d (resp. ρ) is invertible and Γ_d^o (resp. Γ^o) is function of the initial model Γ_d (resp. Γ).

A modeling and a compensation scheme based on this proposed structure and on the inverse multiplicative structure has first been applied to the classical Bouc-Wen model in our papers [BC5][J12], which is monovisible. Then, we extended this into multivariable classical Bouc-Wen modeling and compensation [J24][C48]. Further, we again extended this latter to multivariable generalized Bouc-Wen modeling and compensation [C53] to account for the asymmetry in hysteresis. Prior to these works, no compensation study existed for the Bouc-Wen approach, even in monovisible case.

In parallel, we also apply the method to the Prandtl-Ishlinskii approach. First, a new compensation for the classical Prandtl-Ishlinskii technique was proposed based on the inverse multiple structure [C36]. Then, we extended this to multivariable classical Prandtl-Ishlinskii

modeling and compensation⁶. The application to other techniques (rate-dependent PI, generalized PI) technique, is also being investigated⁷.

Since, the proposed structure of modeling (Eq. (4.15) and Eq. (4.16)) and the compensation (inverse multiplicative structure) were employed by external researchers for other hysteresis approach, for example for the Preisach [304].

4.3.2 Inverse multiplicative structure combined with monovariate and rate-independent cases

For the monovariate and rate-independent case, if we can rearrange a hysteresis model to have the structure in Eq. (4.16), we can calculate a hysteresis compensator with which the output δ meets the reference input δ_r ($\delta(t) = \delta_r(t)$, for $t > t_1$ and $t_1 \geq 0$) as follows [BC5][J12][C36]:

$$u(t) = \frac{1}{\rho} (\delta_r(t) - \Gamma^o(u(t))) \quad (4.17)$$

The block diagram of this compensator has the same structure than for the creep as depicted in Fig. 4.3-a. This structure is an inverse multiplicative structure with a nonlinear (local) feedback which is $\Gamma^o(u(t))$, contrary to the creep which is a linear feedback. The compensator is a rearrangement of the initial model. As soon as the model is identified, the compensator is also obtained. This is a great advantage because there is no need to extracalculate the compensator parameters.

4.3.2.1 Application to the classical Bouc-Wen model

The Bouc model of hysteresis [305] - further modified by Wen [306] - was initially used for nonlinear vibrational mechanics [307; 308]. The Bouc-Wen model has an interesting simplicity and is able to represent a large class of hysteresis. It is based on a state variable h . The classical Bouc-Wen model that is adapted for piezoelectric actuators [309] is:

$$\begin{cases} \delta(t) = d_p u(t) - h(t), & \delta(t_0) = y_0 \\ \frac{dh}{dt} = A_{bw} \frac{du}{dt} - B_{bw} \left| \frac{du}{dt} \right| h - G_{bw} \frac{du}{dt} |h|, & h(t_0) = h_0 \end{cases} \quad (4.18)$$

where A_{bw} controls the restoring force amplitude, B_{bw} and G_{bw} control the shape of the hysteresis loop. Parameter d_p represents the piezoelectric coefficient and is strictly positive. This model is valid for rate-independent and symmetrical monovariate hysteresis. The first equation is the output equation and the second equation (nonlinear and differential) is the hysteresis state equation. Many works reported on the identification procedure of these coefficients [310; 311]. This model can be rewritten to have the same structure than in Eq. (4.16), that is [J12]:

⁶ The results on the modeling and compensation of multivariable classical Prandtl-Ishlinskii technique have been submitted at IEEE Transactions on Control Systems Technology in July 2014.

⁷ The results on inverse multiplicative structure based compensation of rate-dependent Prandtl-Ishlinskii technique have been submitted at IEEE/ASME Transactions on Mechatronics in September 2014.

$$\delta(t) = d_p u(t) - H(u(t)) \quad (4.19)$$

where $H(u(t))$ is a nonlinear operator that describes the state $h(t)$, i.e. $h(t) = H(u(t))$. This operator is characterized by the second equation of Eq. (4.18).

Having the model Eq. (4.19), we easily derive the compensator based on the inverse multiplicative structure in Eq. (4.17) [BC5][J12]:

$$u(t) = \frac{1}{d_p} (\delta_r(t) + H(u(t))) \quad (4.20)$$

4.3.2.2 Application to the classical Prandtl-Ishlinskii technique

A classical Prandtl-Ishlinskii model of hysteresis $\Gamma(u(t))$ is based on the superposition of n_h elementary hysteresis called hysterons. The hysteron itself is the play-operator, also called backlash, that we denote $\gamma(u(t))$ and which is defined by:

$$\delta(t) = \gamma(u(t)) = \max\{u(t) - r, \min\{u(t) + r, \delta(t - T_s)\}\} \quad (4.21)$$

where T_s is the sampling period and $\delta(t - T_s)$ is the output of the backlash at the previous sampling time. The threshold of the backlash is given by r .

The classical Prandtl-Ishlinskii model of hysteresis is therefore [71]:

$$\delta(t) = \Gamma(u(t)) = \sum_{k=1}^{n_h} w_k \gamma_k(u(t)) = \sum_{k=1}^{n_h} w_k \max\{u(t) - r_k, \min\{u(t) + r_k, \delta_{ek}(t - T_s)\}\} \quad (4.22)$$

where w_k is the weightings (or slope), r_k the threshold and δ_{ek} the elementary output of the k^{th} backlash. We have: $0 \leq r_1 \leq r_2 \leq \dots \leq r_k$, and $w_k > 0$. The identification procedure of the parameters w_k and r_k can be done with the least-square method [295] or by closed-form formula [288][J7].

To compensate for a hysteresis modeled by the classical Prandtl-Ishlinskii technique, the existing technique consists in cascading with the plant another classical Prandtl-Ishlinskii model [288]. To obtain the compensation condition $\delta(t) = \delta_r(t)$ for $t > t_1$ (with $t_1 \geq 0$), the hysteresis of the compensator is taken as symmetrical with the hysteresis of the initial model relative to the unitary straightline. A closed form formula based on this symmetry permits afterwards to calculate the parameters (thresholds and weightings) of the compensator.

An alternative way to this existing compensator is based on the inverse multiplicative structure, as we propose in Eq. (4.17). This requires that the model Eq. (4.22) be rearranged to have the same structure than Eq. (4.16). We have the following proposition:

Proposition 4.3.1. *The classical Prandtl-Ishlinskii model in Eq. (4.22) is equivalent to:*

$$\delta(t) = -u(t) + \sum_{k=0}^{n_h} w_k \cdot \max \{u(t) - r_k, \min \{u(t) + r_k, \delta_{ek}(t - T_s)\}\}$$

with $r_0 = 0$ and $w_0 = 1$.

Proof. See [C36]. □

We have therefore the following compensator which has an inverse multiplicative structure.

Theorem 4.3.1. *Reconsider the classical Prandtl-Ishlinskii hysteresis model in Eq. (4.22) which is rewritable like in Proposition. 4.3.1. The following control law:*

$$u(t) = \sum_{k=0}^n w_k \cdot \max \{u(t - T) - r_i, \min \{u(t - T_s) + r_k, \delta_{ek}(t - 2T_s)\}\} - \delta_r(t)$$

yields

$$\frac{\partial \delta}{\partial \delta_r} \simeq 1$$

and therefore results in the (approximate) compensation of the hysteresis.

Proof. See [C36]. □

Let us rewrite the compensator in Theorem. 4.3.1 to be in function of the initial model Eq. (4.22):

$$\begin{aligned} u(t) &= \delta_r(t) + u(t - T_s) - \sum_{k=1}^{n_h} w_k \max \{u(t - T_s) - r_k, \min \{u(t - T_s) + r_k, \delta_k(t - 2T_s)\}\} \\ &= \delta_r(t) + u(t - T_s) - \Gamma(u(t - T_s)) \end{aligned} \tag{4.23}$$

which has the same structure than Eq. (4.17), with $\rho = 1$ and $\Gamma^o(u(t)) = u(t - T_s) - \Gamma(u(t - T_s))$. Again the compensator is a rearrangement of the initial model, at a one sampling period delay. The advantage of this compensator compared to the method in [288] is the no need of extra calculation of the compensator. This advantage is highly appreciated when we extend the technique to multivariable hysteresis.

4.3.3 Inverse multiplicative structure combined with multivariable and rate-independent hysteresis

First we provide the definition of multivariable rate-independent hysteresis [B4].

Definition 4.3.1. *A multivariable rate-independent hysteresis $\Gamma(u(t))$ is an operator that has a vector of inputs $u(t) = (u_1(t) \ u_2(t) \ \cdots \ u_m(t))^T$ and a vector of outputs $\delta(t) = (\delta_1(t) \ \delta_2(t) \ \cdots \ \delta_p(t))^T$ such that*

$$\delta(t) = \Gamma(u(t)) \Leftrightarrow \begin{pmatrix} \delta_1(t) \\ \delta_2(t) \\ \vdots \\ \delta_p(t) \end{pmatrix} = \begin{pmatrix} \Gamma_1(u_1(t), u_2(t), \dots, u_m(t)) \\ \Gamma_2(u_1(t), u_2(t), \dots, u_m(t)) \\ \vdots \\ \Gamma_p(u_1(t), u_2(t), \dots, u_m(t)) \end{pmatrix}$$

where each of the operators $\Gamma_i(u(t))$, $i = 1 \dots p$, are either hysteresis or affine⁸.

Similarly to the creep, let us assume that the cross-couplings are additive. The model in [Definition 4.3.1](#) becomes:

$$\delta(t) = \begin{pmatrix} \delta_1(t) \\ \delta_2(t) \\ \vdots \\ \delta_p(t) \end{pmatrix} = \Gamma(u(t)) = \begin{pmatrix} \sum_{j=1}^m \Gamma_{1j}(u_j(t)) \\ \sum_{j=1}^m \Gamma_{2j}(u_j(t)) \\ \vdots \\ \sum_{j=1}^m \Gamma_{pj}(u_j(t)) \end{pmatrix} \quad (4.24)$$

The rewriting of the model [Eq. \(4.24\)](#) to match with the structure in [Eq. \(4.16\)](#) yields a matrix $\rho \in \mathbb{R}^{p \times m}$ and a vector $\Gamma^o(u(t)) = (\Gamma_1^o(u(t)) \quad \Gamma_2^o(u(t)) \quad \dots \quad \Gamma_p^o(u(t)))^T$.

For square systems ($m = p$), ρ is assumed to be nonsingular. In fact, during the actuator or system design, the designer will do such that each input u_i will drive an output δ_i . In the ideal case where no cross-couplings exist, this matrix is diagonal with non-null components. In the real case, the system exhibits cross-couplings. The only situation in which ρ is singular is that all cross-couplings in one axis i caused by all inputs u_j ($j = 1 \dots m$ and $j \neq i$) compensate for the direct transfer from u_i . This case is very rare and in general the designers will not allow such case. For nonsquare systems ($m \neq p$), which stands for over or underactuated systems, we assume that $\text{rank}(\rho) = \min\{p, m\}$.

When the number of degrees of freedom of the systems or of the actuators increases, the number of parameters of the model $\Gamma(u(t)) = \rho + \Gamma^o(u(t))$ substantially increases. For instance, if we extend the classical Prandtl-Ishlinskii model extended into multivariable with m inputs and p outputs and where each of the operator Γ_{ij} ($i = 1 \dots p$ and $j = 1 \dots m$) of the [Eq. \(4.24\)](#) has n_{ij} backlashes, the total number of parameters to be identified is:

$$2 \times \left(\sum_{i=1}^p \sum_{j=1}^m n_{ij} \right) \quad (4.25)$$

where there are $\sum_{i=1}^p \sum_{j=1}^m n_{ij}$ weightings and $\sum_{i=1}^p \sum_{j=1}^m n_{ij}$ thresholds. If the number of hysterons of each component $\Gamma_{ij}(u_j(t))$ is the same and equal to n_h , we have [Eq. \(4.25\)](#) equal to:

⁸It is worth to notice that affine, and consequently linear, models are particular cases of almost all hysteresis models.

$$2 \times p \times m \times n_h \quad (4.26)$$

If identifying the model parameters is an inevitable step, we can avoid or lessen the calculation of the compensator parameters. This is what the inverse multiplicative structured compensator also brings. As soon as the multivariable model is known and identified, the compensator is yielded by restructuring this. Lessening the calculation will reduce the time spent, the risk of errors and the complexity of the technique. Regarding the identification procedure of the initial model itself, the steps are similar to that of the multivariable creep, but a sine input voltage is applied instead of a step.

When the multivariable model parameters are identified, the multivariable compensator based on the inverse multiplicative structure with which the output δ meets the reference δ_r is derived:

$$u(t) = \rho^+ (\delta_r(t) - \Gamma^o(u(t))) \quad (4.27)$$

This above method multivariable modeling and compensation have been applied to extend the classical Bouc-Wen technique and the classical Prandtl-Ishlinskii technique. They will be reminded below.

4.3.3.1 Extension of the classical Bouc-Wen technique

The works here are detailed in [J24][C48].

The proposed multivariable classical Bouc-Wen model is:

$$\begin{cases} \delta(t) = d_p u(t) - h(t) \\ \frac{dh}{dt} = A_{bw} \frac{du}{dt} - B_{bw} (|\frac{d\bar{u}}{dt}| \circ \bar{h}) - G_{bw} (\frac{d\bar{u}}{dt} \circ |\bar{h}|) \end{cases} \quad (4.28)$$

where $i = 1 \cdots p$ and $j = 1 \cdots m$, and where the matrices are

$$d_p = (d_{pij}); \quad A_{bw} = (A_{bwi j}); \quad B_{bw} = (B_{bwi j}); \quad G_{bw} = (G_{bwi j}) \quad (4.29)$$

with⁹

⁹ $[O]_{k \times l}$ is the matrix of zero with dimension of: $k \times l$.

$$\begin{aligned}
& \text{if } p > m \\
& \quad \bar{u} = \begin{pmatrix} u \\ [0]_{(p-m) \times 1} \end{pmatrix} \\
& \quad \bar{h} = h \\
& \text{if } p < m \\
& \quad \bar{h} = \begin{pmatrix} u \\ [0]_{(m-p) \times 1} \end{pmatrix} \\
& \quad \bar{u} = u \\
& \text{if } p = m \\
& \quad \bar{u} = u \\
& \quad \bar{h} = h \\
& \text{endif}
\end{aligned} \tag{4.30}$$

This multivariable classical Bouc-Wen model already has the model structure in Eq. (4.16), in which $\rho = d_p$ and $\Gamma^o(u(t)) = -H(u(t))$. The hysteresis state $h(t) = H(u(t))$ is defined by the second equation of Eq. (4.28). The multivariable compensator such that the output δ meets the reference input δ_r is therefore deduced from the compensator structure Eq. (4.27) and from the model Eq. (4.28):

$$\begin{cases} u(t) = d_p^+ (\delta_r(t) + H(u(t))) \\ H(u(t)) = h(t) \\ \frac{dh}{dt} = A_{bw} \frac{du}{dt} - B_{bw} (|\frac{d\bar{u}}{dt}| \circ \bar{h}) - G_{bw} (\frac{d\bar{u}}{dt} \circ |\bar{h}|) \end{cases} \tag{4.31}$$

4.3.3.2 Extension of the classical Prandtl-Ishlinskii technique

The monovariale classical Prandtl-Ishlinskii model is extended into multivariable in this subsection. The multivariable compensation is based on the inverse multiplicative structure of Eq. (4.27)¹⁰.

A multivariable classical Prandtl-Ishlinskii model is:

$$\begin{cases} \delta(t) = \begin{pmatrix} \delta_1(t) \\ \delta_2(t) \\ \vdots \\ \delta_p(t) \end{pmatrix} = \Gamma(u(t)) = \begin{pmatrix} \sum_{k=1}^m \Gamma_{1k}(u_k(t)) \\ \sum_{k=1}^m \Gamma_{2k}(u_k(t)) \\ \vdots \\ \sum_{k=1}^m \Gamma_{pk}(u_k(t)) \end{pmatrix} \\ \Gamma_{ij}(u_j(t)) = \sum_{k=1}^{n_{ijh}} w_{ijk} \gamma_{ijk}(u_j(t)) = \sum_{k=1}^{n_{ijh}} w_{ijk} \max \{u_j(t) - r_{ijk}, \min \{u_j(t) + r_{ijk}, \delta_{ijk}(t - T_s)\}\} \end{cases} \tag{4.32}$$

¹⁰The results on the modeling and compensation of multivariable classical Prandtl-Ishlinskii technique have been submitted at IEEE Transactions on Control Systems Technology in July 2014.

where γ_{ijk} , with $i \in \{1, 2, \dots, p\}$ and $j \in \{1, 2, \dots, m\}$, is the k^{th} backlash and its elementary output is δ_{ijk} . The number of backlashes in $\Gamma_{ij}(u_j(t))$ is n_{ijk} and its weighting as well as its threshold are w_{ijk} and r_{ijk} respectively. The total number of parameters to be identified for the whole multivariable classical Prandtl-Ishlinskii model is given by Eq. (4.25).

The following theorem gives a multivariable compensator for the model in Eq. (4.32).

Theorem 4.3.2. *The following compensator:*

$$u(t) = \delta_r(t) + u(t - T_s) - \Gamma(u(t - T_s))$$

is a multivariable approximate compensator for the multivariable classical Prandtl-Ishlinskii hysteresis model defined by Eq. (4.32).

Proof. See ¹¹

□

4.3.3.3 Experimental results

The multivariable modeling and compensation (classical Bouc-Wen and classical Prandtl-Ishlinskii) have been successfully applied to the multimorph 2-DOF piezoelectric actuator and to a 3-DOF piezoelectric tube (piezotube) scanner [J24][C48]¹². Fig. 4.4 presents the results with the piezotube when two axes (x and y) are controlled. The piezotube, depicted in Fig. 4.4-a, b and c, can provide bendings δ_x and δ_y along the two axes when subjected to a voltage u_x and u_y respectively. Fig. 4.4-d and g present the hysteresis nonlinearities exhibited by the actuator along these axes. The amplitudes of the hysteresis are $\frac{h}{H} = 36\%$ and 33% respectively. Additionally to these nonlinearities, the actuator also exhibits cross-couplings. They are depicted in Fig. 4.4-e and f. The proposed multivariable classical Prandtl-Ishlinskii compensator permits to reduce the hysteresis and to linearize the direct transfer. Fig. 4.4-h and k show these compensated results. Furthermore, the compensator also permits to substantially reduce the cross-couplings. Fig. 4.4-i and j show the results. Different tests of tracking of complex spatial trajectories have also been carried out: tracking of spatial circular (Fig. 4.4-l) and spatial Lissajous trajectories (Fig. 4.4-m). Lissajous curves have been considered as interesting reference signal for high speed scanning in atomic force microscopy in these piezotubes are widely used [312]. The experimental results demonstrated that the absolute error does not exceed $0.8\mu m$. Although the frequency of identification is $0.1Hz$, the experiments also demonstrate that the bandwidth (in excess of $10Hz$) can be higher. Generally, $10Hz$ of bandwidth is still low for certain applications. In fact, the classical Prandtl-Ishlinskii model and the classical Bouc-Wen model are rate-independent. To increase the bandwidth therefore, rate-dependent hysteresis models should be used instead. This is one of the ongoing works carried out.

¹¹The results on the modeling and compensation of multivariable classical Prandtl-Ishlinskii technique have been submitted at IEEE Transactions on Control Systems Technology in July 2014.

¹²Submitted to IEEE TCST 2014.

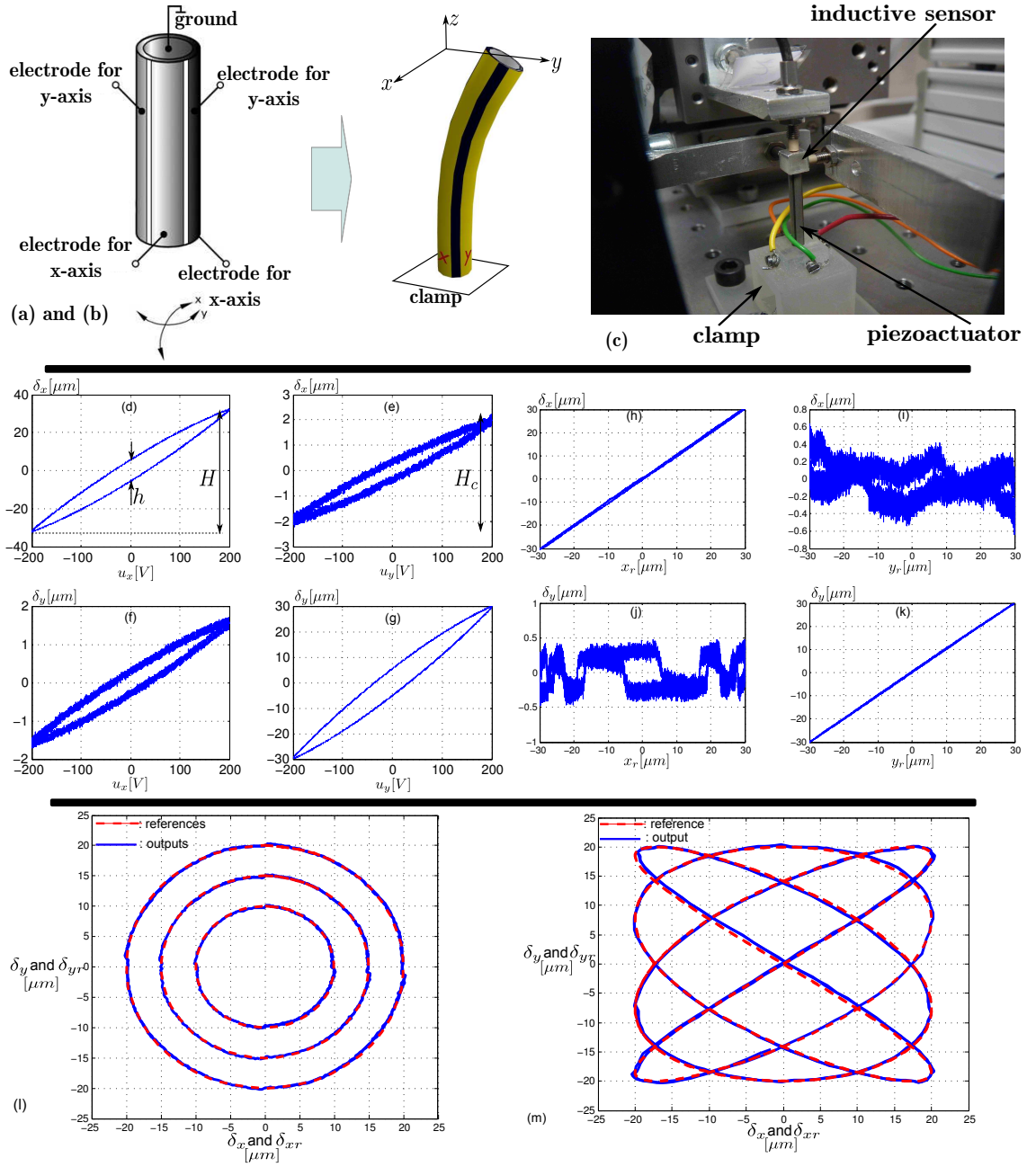


Figure 4.4: Feedforward control of a 2-DOF piezoelectric actuator.

4.3.4 Other ongoing works and perspectives

One of the main advantages of the inverse multiplicative as compensators structure is its applicability in many hysteresis models as long as it is possible to express them with the same structure than Eq. (4.15) for the rate-dependent case or Eq. (4.16) for the rate-independent

case. In [C53], we dealt with a novel multivariable generalized Bouc-Wen technique that consists of compensating asymmetrical hysteresis in multi-DOF systems. Additionally to the compensation, the proposed technique is an extension of the monovaryable generalized Bouc-Wen model described in [313]. The compensation of multivariable rate-dependent hysteresis (Bouc-Wen and Prandtl-Ishlinskii approaches) has also been started.

4.3.5 Acknowledgements

The works regarding the feedforward control of hysteresis have been or are carried out within the postdoctoral fellowship of Dr. Omar Al Janaideh, the PhD fellowship of Didace Habineza and the internships of Qihong Zhou and Mamadou Cissé Diouf.

4.4 Badly damped vibration modeling and control

In precise positioning, the badly damped vibration exhibited by piezoelectric actuators when excited to brusque driving voltage is an unwanted phenomenon. As an example, during an image scanning with a scanning probe microscope, this vibration deforms the scanned image and induces errors. The errors can be reduced by limiting the rate of the driving input, however this will affect the scanning speed. Another example is when performing micromanipulation or microassembly tasks with microgrippers, the overshoots from the vibration may destroy the manipulated objects or the manipulators themselves. In a performances point of view, a badly damped vibration unfortunately increases the settling time of a system, even if this latter has a wide bandwidth. It is therefore important to attenuate the vibration.

The feedforward control of vibration in piezoelectric actuators raised less studies than the feedforward control of the hysteresis, contrary to its feedback control which is very common (see Chapter. 3 and Chapter. 5). The main and initial works of feedforward vibration control in piezoelectric systems dealt with the vibration in piezotube scanners for scanning probe microscopes. Due to the vibration, the images provided by the scanning are deformed and thus erroneous. In order to increase the images precision, the scanning speed should be reduced. However, a too low scanning speed will limit the throughput of the microscopes. The objective consisted therefore in constructing precise scanned images with a high speed scanning.

The vibration compensator is calculated from a linear dynamic model $D(s)$ that was separated from the hysteresis nonlinearity thanks to the Hammerstein principle. In [234; 257], (exact or standard) model based inversion technique was utilized to compensate for the vibration in piezotube scanners of scanning probe microscopes. The compensator was the direct inversion (D^{-1}) of the model. This calculation of the inverse was also carried out in the time-domain [314]. Subsequently, optimal inversion technique was applied in order to account for model uncertainties or to avoid actuators limitations (bandwidth or input saturation violation) that exact inversion cannot tackle [238; 286]. The main principle consisted in only inverting the model in frequency regions where the modeling uncertainties are supposed to be small. In addition, the actuators constraints such as input energy or the bandwidth limitations can be accounted for by a trade-off on the precision needed. A limitation of the optimal inverse and

of the stable exact inverse is that the inverse input tends to be noncausal [315]. This implies that these techniques can only be applied with reference or desired inputs which are known in advance, which is the case for most of the surface or images scanning in microscopes where the trajectories along axis x and along axis y are repetitive and pre-specified. In [316], the previous optimal technique was extended to preview-based optimal technique such that the reference trajectories can be modified or changed every finite-time (preview-time). Different techniques that permitted to overcome the necessity to pre-specify the trajectories in piezotube scanners were developed later [235–237]. The approaches were based on the zero magnitude tracking error (ZMTEC) and the zero phase tracking error (ZPTEC): the compensators are causal and stable discrete transfer functions that have magnitude or phase equivalent to those of the exact inverses of the models.

All the above employed feedforward control that have been applied to piezoelectric systems are among the class of *model inversion based vibration techniques* and the main applications dealt with actuators in scanning probe microscopes. Another class of feedforward control of vibration is the *input shaping techniques*. In this, the controller, called shaper, transforms the input reference into a superposition of two or several elementary commands that results in the elimination of the vibration. In term of calculation and implementation, this class is very interesting. Even if the order of the system is high or if it has multiple resonances, it is still possible to obtain a good damping with a simple controller calculated only with the first resonance. The first work on input shaping technique, called Posicast technique, was proposed by O.J.M. Smith [317] for mechanical systems. The principle consisted in splitting a step input reference into a stair of two lower steps that permit to the output reach the reference without vibration.

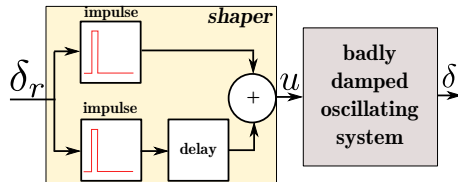


Figure 4.5: Principle of the input shaping technique: a shaper with two impulses.

The technique remained unexplored until the work of Singer and Seering in 1990 who presented a similar strategy, called zero vibration (or traditional) input shaping technique (ZVIS), but which is capable of shaping any input reference by convolving this with a sequence of impulses delayed themselves [318; 319]. Fig. 4.5 depicts an implementation example of a shaper based on two impulses. Since, there have been many ex-

tensions and developments of the traditional techniques which permitted to reach different objectives: simplicity of calculation, robustness, rapidity of responses, multi-modal compensation, multivariable compensation,... This class is very attractive to control piezoelectric systems and actuators because of the good performances and the robustness that can be obtained with simple controllers. We have therefore chosen this class. Different tests with different types of piezoelectric actuators demonstrated that overshoots which are in excess of 62% can be completely removed [BC11][BC11][J7][C14]. For example, Fig. 4.6 depicts the experimental vibrations of a piezoelectric cantilevered actuator without control and with a zero vibration input shaping feedforward control. The two figures represent the step response and the harmonic response of the actuator. Two types of shapers have used: one shaper with two impulses, and one shaper with three impulses. These results clearly show the substantial reduction of the

vibration when using the compensators. When the compensator has two impulses, we observe a small residual vibration. This is due to a bad identification of the model. By increasing the number of the impulses, the residual vibration are diminished. The technique has also been applied to multi-DOF piezoelectric actuators and a successfull damping of the vibration in the direct transfers was obtained [J13][C18]. These techniques still remained monovariable however. Their extension to control multi-DOF piezoelectric actuators with consideration of the cross-couplings is an ongoing work within the PhD workd of Yasser Al Hamidi.

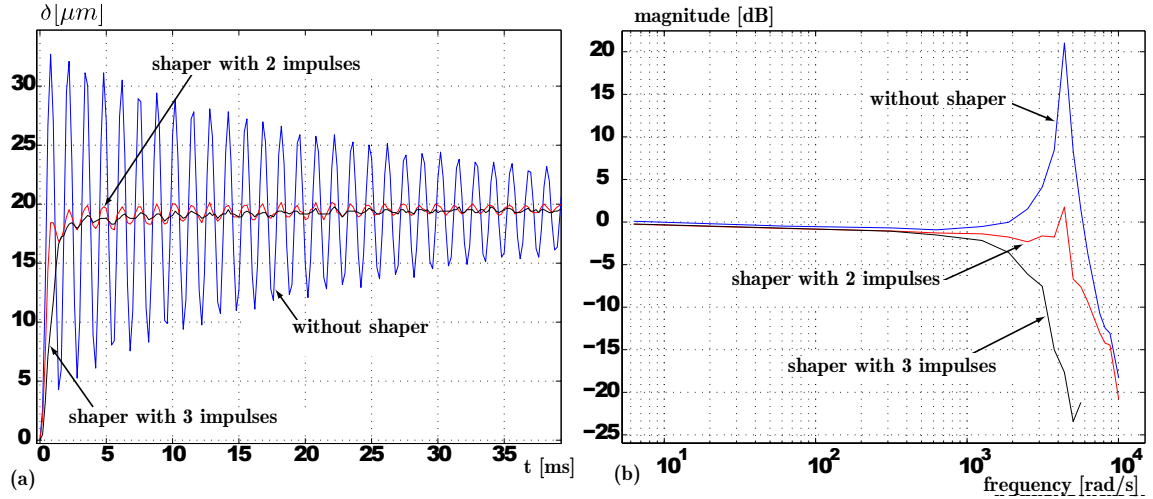


Figure 4.6: Experimental results of input shaping control of a piezoelectric cantilevered actuator.

Acknowledgements - The works regarding the feedforward control of vibrations in multi-DOF piezoelectric systems are within the PhD fellowship of Yasser Al Hamidi.

4.5 Complete feedforward control

So far, we tackled the individual control of the hysteresis, of the creep or of the vibration in piezoelectric systems. In the utilizations however, these three phenomena may appear simultaneously and a combination of the three control techniques is required in that case. Simultaneous feedforward control of the hysteresis and of the creep have been studied in different papers [256; 259–263]. This is because the two nonlinearities are both strong at low frequencies and greatly affect the accuracy of the precise positioning systems. In [J13][C14], we have shown that the vibration and the hysteresis can be simultaneously compensated together by blending the input shaping technique with the classical Prandtl-Ishlinskii. To fully control the hysteresis, the creep and the vibration, the easier way consists in cascading the three compensators as depicted in Fig. 4.7. This structure has been employed by Croft *et al.* [257]. They proposed to compensate first for the hysteresis with the classical Preisach technique, then the creep and finally the dynamics both with the standard dynamics inversion. Their application was the piezotube scanners in atomic force microscopes. In [J7], we

employed the classical Prandtl-Ishlinskii approach, the inverse multiplicative structure of LTI and the input shaping technique to highly reduce the hysteresis, the creep and the vibrations in a unimorph piezoelectric actuator. In fact, cascading the compensators eases the identification procedure. When the hysteresis is compensated, a new system which is composed of the hysteresis compensator and the actuator is obtained. The creep is therefore identified from this new system. Finally, the vibration is identified and controlled from the system composed of the creep compensator, the hysteresis compensator and the actuator. It is possible to commute the different compensators subject to an identification procedure with the right systems.

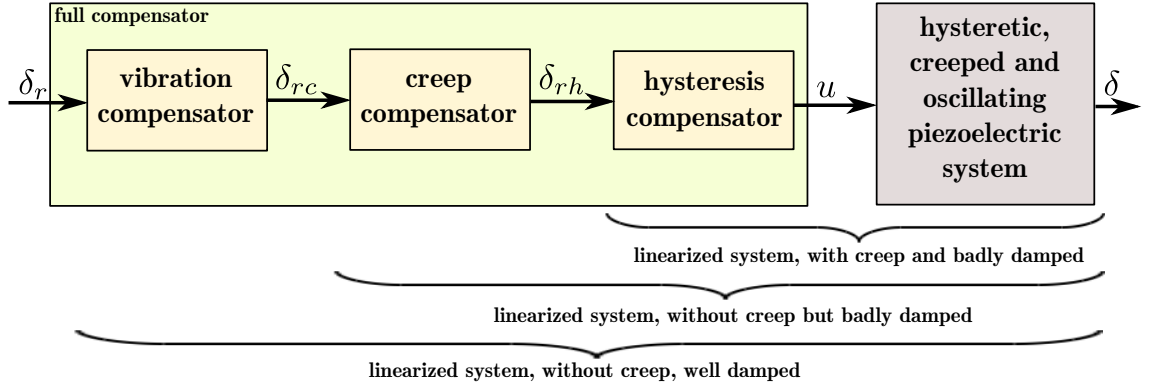


Figure 4.7: Full (or complete) compensation of the hysteresis, creep and badly damped vibration.

4.6 Conclusion and perspectives

Feedforward control techniques are well appreciated in the control of miniaturized systems. This recognition is thanks to the high level of packaging that feedforward control offers to the final devices since no sensors are required. Regarding the control of piezoelectric systems, the main challenges are the hysteresis and the creep nonlinearities. In addition, most of piezoelectric actuators exhibit badly damped vibrations which also requires control. Many works have been raised in the litterature regarding the modeling and control of the hysteresis and of the creep in these actuators and systems. These works mainly adapt existing nonlinear models (Prandtl-Ishlinskii, Preisach, LTI...) to the case of these systems. Our direction is twofold: 1) proposing new compensators schemes with reduced calculation and reduced complexity, 2) and extending the compensation to multivariable. We have demonstrated that a model (of the hysteresis or of the creep) can be judiciously combined with an inverse multiplicative structure to yield a compensator. To reach these objectives, we have proposed to use the inverse multiplicative structure in the compensator. The main advantage is that we do not need an extra calculation of the compensator's parameters: as soon as the model parameters are identified, the compensator is derived by restructuring the model. Regarding the hysteresis, the only condition required on the model such that this technique works is to have the same structure than in Eq. (4.15) (for rate-dependent hysteresis) or Eq. (4.16) (for rate-independent hystere-

sis). The proposed inverse multiplicative structure also permitted to extend the hysteresis and the creep compensation into multivariable. Regarding the vibration, the literature has shown that damping the vibration in piezoelectric systems was mainly based on the model inversion. An alternative way that we proposed consisted in employing input shaping techniques which are efficient and simple for implementation. The feedforward approach proposed in this thesis, mainly based on the inverse multiple structure and on the input shaping techniques, is competitive relative to the other employed techniques, and has an advantage of calculation and implementation simplicity. An essential perspective on feedforward control lies in the development of multivariable compensators that are capable of suppressing the hysteresis, the creep, the vibration and the cross-couplings. Two PhD thesis (by Didace Habineza, and by Yasser Al Hamidi) are ongoing and are focused on this direction.

Chapter 5

Signals measurement and estimation

Chapter. 4 dealt with the feedforward control of piezoelectric systems. Feedforward control techniques permit a high level of integration and a low cost (no sensors required). However, they fail when the models used are uncertain or when external disturbances perturb the systems during their functioning. To account for these uncertainties and dirtubances, there are many techniques available in feedback control schemes. Nevertheless, there is a great lack of convenient sensors to perform feedback control in piezoelectric miniaturized systems and in miniaturized systems in general. The aim of this chapter is to present novel or alternative measurement techniques for feedback use.

Contents

5.1	Introduction	110
5.2	Development of force measurement platform for micromanipulation and microassembly tasks	111
5.3	Observers as complementary tools for signal measurements	113
5.4	Self-sensing techniques in piezoelectric actuators	115
5.4.1	Overview	115
5.4.2	Modeling the electrical circuit and the actuator	117
5.4.3	Static self-sensing	118
5.4.4	Dynamic self-sensing	119
5.4.5	Towards multivariable self-sensing	120
5.4.6	Acknowledgements	121
5.5	Conclusions and perspectives	121

5.1 Introduction

Two of the interesting piezoelectric systems properties are the high bandwidth and the high resolution. However, the nonlinearities (hysteresis and creep), the lightly damped vibrations and the high sensitivity to the environment (temperature variation, surrounding vibrations, interaction force with the objects) that they exhibit compromise certain performances like the accuracy or the damping, or compromise even the stability.

Feedback control of piezoelectric systems with consideration of this negative side has been treated in [Chapter. 3](#) and we demonstrated that very good performances can be reached. A main limitation of feedback control of piezoelectric systems and of miniaturized systems in general is the lack of convenient sensors. Sensors that have the required performances (resolution, accuracy, range and bandwidth) have dimensions that are not necessarily adapted and are very expensive (thousands of €). These sensors cover optical sensors based on triangulation and interferometers. They are adapted for laboratory tests but, as soon as a duplication is required (industrialization for example), they are not the good solution. Another complication with these sensors happens when the number of the degrees of freedom of the system increases. It is frequently impossible to setup several sensors simultaneously to measure the different signals in the different axes of the system [\[BC3\]](#). With regards to sensors that are embeddable (strain gages), they do not have the necessary performances for most of the piezoelectric systems in precise and high dynamics positioning. We often face to sensors that have limited range, limited bandwidth, or that are noisy... There have been works to reduce the noise in these sensors when integrating them in piezoelectric systems by using Kalman filtering [\[74–76\]\[BC7\]](#), but the other limitations (like range) still remain.

In [Chapter. 4](#), feedforward control has been proposed to bypass the usage of sensors. This approach permits a low cost and a high level of integration of the controlled piezoelectric systems. However, feedforward control suffers from the lack of robustness against models uncertainties and against external disturbances.

A part of the works we carried out is the development of novel or alternative measurement techniques devoted to piezoelectric systems to permit feedback control. Treated as part of three projects that I coordinated (european μ PAdS project, ANR MYMESYS project, ANR young investigator C-MUMS project), the target is to be capable of measuring the required signals for feedback by using integrated sensors and a minimum number of them. Generally speaking, tools from control theory (observers...) bring complementary capability to move forward towards this target. In fact, by combining well adapted observers with the measurement systems designed, it is possible to reach certain objectives of measurements that sensors only could not provide.

The chapter is organized as follows. First we present the development of a force measurement platform devoted to microassembly applications. This will be in [Section. 5.2](#). Then, we will present in [Section. 5.3](#) the approach of combining observers and existing sensors to increase the measurement capabilities in piezoelectric systems. Finally, [Section. 5.4](#) will be devoted to

the self-sensing measurement approach. This consists in using the actuator as sensor at the same time. This approach has a very high level of packageability, is cheap and is considered as a very interesting feature in miniaturized systems.

5.2 Development of force measurement platform for micromanipulation and microassembly tasks

During a micromanipulation or a microassembly task, knowing the manipulation force is essential and its control might be necessary for some situations. By doing so, we can avoid the destruction of the manipulated object or of the actuators themselves. The force measurement in these particular tasks has raised several works and a complete discussion and comparison can be found in [320; 321], in particular if the manipulators are based on two close actuators (two fingered grippers). The most used approaches will be reminded below.

An approach to measure the force in systems during micromanipulation or a microassembly task is through strain gages that are implemented in the actuators. This technique is very common [74; 321–326] but the range of the measurable force is limited to some milliNewtons only which is not sufficient for certain tasks. In addition to this, the noise observed in the measured signals are frequently non-negligible making finally the requirement of well designed filters [74–76][BC7]. Another approach to measure the force during micromanipulation and microassembly tasks is proposed in [327; 328] and discussed in [321]. The principle consists in utilizing only one element of the microgripper as actuator and the other element as force sensor. The force sensor itself is integrated as a component of the microgripper and co-designed with the actuator. A limitation of this approach is the fact that only one signal can be controlled: either the positioning or the force. In [329], Agnus *et al.* proposed an end-effector sensorized by strain gages and placed at the tip of the actuators of microgrippers. The end-effector permits to measure the force when it is in contact with the manipulated objects. The end-effector was based on silicon which permitted to fabricate it in batch. Later on, we redesigned the end-effector to measure the force in two directions [C47]. However, again, the range of measurement is limited for this approach. In fact, the range of measurement is principally dependent on the stiffness of the sensitive parts of the integrated sensors. An alternative way that overcomes this limitation and which is developed at the department consists in utilizing SU-8 polymers instead of silicon. In fact, there are many advantages gained with SU-8. First the range of measurement is more adaptable than with silicon. The fabrication of more complex and 3D structures is also rendered easier than with silicon. Finally, SU-8 is compatible with certain applications (manipulation under X-ray), whilst silicon is not. In counterpart, SU-8 has a quicker ageing than silicon, which is a drawback.

All these above mentionned force measurement approaches for micromanipulation and microassembly tasks are proprioceptive: the sensors are integrated in the actuated systems. In [330; 331] camera combined with visual servoing has been used to visualize the deformation of the actuator or of the manipulated object and thus to estimate the force. The great advantage of camera and related optical amplifiers is that, when the manipulated object is very small,

they are the best way to track its position. As the objects to manipulate downscale, these tools are more and more necessary to visualize and to ensure the success of the tasks of manipulation or of assembly. Nowadays, we even assist to the utilization of microscopes (scanning electronic microscopes, atomic force microscopes) as visual measurement and as actuators in nanomanipulation and nanoassembly [331]. Nonetheless, it remains essential to have sensors that are nearby the manipulated objects or integrated with the actuators (proprioceptive). Therefore, it is generally common to combine proprioceptive sensors with camera and visual servoing to increase the chance of success of the tasks [321].

The force measurement system proposed in this subsection is not among the two classes discussed above, it is complementary to them. During a microassembly task, for instance when a microgripper attempts to insert (resp. to place) a manipulated object inside (resp. on) another object, there is an interaction force between the two objects. Our objective here deals with the measurement of this third force which is as important as the force between the actuator and the handled object. An interesting utilization of this third force is to control the insertion of a microassembly. Fig. 5.1-a pictures the first version of the platform [C22]. Called instrumented platform, it integrates a commercial force sensor (from Femtotools [328]). The novelty of the instrumented platform is that it adapts the range of manipulation force to the range of the integrated force sensor so that it is possible to precisely measure or estimate large force. In this fabricated example, the integrated commercial sensor's measurement capability ranges between 0 and $50\mu N$, but the whole developed platform can measure a manipulation force up to $1800\mu m$. An estimator is used to provide an estimate \hat{F} of this manipulation force F on the basis of the measurement from the sensor F_m and on the basis of the mechanical model of the platform. Again, we utilize here the inverse multiplicative structure for the estimator, as depicted in Fig. 5.1-b. This permits to track the force at low and high frequency without performing standard inversion of models. The estimator's gains are: $D_1(s) = \frac{1}{K}$ and $D_2(s) = G(s)$, the model of the platform with the integrated sensor being $F_m = (K + D(s)) F$. Fig. 5.1-c depicts an example of performances of the platform which shows that the estimate force well tracks both the transient part and the final value of the real force. This first version is devoted to measure/estimate the force in one axis. A new design and development has been made to measure the force along two directions [C34]. Finally, ongoing works consist in the development of smaller version (less than the cubic centimeter) of this instrumented platform. Based on the microfabrication technology and on the cartesian piezoelectric microsystem presented in Section. 2.5, the instrumented microplatform will contain not only an integrated measurement but also an actuation. The actuation is piezoelectric and is used to offer other possibilities than measurement. The measurement will be based on the self-sensing that will be presented in Section. 5.4.

Acknowledgements - The works reported here were within the internships of Paul Michaël Moore and Kamel Neir.

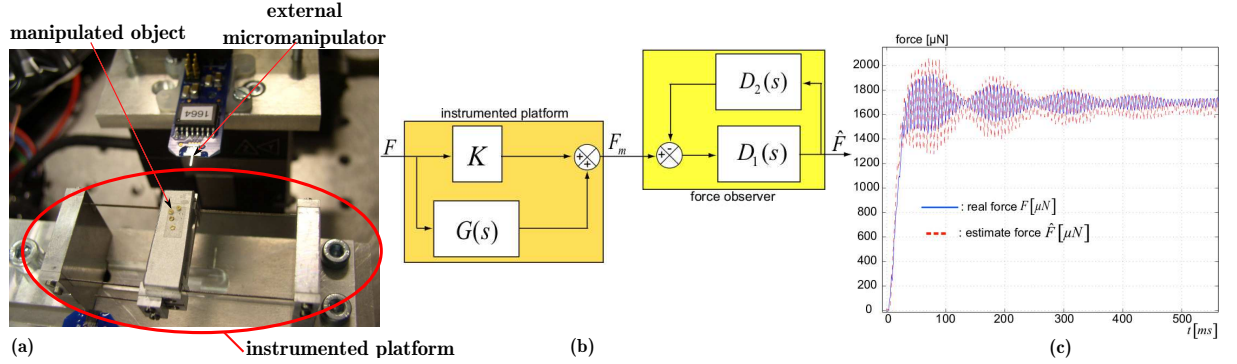


Figure 5.1: Instrumented platform. (a): a view. (b): the estimator. (c): example of force estimation.

5.3 Observers as complementary tools for signal measurements

When the number of sensors is insufficient, observers are essential tools that can be used to complement the measurement. Thus, observers evidently find their place in miniaturized systems and related applications such as precise and high dynamics positioning where it is difficult to find convenient sensors. Observers have been extensively used to measure force in scanning probe microscopes [332–336]. Observers have also been used to estimate the state and to remove the sensors noise in capacitively actuated microsystems [76; 337]. Regarding piezoelectric cantilevered actuators, references [74; 75] utilized observers to estimate the state (displacement and position) and to filter the signals based on the applied voltage and on the measured displacement by strain gages sensors. This dealt however with the displacement estimation, and the manipulation force, which is essential during a micromanipulation or a microassembly, was not furnished. To estimate the force in a piezoelectric actuator in a microgripper, Haddab et al. [59] includes this in the state vector of the actuator. Then, he applied a Luenberger observer to provide the estimate state, including the force. A main interest of this is that the same actuator used for the force estimation can still be used as displacement actuation, or as force actuation. A limitation of the approach is that the observer synthesis necessitates the dynamics of the force to be known, which is generally *a priori* unknown because it depends on the manipulated objects characteristics. For the experimental case, the author therefore utilizes a zero dynamics which restricts the observer for low frequency force only.

To estimate the force applied in a piezoelectric actuator at low and high frequency, a way consists in taking the model of the actuator and directly deriving from this the force [C10]. Reconsider the generalized model of a piezoelectric actuator described by Eq. (2.8) in Chapter 2:

$$\delta(s) = \Gamma(u(s)) D(s) + C_{creep}(u(s), s) + s_p D(s) F(s) + \Gamma_T(T(s)) D_T(s) \quad (5.1)$$

The manipulation force $F_m = -F$ is the force we want to estimate. Considering a stationary temperature ($\Gamma_T(T(s)) = 0$), the estimate force can be directly derived from the model:

$$\hat{F}_m(s) = -\hat{F}(s) = \frac{1}{s_p D(s)} (\Gamma(u(s)) D(s) + C_{creep}(u(s)) - \delta(s)) \quad (5.2)$$

A challenge in this technique is that we need a minimum phase dynamics $D(s)$. If the hysteresis and if the creep are well modeled, it can be a very precise estimation technique, in particular at low frequency [C10].

A second way we have proposed to estimate the manipulation force is in [C15]. It consists in considering the force as an unknown input disturbance and thus employing an unknown input observer (UIO) to estimate it. Still assuming that the temperature is stationary ($\Gamma_T(T(s)) = 0$), let the following model be a state-state representation of the model in Eq. (5.1):

$$\begin{cases} \frac{dX(t)}{dt} = AX(t) + \Gamma^{ss}(u(t)) + B_f F(t) \\ \delta(t) = CX(t) \end{cases} \quad (5.3)$$

where:

- $X(t)$ is the state of the actuator,
- A and C are the state matrix and the output matrix respectively,
- B_f is the input disturbance matrix,
- and $\Gamma^{ss}(u(t))$ is a nonlinear term that encompasses the hysteresis and eventually the creep.

Thus, an UIO observer with the following structure can be used to estimate both the unknown input $F(t)$ (and therefore the manipulation force $F_m(t) = -F(t)$) and the state of the actuator from all available signals:

$$\begin{cases} \frac{d\hat{X}(t)}{dt} = A\hat{X}(t) + \Gamma^{ss}(u(t)) + B_f \hat{F}(t) + K_o (\delta(t) - \hat{\delta}(t)) \\ \hat{\delta}(t) = C\hat{X}(t) \end{cases} \quad (5.4)$$

and

$$\hat{F}(t) = f_1 \delta(t) + f_1 \frac{d\delta(t)}{dt} + g_1 \hat{X}(t) + g_2 \frac{d\hat{X}(t)}{dt} + g_3 \Gamma^{ss}(u(t)) \quad (5.5)$$

In fact, the observer is composed of two (sub)observers which are the state-observer (given by Eq. (5.4)) and the unknown input (force) observer (given by Eq. (5.5)), with K_o , f_1 , f_2 , g_1 , g_2 and g_3 are the gains to synthesize. In the state observer, additionally to the known driving voltage $u(t)$ and the measured displacement δ , the force is also used as available signal. In fact, it is taken from the force observer. In this second observer, the employed signals are the measured displacement $\delta(t)$, its derivative $\frac{d\delta(t)}{dt}$, the estimate state $\hat{X}(t)$ and its derivative $\frac{d\hat{X}(t)}{dt}$ from the previous observer, and the driving voltage $u(t)$. To avoid numerical derivative of the signal δ , it is possible to employ $f_1 C \frac{d\hat{X}(t)}{dt}$ instead of $f_1 \frac{d\delta(t)}{dt}$ in Eq. (5.5).

To calculate the observer gains K_o , f_1 , f_2 , g_1 , g_2 and g_3 for this structure of observer, the technique proposed by Liu and Peng [338] called inverse-dynamics-based UIO has been applied. In [C15], we successfully utilized this to estimate the manipulation force with a piezoelectric actuator. The main difficulty in using the observer in Eq. (5.4) and Eq. (5.5) is the more complex calculation of the gains and the implementation. In fact, the gains calculated with the method in [338] require very low sampling time for the case of piezoelectric actuators, which will demand a high power machine for the implementation. It is difficult to find the gains with convenient sampling time from the model of the piezoelectric actuator, although the condition on the sampling and actuator's dynamics is respected. This may be due to the high Q-factor of the actuator because, when employing a feedforward vibrations controller to the actuator before the observer synthesis, the gains are found more easily. Apart from this calculation and implementation difficulty, this observer can track very well the force both at low and at high frequency, without knowing any property or any model of the force. Additionally to the force, the whole state of the actuator is also estimated. The application of this force observer is multiple: feedback control of the displacement (state-feedback or output feedback schemes) with a display of the force, force feedback control. Fig. 5.2-a depicts the principle scheme of the observer. In the figure, $F(t)$ is the force applied by the object to the actuator, and $F_m(t) = -F(t)$ is the manipulation force. Fig. 5.2-b presents the output displacement (measured and estimate) obtained when a step input voltage is applied to the piezoelectric actuator initially in close contact with an object. Fig. 5.2-c is the force (measured and estimate) due to the movement of the actuator towards the object. In these two curves, the measured displacement and the force are experimentally obtained from an external optical sensor and an external Femtotools force sensor. The comparison of these experimental signals with the estimate signals show a great agreement between them which demonstrate the efficiency of the observer.

5.4 Self-sensing techniques in piezoelectric actuators

5.4.1 Overview

Piezoelectric materials are well known in the development of actuators thanks to the converse piezoelectricity effect, or in the development of sensors thanks to the direct effect. Notwithstanding, it is possible to employ piezoelectric materials as sensor and actuator simultaneously, by exploiting the charges that appear on the electrodes during the deformation. This is called the self-sensing. By definition, self-sensing is an approach that consists in utilizing an actuator as a sensor at the same time.

The first use of the "self-sensing" term goes back to 1992 when J.J. Dosch et al. [339] successfully damped the vibrations of a piezoelectric beam without using the aid of external sensors. In their works, the voltage provided from a capacitive bridge and from the charge amplification was processed in an analog circuit, amplified and returned back to the piezoelectric element. In that time, several independent applications began to emerge for cantilevers vibrations control or stack piezo devices for micropositioning. Several years later T. Taigami et al. [340] applied the method for force self-sensing and for the control of a large size bimorph

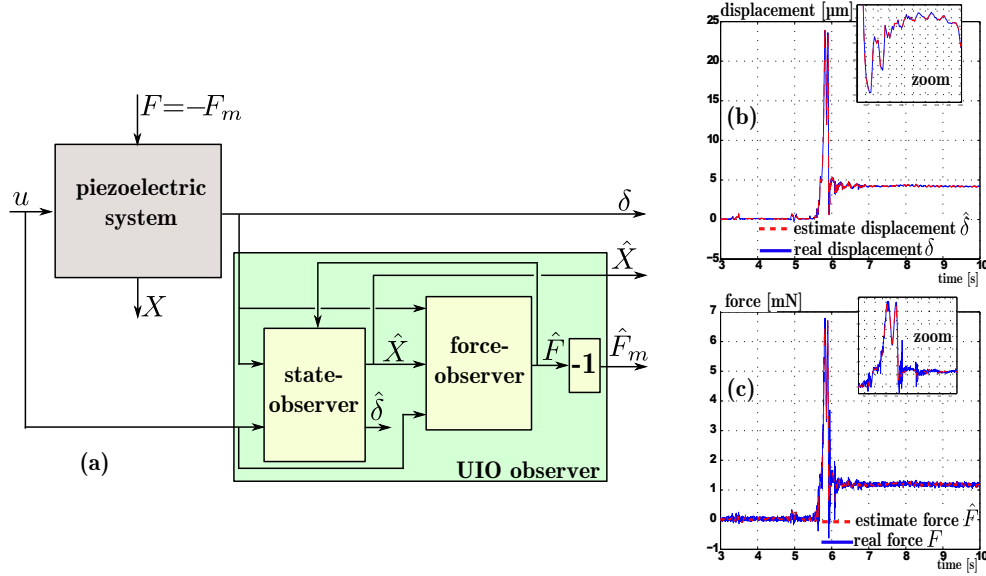


Figure 5.2: (a): scheme of the observer and of the piezoelectric system. (b): measured output displacement $\delta(t)$ and its estimate $\hat{\delta}(t)$. (c): measured force $F_m(t) = -F(t)$ and estimate force $\hat{F}_m(t) = -\hat{F}(t)$.

actuator by using a half-bridge circuit, a voltage follower and a computer based data acquisition system. The authors experimentally verified that the stiffness of the grasping object does not affect the measurement; however the electronic schematic limited the applied voltage range and the nonlinearities (hysteresis and creep) were not compensated. Since, self-sensing is widely used for vibrations control of flexible structures [341–346]. All these self-sensing works deal however with high frequency signals, with applications the vibrations damping. They are not efficient to track low frequency signals or to track constant signals for a duration more than seconds. In fact, due to the internal charge leakage in the piezoelectric device, a low frequency or constant deformation can not be traced back. Consequently, the existing self-sensing techniques can not be utilized in micromanipulation or microassembly applications where the displacements or the force can be constant during tens or hundreds of seconds.

The main contribution of our works lies in the development of self-sensing capable of providing an estimate measure of the displacement or of the force both at low and at high frequencies in order to be congruent with the need in micromanipulation or microassembly applications. The principle, pictured in Fig. 5.3-a, is as follows. When a piezoelectric actuator is supplied by a driving voltage $u(t)$, we obtain a displacement $\delta(t)$. In the meantime, a charge $Q(t)$ appears on the actuator's electrodes. An electrical circuit is used to amplify this charge $Q(t)$ and to transform it into an exploitable voltage $u_o(t)$. Finally, an observer exploits the available signals (the driving voltage $u(t)$ and the exploitable voltage $u_o(t)$) to provide an estimate $\hat{\delta}(t)$ of the displacement or an estimate $\hat{F}(t)$ of the force, or both. Both the electrical circuit and the observer constitute the self-sensing. To reach the targeted performances (measurement at

low and high frequencies), the novelty in our works is mostly in the observer, and for certain cases in the electrical circuit. The observer judiciously accounts for the leakage in the actuator and the imperfection in the electrical circuit that were sources of charge leakage which did not permit a measurement at low frequencies. The observer is thus based on the precise model of the actuator and of the circuit with consideration of these leakages.

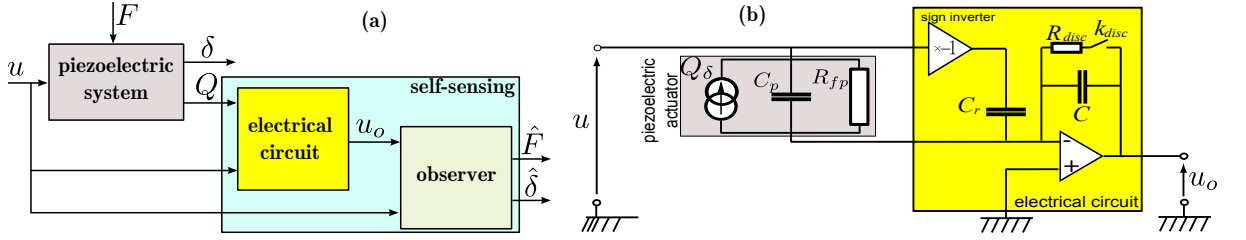


Figure 5.3: (a): principle scheme of a self-sensing. (b): the electrical circuit.

5.4.2 Modeling the electrical circuit and the actuator

The charge $Q(t)$ that appears on the actuator's electrodes is composed of the charge $Q_u(t)$ due to the dielectric effect (due to $u(t)$) and of the charge $Q_\delta(t)$ due to the direct piezoelectric effect (due to $\delta(t)$). The piezoelectric charge $Q_\delta(t)$ is very weak relative to the dielectric charge $Q_u(t)$ and this may strongly compromise the efficiency of the self-sensing measurement. To increase the self-sensing sensitivity, the electrical circuit figured in Fig. 5.3-b has been proposed [J5]. In the figure, the equivalent electrical circuit at low frequency of the piezoelectric actuator is also presented [347]. Let C_p be the equivalent capacitor of the actuator such that the dielectric charge is: $Q_u(t) = C_p u(t)$. If the reference capacitor C_r is chosen to be equal to C_p ($C_r = C_p$), the dielectric effect inside $Q(t)$ is minimized and thus the sensitivity of the self-sensing is increased. In this case, the total charge that will be amplified by an operational amplifier (op-amp) is: $Q_{oa}(t) = Q(t) - C_r u(t) = C_p u(t) - C_r u(t) + Q_\delta(t) \approx Q_\delta(t)$. The relation between the charge $Q_\delta(t)$ and the output displacement $\delta(t)$ is linear when the external force is null: $Q_\delta(t) = \alpha \delta(t)$, where α is the charge-displacement coefficient. Let R_{fp} be the internal leakage resistor of the actuator and $Q_{da}(u(t), t)$ be its dielectric absorption. Let $i_b(t)$ be the bias current in the non-ideal op-amp and C be the capacitor for the charge amplification. Then, taking the charge $Q_{oa}(t)$ and accounting for the different leakages, we derive the equation of the output voltage $u_o(t)$ [J5]:

$$u_o(t) = \frac{-1}{C} \left(\alpha \delta(t) - (C_p - C_r) u(t) - Q_{da}(u(t), t) - \frac{1}{R_{fp}} \int_0^t u(t) dt + \int_0^t i_b(t) dt \right) \quad (5.6)$$

The dielectric absorption $Q_{da}(u(t), t)$ can be approximated by a first order linear model. In the Laplace domain, this is given by:

$$Q_{da}(u(s), s) = Q_{da}(s) u(s) = \frac{k_{da}}{\tau s + 1} u(s) \quad (5.7)$$

where $Q_{da}(s) = \frac{k_{da}}{\tau s + 1}$ is the dielectric absorption transfer function, k_{da} and τ_{da} are the related gain and constant time respectively.

The parameters to be identified experimentally are C_p , R_{fp} , k_{da} , τ_{de} , α and i_b . A procedure for their identification is detailed in [J5]. Notice that the commutator k_{disc} and the resistor R_{disc} in Fig. 5.3-b are used to discharge the capacitor C if the circuit is saturated.

5.4.3 Static self-sensing

From the model Eq. (5.6), the estimate displacement $\hat{\delta}(t)$ is derived [J5]:

$$\hat{\delta}(t) = \frac{1}{\alpha} \left((C_p - C_r) u(t) + Q_{da}(u(t), t) + \frac{1}{R_{fp}} \int_0^t u(t) dt - \int_0^t i_b(t) dt - C u_o(t) \right) \quad (5.8)$$

The observer Eq. (5.8) is valuable to estimate low frequency or constant signal because the dynamics of the actuator was not considered in the model Eq. (5.6). In addition, this observer is only valuable when the actuator is force-free, i.e. there is no interaction force F between the actuator and the external. We call the self-sensing that uses this observer *static displacement self-sensing technique*. It is important to notice that the model and the observer are linear because the relation between the charge and the displacement is linear.

To estimate the force, the relation between the charge $Q(t)$ and the force $F(t)$ applied to the piezoelectric actuator by the external is first described. It is shown that this relation is also linear: $Q_F(t) = \beta F(t)$. Thus, the charge that will be amplified by the op-amp is: $Q_{oa}(t) = Q(t) - C_r u(t) = (C_p - C_r) u(t) + \beta F(t)$. In a similar manner than with the displacement modeling in Eq. (5.6) and observer in Eq. (5.8), we obtain the estimate force as given by the first equation of Eq. (5.9). The displacement is calculated as the difference between the free-displacement $\hat{\delta}^{free}(t)$ already described by Eq. (5.8) (and reminded in the second equation of Eq. (5.9)), and the displacement due to the force. The new observer to estimate both the force and the displacement is [J6]:

$$\begin{cases} \hat{F}(t) = \frac{1}{\beta} \left((C_p - C_r) u(t) + \Gamma^F(t) + \frac{1}{R_{fp}} \int_0^t u(t) dt \right) \\ \hat{\delta}^{free}(t) = \frac{1}{\alpha} \left((C_p - C_r) u(t) + Q_{da}(u(t), t) + \frac{1}{R_{fp}} \int_0^t u(t) dt - \int_0^t i_b(t) dt - C u_o(t) \right) \\ \hat{\delta}(t) = \hat{\delta}^{free}(t) - s_p \hat{F}(t) \end{cases} \quad (5.9)$$

where s_p is the compliance of the actuator, and $\Gamma^F(t)$ is a nonlinear operator that includes the hysteresis and the creep if eventually they exist (to be verified experimentally), but also the dielectric absorption and the non-ideal behavior of the op-amp.

We call *static force-displacement self-sensing technique* the self-sensing that uses the observer in Eq. (5.9). This is valuable to estimate low frequency and constant force and displacement. When the frequency of the displacement $\delta(t)$ or of the force $F(t)$ to be estimated increases, the above estimate signals $\hat{\delta}(t)$ and $\hat{F}(t)$ are biased.

5.4.4 Dynamic self-sensing

The previous static self-sensing permits to estimate constant signals or low frequency signals. The estimated signals can not be used in a feedback dynamic control. For this aim, we need to extend the previous self-sensing techniques into dynamic self-sensing. The principle is to add a dynamic observer in cascade with the already developed static observer [BC2][J23][C41][C20].

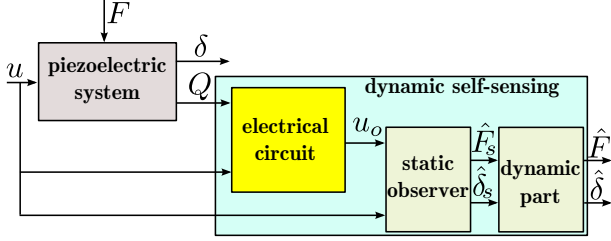


Figure 5.4: Diagram of a dynamic self-sensing in a piezoelectric actuator.

The new self-sensing is therefore schemated in Fig. 5.4. In the figure, $\delta_s(t)$ and $F_s(t)$ represent the steady-state estimate signals and are from the static observer in Eq. (5.8) or Eq. (5.9). The static observer augmented with the dynamics part constitutes the dynamic observer of the self-sensing technique. The synthesis of the dynamic part necessitates a dynamic model between the driving voltage $u(t)$, the output displacement $\delta(t)$ or the force $F(t)$ and the output steady-state $\delta_s(t)$ or $F_s(t)$.

In [J23], we developed this scheme to be able to estimate low and high frequency displacement and only low frequency force. The self-sensing was afterward used in a feedback control of the displacement based on the standard H_∞ robust control technique, with a display of the manipulation force. Let $\Delta(s) = \frac{\hat{\delta}(s)}{\hat{\delta}_s(s)}$ be the transfer function of the dynamic part of the observer. Thus, the observer that provides the steady-state of the force and the complete information on the displacement is [J23]:

$$\begin{cases} \hat{F}(t) = \hat{F}_s(t) = \frac{1}{\beta} \left((C_p - C_r) u(t) + \Gamma^F(t) + \frac{1}{R_{fp}} \int_0^t u(t) dt \right) \\ \hat{\delta}_s^{free}(t) = \frac{1}{\alpha} \left((C_p - C_r) u(t) + Q_{da}(u(t), t) + \frac{1}{R_{fp}} \int_0^t u(t) dt - \int_0^t i_b(t) dt - C u_o(t) \right) \\ \hat{\delta}(s) = \Delta(s) \hat{\delta}_s^{free}(s) - s_p \hat{F}(s) \end{cases} \quad (5.10)$$

with:

$$\Delta(s) = \frac{\alpha d_p D(s)}{\left((C_p - C_r) - \frac{1}{R_{fp}s} - \frac{i_b}{s} - Q_{da}(s) - H(s) \right)} \quad (5.11)$$

where d_p is the piezoelectric coefficient of the actuator, $D(s)$ is its normalized dynamics of the actuator and $H(s)$ is the dynamics between the driving voltage and the exploitable voltage ($H(s) = \frac{u_o(s)}{u(s)}$). In this dynamic self-sensing, we assumed that the actuator behaves linearly: $\delta(s) = d_p D(s) u(s) + s_p F(s)$. The nonlinearities (hysteresis and creep) needs to be accounted for if we would like to use the self-sensing to estimate signals in a larger range. We also assumed that the bias current i_b was constant.

Experimental investigation has been carried out to compare the efficiency of the dynamic self-sensing with the static self-sensing. The experimented actuator is a unimorph piezoelectric cantilever [J23]. For that, a step input voltage $u = 20V$ is applied. Fig. 5.4-a depicts the estimate displacement $\hat{\delta}(t)$ when the static self-sensing is used. In the same figure is also pictured the real displacement $\delta(t)$ measured with an external optical sensor. As we can see, the estimate displacement well tracks the steady state but not the transient part of the real displacement. In Fig. 5.5-b are pictured the estimate $\hat{\delta}(t)$ from the dynamic self-sensing and the real displacement $\delta(t)$. This figure shows that both the steady-state and the transient part are well tracked. These experiments demonstrate that if the objective is to perform a dynamic control, the dynamic self-sensing is the most adequate because it accounts for the dynamics of the actuator. The price of a dynamic self-sensing is a thorough and precise characterization of the dynamics of the actuator and of the electrical circuit.

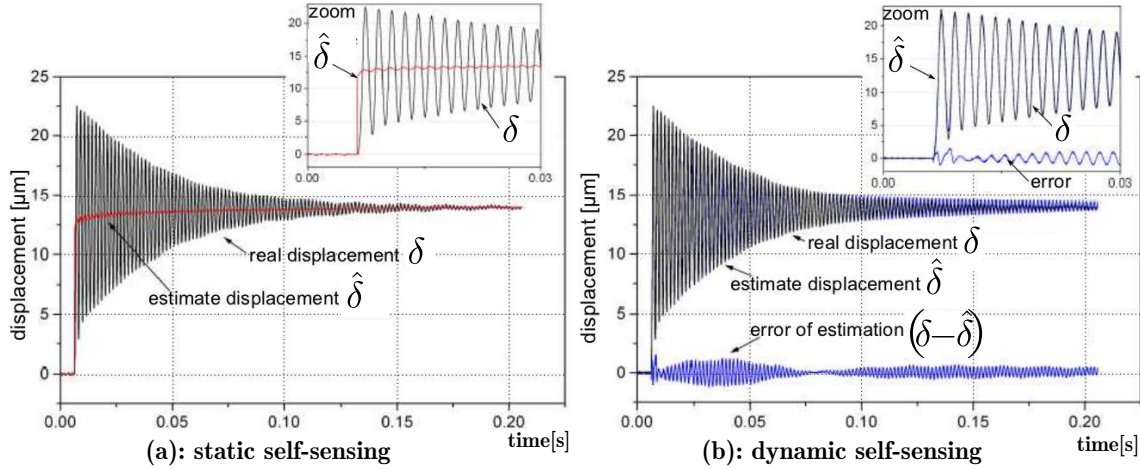


Figure 5.5: (a): estimation of the displacement with the static self-sensing. (b): estimation of the displacement with the dynamic self-sensing.

5.4.5 Towards multivariable self-sensing

The static and dynamic self-sensing techniques above are called monovariable self-sensing and apply for the estimation of displacement or of force (or both) along one axis in piezoelectric actuators. If the actuator has several degrees of freedom (DOF), a monovariable self-sensing technique does not apply anymore.

A multi-DOF piezoelectric actuator has several supply-electrodes additionally to the ground-electrode. The electrical circuit of the self-sensing to be designed needs to have several canals. The observer needs also to be multivariable. A matter in multivariable self-sensing is when several of the supply-electrodes are supplied simultaneously. This may cause a high potentials difference even if the voltages are low, and thus the electrical circuit may be destroyed. In the french patent [P2] and in its extension into international patent [P3], we presented an original electrical circuit and an observer devoted to self-sensing in multi-DOF piezoelectric actuators.

The claim in the patents is multiple.

→ A protection of the electrical components from high potentials difference is proposed. The protection is based on a judicious scheme with ground-electrodes and floating electrodes. Thanks to this protection, the multivariable self-sensing can be used not only for low voltages but also for high voltages actuators like piezotube scanners in scanning probe microscopes.

→ The self-sensing accounts for the couplings of the actuator and can precisely track them too.

5.4.6 Acknowledgements

The works regarding the self-sensing techniques were within the postdoctoral fellowships of Dr. Ioan Alexnadru Ivan and Dr. Omar Al Janaideh.

5.5 Conclusions and perspectives

This chapter dealt with some approaches to carry out signal measurements and estimation in piezoelectric systems. Due to the lack of convenient sensors to measure the force or the displacement in these systems, novel techniques have been proposed. The deal consists in combining measurement devices (commercial or developed) with control theory tools to perform more precise, more dynamic measurement or to estimate the missing signals that the available sensors only could not do. We have shown that observers tools are very interesting tools to help us reaching this target. One of the approach proposed consists in exploiting the charge that appears in the piezoelectric systems electrodes during their actuation and tracking or estimating their displacement or force from well designed observer and electrical circuit. Called self-sensing, this approach is very attractive because of the high level of packaging it offers. Several tests of different cases (1-DOF or multi-DOF piezoelectric actuator, force or displacement signals, static and dynamics) have been carried out to validate the approach. However, the limitation of the self-sensing is the fact that the observers are "open-loop" (no correction gain). Thus the self-sensing may be sensitive to models uncertainties. Furthermore, it cannot account for the external perturbation (temperature variation, ...) that may affect the models parameters during the functioning and affect the precision of the measurement/estimation. An interesting extension of the self-sensing consists in measuring the temperature variation additionally to the force and to the displacement. As the temperature variation results in a deformation of the actuator too which therefore yields an additional charge, a feature is to synthesize an observer that will provide the estimate of the displacement, of the force and of the temperature.

Chapter 6

General conclusions and perspectives

This chapter ends the thesis by synthesizing the contribution of the works carried out and by presenting some possible perspectives explorable in the medium and in the long terms. Whilst the works contribution lied in the precise and high dynamics positioning context, the perspectives are opened to other kinds of applications.

Contents

6.1	General conclusions	123
6.2	General perspectives	126
6.2.1	Going further in the miniaturization of high performances and high dexterity piezoelectric systems	127
6.2.2	Towards highly autonomous and smart miniaturized systems	129
6.2.3	From MEMS harvesters to matters harvesters	135

6.1 General conclusions

THE context of the works reported in this thesis is the positioning in micromanipulation, microassembly and medical applications. These applications require a high precision (micrometric or submicrometric) and a high dynamics. Miniaturized systems are considered as the best candidates to execute these high precision and high dynamics positioning tasks. They can offer a very high resolution and because of other appreciable properties such as low consumption, relatively low costs and small sizes. There have been different principles and actuation techniques to develop miniaturized systems, but piezoelectric actuation is one of the most employed. This recognition is thanks to its nanometric resolution, high bandwidth (tens of kHz) and ease of integration and powering. The contribution of this thesis in the context is the development of novel piezoelectric devices, their modeling and control, and the estimation and measurement of signals in them for precise and high dynamics positioning.

Piezoelectric cantilever actuators with rectangular section (we call multimorph) are simple structures that are involved in many studies and in many applications: switches, microgrippers,

micro-valves, micro-air-vehicles, tips in atomic force microscopes. Two conclusions are raised regarding their design and development. The first conclusion is that they can be exploited to develop more performant or more complex structured systems. An example consists in judiciously combining multimorph actuators with the thermal actuation principle to result in a high resolution, high bandwidth and high range of positioning actuator, called hybrid thermopiezoelectric actuator. Another example deals with the development of a compact, high resolution, high range and high bandwidth two degrees of freedom (2-DOF) system devoted to laser phonomicrosurgery. In this, the simple bendings of well interconnected cantilever actuators are transformed into high range of orientation in two directions. In the second conclusion, we have observed that the level of miniaturization of piezoelectrically actuated systems is still limited. In fact, actuated MEMS¹ based on piezoelectric materials are mostly based on aluminum nitride (AlN). The clean-room process and the machining of these piezoelectric materials are well furnished in the literature which permits to fabricate very miniaturized systems. However, AlN materials have very weak coupling factors (less than 15%) and are not the good solution to develop high displacement and high torque actuators. In contrary, PZT (lead zirconate titanate) piezoelectric bulks are commercially available at low costs and have very remarkable properties (coupling factors around 50%), and thus well adapted for high performant actuation. However their microfabrication process is not well settled. We have shown that a possible way to bypass this limitation is using low temperature bonding and thinning process to PZT bulks. This way permits to go further on the miniaturization of low costs, high range of displacement, high torque, high resolution and high bandwidth systems.

Another important matter to success precise and high dynamics positioning is the control of the systems used to execute the tasks. There are two well-known challenges: the lack of convenient sensors, and the overall high sensitivity to the environment. Additionally to these, piezoelectric based positioning systems are characterized by nonlinearities (hysteresis and creep) and by badly damped vibrations which strongly compromise the precision and the stability of the tasks. Consequently efficient controllers and novel techniques of measurements capable to track the signals should be studied. Regarding the modeling of piezoelectric cantilever actuators, the classical linear model (Ballas model) is not anymore usable because it cannot track the nonlinearities and the sensitivity to the environment. One of the contribution of the works reported in the thesis consisted therefore in generalizing the model in order to account for the nonlinear phenomena and for the ambient temperature effect. A major advantage of this model is that it is the basis for the modeling of more complex structures, for the controllers synthesis, and for the development of measurement techniques and related observers in many works reported in this thesis. With regards to the control, the main guideline is to develop easy to implement and simple controllers which are capable of ensuring the required performances (high accuracy, high dynamics, no overshoots...), knowing the above negative properties (nonlinearities,...). Two control architectures have been proposed. The first architecture is feedforward which is well adapted to miniaturized systems where there is a great lack of convenient sensors to make feedback. The challenges posed in feedforward control consisted in accounting for the nonlinearities and for the vibrations. In principle, their

¹MEMS: MicroElectroMechanical Systems.

compensation can be performed by models inversion but this requires some conditions in the models. In our approach, the inverse multiplicative structure was exploited and combined with the models to construct the compensators (controllers). The advantage is double: i) the conditions on the models are avoided, ii) and the calculation of the compensators is avoided because as soon as a model is identified, a compensator is yielded by structure. Feedforward control architecture suffers however from the lack of robustness face to models uncertainties and to external disturbances. To deal with this lack, feedback architecture has also been tackled. H_∞ robust control technique and its derivative are the classical and efficient way to handle uncertainties and disturbances. However they often yield high order controllers, which are not congruent with the guideline here. To result in low orders controllers, we combined the H_∞ technique with a proposed plurilinear model in which the nonlinearities are approximated by a linear model, uncertainties and fictive external disturbances. The different experiments demonstrate that the proposed combination permitted to reach the performances required in micromanipulation and microassembly applications under different situations (with or without manipulated objects, with or without thermal disturbances, ...). A parallel study in feedback architecture that we have also investigated is the combination of intervals with control theory. We show that by doing so, it is possible to develop very simple but robust controllers where the orders can be much lower than the orders of the models. An additional advantage of the proposed interval control techniques is the ease of modeling of the parametric uncertainties by just bounding them. These control techniques have been tested with laboratory sensors which are bulky and expensive. The last part of the thesis dealt therefore in the study of novel measurement techniques devoted to miniaturized piezoelectric systems in order to make the feedback control techniques possible at low costs and at a high level of packageability. Roughly speaking, the core of the works carried out proposed two main and interesting directions: i) exploiting observers techniques, ii) and exploiting the sensing capability of piezoelectric materials to develop self-sensing actuators, i.e. the actuator is also sensor. Observers are essential complementary tools in these miniaturized systems where the convenient sensors capable to track the required signals are very limited. Finally, self-sensing features a high packaging level to measure signals in piezoelectric actuators. Initially adapted to vibrations damping, we show here that this approach can also be adapted to micromanipulation and microassembly applications.

Temporally, the works carried out since 2006 are in a continual evolution. We started with simple piezoelectric multimorph, i.e. monovaryable systems. Their modeling and control and the signal measurement and estimation in them have been extensively investigated and led to important results recognized at the international level. Over the time, these different contributions have been being gradually extended to multivariable due to the raise of multi-DOF piezoelectric systems. Finally, these last years, we have started to investigate on even more miniaturized, highly performant, highly dexterous and low costs piezoelectric MEMS.

6.2 General perspectives

Piezoelectric actuators bring high resolution, high bandwidth and ease of integration in precise and high dynamics positioning tasks. Control theory contributes to the design optimization of the systems, brings performances enhancement and robustness of the tasks thanks to the controllers, and participates to the packaging and to the efficiency of the measurement thanks to observers. Microtechnologies and related techniques permit to miniaturize the systems. As described in this thesis, the combination of control theory and PZT piezoelectric materials based cantilever actuators have been proved to provide unrivalled high precision and high dynamics miniaturized positioning systems utilizable in tremulous applications like micromanipulation, microassembly and phonomicrosurgery. However, there is still an open space in all these developments. An essential part in this open space deals with going further on the miniaturization of high performances and dexterous systems. We will discuss about this aspect in [Section. 6.2.1](#).

An essential concern when developing smaller and smaller functional systems relates to their powering. On the one hand, using external electrical generators to power the miniaturized systems strongly limits the flexibility and the portability in their utilization. On the other hand, the actual batteries are very limited in autonomy. The second perspective that we will discuss in [Section. 6.2.2](#) evidently deals with the powering and the autonomy of miniaturized systems. The undeniable solution is the energy harvesting. As we will see, piezoelectric based energy harvesting, yet well studied, can largely be rendered more efficient and highly autonomous by going beyond the simple cantilevers-mass system as classically employed. The concept will involve several disciplinaries, among which control theory and microfabrication have notable positions.

In the last perspective, a question or two is proposed: can macrosystems be developed from MEMS? What is the gain? An example which lies in this direction is the LABEX ACTION project [\[350\]](#) that deals with the development of intelligent matters from intelligent MEMS. In the long-term perspective that will be discussed in [Section. 6.2.3](#), with the same fashion than intelligent matters, there is an interesting scope to explore in harvesting matters developed from harvesting MEMS. The key idea consists in exploiting the high efficiency and high autonomy harvesting MEMS explored in [Section. 6.2.2](#) as basis of the harvesting matter, which therefore features a high energy density, more flexibility, high autonomy and low costs making the difference relative to the actual green energy.

Many of the general perspectives described here are also from the fruitful exchanges and discussions with colleagues or acquaintances, at the local level (FEMTO-ST), at the national and at the international level, some of whom are not in the domain of piezoelectricity, of control theory, of miniaturized systems or of precise and high dynamics positioning.

6.2.1 Going further in the miniaturization of high performances and high dexterity piezoelectric systems

The high coupling factors of PZT (Lead zirconate titanate) bulks materials compared to the other piezoelectric materials makes them very well appreciated in the development of high efficiency miniaturized actuators. The piezoelectric material admitted to be competitive face to PZT is the single crystal PMN-PT (lead magnesium titanium niobium oxyde crystal) of which the high coupling factors can reach 90%. However, PMN-PT are not yet mature, still in research phase, rare and expensive unlike PZT which are commercially available at low costs. This finally places PZT on the first step of the podium. In counterpart PZT bulks suffer from the lack of well established process of microfabrication in clean room which limits the level of miniaturization with them. One of the perspectives in miniaturization deals therefore with the processes of microfabrication. The efforts that have been started (see [Section. 2.5](#)) regarding the room temperature metal-PZT bonding and thinning and that permitted to go towards PZT-MEMS, i.e. very miniaturized PZT devices, are to be continued and to be exploited. Yet the proof-of-concept has been validated through the success fabrication of PZT cantilever structures without disrupting the properties of the materials, the fabrication of more complex structures has to be tackled, in particular 3D structures and hybrid structures. For hybrid structures, which are the combination of two or several different principles of actuation (thermal and piezo, electrostatic and piezo, electroactive polymers and piezo,...), an additional challenge is posed if the process and the materials played into role are not compatible.

We assisted to the raise of multi-DOF MEMS with integrated actuation these last years. Due to the limitation of the microfabrication technologies, the number of degrees of freedom are generally two or three. Nevertheless, there are important benefits in the capability to develop higher degrees of freedom: we gain more dexterity and more flexibility in positioning applications, we improve the efficiency in energy harvesting applications (see [Section. 6.2.2](#))... Two non-exclusive solutions are possible. In the first solution, the development of these highly dexterous MEMS can be tackled by employing not only clean room technologies but also microassembly tasks to make the fabrication. This technique has been widely used at the department, in the national and in the international community of microrobotics in order to realise complex non-actuated microstructures. Here we can exploit the technique to realise complex and dexterous actuated piezoelectric MEMS. In the second solution that is considered as a perspective of research , we propose to explore the hybridization technique to combine piezoelectric actuation with other principles. Hence we can create the additional degrees of freedom that the piezoelectric actuation only could not provide. To summarize, hybridization will be used to increase the performances of the final actuated systems (see the proof of concept in [Section. 2.3](#)) and to bring additional dexterity.

The contribution of the control theory in precise and high dynamics positioning systems is undeniable. Designing these systems thanks to tools from this disciplinary is very few in the litterature, though, such formal methods can bring an ease of design and a guarantee in the results. The combination of interval techniques and control tools to design permits to develop actuated structures with guaranteed static and dynamical performances. We have proved the

concept through the design of piezoelectric actuators that have simple cantilever structures. A perspective in this direction consists in extending the approach to design more complex, hybrid, multi-DOF and dexterous miniaturized systems from which the specified performances are guaranteed. The extension may involve new problems such as: existence of solutions in the research domain, optimal solutions among the results, ...

Regarding the control and the signals measurement/estimation, there is still a lot to do in their study for piezoelectric systems and for miniaturized systems in general. Going further in the miniaturization and increasing the number of DOF of the piezoelectric systems doubtlessly augment the challenges in the controllers synthesis. As the systems are downscaled: their sensitivity to the environment (surrounding vibrations, thermal noise, ambient temperature, adhesion forces...) are increased, their models are more and more uncertain and the cross-couplings are stronger. Robust control techniques (intervals, H_∞ , nonlinear robust techniques,...) are therefore to be used in that case. Adaptive robust techniques (gain-scheduled H_∞ , LPV, NLPV, ...) would be the ideal proposition when the uncertainties are too large, however the lack of performant and convenient sensors for miniature systems make impossible their use because the techniques require a realtime measurement of defined signals or of defined parameters. Finally, the measurement of signals in smaller and smaller actuated systems is a great challenge. Piezoelectric systems have the advantage of sensing capability which are potentially profitable here. But advanced studies should be carried out in self-sensing for these miniaturized and multi-DOF systems in order to ensure the precision and the dynamics in the measurement against the models uncertainties and the high sensitivity to the environment which are higher. Hybridizing the measurement can also be another solution. If we hybridize the actuation (see above discussion), we can employ these different transducers to also perform the measurement in a self-sensing fashion (all the transducers are actuators and sensors), or in a switched fashion (some transductions are for the sensing and some for the actuation).

To summarize, going further in the miniaturization of high performances and high dexterity piezoelectric systems with the actual performant and low costs piezoelectric materials (PZT) implies the improvement and the maturation of the microfabrication processes, the involvement of other method in the fabrication (microassembly), the introduction of novel principle of actuation (such as hybridization) that permits to gain in performances and in dexterity, and the strong involvement of control theory at different stages (design, signals estimation, and control). We place this target as medium term perspective.

6.2.2 Towards highly autonomous and smart miniaturized systems

6.2.2.1 The key motivation

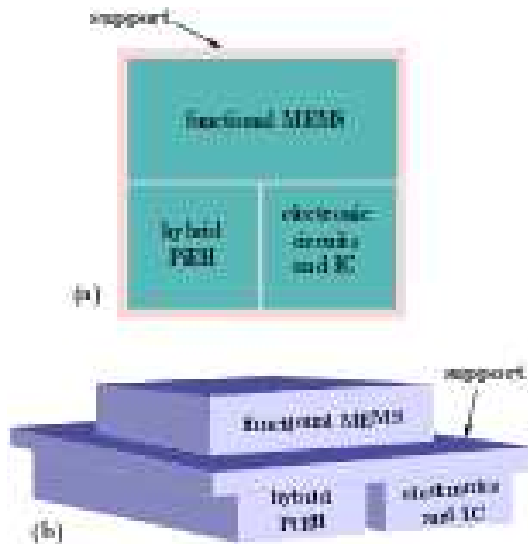


Figure 6.1: Towards autonomous and smart miniaturized devices.

When we go further in the miniaturization, an essential question concerns the power supply. Employing external generators will limit the flexibility and the portability of the miniaturized systems. On the other hand, the actual batteries are limited in autonomy. The aim in this medium/long term perspective consists in investigating energy harvesting techniques to render highly autonomous miniaturized systems. The key motivation is to result in autonomous and smart packaged devices that contain: the energy generation based on energy harvesters, the functionality, the conditioning elements (electronic circuits) and the intelligency such as control and signals treatments in IC (integrated circuits), all packaged within less than some cubic centimeters as depicted in Fig. 6.1. In the figure, PiEH means piezoelectric hybrid energy harvester. The entire package is composed of the

functional MEMS, the harvester mechanical structure, and an electronics for the harvester and for the intelligency management (memory and microprocessor...). All these components can be placed in a planar fashion (Fig. 6.1-a) or in a vertical arrangement (Fig. 6.1-b). In the figure, the functional MEMS can be a precise positioner, a scanners for medical or optical applications, a system for flapping-wings in flying microrobot, a wireless sensor,... Three applications related to sensors in automotives, animals tracking devices, and medical microrobots will be discussed latter. Let us first discuss about the energy harvesting itself.

6.2.2.2 Study of novel high autonomy and high efficiency energy harvesters

Energy harvesting consists to scavenge the energy from the ambient background, this energy being free and considered lost if not exploited. The different sources of background energy are: solar, thermal, wind, waves, sounds, ambient vibrations... Example of commercially and well settled energy harvesters are photovoltaic solar panels and wind energy generators. Vibrational energy harvesting can be effectuated with piezoelectric materials. The principle lies in the exploitation of the ambient vibrations to excite and deform the piezoelectric devices which permits to generate electrical charge thanks to the direct piezoelectric effect. Vibrational piezoelectric energy harvesting has raised many studies and projects at the national, european and international levels. The litterature is dense in the subject. Cantilevers-mass structures have been extensively employed in these studies and proved the concept of inertial (vibrational) piezoelectric energy harversting with compact devices. Thanks to the small

sizes, they are compatible with miniaturized systems. The power-efficiency in this traditional technology is however limited. An actual trend to increase the power-efficiency in interial piezoelectric harversting is the hybrid piezoelectric harvesters (see for instance [352; 353] and references herein). The principle is based on the introduction of additional transducers in the same package. This technique is efficient but the complexity of the conditioning electronics and the volume of the final device are increased.

The potential perspective in piezoelectric energy harvesters which is proposed here to reach the endeavor schemated in Fig. 6.1 is distinguished by four breakthroughs: high miniaturization, flexibility, very high autonomy, and very high efficiency energy harvesting. The endeavor can only be reached by putting in interaction several disciplinaries: materials science, micro-fabrication, systems design and control theory, electrical engineering, and packaging. The perspective will inevitably involve several different departments intra-FEMTO-ST or even other laboratories in France or abroad. The contribution in each disciplinary is discussed below.

Materials science - PZT contains lead-element (typically above 60 weight percent lead in commercial products) directly associated to health and environmental problems due to its harmful effects. The European Standardisation Organization ranks PZT as a chemical element of which the quantities should be reduced or replaced in its legislation as hazardous substances since 2003. Novel materials are now under studies to rival the PZT. Single crystal niobate lithium is one of these potential materials that have transduction performances and costs which can compete those of PZT. Colleagues in another department at FEMTO-ST are focusing in the synthesis and improvement of this novel material. There is a great gain to employ this materual to the development of safe and harmless miniaturized devices.

Microfabrication - Microfabrication technologies are the tools that permit to machine and to fabricate miniaturized structures from materials. According to the designs of the energy harvesting devices and to the materials employed (piezo only, hybrid,...), new microfabrication processes may be necessary. Thus more efforts should also be given to the development of these new processes. FEMTO-ST has a microfabrication technology central (the large clean room MIMENTO) that is part of the national net of large centrals (RTB).

Structures design and control theory - The main technical and scientific contribution of AS2M department in this large perspective deals with the design and development of the structures in order to maximize the harvesting efficiency and the autonomy, or in order to ensure some predefined performances with minimal dimensions. Four major themes are proposed for that: i) hybridization of the harvesting, ii) multiple degrees of freedom (multi-DOF) and multi-modal of the harvesters structures, iii) two modes of functioning (recharge mode and autonomous mode), iv) and optimal and robust design of the structures.

i) Classical hybrid piezoelectric harvesters utilized several transducers in one package. This technique is efficient but leads to large volume and complex conditioning electronics. We propose here to employ one transducer as basis of the hybrid harvesting. By using a piezoelectric material, deposited or bonded on metal, we will exploit the thermal effects (pyroelectricity

and thermal expansion) and the vibrations as sources of energy to be scavenged: a hybrid thermal/vibrational piezoelectric harvester. This hybridization has been demonstrated to be efficient in the design of actuators (see [Section. 2.3](#)) and is exploited here for harvesting. Its main advantage is, if the structures are well designed, the limited efficiency of vibrational energy harvesting only will be highly amplified with the hybrid energy harvesting within compact sizes.

ii) Multi-DOF and multi-modal structures permit to increase the sensitivity of the harvesters. First, whatever the directions of the vibrations, and thus whatever the orientation and emplacement of the harvesters in its working environment, the output energy is always maximized and consequently the autonomy is increased. We call this the spatial sensitivity. In the second interest which we call the modal sensitivity, the harvesters can be designed to "capt" many frequencies contained in one vibrational environment. As the environment is not only typified by its fundamental frequency, but also by additional noise and "harmonics", we can exploit all these to increase the efficiency. Finally, multi-modal harvesters can be used in different vibrational environments that are characterized by different fundamental frequencies.

iii) An interesting principle that can be taken from daily-life applications (for eg. cell phones) is to have two modes: recharge mode and utilization mode. We propose here to introduce the recharge mode additionally to the autonomy mode of the harvesters. Whilst the autonomy mode is based on the vibrations and the temperature that surrounds the harvesters, the recharge mode is from forced vibrations. More precisely, we propose to make possible a quick recharge of the whole energy harvesters (and of the miniaturized systems that encompass the harvesters) thanks to a conveniently designed "charger" that excites at high frequency. The recharge mode allows to give initial energy to the packaged systems before they are left for autonomous functioning. To have a high frequency of vibrational excitation, the charger can be based on ultrasonic or magnetic principles.

iv) To tackle the mechanical structures design and to reach or to guarantee the specified performances from the harvesting, we propose to employ control theory tools (optimality, robustness, dynamical modeling, uncertainties modeling, interval tools,...). Yet, these tools have been demonstrated to provide robust or optimal performances in the design of piezoelectric actuators in the past (see for instance [Section. 2.6](#) and references herein). For instance, if the harvesters have been designed to track a frequency f of vibrations, and if in the real situations the frequency is $f + \Delta f$ where Δf is the difference or error, the robust design should still ensure the specified output-energy.

Electronics - Electrical circuits are required to transform the charge furnished by the piezoelectric transducer during the harvesting into exploitable voltages. Many works have been raised in these circuits in order to have regulated output voltages. In the proposed perspective here, challenges are posed in the design of the electronics to maintain regulated voltages because of the hybrid thermal/vibrational principle, multi-DOF deformation of the structures and multi-modal functioning. Furthermore, in order to maintain an unrivalled autonomy of the whole miniaturized systems, the electronics should feature low consumption. Discussions

have been launched with some specialized laboratories in France (including LGEF INSA Lyon) for this aspect.

Packaging - Packaging consists in studying how to rassemble these different results into one technological package. This disciplinary is of great interest if there is an objective of batch development or of industrialization. Whilst there are research laboratories specialized on packaging, industrial partners may be the the most appropriate to do this, in order to benefit from their point of view on industrializable devices.

Other disciplinaries - The functionality of the smart MEMS and the expected applications for the entire miniaturized devices certainly involve other disciplinaries. For instance, if the functional MEMS is a sensor that emits analogical or digital signal wirelessly, telecommunication and sensors disciplinaries will be involved.

Remark - Another contribution of control theory deals with the design and the control of the functional MEMS itself. First, we can employ control theory tools (optimality, robustness, intervals...) to design the MEMS to have minimal consumption by still maintaining the maximal performances. This is a dual problem of the design of the harvesters, where we utilize control theory tools to design their structure for a maximal output-energy with reduced sizes. Second, if the functional MEMS needs controllers, these latter can be synthesized such that the electrical consumption is also reduced (with optimal controllers deisgn,...).

6.2.2.3 Applications that are in the loop, or almost

Three applications are proposed here. The first application deals with sensors in automotives and a national ANR project has just been submitted for that. The second application (animal tracking) was the result of fruitful discussions with some associations in the Franche-Comté region and farmers and researchers in Australia, when I have been visiting researcher there. No project is in the loop but this can be a good applicative perspective. The last application is linked to medical microrobotics that is carried out by the MINAROB team at the department of AS2M and is from discussions with related colleagues.

First application: energy harvesting for flexible and autonomous sensors in automotives

A modern car contains over 100 different sensors. Sensors and actuators based on MEMS are used to control various elements of automobiles and aircrafts, such as the powertrain and chassis control, advanced areas of driver assistance systems and telematics applications, see Fig. 6.2 [354]. MEMS sensors offer high accuracy, produce a digital signal on their own and are robust in the temperature and pressure ranges used in automobiles. Low-power MEMS sensors, based on silicon technology, became the devices of choice offering cost effective solutions and high yield in automotive and aerospace industry [354]. These sensors are all operated by electrical power. Thus, the signal transfer and alimentation of the big number of sensors in a vehicle introduce a complex network of wires. To minimize costs, automotive sensors

may not have more than three connected wires [355]. The connecting cables have quite an impact on the mass of vehicles (up to 50kg , several km in length) and add complexity and costs to installation and maintenance diagnostics [356]. Moreover, the wire connections have to be protected from heat close to solder points, or hot places near the engine or exhaust

pipe [354]. Furthermore, 80% of the maintenance costs are related to wiring and contact problems. Thus, simplification and miniaturization of these networks is a key issue in order to reduce weight, space and cost of future automobiles and aircrafts [355]. One big step forward in the integration of sensors would be the usage of maintenance-free sensors operating in wireless mode and drawing the source of power from the environment, as i.e. from vibrations, heat or solar energies. The deal consists therefore to develop high autonomy and high efficiency miniaturized energy harvesters based on the hybridization of piezoelectric transducer and the thermal principle to supply the MEMS sensors in the automotives. A national project² has just been submitted. Five partners, listed below, are involved.

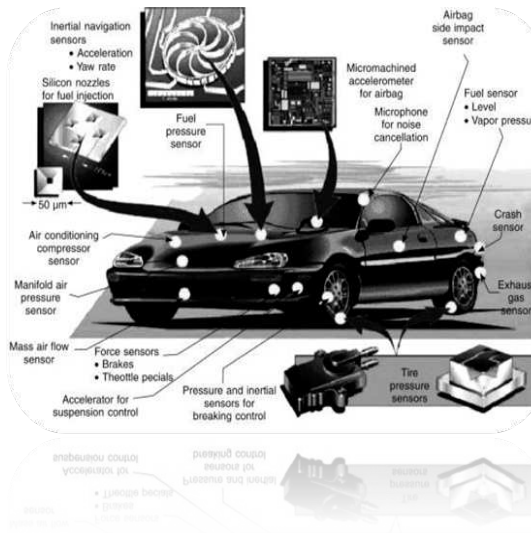


Figure 6.2: MEMS in automotive (Precision Engineering, by V.C. Venkatesh, Sudin Izman).

- FEMTO-ST institute at Besançon: design of the harvesters structures by using control theory (AS2M department), niobate lithium materials synthesis and improvement (MN2S department), deposition of niobate lithium films by spray/aerosol pyrolysis (TF department).
- LGEF laboratory at INSA Lyon: design of smart electronic circuits.
- Cedrat Technology company at Grenoble: guidelines, requirements/constraints of industrial fabrication of energy harvesters, integration in sensors.
- Frec|n|sys company at Besançon: wafer on wafer technology, piezoelectric simulation.
- PSA Peugeot Citroën company: guidelines, harvesters working conditions, in-situ test.

Project coordinators: Ausrine Bartasyte and Micky Rakotondrabe, FEMTO-ST Institute.

Second application: energy harvesting and animal tracking

Animal tracking is an application that has been raised in many research projects and has produced industrialized devices. Active tags in animal tracking are embedded devices that can save data autonomously or emit signals by their own. This permits to record, to follow and to

²ENHANCE project: ENergy Harvesters for self powered automotive sensors: from advANCED materials to smart devices.

analyze their movements, to identify and to trace their origins (mainly for animals for foods), to track their positions, to health-monitor, or to understand their ways of life. Many animals types are involved, for instance: livestock, snakes, birds, lynxes,... Active tracking devices require however energy. The miniaturized and highly autonomous energy harvesters proposed in the above perspective certainly present many advantages in animals tracking application. First, the tracking devices will not disrupt the animals, as the devices are very small and their masses very light. Second, the devices can be injected in the animals or well dissimulated on them, and thus discreet. This latter advantage is particularly interesting in situations where animals theft is common (eg. livestock theft). Indeed, the desactivation or the remove of the devices by the thieves are avoided allowing a chance to locate the position of the stolen livestock. Fig. 6.3 picture an example of active tracking device industrialized by *Tekvet* and *IBM* companies to track livestock [357; 358]. The figure shows that the actual device is still bulky, may be uncomfortable for the animals, and are not concealable. This device is powered by a battery and thus not autonomous. The last advantage of the energy harvesters proposed in the above perspective concerns the autonomy itself. Some animal tracking applications like migratory birds tracking require a very high autonomy of the electrical generator (several months) which can only be satisfied by highly autonomous energy harvesters.



Figure 6.3: An active tracking device to track livestock, developed and industrialized by *Tekvet* and *IBM* [357; 358].

Medical applications

An application to which the MINAROB team of the AS2M department is nowadays facing is the medical application. Intra-body capsules and microrobots require energy to perform the tasks they have to do: surgery, filming thanks to embedded cameras, ... The capsules and microrobots are guided from the external with a magnetic field [8; 359]. The same guidance magnetic field can also be used to convey additional magnetic signal that will excite at high frequency an energy harvester device embedded in the capsule.

6.2.3 From MEMS harvesters to matters harvesters

A long term and remarkable perspective deals with the exploitation of the developed miniaturized and MEMS hybrid thermal/vibrations piezoelectric harvesters previously proposed to create a harvester matter with surface or volume shape, deformable/flexible or rigid structure. As the individual MEMS harvesters are designed to be highly autonomous and highly efficient, we can assess that the matter over which the MEMS harvesters are distributed will features a high autonomy and a high energy density. Possible applications of harvester matters include the energy harvesting in very isolated area, in aerospace, ... Beyond the good energy density itself and the electrical generator applications, one of the main interests here is the fact that we can extend the concept of "intelligent matter" (developed in the LABEX ACTION [350]) to "autonomous intelligent matter" and "self-supplied intelligent matter". The entire autonomous and smart miniaturized system developed in Section. 6.2.2) can be taken as the basic elements of a smart and autonomous matter, as depicted in Fig. 6.4.

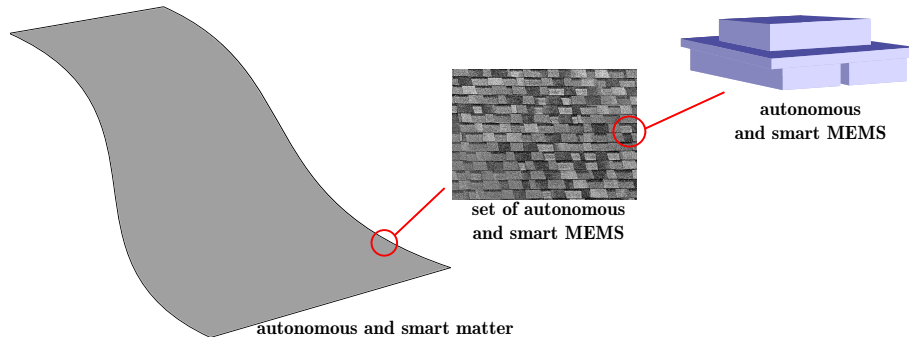


Figure 6.4: High autonomy and smart miniaturized systems as basic element of high autonomy and smart matter.

Chapter 7

Appendix

Appendix A

Curriculum Vitae

A.1 Personal track

- A.1.1 Positions
- A.1.2 Education and diploma
- A.1.3 Research activities: summary
- A.1.4 Teaching activities: summary
- A.1.5 Prizes, awards and distinctions
- A.1.6 Misc

A.2 Research activities

- A.2.1 Journals editorial activities
- A.2.2 Editorial and organization responsibilities in conferences
- A.2.3 Supervising: post-doc, PhD, BSc, MSc
- A.2.4 Projects responsibilities
- A.2.5 Projects participation
- A.2.6 Other responsibilities
- A.2.7 Workshops/tutorials organization
- A.2.8 PhD Committee member
- A.2.9 Reviewing
- A.2.10 Societies and group memberships

A.3 Teaching activities

- A.3.1 Pedagogic and administrative responsibilities
- A.3.2 Teaching for undergrads (BSc)¹⁴⁰, UFC University
- A.3.3 Teaching for MSc UFC University and *écoles d'ingénieurs* at Besançon
- A.3.4 Invited lecture

A.1 PERSONAL TRACK

Manitrarivo Micky John RAKOTONDRABE

Associate Professor (Maître de Conférences), University of Franche-Comté (UFC)

AS2M department of the FEMTO-ST Institute
CNRS URM6174 – UFC – ENSMM – UTBM
24, rue Alain Savary, 25000 Besançon, FRANCE

Tel: +33 381 402 810 – Fax: +33 381 402 809

mrakoton@femto-st.fr ; <http://sites.femto-st.fr/~micky.rakotondrabe/>

Date of birth: February 8, 1978 in Ambohijanajary, MADAGASCAR

Citizenships: French, Malagasy



A.1.1 POSITIONS

2012	Visiting researcher, University of Newcastle/CDSC - Australia, 3 months (march to june)
2011	Visiting researcher, University of Texas at Arlington/ARRI Institute - TX USA, 1 month (nov.)
2011-2012	CNRS fellow (<i>délégation CNRS</i>), 1 year
2007 onwards	Associate Professor, UFC at Besançon; research appointment at FEMTO-ST Institute
2006-2007	Assistant Professor, UFC at Besançon; research appointment at FEMTO-ST Institute

A.1.2 EDUCATION and DIPLOMA

2014	Habilitation to Direct Research diploma (HDR) , UFC at Besançon
2006	PhD on Control Systems , UFC at Besançon
2003	MSc on Control Systems, National Institute of Applied Sciences (INSA) Lyon, France
2002	'diplôme d'Ingénieur', Catholic Institute of Arts and Métiers (ICAM) Lille, France

A.1.3 RESEARCH ACTIVITIES: summary

My research activities are led at the department of AS2M of FEMTO-ST Institute. They deal with the: design, development, modeling, control and signals measurement and estimation in piezoelectric based microsystems. The systems behaviors include linear and nonlinearities (hysteresis and creep) and badly damped vibrations. The proposed control techniques enclose feedforward and feedback schemes. In feedback schemes, mainly robust techniques are studied: H-infinity techniques and interval control techniques. In the use of intervals, new theoretical results are also proposed and are applied to different applications: design, control, structural analysis.

A.1.4 TEACHING ACTIVITIES: summary

My teaching activities are principally for 3rd year undergrad (EEA: Electrical and Control Engineering department) students and for Master 1st and 2nd year (Mechatronics). My lectures are: robotics, control systems.

A.1.5 PRIZES, AWARDS and DISTINCTIONS

2013	Among the 5 most cited papers of IEEE TASE (' <i>Complete open loop control of hysteretic...</i> ')
Nov 2011	Romanian Scientific-Activities-Award (shared with Dr I. A. Ivan, Univ. Targoviste Romania)
Oct 2011	French Scientific-Excellence-Award (the national PES award)
2011	CNRS fellow (1 year)
2011	CRCT fellow (6 months), I have declined the CRCT in favour of the CNRS fellow
2011	Best Application Paper finalist, IEEE CASE Triesta Italy
2006	Best PhD thesis finalist, University of Franche-Comté
2006	Best Paper Award finalist (4 selected among 580 papers), IEEE ICARCV Singapour
2003	Ministerial grant award for the PhD works (2003 – 2006)

A.1.6 MISC

2013 onwards	Committee member of the Service of Handicapped Persons at the diocese of Besançon
2012 onwards	Committee member of the Service of Migrants at the diocese of Besançon
summer 2011	International solidarity travel in Tchad for the schooling and integration of disadvantaged youngs
2002-2003	President of an association in Lyon for schooling Malagasy disadvantaged youngs
1996-1997	Placement year in order to travel around Madagascar

A.2 RESEARCH ACTIVITIES

A.2.1 Journal Editorial Activities and Technical Committee Activities

- 2015 Guest Editor of "special issue: High resolution actuators", MDPI ACTUATORS
2015 Guest Editor of "focused section: Hysteresis in Smart Mechatronic Systems: Modeling, Identification, and Control", IEEE/ASME TRANSACTIONS ON MECHATRONICS
2014-*onwards* Active member of the IEEE-RAS Technical Committee on Micro/Nano Robotics and Automation
2012 Guest Editor of "special issue: advanced control in micro/nanosystems", JOURNAL OF CONTROL SCIENCE AND ENGINEERING

A.2.2 Editorial and Organization Responsibilities in Conferences

- 2015 Program Committee, IEEE ICIA Yunnan China
2015 Program Committee, IEEE MSC Sydney Australia
2015 Program Committee, IEEE/ASME AIM Pusan South Korea
2015 Program Committee, IEEE ICRA Seattle WA USA
2015 Program Committee, SPIE Sensing Technology + Applications Baltimore MD USA
2014 Program Committee, IEEE ROBIO Hanoi, Vietnam
2014 Program Committee, IEEE ICRA Hong Kong China
2014 Program Committee, IEEE/ASME AIM Besançon France
2014 IEEE/ASME AIM Besançon France
Organizing Committee Chair,
Webmaster of the conference website,
Papercept and Papercept-registration technical co-administrator,
2013 Program Committee, IEEE/ASME AIM Wollongong Australia
2013 Program Committee, IEEE ICRA Karlsruhe Germany
2012 Programm Committee for the Workshop: "μCONTROL", Besançon France
2012 Committee Member for the IEEE ICRA 2012 Best Automation Paper Award, St Paul MN USA
2010 Program Committee, IEEE-CASE Toronto Canada
2006 Local organization committee, the 'Génie Industrielle (GI)', Besançon France
2006 Local organization committee, the 'International Workshop on MicroFactory (IWMF)', Besançon France

A.2.3 ADVISED post-docs, PhD, Engineers and MSc internships

(for postdoctoral and PhD fellowships, the co-advisors are in parenthesis)

POST-DOCS

- Omar ALJANAIDEH, 2014 (7 months, with Philippe Lutz) .
- Vincent CHALVET, 2014 (6 months, with Cédric Clévy) .
- Eakkachai Ton PENGWANG, 2013-2014 (12 months, with Kanty Rabenorofoa and Nicolas Andreff) .
- Ioan Alexandru IVAN, 2012-2013 (10 months, with Philippe Lutz).
- Alex BIENAIME, 2012-2013 (12 months, with Cédric Clévy).
- Juan Antonio ESCARENO, 2012-2013 (15 months, with Joël abadie).
- Ioan Alexandru IVAN, 2008-2010 (24 months, with Philippe Lutz and Nicolas Chaillet).

PHD

- Yasser Al HAMIDI, UFC Besançon, nov 2013- nov 2016 (with Philippe Lutz until december 2014).
- Didace HABINEZA, UFC Besançon, oct 2012- sept 2015 (with Yann Le Gorrec).
- Sergio Andree LESCANO ALVARADO, UFC Besançon, jan 2012- jan 2015 (with Nicolas Andreff).
- Sofiane KHADRAOUI, UFC Besançon, feb 2009 - jan 2012 (with Philippe Lutz).

ENGINEERS AND MSc INTERNSHIPS

- Ismaël Ahmed ISMAEL, MSc degree UFC Besançon, 2014.
- Fadwa HOUSSALI, MSc degree UFC Besançon, 2014.
- Erwann DUPONT, MSc degree UFC and ENSMM Eng. School Besançon, 2014.
- Vincent TRENCHANT, MSc degree UFC and ENSMM Eng. School Besançon, 2014.
- Yasser Al HAMIDI, MSc degree UFC Besançon, 2013.
- Adiasa ADIASA, MSc degree UFC and ENSMM Eng. School Besançon, 2013.
- Quentin ASSAILLY , Engineering diploma, ENSIAME Valenciennes Eng. School, 2013.
- Mohamed Lamine BERRANDJIA, MSc degree, CDTA, Alger Algeria, 2012.
- Paul Michaël MOORE, BSc/PhD degree, University of Florida, Gainesville, 2011.

- Qihong ZHOU, MSc degree UFC Besançon, 2011.
- Kamel NCIR, MSc degree University of Montpellier, 2009.
- Elodie Havet, Engineering degree IPSA Eng. School Paris, 2008.
- Mamadou Cissé DIOUF, MSc degree UFC Besançon, 2007.

A.2.4 PROJECTS and FUNDINGS Responsibilities

(the amount corresponds to the grant given to the laboratory. The total is: 827k€)

2014 University of Franche-Comté post-doc fellowship funding, 'Self-sensing in 2-DoF piezoelectric actuators: observer and control', 21k€, 7 months. **Coordinators: Micky RAKOTONDRABE.**

2012-2016 National ANR Young Investigator C-MUMS project (<http://sites.femto-st.fr/c-mums/>), 'Control of Multivariable Piezoelectric Microsystems with Minimization of Sensors', 177k€, 42 months. **Principal Investigator and Coordinator: Micky RAKOTONDRABE.**

2012-2013 National ANR Emergence MYMESYS project (<http://sites.femto-st.fr/mymesys/>), 'High Performances Embedded Measurement Systems for multiDegrees of Freedom Microsystems', 300k€, 24 mois. **Principal Investigator and Coordinator: Micky RAKOTONDRABE.**

2013 University of Franche-Comté post-doc fellowship funding, 'Design, development, characterization and modeling of a 3-Dof (rho-theta-z) hybrid piezoelectric micro-platform for laser scanning in phonosurgery ', 27k€, 9 months. **Coordinators: Kanty RABENOROSOA, Nicolas ANDREFF and Micky RAKOTONDRABE.**

2013 University of Franche-Comté BQR funding, 'Energy harvesting for autonomous in-vivo millimetric robots', 16k€, 12 months. **Coordinators: Kanty Rabenorosoa and Micky RAKOTONDRABE.**

2011 University of Franche-Comté BQR funding, 'Interval tools for the modeling, design and robust control of multivariable piezoelectric microgripper', 5k€, 12 months. **Principal Investigator and Coordinator: Micky RAKOTONDRABE.**

2010 ENSMM BQR funding, 'Measurement and control of force/position multidirectional microassembly system', 14k€, 12 months. **Coordinators: Cédric Clévy and Micky RAKOTONDRABE.**

2009-2012 Funding for one PhD student from the Conseil Général du Doubs, 'Interval modeling and control of piezoelectric microactuators', 36 months, 90k€. **Coordinators: Philippe Lutz and Micky RAKOTONDRABE.**

2008-2010 European FP7-PEOPLE-IEF MicroPADS project (<http://sites.femto-st.fr/micropads/>), 'New Micro-Robotic Systems featuring Piezoelectric Adaptive MicroStructures for Sensing and Actuating, with Associated Embedded Control: Microstructured Piezoelectric Adaptronic Systems', 171k€, 24 month, With researcher fellow Dr Ioan Alexandru IVAN. **Scientific Coordinator: Micky RAKOTONDRABE.**

2006 OSEO-ANVAR funding, 'Modeling, identification and control of monovariaable hysteresis', 6k€, 7 months. **Coordinators: Mamadou Cissé DIOUF and Micky RAKOTONDRABE.**

A.2.5 PROJECTS Participation

(active participation to the following past and present funded projects)

2011- 2014 µRALP (european project), coordinators: Nicolas ANDREFF (FEMTO-ST) and Leo de MATOS.
2011-2014 NET4M (european/USA project), coordinator: Philippe LUTZ.
2012-2013 MIM-Hac (regional project), coordinator: Cédric CLEVY.
2008-2012 ANR NANOROL (national project), coordinator: Michaël GAUTHIER and Stéphane REGNIER.
2010- 2011 Maturation-project (regional project), coordinator: Philippe LUTZ.
2010-2012 MicroFactory-2 (regional project), coordinator: Jean-Marc NICOD.
2007-2009 MicroFactory (regional project), coordinator: Laurent PHILIPPE.
2004-2008 EUPASS (european project), coordinators: Philippe LUTZ (FEMTO-ST) and Sergej FATIKOW.

A.2.6 Other responsibilities

2014-onwards Committee member of the “TEMIS Innovation Pépinière d'Entreprises” for the expertise of newly created companies.

A.2.7 Workshops, Tutorials and special sessions organization

- 2015 Organizer of the special session on 'Control of smart mechatronic systems'
ACC Chicago IL USA
- 2014 Organizer of the 2 special sessions on 'Advances in micro and nano-scale positioning: design and control'
IEEE/ASME-AIM Besançon France (11 invited papers for two twin sessions)
- 2014 Organizer of the Tutorial 'Advanced control and noise reduction for micromanipulation'
IEEE/ASME-AIM Besançon France (<http://sites.femto-st.fr/tutoAIM14/>).
- 2011 Organizer of the Workshop 'Automation of assembly and packaging at the micro/nano-world',
IEEE-CASE Trieste Italy (<http://sites.femto-st.fr/WS-case11/>).
- 2011 Organizer of the Tutorial 'Dynamics, characterization and control at the micro/nano-world',
IEEE-ICRA Shanghai China (<http://sites.femto-st.fr/Tuto-icra11/>).
- 2010 Organizer of the Workshop 'Signal measurement and estimation techniques issues in the
micro/nano-world ', IEEE-ICRA Alaska USA (<http://sites.femto-st.fr/WS-icra10/>).
- 2009 Organizer of the Workshop 'Control issue in the micro/nanoworld", IEEE-ICRA Japan (<http://sites.femto-st.fr/~micky.rakotondrabe/icra09/>).

A.2.8 PhD Committee

- 2012 Committee member of the PhD dissertation of Muhamed Rashid PAC, University of Texas at Arlington (UTA TX) USA, title 'Precision and mobility analysis for microrobot desing and control', nov. 2012.

A.2.9 Reviewing

(regular or punctual reviewer for the following book, conferences and journals)

BOOK REVIEWING

- 2014 Reviewer of the book proposal "Precision modeling and control of systems with hysteresis", by Dr Liu Lei, publisher: Elsevier Chandos Publishing.

CONFERENCES

IEEE-ICRA, IEEE-IROS, IEEE-CASE, IEEE-IECON, IEEE-ICIT, IEEE-NANO, IEEE-MSC, IEEE-ROBIO, IEEE/ASME AIM, ASME IDETC, IFAC Symposium on Mechatronics, IFAC Symposium on NOLCOS, IFAC World Congress, WorldHaptics, ROCOND, CDC, ACC, RSI ICRoM.

JOURNALS

- IEEE Transactions on Robotics
- IEEE Transactions on Biomedical Engineering
- IEEE Transactions on Control Systems Technology
- IEEE Transactions on Automation Science and Engineering
- IEEE Transactions on Instrumentation & Measurement
- IEEE Transactions on Industrial Electronics
- IEEE Transactions on Industrial Informatics
- IEEE Transactions on Vehicular Technology
- IEEE/ASME Transactions on Mechatronics
- SIAM Journal of Optimization and Control
- IFAC AUTOMATICA
- IFAC/Elsevier Control Engineering Practice
- IFAC Mechatronics
- International Journal of Control
- Asian Journal of Control
- IET Control Theory & Applications
- Elsevier Sensors & Actuators A: Physical
- Elsevier Energy Conversion and Management
- Elsevier Measurement
- Elsevier Sensors Robotics and Computer Integrated Manufacturing
- Taylor & Francis International Journal of Systems Science
- IOP Journal of Micromechanics and Microengineering
- IOP Review of Scientific Instruments
- IOP Smart Materials and Structures
- Springer Meccanica

- Springer Cell Biochemistry & Biophysics
- Springer Journal of Intelligent and Robotic Systems
- Springer Control Theory and Technology (Journal of Control Theory and Applications)
- Birkhäuser/Springer Journal of Mathematics in Computer Science
- SAGE Journal of Intelligent Material Systems and Structures
- SAGE Journal of Vibration and Control
- SAGE Journal of Systems and Control Engineering
- SAGE Journal of Mechanical Engineering Science
- MDPI International Journal of Molecular Sciences
- MDPI Sensors
- MDPI Materials
- Journal of Low Frequency Noise, Vibration and Active Control
- International Journal of Advanced Robotic Systems
- Hindawi Journal of Robotics
- Hindawi Mathematical Problems in Engineering
- Hindawi Discrete Dynamics in Nature and Society
- Merit Research Journal of Education and Review

A.2.10 Societies and groups memberships

- IEEE: StudM'05, M'07
- Group of Set Membership Computation (the MEA group of the GDR-MACS society, France), member
- Group of Methods and Tools for the Analysis and Synthesis in Robustness (the MOSAR group of the GDR-MACS), member
- Group of Mechatronic Systems (the SYSME group of the GDR-MACS society, France), member
- Group of Multiscale Manipulation (the MM group of the GDR-Robotics society, France), member.

A.3 TEACHING ACTIVITIES

A.3.1 Pedagogic and administrative responsibilities

TEACHING MODULES RESPONSABILITIES

- *Responsible of the module 'Advanced Control Systems' for 2nd year MSc Mechatronics and Microsystems*
- *Responsible of the module 'Control Systems: modeling and basics on control' for 3rd year BSc EEA*
- *Responsible of the module 'Linear Control: Continuous Systems' for 3rd year BSc EEA*
- *Responsible of the module 'Robotics' for 3rd year BSc ARIA (until 2011)*

ADMINISTRATIVE RESPONSABILITIES

- *Elected UFC consultant at the AIP-PRIMECA-pôle of Franche-Comté since march 2012. The AIP-PRIMECA-pôle is one of the competitive and great poles in France for robotics and production platforms devoted to robotics and mechanics teachings. Each of these poles is used by several universities, institutes and “Ecoles d'Ingénieurs”.*

- *Committee member for the Academic Recruitment (Commissions Universitaires) at INSA (National Institute of Applied Sciences), LYON FRANCE, since 2013.*

- *Scientific committee of the AIP-PRIMECA congress, 2015.*

A.3.2 TEACHING for undergrads (BSc), UFC University

TEACHINGS:

- **Introduction to Electrical and Control Engineering** (*Découverte de l'EEA*): labs (until 2011), 1st year BSc EEA
- **Control Systems: modeling and basics on control** (*Introduction à la Commande*): courses/tutorials/labs, 3rd year BSc EEA
- **Linear Control: Continuous Systems** (*Asservissement Continu*): courses/tutorials/labs, 3rd year BSc EEA
- **Digital Control** (*Asservissement Numérique*): labs (until 2011), 3rd year BSc EEA
- **Linear Control Systems** (*Automatique*): labs (until 2011), 2nd year of ISIFC Engineering School
- **Robotics** (*Robotique*): courses/tutorials/labs (until 2011), 3rd year BSc ARIA

SIGNIFICATIONS OF THE ACRONYMS AND TERMS

UFR ST: Unité mixte de Formation et de Recherche, Science et Techniques (*School of Sciences and Techniques*)

EEA: Electronique Electrotechnique Automatique (*Electronics, Electrical and Control Engineering*)

ARIA: Automatique, Robotique, Informatique et Assemblage (*Control Engineering, Robotics, Computer science and Assembly*), BSc with professional qualification

A.3.3 TEACHING for MSc UFC University and “Ecoles d'Ingénieurs”

TEACHINGS:

- **MicroMechatronics** (*Micromécatronique*): courses/tutorials, 2nd year MSc Mechatronics and Microsystems
- **Advanced Control Systems: H-inf and μ -synthesis theories** (*Automatique Avancée*): courses/tutorials/labs, 2nd year MSc Mechatronics and Microsystems
- **Multivariable Control Systems** (*Commande des Systèmes Multivariables*): labs, 1st year MSc Mechatronics and Microsystems
- **Robotics** (*Robotique*): labs (until 2011), 1st year MSc Mechatronics and Microsystems
- **Robotics** (*Robotique*): labs (until 2011), 2nd year of MSc SAPIAA
- **Robotics** (*Robotique*): labs (until 2011), 3rd year of ISIFC “Ecole d'Ingénieurs”

SIGNIFICATIONS OF THE ACRONYMS AND TERMS

SAPIAA: Systèmes Automatisés de Production dans les Industries Agro-Alimentaires (*Automated production systems in food-processing industry, MSc with professional qualification*)

ISIFC: Institut Supérieur des Ingénieurs de Franche-Comté (*Institute of Engineers of Franche-Comté, “Ecole d'Ingénieurs”*)

A.3.4 INVITED LECTURE

- *Invited lecture (1h) on 'Control of microrobots' at the University of Texas at Arlington (UTA TX USA) in november 2012: courses for BSc, MSc and PhD.*

Appendix B

Personal publications (accepted or published) and invited talks/seminars

B.1 Book and edited books

B.2 Book chapters

B.3 Patents

B.4 Journal papers

B.5 International conferences

B.6 Workshops

B.7 Invited talks and seminars

B.7.1 Invited talks in organized workshops and tutorials

B.7.2 Invited seminars in research institutes and universities

B.1 BOOK and EDITED BOOKS

[B4] **Micky Rakotondrabe**, 'Piezoelectric cantilevered structures: modeling control and measurement/estimation aspects', [Springer - Verlag](#), **Monography** in preparation (still !!).

[B3] **Micky Rakotondrabe**, 'Smart materials-based actuators at the micro/nano-scale: characterization, control and applications', **edited book**, [Springer - Verlag](#), New York, ISBN 978-1-4614-6683-3, 2013.

[B2] Cédric Clévy, **Micky Rakotondrabe** and Nicolas Chaillet, 'Signal measurement and estimation techniques issues in the micro/nano world', **edited book**, [Springer - Verlag](#), New York, ISBN 978-1-4419-9945-0, 2011.

[B1] **Micky Rakotondrabe**, 'Microrobots et stations de microassemblage', **Monography**, [Editions Universitaires Européennes](#), ISBN: 978-613-1-51443-2, June 2010. (*related to my phd works*)

B.2 BOOK CHAPTERS

[BC11] Yassine Haddab, Vincent Chalvet et **Micky Rakotondrabe**, 'Open-loop control approaches of compliant micromanipulators', a chapter in 'Flexible robotics: Applications to Multiscale Manipulations' edited by Mathieu Grossard, Nicolas Chaillet et Stéphane Régnier, [Wiley - ISTE](#), ISBN 978-1-84821-520-7, July 2013.

[BC10] Yassine Haddab, Vincent Chalvet et **Micky Rakotondrabe**, 'Approches de commande en boucle ouverte pour les micro-manipulateurs flexibles à base de matériaux actifs', a chapter in 'Robotique flexible: manipulation multi-échelle' edited by Mathieu Grossard, Nicolas Chaillet et Stéphane Régnier, [Hermès Science](#), ISBN 9782746245099, July 2013.

[BC9] **Micky Rakotondrabe**, Mohammad Al Janaideh, Alex Bienaimé and Qingsong Xu, 'Introduction: smart materials as essential base for actuators in micro/nanopositioning', a chapter in 'Smart materials-based actuators at the micro/nano-scale: characterization, control and applications' edited by Micky Rakotondrabe, [Springer - Verlag](#), New York, ISBN 978-1-4614-6683-3, 2013.

[BC8] **Micky Rakotondrabe** and Sofiane Khadraoui, 'Design of piezoelectric actuators with guaranteed performances using the performances inclusion theorem and interval tools', a chapter in 'Smart materials-based actuators at the micro/nano-scale: characterization, control and applications' edited by Micky Rakotondrabe, [Springer - Verlag](#), New York, ISBN 978-1-4614-6683-3, 2013.

[BC7] **Micky Rakotondrabe**, Juan-Antonio Escareno, Didace Habineza and Sergio Lescano 'Kalman filtering and state-feedback control of a nonlinear piezoelectric cantilevered actuator', a chapter in 'Smart materials-based actuators at the micro/nano-scale: characterization, control and applications' edited by Micky Rakotondrabe, [Springer - Verlag](#), New York, ISBN 978-1-4614-6683-3, 2013.

[BC6] **Micky Rakotondrabe**, 'Modeling and robust H -inf control of a nonlinear and oscillating 2-dof multimorph cantilevered piezoelectric actuator', a chapter in 'Smart materials-based actuators at the micro/nano-scale: characterization, control and applications' edited by Micky Rakotondrabe, [Springer - Verlag](#), New York, ISBN 978-1-4614-6683-3, 2013.

[BC5] **Micky Rakotondrabe**, 'Feedforward control of flexible and nonlinear piezoelectric actuators', a chapter in 'Smart materials-based actuators at the micro/nano-scale: characterization, control and applications' edited by Micky Rakotondrabe, [Springer - Verlag](#), New York, ISBN 978-1-4614-6683-3, 2013.

[BC4] Sofiane Khadraoui, **Micky Rakotondrabe** and Philippe Lutz, 'Interval modeling and robust feedback control of piezoelectric-based microactuators', a chapter in 'Smart materials-based actuators at the micro/nano-scale: characterization, control and applications' edited by Micky Rakotondrabe, [Springer - Verlag](#), New York, ISBN 978-1-4614-6683-3, 2013.

[BC3] Cédric Clévy and **Micky Rakotondrabe**, 'Microscale specificities', a chapter in 'Signal measurement and estimation techniques issues in the micro/nano world' edited by Cédric Clévy, Micky Rakotondrabe and Nicolas Chaillet, [Springer - Verlag](#), ISBN 978-1-4419-9945-0, August 2011.

[BC2] Ioan Alexandru Ivan, **Micky Rakotondrabe**, Philippe Lutz and Nicolas Chaillet, '*Self-sensing measurement in piezoelectric cantilevered actuators for micromanipulation and microassembly contexts*', a chapter in '*Signal measurement and estimation techniques issues in the micro/nano world*' edited by Cédric Clévy, Micky Rakotondrabe and Nicolas Chaillet, [Springer - Verlag](#), ISBN 978-1-4419-9945-0, August 2011.

[BC1] **Micky Rakotondrabe**, Yassine Haddab and Philippe Lutz, '*Modeling and control of stick-slip micropositioning devices*', a chapter in '*Micro nanosystems & systems on chips: modeling, control and estimation*' edited by Alina Voda, [Wiley - ISTE](#), ISBN: 978-1-84821-190-2, Jan. 2010. *(related to my phd works)*

B.3 PATENTS ---

[PT3] Ioan Alexandru Ivan, Joël Agnus and **Micky Rakotondrabe**, '*Multi-DOF micropositioning techniques for piezoelectric actuators and relative devices*', PCT procedure finished N°PCT/FR2013/050622, [patent extension](#) is ongoing for the following countries: european countries, Switzerland and USA.

[PT2] Ioan Alexandru Ivan, Joël Agnus and **Micky Rakotondrabe**, '*Technique de micropositionnement à multidegrés de liberté pour actionneurs piézoélectriques et dispositifs associés*', [french Patent](#), INPI FR-N°12/52554, march 2013.

[PT1] Ioan Alexandru Ivan and **Micky Rakotondrabe**, '*Micro-actionneur et Micro-pince*', [french Patent](#), INPI FR1053377, delivered in 8th june 2012.

B.4 JOURNAL PAPERS ---

[J24] Didace Habineza, **Micky Rakotondrabe** and Yann Le Gorrec, '*Bouc-Wen Modeling and Feedforward Control of multivariable Hysteresis in Piezoelectric Systems: Application to a 3-DoF Piezotube scanner*', [IEEE - Transactions on Control Systems Technology \(T-CST\)](#), DOI.10.1109/TCST.2014.2386779, in press.

[J23] **Micky Rakotondrabe**, Alexandru Ivan, Sofiane Khadraoui, Philippe Lutz and Nicolas Chaillet, '*Simultaneous displacement and force self-sensing in piezoelectric actuators and applications to robust control of the displacement*', [IEEE/ASME - Transactions on Mechatronics \(T-mech\)](#), DOI.10.1109/TMECH.2014.2300333, Jan 2014.

[J22] Sofiane Khadraoui, **Micky Rakotondrabe** and Philippe Lutz, '*Interval force/position modeling and control of a microgripper composed of two collaborative piezoelectric actuators and its automation*', [Springer - International Journal of Control, Automation and Systems \(IJCAS\)](#), Vol 12, No 2, Page 358-371, April 2014.

[J21] Sofiane Khadraoui, **Micky Rakotondrabe** and Philippe Lutz, '*Optimal design of piezoelectric cantilevered actuators with guaranteed performances by using interval techniques*', [IEEE/ASME - Transactions on Mechatronics \(T-mech\)](#), Volume 19, Issue 5, Page 1660-1668, October 2014.

[J20] **Micky Rakotondrabe**, Anthony Fowler and S.O. Reza Moheimani, '*Control of a novel 2-DoF MEMS nanopositioner with electrothermal actuation and sensing*', [IEEE - Transactions on Control Systems Technology \(T-CST\)](#), Volume 22, Number 4, Page 1486-1497, July 2014.

[J19] Joël Agnus, Nicolas Chaillet, Cédric Clévy, Sounkalo Dembélé, Michaël Gauthier, Yassine Haddab, Guillaume Laurent, Philippe Lutz, Nadine Piat and **Micky Rakotondrabe**, '*Robotic Microassembly and micromanipulation at FEMTO-ST*', [Journal of Micro-Bio Robotics \(JMBR\)](#), Volume 8, Issue 2, Page 91-106, 2013.

[J18] Sofiane Khadraoui, **Micky Rakotondrabe** and Philippe Lutz, '*Design of RST-structured controller for parametric uncertain system using interval analysis: application to piezocantilever*', [Asian Journal of Control \(AJC\)](#), Vol.15, Num.1, pp.142-154-13, January 2013.

[J17] Qingsong Xu, Pak-Kin Wong, Minping Jia, **Micky Rakotondrabe** and Li Zhang, 'Guest editorial introduction to the special issue on advanced control in micro/nanosystems', [Journal of Control Science and Engineering](#), vol. 2012, Article ID 827479, 2 pages, doi:10.1155/2012/827479, 2012.

[J16] Sofiane Khadraoui, **Micky Rakotondrabe** and Philippe Lutz, 'Combining H_{∞} approach and interval tools to design a low order and robust controller for systems with parametric uncertainties: application to piezoelectric actuators', [International Journal of Control \(IJC\)](#), vol. 85, no1-3, pp. 251-259, 2012.

[J15] Sofiane Khadraoui, **Micky Rakotondrabe** and Philippe Lutz, 'Interval Modeling and Robust Control of Piezoelectric Microactuators', [IEEE - Transactions on Control Systems Technology \(T-CST\)](#), Vol.20, Num.2, pp.486-494, March 2012.

[J14] **Micky Rakotondrabe** and Alexandru Ivan, 'Development and Force/Position Control of a New Hybrid Thermo-Piezoelectric microGripper dedicated to micromanipulation tasks', [IEEE - Transactions on Automation Science and Engineering \(T-ASE\)](#), Vol.8, Issue.4, pp.824-834, October 2011.

[J13] **Micky Rakotondrabe**, Kanty Rabenorosoa, Joël Agnus and Nicolas Chaillet, 'Robust feedforward-feedback control of a nonlinear and oscillating 2-dof piezocantilever', [IEEE - Transactions on Automation Science and Engineering \(T-ASE\)](#), Vol.8, Issue.3, pp.506-519, July 2011.

[J12] **Micky Rakotondrabe**, 'Bouc-Wen modeling and inverse multiplicative structure to compensate hysteresis nonlinearity in piezoelectric actuators', [IEEE - Transactions on Automation Science and Engineering \(T-ASE\)](#), Vol.8, Issue.2, pp.428-431, April 2011.

[J11] Ioan Alexandru Ivan, Valentin Stih, Michaela Ivan, C. Stih, **Micky Rakotondrabe**, A. Jelea, 'Battery powered cost effective TDS logger intended for water testing', [Romanian Journal of Physics \(RJP\)](#), ISSN 1221-146X, Vol.56(3-4), 2011.

[J10] **Micky Rakotondrabe**, Ioan Alexandru Ivan, Valentin Stih, Simona Noveanu and Eugenia Minca, 'Design and modeling of a piezoelectrically actuated microvalve', [Romanian Journal of Physics \(RJP\)](#), Vol.56, pp.141-149, 2011.

[J9] **Micky Rakotondrabe** and Alexandru Ivan, 'Development and dynamic modeling of a new hybrid thermo-piezoelectric micro-actuator', [IEEE - Transactions on Robotics \(T-RO\)](#), Vol.26, Issue.6, pp.1077-1085, Dec 2010.

[J8] Ioan Alexandru Ivan, **Micky Rakotondrabe**, Joël Agnus, Roger Bourquin, Nicolas Chaillet, Philippe Lutz, Jean-Claude Ponçot, Roland Duffait, Olivier Bauer, 'Comparative material study between PZT ceramic and newer crystalline PMN-PT and PZN-PT materials for composite bimorph actuators', [Review on Advanced Materials Science \(RAMS\)](#), Vol.24(1), 2010.

[J7] **Micky Rakotondrabe**, Cédric Clévy and Philippe Lutz, 'Complete open loop control of hysteretic, creeped and oscillating piezoelectric cantilever', [IEEE - Transactions on Automation Science and Engineering \(T-ASE\)](#), Vol.7(3), pp:440-450, July 2010.

[J6] Alexandru Ivan, **Micky Rakotondrabe**, Philippe Lutz and Nicolas Chaillet, 'Current integration force and displacement self-sensing method for cantilevered piezoelectric actuators', [Review of Scientific Instruments \(RSI\)](#), Vol.80(12), 2126103, December 2009.

[J5] Alexandru Ivan, **Micky Rakotondrabe**, Philippe Lutz and Nicolas Chaillet, 'Quasi-static displacement self-sensing method for cantilevered piezoelectric actuators', [Review of Scientific Instruments \(RSI\)](#), Vol.80(6), 065102, June 2009.

[J4] Hui Xie, **Micky Rakotondrabe** and Stéphane Régnier, 'Characterizing piezoscanner hysteresis and creep using optical levers and a reference nanopositioning stage', [Review of Scientific Instruments \(RSI\)](#), Vol.80, 046102, April 2009.

[J3] **Micky Rakotondrabe**, Yassine Haddab and Philippe Lutz, 'Development, Modeling, and Control of a Micro-/Nanopositioning 2-DOF Stick-Slip Device', [IEEE/ASME - Transactions on Mechatronics \(T-mech\)](#), Vol.14, Issue 6, pp:733-745, December 2009. (related to my phd works)

[J2] **Micky Rakotondrabe**, Yassine Haddab and Philippe Lutz, '*Quadrilateral modeling and robust control of a nonlinear piezoelectric cantilever*', [IEEE - Transactions on Control Systems Technology \(T-CST\)](#), Vol.17, Issue 3, pp:528-539, May 2009. (*related to my phd works*)

[J1] **Micky Rakotondrabe**, Yassine Haddab and Philippe Lutz, '*Voltage/frequency proportional control of stick-slip microsystems*', [IEEE - Transactions on Control Systems Technology \(T-CST\)](#), Vol.16, Issue 6, pp:1316-1322, November 2008. (*related to my phd works*)

B.5 INTERNATIONAL CONFERENCES

[C55] Ton E. Pengwang, Kanty Rabenorosoa, **Micky Rakotondrabe** and Nicolas Andreff, '*Characterizations and Micro-assembly of Electrostatic Actuators for 3-DOF Micromanipulators in Laser Phonomicrosurgery* ', [IEEE/ASME-MESA, \(International Conference on Mechatronic and Embedded Systems and Applications\)](#), accepted, Senigallia Ancona Italy, September 2014.

[C54] Juan Antonio Escareno, Didace Habineza and **Micky Rakotondrabe**, '*Tracking Control of a Piezocantilever Using a Bounded-Input Adaptive Backstepping Scheme and Sliding-Mode Observer*', [IFAC - WC , \(World Congress\)](#), accepted, Cape Town, South Africa, August 2014.

INVITED SESSION.

[C53] Didace Habineza, **Micky Rakotondrabe** and Yann Le Gorrec, '*Multivariable generalized Bouc-Wen modeling, identification and feedforward control and its application to a 2-DoF piezoelectric multimorph actuator* ', [IFAC - WC , \(World Congress\)](#), accepted, Cape Town, South Africa, August 2014.

[C52] Juan Antonio Escareno, Joël Abadie, **Micky Rakotondrabe** and Emmanuel Piat, '*H-inf based Trajectory Control of a 2DOF piezo-cantilever Using Embedded/Integrated Magnetic Sensors*', [IEEE/ASME - AIM, \(International Conference on Advanced Intelligent Mechatronics\)](#), pp.1676-1682, Besançon, France, July 2014

INVITED SESSION.

[C51] Omar Aljanaideh, Mohammad Al Janaideh and **Micky Rakotondrabe**, '*Enhancement of Micro-positioning Accuracy of a Piezoelectric Positioner by Suppressing the Rate-Dependant Hysteresis Nonlinearities*', [IEEE/ASME - AIM, \(International Conference on Advanced Intelligent Mechatronics\)](#), pp.1683-1688, Besançon, France, July 2014

INVITED SESSION.

[C50] Bilal Komati, Cédric Clévy, **Micky Rakotondrabe** and Philippe Lutz, '*Dynamic Force/Position Modeling of a one-DOF Piezoelectric Smart Micro-Finger with sensorized end-effector*', [IEEE/ASME - AIM, \(International Conference on Advanced Intelligent Mechatronics\)](#), pp.1474-1479, Besançon, France, July 2014

INVITED SESSION.

[C49] Juan Antonio Escareno, Gerardo Ramon Flores Colunga, **Micky Rakotondrabe** and Rogelio Lozano, '*Task-based Control of a Multirotor Miniature Aerial Vehicle Having an Onboard Manipulator*', [ICUAS, \(International Conference on Unmanned Aircraft Systems\)](#), accepted, Orlando, FL USA, May 2014

[C48] Didace Habineza, **Micky Rakotondrabe** and Yann Le Gorrec, '*Modeling, identification and feedforward control of multivariable hysteresis by combining Bouc-Wen equations and the inverse multiplicative structure*', [ACC, \(American Control Conference\)](#), pp.4783-4789, Portland Oregon USA, June 2014.

INVITED SESSION.

[C47] Xin Xu, Joël Agnus and **Micky Rakotondrabe**, '*Development and characterization of a new silicone / platine based 2-DoF sensorized end-effector for micromanipulators*', [SPIE - Sensing Technology+Applications; Sensors for Next Generation Robots conference](#), Baltimore Maryland USA, May 2014.

[C46] Ton E. Pengwang, Kanty Rabenorosoa, **Micky Rakotondrabe** and Nicolas Andreff, '*Integrative Micro Actuators for Robot-assisted Laser Phonomicrosurgery*', [RGC, Russian German Conference \(Russian Bavarian Conference on Bio-Medical Engineering\)](#), Hannover Germany, October 2013.

[C45] Sergio Lescano, Dimiter Zlatanov, **Micky Rakotondrabe** and Nicolas Andreff, '*Kinematic Analysis of a Meso Scale Parallel Robot for Laser Phonomicrosurgery*', [IAK, \(International Conference on Interdisciplinary Applications in Kinematic\)](#), Lima Peru, September 2013.

[C44] Muhammed Rashid Pac, **Micky Rakotondrabe**, Sofiane Khadraoui, Dan O. Popa and Philippe Lutz, '*Guaranteed Manipulator Precision via Interval Analysis of Inverse Kinematics*', [ASME - IDETC/CIE, \(International Design Engineering Technical Conference & Computers and Information in Engineering Conference\)](#), Portland Oregon USA, August 2013.

[C43] **Micky Rakotondrabe**, '*Towards high autonomy energy harvesters based on piezoelectric MEMS*', [Nanoenergy, \(International Conference on Nanoenergy\)](#), Perugia Italy, July 2013.

[C42] Juan Antonio Escareno, **Micky Rakotondrabe**, Gerardo Ramon Flores Colunga and Rogelio Lozano, '*Rotorcraft MAV Having an Onboard Manipulator: Longitudinal Modeling and Robust Control*', [ECC, \(European Control Conference\)](#), Zürich Switzerland, pp.3258-3263, July 2013.

[C41] **Micky Rakotondrabe**, '*Combining self-sensing with an Unkown-Input-Observer to estimate the displacement, the force and the state in piezoelectric cantilevered actuator*', [ACC, \(American Control Conference\)](#), pp.4523-4530, Washington DC USA, June 2013.

[C40] Anthony Fowler, **Micky Rakotondrabe**, and S.O. Reza Moheimani, '*Closed-Loop Control of a Novel 2-DOF MEMS Nanopositioner with Electrothermal Actuation*', [IFAC Mechatronics, \(Symposium on Mechatronic Systems\)](#), pp.391-398, Hangzhou China, April 2013.

[C39] **Micky Rakotondrabe**, Anthony Fowler and S.O. Reza Moheimani '*Characterization of a 2-dof electrothermal MEMS with integrated actuation and sensing capability*', [IEEE - Sensors](#), pp.973-976, Taipei Taiwan, October 2012.

[C38] Dominique Gendreau, **Micky Rakotondrabe** and Philippe Lutz, '*Towards reconfigurable and modular microfactory based on the TRING-module stick-slip microrobot*', [IWME, \(International Workshop on MicroFactory\)](#), Tampere, Finland, June 2012.

[C37] Sofiane Khadraoui, **Micky Rakotondrabe** and Philippe Lutz, '*Combining H-inf and interval techniques to design robust low order controllers: application to piezoelectric actuators*', [ACC, \(American Control Conference\)](#), pp.104-110, Montréal Canada, June 2012.

[C36] **Micky Rakotondrabe**, '*Classical Prandtl-Ishlinskii modeling and inverse multiplicative structure to compensate hysteresis in piezoactuators*', [ACC, \(American Control Conference\)](#), pp.1646-1651, Montréal Canada, June 2012.

[C35] **Micky Rakotondrabe**, '*Modeling and Compensation of Multivariable Creep in multi-DOF Piezoelectric Actuators*', [IEEE - ICRA, \(International Conference on Robotics and Automation\)](#), pp.4577-4581, St Paul Minnesota USA, May 2012.

[C34] Paul M. Moore, **Micky Rakotondrabe**, Cédric Clévy and Gloria J. Wiens, '*Development of a modular and compliant micro-assembly platform with integrated force measurement capabilities*', [ICOMM, \(International Conference on MicroManufacturing\)](#), Northwestern University, March 2012.

[C33] Ioan Alexandru Ivan, Joël Agnus, **Micky Rakotondrabe**, Philippe Lutz and Nicolas Chaillet, '*PMN-PT piezoelectric material and related applications in silicon-integrated devices like microactuators and energy harvesting*', [IEEE - CAS, \(International Semiconductor Conference CAS2011\)](#), Sinaia Romania, October 2011.

[C32] Gilgueng Hwang, Ioan Alexandru Ivan, Joël Agnus, **Micky Rakotondrabe**, Edgar Leon Perez, Stamboul Meriemn Hugo Salmon, Sinan Haliyon, Nicolas Chaillet, Stéphane Régner and Anne-Marie Hanghiri-Gosnet, '*Remotely powered floating microswimmers as colloidam microparticle manipulators*', [MNE, \(International Conference on Micro and Nano Engineering\)](#), Berlin Germany, September 2011.

[C31] **Micky Rakotondrabe**, Joël Agnus and Philippe Lutz, '*Feedforward and IMC-feedback control of a nonlinear 2-DOF piezoactuator dedicated to automated micropositioning tasks*', [IEEE - CASE, \(International Conference on Automation Science and Engineering\)](#), pp.393-398, Trieste Italy, August 2011.

BEST PAPER AWARD FINALIST.

- [C30] Sofiane Khadraoui, **Micky Rakotondrabe** and Philippe Lutz, '*Modeling and Robust Deflection Control of Piezoelectric microActuators modeled by Zero-Order Numerator Interval System*', [IFAC - WC, \(World Congress\)](#), pp.9763-9768, Milano Italy, August 2011.
- [C29] Ioan Alexandru Ivan, Joël Agnus, **Micky Rakotondrabe**, Philippe Lutz and Nicolas Chaillet, '*Microfabricated PMN-PT on Silicon cantilevers with improved static and dynamic piezoelectric actuation: development, characterization and control*', [IEEE/ASME - AIM, \(International Conference on Advanced Intelligent Materials\)](#), pp.403-408, Budapest Hungary, July 2011.
- [C28] **Micky Rakotondrabe**, '*Performances inclusion for stable interval systems*', [ACC, \(American Control Conference\)](#), pp.4367-4372, San Francisco CA USA, June-July 2011.
- [C27] Sofiane Khadraoui, **Micky Rakotondrabe** and Philippe Lutz, '*PID-Structured Controller Design for Interval Systems: Application to Piezoelectric Microactuators*', [ACC, \(American Control Conference\)](#), pp.3477-3482, San Francisco CA USA, June-July 2011.
- [C26] Ioan Alexandru Ivan, Gilgueng Hwang, Joël Agnus, **Micky Rakotondrabe**, Nicolas Chaillet and Stéphane Régnier, '*First experiments on MagPieR: a planar wireless magnetic and piezoelectric microrobot*', [IEEE - ICRA, \(International Conference on Robotics and Automation\)](#), pp.102-108, Shanghai China, May 2011.
- [C25] Sofiane Khadraoui, **Micky Rakotondrabe** and Philippe Lutz, '*Robust control for a class of interval model: application to the force control of piezoelectric cantilevers*', [IEEE - CDC, \(Conference on Decision and Control\)](#), pp.4257-4262, Atlanta Georgia USA, December 2010.
- [C24] Dominique Gendreau, **Micky Rakotondrabe** and Philippe Lutz, '*Modular design method applied to a micromanipulation station*', [IWME, \(International Workshop on MicroFactory\)](#), Daejeon, Korea, October 2010.
- [C23] **Micky Rakotondrabe** and Yann Le Gorrec, '*Force control in piezoelectric microactuators using self scheduled H_{∞} technique*', [IFAC - Mech, \(Symposium on Mechatronic Systems\)](#), pp.417:422, Cambridge Massachusetts USA, September 2010.
- INVITED SESSION.**
- [C22] **Micky Rakotondrabe**, Cédric Clévy, Kanty Rabenorosoa and Kamel Ncir, '*Presentation, Force Estimation and Control of an Instrumented platform dedicated to Automated Micromanipulation Tasks*', [IEEE - CASE, \(International Conference on Automation Science and Engineering\)](#), pp:722-727, Toronto Ontario CA, Aug 2010.
- [C21] Kanty Rabenorosoa, Cédric Clévy, **Micky Rakotondrabe** and Philippe Lutz, '*Guiding strategies for the assembly of micro-components subjected to planar pull-off force*', [ASME - DETC/CIE, \(International Design Engineering Technical Conference & Computers and Information in Engineering Conference\)](#), DETC2010-29213, Montreal Canada, August 2010.
- [C20] **Micky Rakotondrabe**, Ioan Alexandru Ivan, Sofiane Khadraoui, Cédric Clévy, Philippe Lutz and Nicolas Chaillet, '*Dynamic displacement self-sensing and robust control of cantilevered piezoelectric actuators dedicated to microassembly tasks*', [IEEE/ASME - AIM, \(International Conference on Intelligent Materials\)](#), pp:557-562, Montreal Canada, July 2010.
- [C19] **Micky Rakotondrabe** and Ioan Alexandru Ivan, '*Principle, characterization and control of a new hybrid thermo-piezoelectric microactuator*', [IEEE - ICRA, \(International Conference on Robotics and Automation\)](#), pp:1580-1585, Anchorage Alaska USA, May 2010.
- [C18] **Micky Rakotondrabe**, Joël Agnus, Kanty Rabenorosoa and Nicolas Chaillet, '*Characterization, modeling and robust control of a nonlinear 2-dof piezocantilever for micromanipulation/microassembly*', [IEEE/RSJ - IROS, \(International Conference on Intelligent Robots and Systems\)](#), pp:767-774, St Louis MO USA, October 2009.
- [C17] Ioan Alexandru Ivan, **Micky Rakotondrabe** and Nicolas Chaillet, '*High Coupling Factor Materials for Bending Actuators: Analytical and Finite Elements Modeling Results*', [COMSOL Conference](#), Milan Italy, October 2009.

[C16] **Micky Rakotondrabe** and Patrick Rougeot, '*Presentation and improvement of an AFM-based system for the measurement of adhesion forces*', [IEEE - CASE, \(International Conference on Automation Science and Engineering\)](#), pp:585-590, Bangalore India, August 2009.

[C15] **Micky Rakotondrabe** and Philippe Lutz, '*Force estimation in a piezoelectric cantilever using the inverse-dynamics-based UIO technique*', [IEEE - ICRA, \(International Conference on Robotics and Automation\)](#), pp:2205-2210, Kobe Japan, May 2009.

[C14] **Micky Rakotondrabe**, Cédric Clévy and Philippe Lutz, '*Hysteresis and vibration compensation in a nonlinear unimorph piezocantilever*', [IEEE/RSJ - IROS, \(International Conference on Intelligent Robots and Systems\)](#), pp:558-563, Nice France, Sept 2008.

[C13] **Micky Rakotondrabe**, Mamadou Cissé Diouf and Philippe Lutz, '*Robust feedforward-feedback control of a hysteretic piezocantilever under thermal disturbance*', [IFAC - WC , \(World Congress\)](#), pp:13725-13730, Seoul Korea, July 2008.

INVITED SESSION.

[C12] **Micky Rakotondrabe**, Cédric Clévy and Philippe Lutz, '*H-inf deflection control of a unimorph piezoelectric cantilever under thermal disturbance*', [IEEE/RSJ - IROS, \(International Conference on Intelligent Robots and Systems\)](#), pp:1190-1197, San Diego CA USA, Oct-Nov 2007.

[C11] **Micky Rakotondrabe**, Cédric Clévy and Philippe Lutz, '*Modelling and robust position/force control of a piezoelectric microgripper*', [IEEE - CASE, \(International Conference on Automation Science and Engineering\)](#), pp:39-44, Scottsdale AZ USA, Sept 2007.

[C10] **Micky Rakotondrabe**, Yassine Haddab and Philippe Lutz, '*Nonlinear modelling and estimation of force in a piezoelectric cantilever*', [IEEE/ASME - AIM, \(International Conference on Advanced Intelligent Mechatronics\)](#), Zurich Switzerland, Sept 2007. *(related to my phd works)*

[C9] **Micky Rakotondrabe**, Yassine Haddab and Philippe Lutz, '*Modelling and H-inf force control of a nonlinear piezoelectric cantilever*', [IEEE/RSJ - IROS, \(International Conference on Intelligent Robots and Systems\)](#), pp:3131-3136, San Diego CA USA, Oct-Nov 2007. *(related to my phd works)*

[C8] **Micky Rakotondrabe**, Yassine Haddab and Philippe Lutz, '*High-stroke motion modelling and voltage/frequency proportional control of a stick-slip microsystem*', [IEEE - ICRA, \(International Conference on Robotics and Automation\)](#), pp:4490-4496, Roma Italy, April 2007. *(related to my phd works)*

[C7] **Micky Rakotondrabe**, Yassine Haddab and Philippe Lutz, '*Plurilinear modeling and discrete μ -synthesis control of a hysteretic and creeped unimorph piezoelectric cantilever*', [IEEE - ICARCV, \(International Conference on Automation, Robotics, Control and Vision\)](#), pp:57-64, Grand Hyatt Singapur, December 2006. **BEST PAPER AWARD FINALIST.** *(related to my phd works)*

[C6] **Micky Rakotondrabe**, Yassine Haddab and Philippe Lutz, '*Results on the closed-loop control of the TRING-module dedicated to a modular micromanipulation station*', [IWMF, \(International Workshop on MicroFactory\)](#), Besançon, October 2006. *(related to my phd works)*

[C5] **Micky Rakotondrabe**, Yassine Haddab and Philippe Lutz, '*TRING-module : a high-range and high-precision 2DoF microsystem dedicated to a modular micromanipulation station*', [IWMF, \(International Workshop on MicroFactory\)](#), Besançon, October 2006. *(related to my phd works)*

[C4] **Micky Rakotondrabe**, Yassine Haddab and Philippe Lutz, '*Design, development and experiments of a high stroke-precision 2DoF (linear-angular) microsystem*', [IEEE - ICRA, \(International Conference on Robotics and Automation\)](#), pp:669-674, Orlando FL USA, May 2006. *(related to my phd works)*

[C3] **Micky Rakotondrabe**, Samir Benbelkacem, Yassine Haddab, Christophe Perrard, Philippe Lutz, '*Approche architecturale pour la ré-organisabilité d'une micro-usine hautement modulaire*', [GI, \(franco-Canadian Industrial Engineering Conference\)](#), poster session, Besançon France, June 2005. *(related to my phd works)*

[C2] **Micky Rakotondrabe**, Yassine Haddab and Philippe Lutz, '*Step modelling of a high precision 2DoF (linear-angular) microsystem*', [IEEE - ICRA, \(International Conference on Robotics and Automation\)](#), pp:151-157, Barcelona Spain, April 2005. *(related to my phd works)*

[C1] **Micky Rakotondrabe**, Yassine Haddab and Philippe Lutz, '*Modelling and control of a highly modular microassembly system*', [IWMEF, \(International Workshop on MicroFactory\)](#), pp:140-145, Shanghai China, October 2004. *(related to my phd works)*

B.6 WORKSHOPS

[WT15] Alex Bienaimé, Cédric Clévy and **Micky Rakotondrabe**, '*High performance piezoelectric microactuators: toward a new 6 DOF microactuated platform*', [PiezoNEMS 2013 Workshop](#), november 2013.

[WT14] Sergio Lescano, **Micky Rakotondrabe** and Nicolas Andreff, '*Conception d'un Microrobot Parallèle Destiné à la Phonomicrochirurgie Laser*', [GT6 of the GDR-Robotique, \(Workshop on Robts Design\)](#), Paris France, September 2013.

[WT13] **Micky Rakotondrabe**, '*Control of piezoelectric microsystems with minimization of sensors: feedforward control and feedback control with self-sensing*', [GDR MNS - MNE, \(National Workshop - Micro Nano Systems - Micro Nano Fluidics\)](#), Bordeaux France, July 2012.

[WT12] Sofiane Khadraoui, **Micky Rakotondrabe** and Philippe Lutz, '*Interval control design and Hinf based performances analysis for piezoelectric microactuators*', [GT-MOSAR of the GDR-MACS \(Workshop on Methods and Tools for the Synthesis and Analysis on Robustness\)](#), Paris France, January 2011.

[WT11] Sofiane Khadraoui, **Micky Rakotondrabe** and Philippe Lutz, '*Performances analysis of controlled interval systems using Hinf approach*', [GT-MEA of the GDR-MACS, \(Workshop on Set Computations for Automatic control\)](#), Paris France, December 2010.

[WT10] Sofiane Khadraoui, **Micky Rakotondrabe** and Philippe Lutz, '*Modélisation et Commande Robuste par Intervalle des Micropinces Piézoélectriques dédiées à la Micromanipulation et au Microassemblage*', Poster, [JJCR, \(Journées des Jeunes Chercheurs en Robotique\)](#), Paris France, November 2010.

[WT9] Sofiane Khadraoui, **Micky Rakotondrabe** and Philippe Lutz, '*Robust control of parametric uncertain systems: application to the control of piezoelectric cantilevers*', [SWIM, \(Small Workshop on Interval Methods\)](#), Nantes France, June 2010.

[WT8] Sofiane Khadraoui, **Micky Rakotondrabe** and Philippe Lutz, '*Control of microsystems: introducing interval computation to account the model uncertainties*', [LEA, \(Workshop with Associated European Laboratories\)](#) Arc-et-Senans France, September 2009.

[WT7] **Micky Rakotondrabe**, Ioan Alexandru Ivan, Valentin Stih, Simona Noveanu and Eugenia Minca, '*Design and modeling of a piezoelectrically actuated microvalve*', [IBWAP, \(International Balkan Workshop on Applied Physics\)](#), Constanta Romania, July 2009.

[WT6] Sofiane Khadraoui, **Micky Rakotondrabe** and Philippe Lutz, '*Design of a robust controller for guaranteed performances: application to piezoelectric cantilevers*', [SWIM, \(Small Workshop on Interval Methods\)](#), Lausanne Switzerland, June 2009.

[WT5] **Micky Rakotondrabe**, '*Modélisation et commande des poutres piézoélectriques dédiées à la micromanipulation*', [GT-Manipulation Multi-échelle of the GDR-Robotique, \(Workshop on Multi-Scale Manipulation\)](#), Besançon France, February 2008.

[WT4] **Micky Rakotondrabe**, '*TRING-module : développement, modélisation et commande*', [GT SYSME of the GDR-MACS, \(Workshop on Mechatronic Systems\)](#), Lyon France, March 2007. *(related to my phd works)*

[WT3] **Micky Rakotondrabe**, Yassine Haddab and Philippe Lutz, '*Le TRING-module : un microsystème à 2DdL (linéaire et angulaire) de très haute précision (submicrométrique) et de grande course (quelques centimètres)*',

INTERCONNEX , (Meeting of research institutes and industries on microelectronic and micromechanics), Besançon France, Septembre 2006. *(related to my phd works)*

[WT2] **Micky Rakotondrabe**, Yassine Haddab and Philippe Lutz, '*Modular and re-organizable micromanipulation station*', RTP-Microrobotiques, (Workshop on Microrobotics), EPFL Lausanne Switzerland, December 2004. *(related to my phd works)*

[WT1] **Micky Rakotondrabe**, Yassine Haddab and Philippe Lutz, '*Commande d'une station de micro-assemblage modulaire*', LEA, (Workshop with Associated European Laboratories), Arc-et-Senans France, September 2004. *(related to my phd works)*

B.7 INVITED TALKS and SEMINARS

B.7.1 Invited talks in organized workshops and tutorials

[IT8] **Micky Rakotondrabe**, 'Feedforward control of hysteresis: the classical Prandtl-Ishlinskii approach', lecture presented at the tutorial: 'Advanced control and noise reduction for micromanipulation', IEEE/ASME - AIM, (International Conference on Advanced Intelligent Mechatronics), **Lecture at the tutorial session.**

[IT7] **Micky Rakotondrabe** and Philippe Lutz, 'Using interval techniques for the design of robust controllers and for the robust performances analysis: application to piezoelectric microactuators', talk at the Workshop on New Trends and Challenges in Modeling and Control of Microsystems (μ Control), Besançon, June 2012. **Workshop talk.**

[IT6] Sergio Lescano, **Micky Rakotondrabe** and Nicolas Andreff, '*Micromechanisms for laser phonosurgery: A Review of Actuators and Compliant Parts*', talk presented at the workshop: 'Robot-Assisted Laryngeal Microsurgery', IEEE - BIOROB, (International Conference on Biomedical Robotics and Biomechatronics), Roma Italy, June 2012. **Workshop talk.**

[IT5] Sofiane Khadraoui, **Micky Rakotondrabe** and Philippe Lutz, '*Robust automated pick-and-place tasks using piezoelectric microgripper with force/position interval control*', talk at the workshop 'Automation of assembly and packaging at the micro/nano-scale', IEEE - CASE (International Conference on Automation Science and Engineering), Trieste Italy, August 2011. **Workshop talk.**

[IT4] **Micky Rakotondrabe**, '*Hysteresis modelling, identification and feedforward control for piezoelectric based Microsystems*', lecture presented at the tutorial: 'Dynamics, characterization and control at the micro/nano scale', IEEE - ICRA, (International Conference on Robotics and Automation), Shanghai China, May 2011. **Lecture at the tutorial session.**

[IT3] **Micky Rakotondrabe**, '*Force observation and force/position control of a micromanipulation / microassembly system*', presented in the workshop: 'Automation at the Microscale and Beyond', IEEE - CASE, (International Conference on Automation Science and Engineering), Toronto Ontario CA, August 2010. **Workshop talk.**

[IT2] **Micky Rakotondrabe**, Cédric Clévy, Ioan Alexandru Ivan and Nicolas Chaillet, '*Observer Techniques Applied to the Control of Piezoelectric Microactuators*', presented in the workshop: 'Signals Measurement and Estimation Techniques Issues in the Micro/Nano-World', IEEE - ICRA, (International Conference on Robotics and Automation), Workshop, Anchorage Alaska USA, May 2010. **Workshop talk.**

[IT1] **Micky Rakotondrabe** and Philippe Lutz, '*Main aspects of the control issues in the micro/nano-world*', presented in the workshop: 'Control issues in the micro/nano-world', IEEE - ICRA, (International Conference on Robotics and Automation), Workshop, Kobe Japan, May 2009. **Workshop talk.**

B.7.2 Invited seminars in research institutes and universities

[IS9] **Micky Rakotondrabe**, 'Modeling and control of systems: feedforward control', presented at the [University of Science and Technologies of Oran, Algeria](#), June 2014.

[IS8] **Micky Rakotondrabe**, 'Introduction to feedforward control of vibration in systems', presented at the [Texas A & M University at Qatar, Qatar](#), May 2013.

[IS7] **Micky Rakotondrabe**, 'Using Interval techniques to synthesis robust controllers and to perform an à posteriori performances analysis of closed-loop: application to piezoelectric actuators', seminar at the [University of Newcastle, Australia](#), June 2012.

[IS6] **Micky Rakotondrabe**, '*Hysteresis modeling, identification and feedforward control for piezoelectric based Microsystems and microrobots*', guest lecture at the [University of Texas at Arlington \(UTA\), Arlington Texas USA](#), Nov 2011. **Guest lecture for undergraduate, graduate and phd students.**

[IS5] **Micky Rakotondrabe**, '*Interval tools for design, modeling, signal estimation and control of systems working at the microworld*', seminar at the [University of Texas at Arlington \(UTA\), Arlington Texas USA](#), Nov 2011.

[IS4] **Micky Rakotondrabe**, '*Control of piezoelectric microsystems with minimized number of sensors: from feedforward to combined observer/feedback approach*', seminar at the [ARRI Institute, Arlington Texas USA](#), Nov 2011.

[IS3] **Micky Rakotondrabe**, '*Design and development of piezoelectric microsystems, modeling, observer techniques and feedback/feedforward control*', seminar at the [Néel Institute - University of Joseph Fourier, Grenoble FR](#), June 2011

[IS2] **Micky Rakotondrabe**, '*Modeling, estimation and control of piezoelectric microsystems*', seminar at the [Italian Institute of Technology \(IIT\), Genoa Italy](#), 27 April 2010.

[IS1] **M. Rakotondrabe**, '*Control of piezoelectric microsystems*', seminar at the [ARRI Institute, Arlington Texas USA](#), September 2007.

Appendix C

Ballas linear model of multimorph piezoelectric cantilevers

Contents

C.1	Introduction	159
C.2	Model of multimorph piezoelectric cantilevers	161
C.2.1	Static behavior	161
C.2.2	Dynamic behavior	162
C.3	Usual cases	162
C.3.1	Unimorph actuators	162
C.3.2	Bimorph actuators	163

C.1 Introduction

The Ballas model [73] is a linear model of multilayered piezoelectric cantilevers (or multimorph) that have rectangular section. The cantilever is depicted in Fig. C.1-a. The model includes the static and the dynamic behaviors. It provides the relation between four external excitations (voltage u , moment M , force at the tip F and uniform pressure load p) applied to the cantilever and four resulting outputs at any arbitrary point x (charge $Q(x)$, bending angle $\alpha(x)$, bending or displacement $\delta(x)$ and displaced volume $V(x)$), see Fig. C.1-b. In the figures, \bar{z} indicates the distance between the neutral axis and the bottom surface of the cantilever. The piezoelectric cantilever should include at least one piezoelectric layer (piezolayer). The non-piezoelectric layers are called passive layers. The cantilever has a length L and a total thickness $h = \sum_{i=1}^n h_i$ where h_i is the thickness of the i^{th} layer and n is their total number. All layers have the same width w . The i^{th} layer has a transversal piezoelectric coefficient $d_{31,i}$ and a longitudinal compliance $s_{11,i}$. The local axis (3) in the coefficients $d_{31,i}$ and $s_{11,i}$ corresponds to the axis of poling of the piezolayer (axis z in the figure) and the local axis (1) corresponds

to the axis x before bending. Coefficient $d_{31,i}$ is taken to be zero for all non-piezoelectric layers.

If the cantilever contains two layers, one being piezoelectric and one passive, the actuator is commonly called unimorph piezoelectric cantilever. When the two layers are both piezoelectric, the actuator is called bimorph piezoelectric. The electrical connection in an unimorph is easier than in a bimorph. In counterpart, in bimorph, it is possible to obtain similar displacement than in unimorph with lower voltages.

When an electrical field is applied to the piezoelectric layers through the voltage u , they contract or expand along the x -axis thanks to the d_{31} coefficient. Due to the interfaces connection between the layers, these contraction or expansion will result in a deflection δ of the whole cantilever Fig. C.1-b. This bending is much larger than the contraction or expansion of the layers, which is the main interest of cantilever structures.

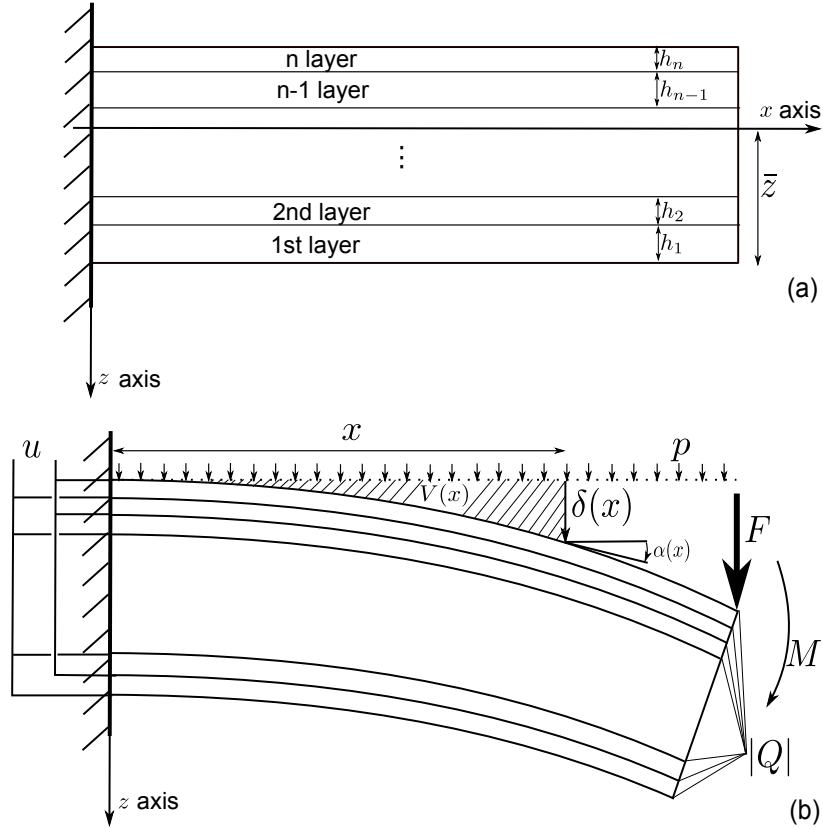


Figure C.1: A multilayered piezoelectric cantilever.

C.2 Model of multimorph piezoelectric cantilevers

C.2.1 Static behavior

The Ballas static model of a multilayered piezoelectric cantilever is given by:

$$\begin{pmatrix} \alpha(x) \\ \delta(x) \\ V(x) \\ Q(x) \end{pmatrix} = \underbrace{\begin{pmatrix} m_{11}(s) & m_{12}(s) & m_{13}(s) & m_{14}(s) \\ m_{21}(s) & m_{22}(s) & m_{23}(s) & m_{24}(s) \\ m_{31}(s) & m_{32}(s) & m_{33}(s) & m_{34}(s) \\ m_{41}(s) & m_{42}(s) & m_{43}(s) & m_{44}(s) \end{pmatrix}}_{\mathbf{M}} \begin{pmatrix} M \\ F \\ p \\ u \end{pmatrix} \quad (\text{C.1})$$

in which \mathbf{M} is the coupling matrix and. The first row is:

$$\begin{aligned} m_{11}(x) &= \frac{L}{C} \left(\frac{x}{L} \right) \\ m_{12}(x) &= \frac{L^2}{2C} \left[2 \left(\frac{x}{L} \right) - \left(\frac{x}{L} \right)^2 \right] \\ m_{13}(x) &= \frac{wL^3}{6C} \left[3 \left(\frac{x}{L} \right) - 3 \left(\frac{x}{L} \right)^2 + \left(\frac{x}{L} \right)^3 \right] \\ m_{14}(x) &= \frac{m_{piezo}L}{C} \left(\frac{x}{L} \right) \end{aligned} \quad (\text{C.2})$$

the second row is:

$$\begin{aligned} m_{21}(x) &= \frac{L^2}{2C} \left(\frac{x}{L} \right)^2 \\ m_{22}(x) &= \frac{L^3}{6C} \left[3 \left(\frac{x}{L} \right)^2 - \left(\frac{x}{L} \right)^3 \right] \\ m_{23}(x) &= \frac{wL^4}{24C} \left[6 \left(\frac{x}{L} \right)^2 - 4 \left(\frac{x}{L} \right)^3 + \left(\frac{x}{L} \right)^4 \right] \\ m_{24}(x) &= \frac{m_{piezo}L^2}{2C} \left(\frac{x}{L} \right)^2 \end{aligned} \quad (\text{C.3})$$

the third row is:

$$\begin{aligned} m_{31}(x) &= \frac{wL^3}{6C} \left(\frac{x}{L} \right)^3 \\ m_{32}(x) &= \frac{L^4}{24C} \left[4 \left(\frac{x}{L} \right)^3 - \left(\frac{x}{L} \right)^4 \right] \\ m_{33}(x) &= \frac{w^2L^5}{120C} \left[10 \left(\frac{x}{L} \right)^3 - 5 \left(\frac{x}{L} \right)^4 + \left(\frac{x}{L} \right)^5 \right] \\ m_{34}(x) &= \frac{m_{piezo}wL^3}{6C} \left(\frac{x}{L} \right)^3 \end{aligned} \quad (\text{C.4})$$

and the last row is:

$$\begin{aligned} m_{41}(x) &= -\frac{m_{piezo}L}{C} \left(\frac{x}{L} \right) \\ m_{42}(x) &= \frac{m_{piezo}L^2}{2C} \left[2 \left(\frac{x}{L} \right) - \left(\frac{x}{L} \right)^2 \right] \\ m_{43}(x) &= \frac{wm_{piezo}L^3}{6C} \left[3 \left(\frac{x}{L} \right) - 3 \left(\frac{x}{L} \right)^2 + \left(\frac{x}{L} \right)^3 \right] \\ m_{44}(x) &= \left[\sum_{i=1}^n \frac{wL}{h_i} \left(\varepsilon_{33,i}^T - \frac{d_{31,i}^2}{s_{11,i}} \right) + \frac{m_{piezo}^2L}{C} \right] \left(\frac{x}{L} \right) \end{aligned} \quad (\text{C.5})$$

with

$$\begin{cases} m_{piezo} = \frac{1}{2} \sum_{i=1}^n \frac{wd_{31,i}}{s_{11,i}h_i} \left[2\bar{z}h_i - 2h_i \sum_{j=1}^i h_j + h_i^2 \right] \\ C = \frac{1}{3} \sum_{i=1}^n \frac{w}{s_{11,i}} \left[3h_i \left(\bar{z} - \sum_{j=1}^i h_j \right) \left(\bar{z} - \sum_{j=1}^{i-1} h_j \right) + h_i^3 \right] \end{cases} \quad (C.6)$$

The distance the distance between the neutral axis and the bottom surface is defined by:

$$\bar{z} = - \frac{\sum_{i=1}^n \frac{w}{s_{11,i}} h_i^2 - 2 \sum_{i=1}^n \frac{w}{s_{11,i}} h_i \sum_{j=1}^i h_j}{2 \sum_{i=1}^n \frac{w}{s_{11,i}} h_i} \quad (C.7)$$

C.2.2 Dynamic behavior

The dynamic behavior of a multilayered piezoelectric cantilevered is given as the resonant frequencies in the Ballas model. The resonant frequency of the m^{th} mode ($m = 1, 2, \dots, \infty$) is:

$$f_m = \frac{(k_m L)}{2\pi L^2} \sqrt{\frac{C}{\mu}} \quad (C.8)$$

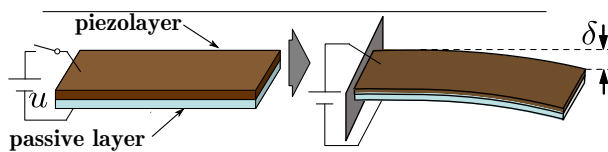
where $\mu = \frac{m_c}{L} = \sum_{i=1}^n \rho_i h_i w$ is the total mass related to the actuator's length, m_c being the mass of the whole cantilever and ρ_i being the density of the i^{th} layer. The multiplication $k_m L$ are given in [Table C.1](#).

Table C.1: Numerical values of $k_m L$ for the m^{th} mode.

m	1	2	3	4	5	\dots
$k_m L$	1.8751	4.6941	7.8548	10.9955	14.137	\dots

C.3 Usual cases

C.3.1 Unimorph actuators



A unimorph piezoelectric cantilever actuator has two layers: one piezolayer and one passive layer. It is very common because of the ease of fabrication and ease of connection. The application of a voltage u to the piezolayer

Figure C.2: A unimorph piezoelectric actuator.

yields an expansion or contraction of this latter and thus results in a bending of the total cantilever, see [Figure 2.1](#). We provide here the model that links the applied force, the applied voltage and the output displacement (bending) of the cantilever.

From the above multilayered model, the static behavior of a unimorph is:

$$\delta(x) = \frac{-3d_{31}s_{11,np}s_{11,p}h_{np}(h_{np} + h_p)x^2}{(s_{11,p})^2h_{np}^4 + s_{11,np}s_{11,p}(4h_ph_{np}^3 + 6h_p^2h_{np}^2 + 4h_p^3h_{np}) + (s_{11,np})^2h_p^4}u \quad (\text{C.9})$$

and the resonant frequency at mode m is:

$$f_m = \frac{(k_m L)^2}{2\pi L^2} \sqrt{\frac{(s_{11,p})^2h_{np}^4 + s_{11,np}s_{11,p}(4h_ph_{np}^3 + 6h_p^2h_{np}^2 + 4h_p^3h_{np}) + (s_{11,np})^2h_p^4}{12s_{11,np}s_{11,p}(s_{11,np}h_p + s_{11,p}h_{np})(\rho_{np}h_{np} + \rho_ph_p)}}} \quad (\text{C.10})$$

where the subscript p means for the piezolayer and the subscript np means for the passive layer (nonpiezoelectric).

C.3.2 Bimorph actuators

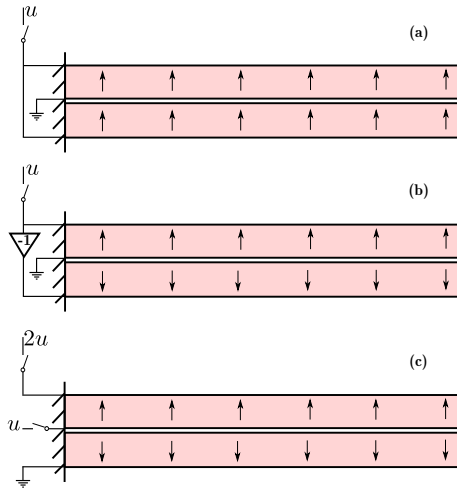


Figure C.3: A bimorph piezoelectric actuator.

[Figure C.3-c](#).

A bimorph actuator is composed of two piezolayers stucked thanks to a thin layer of glue. The obtention of the bending is made by the extension of one layer and the contraction of the other one. Two possibilities exist for that. In the first case depicted in [Figure C.3-a](#), both the two piezolayers have the same direction of poling. Hence, one voltage u suffices to create the expansion and the contraction. The bimorph is said to have parallel poling. The second case is depicted in [Figure C.3-b](#). In this, the two poling directions are opposite and the bimorph is called anti-parallel. To obtain the same bending than the previous case, a voltage u and its opposite $-u$ are required. It is possible to avoid the use of opposite voltage. However, this will require twice the previous voltage as schemated in

An advantage of bimorph relative to unimorph is the higher bending obtained with the same potential u employed. However, the electrical connection is more complex.

Consider a bimorph where the two piezolayers have the same thickness h_p . From the above multilayered model, the static behavior of the bimorph is:

$$\delta(x) = \frac{-3d_{31}x^2}{4h_p^2}u \quad (\text{C.11})$$

and the resonant frequency at mode m is:

$$f_m = \frac{(k_m L)^2 h_p}{2\pi L^2} \sqrt{\frac{1}{3\rho_p s_{11,p}}} \quad (\text{C.12})$$

Appendix D

Basics on intervals and on related techniques

Contents

D.1	Definitions	165
D.2	Operations on intervals	166
D.3	A set inversion problem	167
D.4	Interval systems	167
D.4.1	Definition	167
D.4.2	Kharitonov vertex polynomials	168
D.4.3	Stability of interval systems	168
D.4.4	H_∞ -norm of interval systems	169

References [\[172\]](#) or [\[158\]](#) are suggested if the reader would like to go further on intervals and on interval techniques.

D.1 Definitions

A closed interval denoted by $[x]$, is the set of real numbers given by:

$$[x] = [x^-, x^+] = \{x \in R / x^- \leq x \leq x^+\} \quad (\text{D.1})$$

The endpoints x^- and x^+ are respectively the left and right endpoint of $[x]$.

We say that $[x]$ is degenerate if $x^- = x^+$. Such an interval contains a single real number x . By convention, a degenerate interval $[a, a]$ can be described with the real number a .

The width of an interval $[x]$ is given by:

$$w([x]) = x^+ - x^- \quad (\text{D.2})$$

The midpoint of $[x]$ is given by:

$$mid([x]) = \frac{x^+ + x^-}{2} \quad (D.3)$$

The radius of $[x]$ is defined by:

$$rad([x]) = \frac{x^+ - x^-}{2} \quad (D.4)$$

D.2 Operations on intervals

The elementary mathematical operations are also extended to intervals, the operation result between two intervals is an interval containing all the operations results of all pairs of numbers in the two intervals. So, if we have two intervals $[x] = [x^-, x^+]$ and $[y] = [y^-, y^+]$ and a law $\circ \in \{+, -, \cdot, /\}$, we can write:

$$[x] \circ [y] = \{x \circ y \mid x \in [x], y \in [y]\} \quad (D.5)$$

The four basic operations are:

the sum of two intervals $[x] + [y]$ is defined by:

$$[x] + [y] = [x^- + y^-, x^+ + y^+] \quad (D.6)$$

the difference of two intervals $[x] - [y]$ is given by:

$$[x] - [y] = [x^- - y^+, x^+ - y^-] \quad (D.7)$$

the product of two intervals $[x] \cdot [y]$ is the set:

$$[x] \cdot [y] = [\min(x^- y^-, x^- y^+, x^+ y^-, x^+ y^+), \max(x^- y^-, x^- y^+, x^+ y^-, x^+ y^+)] \quad (D.8)$$

the quotient $[x]/[y]$ is defined as:

$$[x]/[y] = [x] \cdot [1/y^+, 1/y^-], 0 \notin [y] \quad (D.9)$$

The intersection of two intervals $[x] \cap [y]$ is the interval defined by:

1- if $y^+ < x^-$ or $x^+ < y^-$ the intersection is the empty set:

$$[x] \cap [y] = \emptyset \quad (D.10)$$

2- Otherwise:

$$[x] \cap [y] = [\max\{x^-, y^-\}, \min\{x^+, y^+\}] \quad (D.11)$$

In the latter case, the union of $[x]$ and $[y]$ is also an interval:

$$[x] \cup [y] = [\min \{x^-, y^-\}, \max \{x^+, y^+\}] \quad (\text{D.12})$$

When $[x] \cap [y] = \emptyset$, the union of the two intervals is not an interval. For that, the interval hull is defined:

$$[x] \sqcup [y] = [\min \{x^-, y^-\}, \max \{x^+, y^+\}] \quad (\text{D.13})$$

It is verified that: $[x] \cup [y] \subseteq [x] \sqcup [y]$ for any two intervals $[x]$ and $[y]$.

D.3 A set inversion problem

Let $[\mathbf{f}] : \mathbb{R}^p \rightarrow \mathbb{R}^n$ be a continuous function. Let $[\mathbf{Y}] \subseteq \mathbb{R}^n$ be a vector of intervals (also called box) that is known. We wish to find a set \mathbb{S} such that:

$$\mathbb{S} = [\mathbf{f}]^{-1}([\mathbf{Y}]) = \{[\mathbf{x}] \subseteq \mathbb{R}^p \mid [\mathbf{f}]([\mathbf{x}]) \subseteq [\mathbf{Y}]\} \quad (\text{D.14})$$

\mathbb{S} is the reciprocal image of $[\mathbf{x}]$ *via* the function $[\mathbf{f}]$. Finding the set \mathbb{S} of all solutions of Eq. (D.14) is called a set inversion problem.

An algorithm that permits to solve a set inversion problem is the SIVIA algorithm (Set Inversion Via Interval Analysis) [171; 172]. Table D.3 depicts the algorithm. In the table, $w([\mathbf{x}])$ means width of $[\mathbf{x}]$.

	SIVIA(inputs: $[\mathbf{x}], t, \epsilon$; outputs: $\underline{\mathbb{S}}, \overline{\mathbb{S}}$)
1	if $[\mathbf{f}]([\mathbf{x}]) \cap [\mathbf{Y}] = \emptyset$, $[\mathbf{x}]$ is non-solution;
2	if $[\mathbf{f}]([\mathbf{x}]) \subseteq [\mathbf{Y}]$, thus $\underline{\mathbb{S}} := \underline{\mathbb{S}} \cup [\mathbf{x}]$; $\overline{\mathbb{S}} := \overline{\mathbb{S}} \cup [\mathbf{x}]$;
3	if $w([\mathbf{x}]) < \epsilon$ thus $\overline{\mathbb{S}} := \overline{\mathbb{S}} \cup [\mathbf{x}]$;
4	sinon bissecter $[\mathbf{x}]$ en $[\mathbf{x}_1]$ et $[\mathbf{x}_2]$; SIVIA(inputs: $[\mathbf{x}_1], t, \epsilon$; outputs: $\underline{\mathbb{S}}, \overline{\mathbb{S}}$) ; SIVIA(inputs: $[\mathbf{x}_2], t, \epsilon$; outputs: $\underline{\mathbb{S}}, \overline{\mathbb{S}}$).

Table D.1: The SIVIA algorithm [171].

D.4 Interval systems

D.4.1 Definition

Parametric uncertain systems can be modeled by interval systems. An interval system denoted $[G](s, [a], [b])$ is a family of systems:

$$[G](s, [a], [b]) = \frac{[N](s, [\mathbf{b}])}{[D](s, [\mathbf{a}])} = \frac{\sum_{j=0}^m [b_j] s^j}{\sum_{i=0}^n [a_i] s^i} = \left\{ \frac{\sum_{j=0}^m b_j s^j}{\sum_{i=0}^n a_i s^i} \mid b_j \in [b_j^-, b_j^+]; a_j \in [a_j^-, a_j^+] \right\} \quad (\text{D.15})$$

such as: $[b] = [[b_0], \dots, [b_m]]$ and $[a] = [[a_0], \dots, [a_n]]$ are two boxes (vectors of interval numbers) and s the Laplace variable.

An interval system is stable if and only if the four corresponding vertex systems are stable [210]. These vertex are (point) systems whose parameters are based on the endpoints of the interval system parameters.

D.4.2 Kharitonov vertex polynomials

Given the interval system $[G](s, [\mathbf{a}], [\mathbf{b}])$ defined as in Eq. (D.15) such that:

$$\begin{cases} [N](s, [\mathbf{b}]) = [b_0] + [b_1]s + [b_2]s^2 + \dots + [b_m]s^m \\ [D](s, [\mathbf{a}]) = [a_0] + [a_1]s + [a_2]s^2 + \dots + [a_n]s^n \end{cases} \quad (\text{D.16})$$

Thus, the four Kharitonov vertex polynomials corresponding to $[N](s, [\mathbf{b}])$ and $[D](s, [\mathbf{a}])$ are:

$$\begin{aligned} N^{(1)}(s) &= b_0^- + b_1^- s + b_2^+ s^2 + b_3^+ s^3 + b_4^- s^4 + b_5^- s^5 + \dots \\ N^{(2)}(s) &= b_0^- + b_1^+ s + b_2^+ s^2 + b_3^- s^3 + b_4^- s^4 + b_5^+ s^5 + \dots \\ N^{(3)}(s) &= b_0^+ + b_1^- s + b_2^- s^2 + b_3^+ s^3 + b_4^+ s^4 + b_5^- s^5 + \dots \\ N^{(4)}(s) &= b_0^+ + b_1^+ s + b_2^- s^2 + b_3^- s^3 + b_4^+ s^4 + b_5^+ s^5 + \dots \end{aligned} \quad (\text{D.17})$$

and

$$\begin{aligned} D^{(1)}(s) &= a_0^- + a_1^- s + a_2^+ s^2 + a_3^+ s^3 + a_4^- s^4 + a_5^- s^5 + \dots \\ D^{(2)}(s) &= a_0^- + a_1^+ s + a_2^+ s^2 + a_3^- s^3 + a_4^- s^4 + a_5^+ s^5 + \dots \\ D^{(3)}(s) &= a_0^+ + a_1^- s + a_2^- s^2 + a_3^+ s^3 + a_4^+ s^4 + a_5^- s^5 + \dots \\ D^{(4)}(s) &= a_0^+ + a_1^+ s + a_2^- s^2 + a_3^- s^3 + a_4^+ s^4 + a_5^+ s^5 + \dots \end{aligned} \quad (\text{D.18})$$

respectively.

The sixteen Kharitonov (point) systems that corresponds to the interval system $[G]$ are the combination of these vertex polynomials. These sixteen Kharitonov systems are called vertex of $[G]$. We denote these sixteen Kharitonov vertex by $G^{(i)}$, with $i = 1 \rightarrow 16$.

D.4.3 Stability of interval systems

The stability of the interval system in Eq. (D.15) can be decided by analyzing by the polynomial $[D](s)$. A simple way to this analysis consists in directly applying the algebraic Routh-Hurwitz

criteria to $[D](s)$ [172; 216]. In order to introduce a robustness on the stability, the previous result was extended to the δ -stability of interval systems [172]. On the other hand, the stability from the Kharitonov theorem [210] is summarized as follows.

Theorem D.4.1. *Consider the interval system $[G](s, [\mathbf{a}], [\mathbf{b}]) = \frac{[N](s, [\mathbf{b}])}{[D](s, [\mathbf{a}])}$ defined in Eq. (D.15). All point systems in this interval system is stable iif the four vertex polynomials of $[D](s, [\mathbf{a}])$ and given in Eq. (D.18) are Hurwitz.*

Proof. see [210]. □

The above Kharitonov theorem is based in a fact that the interval parameters are independent. When these parameters are dependent, the theorem becomes conservative and the condition is only sufficient. Different works [226–228] have been carried out to generalize the Kharitonov theorem. Finally, the Lyapunov stability was extended to interval systems in [223].

D.4.4 H_∞ -norm of interval systems

Theorem D.4.2. *Consider the interval system $[G](s, [\mathbf{a}], [\mathbf{b}])$ defined in Eq. (D.15). The H_∞ -norm of $[G]$ is the maximal among the H_∞ -norm of the sixteen vertex, i.e.:*

$$\|[G]\|_\infty = \max_{i=1 \rightarrow 16} \|G^{(i)}\|_\infty$$

Proof. see [223; 224]. □

When the interval system $[G]$ is weighted by a function $W(s)$ which is a point, it is not advised to compute the multiplication $W[G]$ first and compute the H_∞ -norm of the resulting interval plant afterwards. Indeed, developping the multiplication of the intervals polynomials produces a multi-occurrence of the parameters and therefore a surestimation of the resulting intervals. Thus, the H_∞ -norm of $W[G]$ is defined as follows:

$$\|W[G]\|_\infty = \max_{i=1 \rightarrow 16} \|WG^{(i)}\|_\infty \quad (\text{D.19})$$

In [225], the H_∞ -norm of the sensitivity function of an interval system $[G](s, [\mathbf{a}], [\mathbf{b}])$ is proposed. The sensitivity of $[G]$ is defined by $[S] = \frac{1}{1+[G]} = \frac{[D]}{[N]+[D]}$, where $[N]$ and $[D]$ are the numerator and denominator defined in Eq. (D.15). It has been then demonstrated that the sensitivity $[S]$ has only twelve vertex instead of sixteen vertex and thus its H_∞ -norm is the maximal among the twelve norms:

$$\|[S]\|_\infty = \left\| \frac{[D]}{[N] + [D]} \right\|_\infty = \max_{i=1 \rightarrow 12} \|S^{(i)}\|_\infty \quad (\text{D.20})$$

Appendix E

Approximation schemes for nonlinear dynamical systems

Contents

E.1	Hammerstein-Wiener scheme	171
E.2	Hammerstein scheme	172
E.3	Wiener scheme	172

Consider the nonlinear and dynamical system pictured in [Fig. E.1](#) with driving input u and output y .

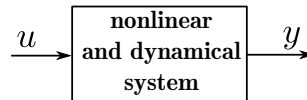


Figure E.1: A nonlinear system.

E.1 Hammerstein-Wiener scheme

It is often possible to approximate or decompose the nonlinear and dynamical system pictured in [Fig. E.1](#) by several elements. For the equivalent Hammerstein-Wiener decomposition is a composition of a linear dynamics and two static nonlinearities at the input and at the output [\[348; 349\]](#). This is figured in [Fig. E.2](#).

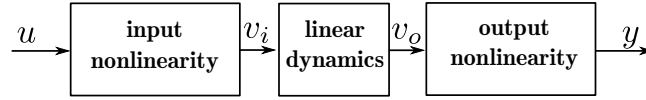


Figure E.2: The Hammerstein-Wiener scheme.

The input nonlinearity generally represents the nonlinear behavior found in the actuators and the output nonlinearity for that in the sensors or in the plant. The Hammerstein-Wiener scheme has a wide range of applications to approximate nonlinear and dynamical systems. The approximation is often easier to handle than dynamic nonlinearities. The Hammerstein-Wiener scheme has two particular cases: the Hammerstein scheme and the Wiener scheme.

E.2 Hammerstein scheme

In the Hammerstein scheme, the nonlinearities are assumed to be only at the input as depicted in [Fig. E.3](#). It is widely employed in actuated systems, in particular to represent systems with hysteresis. This is from the well known Hammerstein theorem.

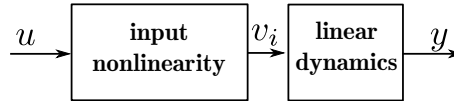


Figure E.3: The Hammerstein scheme.

E.3 Wiener scheme

In the Wiener scheme, the nonlinearities are assumed to be only at the output, see [Fig. E.4](#).

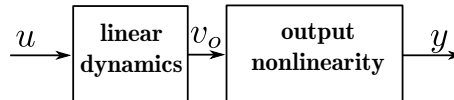


Figure E.4: The Wiener scheme.

References

- [1] José L. Pons, 'Emerging actuator technologies : a micromechatronic approach', Wiley, ISBN 0-470-09197-5, 2005.
- [2] Ankur Jain, Anthony Kopa, Yingtian Pan, Gary K. Fedder and Huikai Xie, 'A Two-Axis Electrothermal Micromirror for Endoscopic Optical Coherence Tomography', IEEE Journal of selected topics in quantum electronics, Vol.10(3), may/june 2004.
- [3] Jingjing Sun and Huikai Xie, 'MEMS-Based Endoscopic Optical Coherence Tomography', Review article, Hindawi, International Journal of Optics, doi:10.1155/2011/825629, 2011.
- [4] A. Espinosa, K. Rabenorosoa, C. Clévy, B. Komati, P. Lutz, X. Zhang, S. Samuelson, and H. Xie, "Piston Motion Performance Analysis of a 3DOF Electrothermal MEMS Scanner for Medical Applications", International Journal of Optomechatronics, vol. 8, issue 3, pp. 179 - 194, 07/2014.
- [5] C. Duan, X. Zhang, D. Wang, Z. Zhou, P. Liang, A. Pozzi, and H. Xie, "An endoscopic forward-viewing OCT imaging probe based on a two-axis scanning mems mirror", Biomedical Imaging (ISBI), 2014 IEEE 11th International Symposium on, pp. 1397-1400, April, 2014.
- [6] The european microRALP project, <http://www.microralp.eu/>.
- [7] Leonardo S. Mattos, Nikhil Deshpande, Giacinto Barresi, Luca Guastini, Giorgio Peretti, "A Novel Computerized Surgeon–Machine Interface for Robot-Assisted Laser Phonomicrosurgery" The Laryngoscope, The American Laryngological, Rhinological and Otological Society, DOI: 10.1002/lary.24566, 2013.
- [8] Michael Gauthier, Nicolas Andreff, Etienne Dombre, "Intracorporeal Robotics: From Milliscale to Nanoscale", Wiley-ISTE, ISBN: 978-1-84821-371-5, february 2014.
- [9] K.B. Yesin, P. Exner, K. Vollmers, N.J. Nelson, "Design and control of in-vivo magnetic microrobots", Medical Image Computing and Computer-Assisted Intervention - MICCAI 2005.
- [10] B.J. Nelson, I.K. Kaliakatsos, J.J. Abbott, "Microrobots for minimally invasive medicine", Annual Review of Biomedical Engineering, DOI: 10.1146/annurev-bioeng-010510-103409, Vol.12:55-85, 2010.

- [11] Olgaç Ergeneman, Christos Bergeles, Michael P. Kummer, Jake J. Abbott, Bradley J. Nelson, "Wireless Intraocular Microrobots: Opportunities and Challenges" *Surgical Robotics*, pp 271-311, 2011.
- [12] F. Ullrich, C. Bergeles, J. Pokki, O. Ergeneman, S. Erni, G. Chatzipirpiridis, S. Pané, C. Framme, B. J. Nelson, "Mobility experiments with microrobots for minimally invasive intraocular surgery", *Investigative Ophthalmology Visual Science*, Vol. 54, No. 4, April 2013, pp. 2853-63.
- [13] G. Binnig, C. F. Quate, Ch. Gerber, "Atomic Force Microscope". *Physical Review Letters* 56 (9): 930–933, 1986
- [14] G. Binnig and H. Rohrer, "The scanning tunneling microscope", *Scientific American*, vol. 253, pp. 50–56, 1986.
- [15] W. J. Kaiser, L. D. Bell, "Direct investigation of subsurface interface electronic structure by ballistic-electron-emission microscopy". *Physical Review Letters* 60 (14): 1406–1409, 1988.
- [16] J. M. R. Weaver, David W. Abraham, "High resolution atomic force microscopy potentiometry". *Journal of Vacuum Science and Technology B* 9 (3): 1559–1561, 1991.
- [17] S. M. Salapaka and M. V. Salapaka, "Scanning probe microscopy," *IEEE Control Systems Magazine*, vol. 28, no. 2, pp. 65–83, 2008.
- [18] Y. K. Yong, B. Arain, S. O. R. Moheimani, "Atomic Force Microscopy with a 12-electrode Piezoelectric Tube Scanner", *Review of Scientific Instruments*, Volume 81, Number 3, page 033701 2010.
- [19] K. K. Leang, A. J. Fleming, "High-speed serial-kinematic AFM scanner: design and drive considerations", *Asian Journal of Control*, Special issue on Advanced Control Methods for Scanning Probe Microscopy Research and Techniques, 11 (2), pp. 144 – 153, 2009.
- [20] A. J. Fleming, B. J. Kenton, K. K. Leang (2010): Bridging the gap between conventional and video-speed scanning probe microscopes. *Ultramicroscopy*, 110 (9), pp. 1205 – 1214, 2010.
- [21] HJ Quenzer, U Drechsler, A Sebastian, S Marauska, B Wagner, "Fabrication of conducting AFM cantilevers with AlN-based piezoelectric actuators"; *Procedia Engineering* 25, 665-6683, 2011.
- [22] A Sebastian, N Shamsudhin, H Rothuizen, U Drechsler, WW Koelmans, "Note: Micro-cantilevers with AlN actuators and PtSi tips for multi-frequency atomic force microscopy", *Review of Scientific Instruments* 83 (9), 096107, 2012.
- [23] A. G. Fowler, A. N. Laskovski, A. C. Hammond, and S. O. R. Moheimani, "A 2-DOF electrostatically actuated MEMS nanopositioner for on-chip AFM", *Journal of Microelectromechanical Systems*, vol. 21, no. 4, pp. 771–773, 2012.

- [24] Y. K. Yong, S. O. R. Moheimani, B. J. Kenton, K. K. Leang, "Invited Review Article: High-Speed Flexure-Guided Nanopositioning: Mechanical Design and Control Issues", *Review of Scientific Instruments*, Volume 83, Number 12, page 121101 2012.
- [25] Y. K. Yong, S. O. R. Moheimani, "Design of an Inertially Counterbalanced Z-nanopositioner for High-Speed Atomic Force Microscopy", *IEEE Transactions on Nanotechnology*, Volume 12, Number 2, page 137–145 March 2013.
- [26] Mohammad Maroufi, Ali Bazaei, and S. O. Reza Moheimani, "A High-Bandwidth MEMS Nanopositioner for On-Chip AFM: Design, Characterization, and Control", *IEEE Transactions on Control Systems Technology*, 2014.
- [27] S. Wadikhaie, Y. K. Yong, S. O. R. Moheimani, "A Serial-Kinematic Nanopositioner for High-Speed AFM", *Review of Scientific Instruments* - 2014.
- [28] A. G. Fowler, M. Maroufi, A. Bazaei, S. O. R. Moheimani, "MEMS Nanopositioner for Lissajous-Scan Atomic Force Microscopy", *ASME Dynamic Systems and Control Conference* - Oct. 22-24 2014.
- [29] P. Vettiger, G. Cross, M. Despont, U. Drechsler, U. Dürig, B. Gotsmann, W. Häberle, M. Lantz, H. Rothuizen, R. Stutz, and G. Binnig, "The 'millipede'—Nanotechnology entering data storage", *IEEE Trans. Nanotechnol.*, vol. 1, pp. 39–55, 2002.
- [30] E. Eleftheriou, T. Antonakopoulos, G.K. Binnig, G. Cherubini, M. Despont, A. Dholakia, U. Dürig, M.A. Lantz, H. Pozidis, H.E. Rothuizen, and P. Vettiger, "Millipede—A MEMS based scanning-probe data storage system", *IEEE Trans. Magn.*, vol. 39, no. 2, pp. 938–945, 2003.
- [31] A. Pantazi, M. A. Lantz, G. Cherubini, H. Pozidis, and E. Eleftheriou, "A servomechanism for a micro-electro-mechanical-system-based scanning-probe data storage device", *Nanotechnology*, vol. 15, no. 10, pp. S612–S621, Oct. 2004.
- [32] A Knoll, P Bächtold, J Bonan, G Cherubini, M Despont, U Drechsler, U Dürig, B Gotsmann, W Häberle, C Hagleitner, D Jubin, MA Lantz, A Pantazi, H Pozidis, H Rothuizen, A Sebastian, R Stutz, P Vettiger, D Wiesmann, ES Eleftheriou, "Integrating nanotechnology into a working storage device", *Elsevier Microelectronic Engineering*, pp.83(4), pp.1692-1697, 2006.
- [33] A. Pantazi, A. Sebastian, G. Cherubini, M. Lantz, H. Pozidis, H. Rothuizen, and E. Eleftheriou, "Control of MEMS-based scanning-probe data-storage devices", *IEEE Transactions on Control Systems Technology*, vol. 15, no. 5, pp. 824–841, 2007.
- [34] M. Lantz, H. Rothuizen, U. Drechsler, W. Häberle, and M. Despont, "A vibration resistant nanopositioner for mobile parallel-probe storage applications", *Journal of Microelectromechanical Systems*, vol. 16, no. 1, pp. 130–139, 2007.
- [35] Aggeliki Pantazi, Abu Sebastian, TA Antonakopoulos, Peter Bächtold, Anthony R Bonaccio, Jose Bonan, Giovanni Cherubini, Michel Despont, Richard A DiPietro, Ute Drechsler,

- Urs Dürig, Bernd Gotsmann, Walter Häberle, Christoph Hagleitner, James L Hedrick, Daniel Jubin, Armin Knoll, Mark A Lantz, John Pentarakis, Haralampos Pozidis, Russell C Pratt, H Rothuizen, Richard Stutz, Maria Varsamou, Dorothea Wiesmann, Evangelos Eleftheriou, "Probe-based ultrahigh-density storage technology", *IBM Journal of Research and Development*, vol.52(4-5), pp.493-511, 2008.
- [36] Abu Sebastian, Angeliki Pantazi, Haris Pozidis, Evangelos Eleftheriou, "Nanopositioning for Probe-Based Data Storage", *IEEE Control Systems*, vol.28(4), pp.26-35, 2008.
- [37] Abu Sebastian, Angeliki Pantazi, S.O.Reza Moheimani, Haris Pozidis, Evangelos Eleftheriou, "Achieving subnanometer precision in a MEMS-based storage device during self-servo write process", *IEEE Transactions on Nanotechnology*, vol.7(5), pp.586-595, 2008.
- [38] C. Clévy, A. Hubert, and N. Chaillet, "Micromanipulation and microassembly systems" in *Proc. IEEE Adv. Robot. Prog.*, Paris, France, 2006.
- [39] J. Cecil, D. Powell, and D. Vasquez, "A review of gripping and manipulation techniques for micro-assembly applications", *Robot. Comp.-Int. Manuf.*, vol. 23, no. 5, pp. 580–588, Oct. 2007.
- [40] M. Savia and H. N. Koivo, "Contact micromanipulation—Survey of strategies", *IEEE/ASME Trans. Mech.*, vol. 14, no. 4, pp. 504–514, Aug. 2009.
- [41] N. Chaillet and S. Régnier, "Microrobotics for Micromanipulation", Hoboken, NJ, USA: Wiley, 2010.
- [42] Ashis Gopal Banerjee, and Satyandra K. Gupta, "Research in Automated Planning and Control for Micromanipulation", *IEEE Trans. Automation Science and Engineering*, vol.10(3), 2013.
- [43] A. Fasoro, A. Patil, D. O. Popa, H. Beardsley, D. Agonafer and H. Stephanou, "Fluxless soldering of MOEMS," *ITHERM Intersociety Conference on Thermal and Thermomechanical Phenomena in Electronic Systems*, San Diego, May, 2006.
- [44] N. Lakhkar, A. Fasoro, A. Patil, W. Lee, D. O. Popa, H. Stephanou, and D. Agonafer, "Process Development and Die Shear Testing in MOEMS Packaging," *ASME InterPACK Conference*, Vancouver, Canada, July 2007.
- [45] A. Fasoro, M. Mittal, D. O. Popa, D.A. Agonafer, and H. E. Stephanou "Design for Reliability Applied to Packaging of a MOEMS Switch," in *ASME Journal of Electronic Packaging*, September 2008.
- [46] A. N. Das, D.O. Popa, J. Sin, and H.E. Stephanou, "Precision Alingment and Assembly for a Fourier Transform Microspectrometer, " in *Journal of Micro-Nano Mechatronics (JNMN)*, Nov. 2009.

- [47] K. Rabenoroso, A.N. Das, R. Murthy, C. Clévy, D. Popa, P. Lutz, "Precise motion control of a piezoelectric microgripper for microspectrometer assembly". In ASME'09 International Design Engineering Technical Conferences Computers and Information in Engineering Conference, San Diego, 2009.
- [48] K. Rabenoroso, C. Clévy, P. Lutz, S. Bargiel, C. Gorecki, "A micro-assembly station used for 3d reconfigurable hybrid moems assembly", In IEEE International Symposium on Assembly and Manufacturing, 2009.
- [49] A. N. Das, D.O. Popa, J. Sin, and H.E. Stephanou, "Precision Alingnment and Assembly for a Fourier Transform Microspectrometer," in Journal of Micro-Nano Mechatronics (JNMN), Nov. 2009.
- [50] D. Hériban, M. Gauthier, P. Lutz, and N. Chaillet, "Station de micro-assemblage", "micron d'or" au salon industriel international des microtechniques Micro- nora, <http://www.femto-st.fr/fr/L-institut/Actualite/?eid=62&y=2008>, 2008.
- [51] S. Bargiel, K. Rabenoroso, C. Clévy, C. Gorecki and P. Lutz, "Towards Micro-Assembly of Hybrid MOEMS Components on Reconfigurable Silicon Free-Space Micro-Optical Bench", Journal of Micromechanics and Microengineering (JMM), 20(4), 2010.
- [52] K. Rabenoroso, S. Bargiel, C. Clévy, P Lutz and C Gorecki, "Assembly of 3D Reconfigurable Hybrid MOEMS through Microrobotic Approach", Lecture Notes in Automation, Frontiers of Assembly and Manufacturing, pp. 99-112, 2010.
- [53] C. Clévy, I. Lungu, K. Rabenoroso and P. Lutz, "Positioning Accuracy Characterization of Assembled Microscale Components for Micro-Optical Benches", Assembly Automation (AA), 34(1), pp. 68-77, January 2014.
- [54] Yu Sun, K-T Wan, Kenneth P Roberts, John C Bischof, Bradley J Nelson, "Mechanical property characterization of mouse zona pellucida", IEEE Transactions on NanoBioscience, vol.2(4), pp.279-286, 2003.
- [55] Felix Beyeler, Adrian Neild, Stefano Oberti, Dominik J Bell, Yu Sun, Jrg Dual, Bradley J Nelson, "Monolithically fabricated microgripper with integrated force sensor for manipulating microobjects and biological cells aligned in an ultrasonic field", Journal of Microelectromechanical Systems, vol.16(1), 2007.
- [56] Keekyoung Kim, Xinyu Liu, Yong Zhang, Yu Sun, "Nanonewton force-controlled manipulation of biological cells using a monolithic MEMS microgripper with two-axis force feedback" Journal of micromechanics and microengineering, vol.18, 2008.
- [57] X.Y. Liu, R. Fernandes, A. Jurisicova, R. Casper, and Y. Sun, "In-situ mechanical characterization of mouse oocytes using a cell holding device" Lab on a Chip, Vol. 10, pp. 2154, 2010.
- [58] M. Sitti, "Survey of nanomanipulation systems", in Proc. IEEE Conf. Nanotech., Maui, HI, pp.75-80, 2001.

- [59] Yassine Haddab, "Conception et réalisation d'un système de micromanipulation contrôlé en effort et en position pour la manipulation d'objets de taille micrométrique", PhD Thesis (in french), Franche-Comté University, FRANCE, 2000.
- [60] Y. Haddab, N. Chaillet, A. Bourjault. A Microgripper Using Smart Piezoelectric Actuators. IEEE/RSJ International Conference on Intelligent Robots and Systems, Kagawa University, Takamatsu, Japon, 2000.
- [61] J. Agnus, "Contribution à la micromanipulation: étude, réalisation, caractérisation et commande d'une micropince piézoélectrique", PhD thesis, University of Franche-Comté, Besançon, 2003.
- [62] J. Agnus, P. De Lit and N. Chaillet, 'Micromanipulateur piézoélectrique notamment pour microrobotique', french Patent, FR0211934, 2002.
- [63] C. Clévy, "Contribution à la micromanipulation robotisée: un système de changement d'outils automatisé pour le microassemblage", PhD thesis, University of Franche-Comté, Besançon, 2005.
- [64] M. Grossard, "Contribution à la conception optimale et la commande de systèmes mécatroniques flexibles à actionnement piézoélectrique intégré - Application en microrobotique", PhD thesis, University of Franche-Comté, Besançon, 2008.
- [65] M. Grossard, C. Rotinat-Libersa, N. Chaillet, M. Boukallel, 'Mechanical and Control-Oriented Design of a Monolithic Piezoelectric Microgripper Using a New Topological Optimization Method', IEEE Transactions on Mechatronics 14, 1, 32-45, 2009.
- [66] R. El Khoury Moussa, "Synthèse optimale, réalisation et caractérisation de micro-articulations flexibles à actionnement et mesure piézoélectriques intégrés" PhD thesis, University of Franche-Comté, Besançon, 2011.
- [67] Dragos Adrian Ciubotariu, Ioan Alexandru Ivan, Cédric Clévy, Philippe Lutz, 'Size-dependent analysis and experiments of bulk PMN-PT [001] piezoelectric actuator for MOEMS micro-mirrors', IEEE/ASME - AIM, (International Conference on Advanced Intelligent Mechatronics), accepted, Besançon, France, July 2014
- [68] X. Tan and J. Baras, "Modeling and control of hysteresis in magnetostrictive actuators," *Automatica*, vol. 40, no. 9, pp. 1469-1480, 2004.
- [69] Ram Venkataraman Iyer, X. Tan, and P. S. Krishnaprasad, "Approximate inversion of the Preisach hysteresis operator with applications to control of smart actuators," *IEEE Trans on Automatic Control*, vol. 50, no. 6, pp. 798-810, 2005.
- [70] I.D. Mayergoyz, "Mathematical Models of Hysteresis", Springer, ISBN-13: 978-1461277675, 1991.
- [71] M. A. Krasnosel'skii and A. V. Pokrovskii, "Systems with hysteresis", Springer-Verlag, Berlin, 1989

- [72] Konstantin Naumenko Holm Altenbach, "Modeling of creep for structural analysis", Springer Verlag, ISBN-13: 978-3-540-70834-6, 2006.
- [73] R. G. Ballas, 'Piezoelectric multilayer beam bending actuators: static and dynamic behavior and aspects of sensor integration', Springer-Verlag, Berlin 2007.
- [74] Yassine Haddab, Qiao Chen, Philippe Lutz, "Improvement of strain gauges micro-forces measurement using Kalman optimal filtering", IFAC International Journal of Mechatronics. Volume 19, Issue 4, 8 pp. 457-462, 2009.
- [75] Abdenbi Mohand, Mathieu Grossard, Mehdi Boukallel, "Adaptive Control Based on an Extended Kalman Filter for Hammerstein System -Application to Piezoelectric Actuators", IFAC - Mech, (Symposium on Mechatronic Systems), pp.417:422, Cambridge Massachusetts USA, September 2010.
- [76] M. Boudaoud, Y. Haddab and Y. Le Gorrec, "Kalman Filtering Applied to Weak Force Measurement and Control in the Microworld", in "Signal Measurement and Estimation Techniques for Micro and Nanotechnology", Clévy, Cédric; Rakotondrabe, Micky; Chaillet, Nicolas (Eds.), pp. 71-91, 2011.
- [77] R. S. Fearing, "Survey of sticking effect for micro parts handling", IEEE International Conference on Intelligent Robots and Systems, IROS, Vol.2, pp.212-227, Pittsburgh, PA, USA 1995.
- [78] Michaël Gauthier, Stephane Régnier, Patrick Rougeot, Nicolas Chaillet, "Analysis of forces for micromanipulations in dry and liquid media", Journal of Micromechatronics, vol.3(3), 2006.
- [79] Pierre Lambert, 'Capillary Forces in Microassembly: Modeling, Simulation, Experiments, and Case Study', Springer Verlag, ISBN-13: 978-0387710884, october 2007.
- [80] Quan Zhou, Carlos del Corral, Pedro J. Esteban, and Keikki N. Koivo. "Environmental influences on microassembly", IEEE/RSJ IROS, 2002.
- [81] The european EUPASS project (Evolvable ultra precision assembly system), 2004 - 2009.
- [82] <http://www.percipio-robotics.com/>
- [83] Maria Chiara Carrozza, Anna Eisinberg, Arianna Menciassi, Domenico Campolo, Silvestro Micera and Paolo Dario, "Towards a force-controlled microgripper for assembling biomedical microdevices", Journal of Micromechanics and Microengineering, doi:10.1088/0960-1317/10/2/328, 2000.
- [84] Domenico Campolo, Ranjana Sahai, and Ronald S. Fearnig, "Development of piezoelectric bending actuators with embedded piezoelectric sensors for micromechanical flapping mechanisms", ICRA, Taipei, Taiwan 2003.

- [85] Deok-Ho Kim, Byungkyu Kim, Sang-Min Kim, and Hyunjae Kang, "Development of a piezoelectric polymer-based sensorized microgripper for microassembly and micromanipulation", IROS, 2003.
- [86] David L. Heiserman, "Piezoelectric polymer micromanipulator", US Patent, N4610475, 1986.
- [87] Steven J. Gross, "Micromachined switches and cantilever actuators based on piezoelectric lead zirconate titanate (PZT)", PhD thesis, The Pennsylvania State University, 2004.
- [88] H.-C. Lee, J. Y. Park, and J.-U. Bu, "Piezoelectrically actuated RF MEMS DC contact switches with low voltage operation," IEEE Microw. Wireless Compon. Lett., vol. 15, no. 4, pp. 202–204, Apr. 2005.
- [89] Gabriel L. Smith, Jeffrey S. Pulskamp, Luz M. Sanchez, Daniel M. Potrepka, Robert M. Proie, Tony G. Ivanov, Ryan Q. Rudy, William D. Nothwang, Sarah S. Bedair, Christopher D. Meyer and Ronald G. Polcawich, "PZT-Based Piezoelectric MEMS Technology", Journal of the American Ceramic Society, DOI: 10.1111/j.1551-2916.2012.05155, 2012.
- [90] Y. Fu, E. C. Harvey, M. K. Ghantasala, and G. M. Spinks, "Design, fabrication and testing of piezoelectric polymer PVDF micro actuators," Smart Mater. Struct., vol. 15, no. 1, pp. 141–146, 2006.
- [91] A. Cox, D. Monopoli, D. Cvetnicanin, M. Goldfarb, and E. Garcia, "The development of elastodynamic components for piezoelectrically actuated flapping micro-air vehicles," J. Intell. Mater. Syst. Struct., vol. 13, no. 9, pp. 611–615, 2002.
- [92] J. Yan, R.J. Wood, S. Avadhanula, D. Campolo, M. Sitti and R.S. Fearing, "Towards Flapping Wing Control for a Micromechanical Flying Insect", IEEE Int. Conference on Robotics and Automation, 2001.
- [93] R.J. Wood, S. Avadhanula, M. Menon, R.S. Fearing, "Microrobotics Using Composite Materials: The Micromechanical Flying Insect Thorax", IEEE Int. Conference on Robotics and Automation, 2003.
- [94] Kevin Y. Ma, Samuel M. Felton, and Robert J. Wood, "Design, Fabrication, and Modeling of the Split Actuator Microrobotic Bee", IEEE/RSJ International Conference on Intelligent Robots and Systems, 2012.
- [95] Z.E. Teoh and R.J. Wood, "A Flapping Wing Microrobot with a Differential Angle-of-Attack Mechanism", IEEE Int. Conference on Robotics and Automation, 2012.
- [96] A.T. Trana, G. Pandrauda, H. Schellevis and P. M. Sarro, "Enhancement of AlN slender piezoelectric cantilevers actuation by PECVD Silicon Nitride coating", Procedia Engineering, 47, pp.104-107, 2012.
- [97] W.P. Robbins, D.E. Glumac, "A planar unimorph-based actuator with large vertical displacement capability", IEEE Trans Ultrason Ferroelectr Freq Control, 45(5):1151-60. doi:10.1109/58.726438., 1998.

- [98] Yiping Zhu, Wenjing Liu, Kemiao Jia, Wenjun Liao, Huikai Xie, "A piezoelectric unimorph actuator based tip-tilt-piston micromirror with high fill factor and small tilt and lateral shift", Elsevier Sensors and Actuators A, 167, 495–501, 2011.
- [99] Ethem Erkan Aktakka, Rebecca L. Peterson, and Khalil Najafi, "High Stroke and High Deflection Bulk-PZT Diaphragm and Cantilever Micro Actuators and Effect of Pre-Stress on Device Performance", Journal of Microelectromechanical Systems, DOI.10.1109/JMEMS.2013.2279079, 2013.
- [100] E.E. Aktakka, R. L. Peterson, and K. Najafi, "A 3-DOF piezoelectric micro vibratory stage based on bulk-PZT/silicon crab-leg suspensions", IEEE 26th International Conference on Micro Electro Mechanical Systems (MEMS), pp.576-579, 2013.
- [101] J. Zhong, S. Seelecke, R. C. Smith and C. Büskens, "Optimal control of piezoceramic actuators", Proceedings of the SPIE Smart Structures and Materials: Modeling, Signal Processing, and Control. Volume 5049, pp. 264-274, 2003.
- [102] "ANSI/IEEE Standard on Piezoelectricity", IEEE Transactions on Ultrasonics, Ferroelectrics and Frequency Control, vol. 45, 1996, p. 717
- [103] Jan G. Smits and Wai-Shing Choi, "The constituent equations of piezoelectric heterogeneous bimorphs", Ultrasonics Symposium, 1990.
- [104] Jan G. Smits and Wai-Shing Choi, 'Equations of state including the thermal domain of piezoelectric and pyroelectric heterogeneous bimorphs', Ferroelectrics, Volume 141, Issue 1, pp.271-276s, 1993.
- [105] Jan G. Smits, Susan I. Dalke, Thomas K. Cooney, 'The constituent equations of piezoelectric bimorphs', Sensors and Actuators A: Physical, Volume 28, Issue 1, Pages 41-61, June 1991
- [106] Qing-Ming Wang and L. Eric Cross, 'Performance analysis of piezoelectric cantilever bending actuators', Ferroelectrics, Volume 215, Issue 1, 1998.
- [107] Sigrun Hirsekorn, 'Flexural Vibration Behavior of Piezoelectric Heterogeneous Bimorph Beams', IEEE transactions on ultrasonics, ferroelectrics, and frequency control, vol. 49, no. 7, July 2002.
- [108] K.J. Yoon, K.H. Park, S.K. Lee, N.S. Goo and H.C. Park, "Analytical design model for a piezo-composite unimorph actuator and its verification using lightweight piezo-composite curved actuators", Smart Materials and Structures, vol.13, pp.459-467, 2004.
- [109] Don L. DeVoe and Albert P. Pisano, 'Modeling and Optimal Design of Piezoelectric Cantilever Microactuators', JOURNAL OF MICROELECTROMECHANICAL SYSTEMS, VOL. 6, NO. 3, SEPTEMBER 1997.
- [110] Marc S. Weinberg, 'Working Equations for Piezoelectric Actuators and Sensors', ASME/IEEE Journal of MEMS, Vol. 8, No. 4, 1999.

- [111] D. O. Popa, B. H. Kang, J. T. Wen, H. E. Stephanou, G. Skidmore, and A. Geisberger, "Dynamic modeling and input shaping of thermal bimorph MEMS actuators," in Proc. IEEE Int. Conf. Robot. Autom., Taipei, Taiwan, pp. 1470–1475, 2003.
- [112] A. Jain, H. Qu, S. Todd, and H. Xie, "A thermal bimorph micromirror with large bi-directional and vertical actuation," Elsevier Sens. Actuators A, vol. 122, pp. 9–15, 2005.
- [113] Wolfgang Benecke, "Micromanipulator for gripping objects", US Patent N5172950, 1992.
- [114] B. Mokaberi and A. A. G. Requicha, "Drift compensation for automatic nanomanipulation with scanning probe microscopes," IEEE Trans. Autom. Sci. Eng., vol. 3, no. 3, pp. 199–207, Jul. 2006.
- [115] Q. Zhou, A. Aurelian, C. del Corral, P. J. Esteban, P. Kallio, B. Chang and H. N. Koivo, 'A microassembly station with controlled environment', SPIE Microrobotics and Microassembly III Conference, Potonics Boston 2001.
- [116] I.A. Ivan, G. Hwang, J. Agnus, N. Chaillet, S. Régnier, "NIST Mobile Microrobotics Challenge. MagPieR: The Fastest Mobile Microrobots in the World", IEEE Robotics and Automation Magazine (RAM), DOI: 10.1109/MRA.2012.2201599, Available online: October 2012.
- [117] D. V. Widder, "The Heat Equation", Academic Press, ISBN.0080873839, 9780080873831, 1976.
- [118] G.R. Liu, S. S. Quek, "The Finite Element Method: A Practical Course", Butterworth-Heinemann, ISBN-13: 978-0750658669, 2003.
- [119] J. P. Holman, "Heat transfer", McGraw-Hill Book Company, ISBN 0-07-029620-0, 6th edition 1986.
- [120] G. Selliger, J. Stephan and S. Lange, "Hydroadhesive gripping by using peltier effect", ASME International Mechanical Engineering Congress & Exposition (IMECE), pp.3-8, Florida USA, November 2000.
- [121] Karnopp D., R. Rosenberg, "Systems Dynamics: a Unified Approach", John Wiley sons, 1975.
- [122] C. Sueur et G. Dauphin-Tanguy, "Bond-graph approach for structural analysis of MIMO linear systems", Journal of the Franklin Institute, vol. 328, No. 1, pp. 55-70, 1991.
- [123] D.W. Roberts, D. J. Ballance et P. J. Gawthrop, "Design and Implementation of a Bond Graph Observer for Robot Control". Technical Report CSC-95004, Glasgow University Centre for Systems and Control (1995).
- [124] E Bideaux, M Smaoui, X Brun, D Thomasset, "Design of a compliant positioning control using an inverse method", Bath Workshop on Power Transmission and Motion Control, 147-164, 2003.

- [125] C. Pichardo-Almarza, A. Rahmani, G. Dauphin-Tanguy, et M. Delgado, "Bond Graph Approach to Build Reduced Order Observers in Linear Time Invariant Systems", Proceedings of 4th MATHMOD, Fourth International Symposium on Mathematical Modelling, 2003.
- [126] Abdechafik Derkaoui, Eric Bideaux, Michel Vergé, Serge Scavarda, "Design of an actuating system using Inverse bond graph methodology: Application of FEM to a tow-links flexible manipulator", IEEE IECON 2006-32nd Annual Conference on Industrial Electronics, pp-4442-4447, 2006.
- [127] Eric BIDEAUX, Jérôme LAFFITE, Wilfrid MARQUIS-FAVRE, Serge SCAVARDA, Franck GUILLEMARD, "System design using an inverse approach : Application to the hybrid vehicle powertrain", Journal européen des systèmes automatisés, vol. 40, no3, 2006.
- [128] Wilfrid Marquis-Favre, Eric Bideaux, Olivier Mechin, Serge Scavarda, Franck Guille-mard, Marc Ebalard, "Mechatronic bond graph modelling of an automotive vehicle", Mathematical and Computer Modelling of Dynamical Systems, vol.12, pp.189-202, 2006.
- [129] Mariem El Feki, Michaël Di Loreto, Eric Bideaux, Daniel Thomasset, Roger Fotsu Ng-wompo, "Structural properties of inverse models represented by bond graph", Proceedings of the 17th IFAC World Congress, 2008.
- [130] Omar Mouhib, Audrey Jardin, Wilfrid Marquis-Favre, Eric Bideaux, Daniel Thomas-set, "Optimal control problem in bond graph formalism", Elsevier Simulation Modelling Practice and Theory, vol.17, pp.240-256, 2009.
- [131] Xavier Roboam, Eric Bideaux, Geneviève Dauphin-Tanguy, Bruno Sareni, Stéphan Astier, "The Bond Graph Formulation for an Energetic and Dynamic Approach of the Anal-ysis and Synthesis of Multiphysical Systems", Systemic Design Methodologies for Electrical Energy Systems: Analysis, Synthesis and Management, pp.39-84, 2012.
- [132] P.J. Gawthrop, B. Bhikkaji, S.O.R. Moheimani, "Physical-model-based control of a piezoelectric tube for nano-scale positioning applications", IFAC Mechatronics, 20, 74-84, 2010.
- [133] <http://www.davincisurgery.com/>.
- [134] W. Piyawattanametha, P. R. Patterson, D. Hah, H. Toshiyoshi, and M. C. Wu, "Surface-and bulk-micromachined two-dimensional scanner driven by angular vertical comb actua-tors," J. Microelectromech. Syst., vol. 14, no. 6, pp. 1329-1338, 2005.
- [135] G. D. J. Su, H. Toshiyoshi, and M. C. Wu, "Surface-micromachined 2-D optical scan-ners with high-performance single-crystalline silicon micromirrors," IEEE Photon. Technol. Lett., vol. 13, no. 6, pp. 606- 608, 2001.
- [136] H. M. Chu and K. Hane, "Design, fabrication and vacuum operation characteristics of two-dimensional comb-drive micro-scanner," Sensors Actuators A, vol. 165, no. 2, pp. 422-430, 2011.

- [137] D. Yan, A. Apsel, and A. Lal, "Fabrication and electromechanical characterization of silicon on insulator based electrostatic microscanners," *Smart materials and structures*, vol. 14, no. 4, p. 775, 2005.
- [138] Y. D. Gokdel, B. Sarioglu, S. Mutlu, and A. Yalcinkaya, "Design and fabrication of two-axis micromachined steel scanners," *J. Micromech. Microeng.*, vol. 19, no. 7, p. 075001, 2009.
- [139] Donglin Wang, Linlai Fu, Xin Wang, Zhongjian Gong, Sean Samuelson, Can Duan, Hongzhi Jia, Jun Shan Ma, Huikai Xie, "Endoscopic swept-source optical coherence tomography based on a two-axis microelectromechanical system mirror", *Journal of biomedical optics*, 2013.
- [140] J. G. Smits, K. Fujimoto, and V. F. Kleptsyn, "Microelectromechanical flexure PZT actuated optical scanner: static and resonance behavior," *J. Micromech. Microeng.*, vol. 15, no. 6, p. 1285, 2005.
- [141] L. Liu, L. Wu, J. Sun, E. Lin, and H. Xie, "Miniature endoscopic optical coherence tomography probe employing a two-axis microelectromechanical scanning mirror with through-silicon vias," *J. Biomed. Opt.*, vol. 16, no. 2, pp. 026006–026006, 2011.
- [142] H. Ra, W. Piyawattanametha, Y. Taguchi, S. Lee, M. J. Mandella, and O. Solgaard, "Two-dimensional MEMS scanner for dual-axes confocal microscopy," *J. Microelectromech. Syst.*, vol. 16, no. 4, pp. 969–976, 2007.
- [143] K. H. Koh, T. Kobayashi, and C. Lee, "A 2-D MEMS scanning mirror based on dynamic mixed mode excitation of a piezoelectric PZT thin film s-shaped actuator," *Opt. Express*, vol. 19, no. 15, pp. 13812–13824, 2011.
- [144] J. M. Zara and S. W. Smith, "Optical scanner using a MEMS actuator," *Sensors Actuators A*, vol. 102, no. 1, pp. 176–184, 2002.
- [145] D. Isarakorn, A. Sambri, P. Janphuang, D. Briand, S. Gariglio, J. M. Triscone, F. Guy, J. W. Reiner, C. H. Ahn, and N. F. de Rooij, "Epitaxial piezoelectric MEMS on silicon," *J. Micromech. Microeng.*, vol. 20, no. 5, p. 055008, 2010.
- [146] K. H. Koh, T. Kobayashi, J. Xie, A. Yu, and C. Lee, "Novel piezoelectric actuation mechanism for a gimbal-less mirror in 2D raster scanning applications," *J. Micromech. Microeng.*, vol. 21, no. 7, p. 075001, 2011.
- [147] C. Gosselin, E. St.Pierre, M. Gagne, "On the development of the Agile Eye", *IEEE Robotics Automation Magazine*, V.3(4), pp.29-37, 1996.
- [148] Clément Gosselin and François Caron, 'Two degree-of-freedom spherical orienting device', US.patent US005966991A, oct. 1999.
- [149] <http://robot.gmc.ulaval.ca/en/research/theme103.html>

- [150] R. Wood, S. Avadhanula, M. Menon, M., R. Fearing, 'Microrobotics using composite materials: the micromechanical flying insect thorax', IEEE International Conference on Robotics and Automation, vol. 2, pp. 1842–1849, 2003.
- [151] R. Wood, S. Avadhanula, R. Sahai, E. Steltz, R.S. Fearing, 'Microrobot design using fiber reinforced composites', Journal of Mechanical Design 130(5), 052,304+ 2008.
- [152] I. Kanno, H. Kotera, K. Wasa, "Measurement of transverse piezoelectric properties of PZT thin films", Sensors and Actuators A: Physical, 107(1), pp. 68-74.
- [153] Z. Wang, J. Miao, C. Tan and T. Xu, "Fabrication of piezoelectric MEMS devices-from thin film to bulk PZT wafer", Journal of Electroceramics, Springer US, 24, pp. 25-32, 2010.
- [154] X. Xu, B. Q. Li, Y. Feng, J.R. Chu, "Design, fabrication and characterization of a bulk-PZT-actuated MEMS deformable mirror", Journal of Micromechanics and Microengineering, 17(12), pp. 2439, 2007.
- [155] Z. Wang, J. Miao, C.W. Tan, "Acoustic transducers with a perforated damping back-plate based on PZT/silicon wafer bonding technique", Sensors and Actuators A: Physical, 149, pp. 277-283, 2009.
- [156] Bharti, M. Frecker, "Compliant mechanical amplifier design using multiple optimally placed actuators", Proceedings of IMECEŠ03 ASME International Mechanical Engineering Congress and Exposition, IMECE, 42658, 139-146, 2003.
- [157] S. Bharti, M. Frecker, "Optimal design and experimental characterization of a compliant mechanism piezoelectric actuator for inertially stabilized rifle", Journal of intelligent material systems and structures, vol.15(2), 93-106, 2004.
- [158] R. E. Moore, 'Interval Analysis', Prentice-Hall, Englewood Cliffs N. J., 1966.
- [159] R. Rao, A. Asaithambi, S.K Agrawal, 'Inverse kinematics solution of robot manipulators using interval analysis', Journal of Mechanical Design, Vol. 120, No. 1, pp.147–150, 1998.
- [160] C. Carreras, I.D. Walker, "Interval methods for fault-tree analysis in robotics", Transaction on Reliability, Vol.50, No. 1, pp.3–11, 2001.
- [161] J.P. Merlet, "Solving the forward kinematics of a Gough-type parallel manipulator with interval analysis", International Journal of Robotics Research, Vol.23, No.3, pp.221–236, 2004.
- [162] H. Fang, J.P. Merlet, "Dynamic interference avoidance of 2-dof robot arms using interval analysis", International Conference on Intelligent Robots and Systems (IROS), Alberta, 2005.
- [163] J.P. Merlet, "Interval Analysis and Robotics", in "Principles and Practice of Constraint Programming", Editor, Frédéric Benhamou, Springer, ISBN: 978-3-540-46267-5, 2006.

- [164] Jean-Pierre Merlet, "Interval analysis and reliability in robotics", *Int. J. Reliability and Safety*, Vol. 3, Nos. 1/2/3, 2009.
- [165] J.-P. Merlet, "Interval analysis and robotics," in *Robotics Research*, Springer Tracts in Advanced Robotics, M. Kaneko and Y. Nakamura, Eds. Springer Berlin Heidelberg, vol.66, pp. 147–156, 2011.
- [166] M. Pac and D. Popa, "Interval analysis for robot precision evaluation," in *IEEE International Conference on Robotics and Automation (ICRA) 2012*. IEEE, 2012, pp. 1087–1092.
- [167] M. Pac and D. Popa, "Interval analysis of kinematic errors in serial manipulators using product of exponentials formula," *IEEE Transactions on Automation Science and Engineering*, vol. 10, no. 3, pp. 525–535, 2013.
- [168] M.-H. Masson and T. Denoeux. Clustering Interval-valued Data using Belief Functions. *Pattern Recognition Letters*, Vol. 25, Issue 2, Pages 163-171, 2004.
- [169] G. Nassreddine, F. Abdallah and T. Denoeux. State estimation using interval analysis and belief function theory: Application to dynamic vehicle localization. *IEEE Transactions on Systems, Man and Cybernetics B*, vol. 40, Issue 5, pages 1205-1218, 2010.
- [170] Christophe Combastel, Rihab El Houda Thabet, Tarek Raissi, Ali Zolghadri, David Gucik, "Set-membership fault detection under noisy environment in aircraft control surface servo-loops", *IFAC World Congress*, August 2014.
- [171] L. Jaulin and E. Walter, "Set-inversion via interval analysis for nonlinear bounded-error estimation", *Automatica*, 29(4) :1053–1064, 1993.
- [172] L. Jaulin, M. Kieffer, O. Didrit and E. Walter, "Applied interval analysis", Springer-Verlag, 2001.
- [173] S. Devasia, E. E. Eleftheriou, R. Moheimani, "A survey of control issues in nanopositioning", *IEEE Transactions on Control Systems Technology*, Vol.15, N^o5, pp.802-823, 2007.
- [174] R. C. Barrett and C. F. Quate, "Optical scan-correction system applied to atomic force microscopy," *Rev. Sci. Instrum.*, vol. 62, no. 6, pp. 1393–1399, Jun. 1991.
- [175] A. Sebastian and S. M. Salapaka, "Design methodologies for robust nano-positioning," *IEEE Trans. Control Syst. Technol.*, vol. 13, no. 6, pp. 868–876, Nov. 2005.
- [176] A. J. Fleming, "Nanopositioning system with force feedback for high-performance tracking and vibration control," *IEEE/ASME Transactions on Mechatronics*, vol. 15, no. 3, pp. 433–447, June 2010.
- [177] S. Salapaka, A. Sebastian, J. P. Cleveland, and M. V. Salapaka, 'High bandwidth nano-positioner: A robust control approach', *Review of Scientific Instruments*, vol. 73, no. 9, pp. 3232–3241, 2002.

- [178] G. Schitter, A. Stemmer, and F. Allgower, 'Robust 2 DOF-control of a piezoelectric tube scanner for high speed atomic force microscopy', in Proc. American Control Conf the 2003, vol. 5, pp. 3720–3725, 2003
- [179] M. Ratnam, B. Bhikkaji, A. J. Fleming and S. O. R. Moheimani, "PPF Control of a Piezoelectric Tube Scanner", IEEE Conference on Decision and Control, and the European Control Conference, Seville, Spain, December 2005.
- [180] I. A. Mahmood and S. O. R. Moheimani, "Making a commercial atomic force microscope more accurate and faster using positive position feedback control," Rev. of Sci. Instrum., vol. 80, no. 6, pp. 063 705(1), 2009.
- [181] A. J. Fleming, S. S. Aphale, and S. O. R. Moheimani, "A new method for robust damping and tracking control of scanning probe microscope positioning stages," IEEE Trans. on Nanotechnology, vol. 9, no. 4, pp.438–448, 2010.
- [182] S. K. Das, H. R. Pota, and I. R. Petersen, "Resonant controller for fast atomic force microscopy," in Proc. Conference on Decision and Control, Maui, Hawaii, USA, Dec 2012, pp. 2471–2476.
- [183] H. Pota, S. Reza Moheimani, and M. Smith, "Resonant controller for smart structures," Smart Materials and Structures, vol. 11, pp. 1–8, 2002.
- [184] Sajal K. Das, Hemanshu R. Pota and Ian R. Petersen, "Resonant Controller Design for a Piezoelectric Tube Scanner: A Mixed Negative-Imaginary and Small-Gain Approach", IEEE Transactions on Control Systems Technology, 10.1109/TCST.2013.2297375, 2014.
- [185] S. K. Das, H. R. Pota, I. R. Petersen, "Damping Controller Design for Nanopositioners: A Mixed Passivity, Negative-Imaginary and Small-Gain Approach", IEEE/ASME Transactions on Mechatronics, 2014.
- [186] Ugur Aridogan, Yingfeng Shan, Kam K. Leang, "Design and Analysis of Discrete-Time Repetitive Control for Scanning Probe Microscopes", ASME Journal of Dynamic Systems, Measurement, and Control, Vol. 131, 2009.
- [187] Yingfeng Shan, Kam K. Leang, "Accounting for hysteresis in repetitive control design: Nanopositioning example", Automatica 48, pp. 1751–1758, 2012.
- [188] G. Schitter, P. Menold, H. F. Knapp, F. Allgower, and A. Stemmer, "High performance feedback for fast scanning atomic force microscopes," Rev. Scientific Instrum., vol. 72, no. 8, pp. 3320–3327, 2001.
- [189] S. Salapaka, A. Sebastian, J. P. Cleveland, and M. V. Salapaka, "High bandwidth nano-positioner: A robust control approach," Rev. Scientific Instrum., vol. 73, no. 9, pp. 3232–3241, Sep. 2002.
- [190] A. Sebastian and S. M. Salapaka, "Design methodologies for robust nano-positioning," IEEE Trans. Control Syst. Technol., vol. 13, no. 6, pp. 868–876, Nov. 2005.

- [191] N. Tamer and M. Dahleh, "Feedback control of piezoelectric tube scanners," in Proc. 33rd IEEE Conf. Dec. Control, pp. 1826–1831, 1994.
- [192] S. Devasia, "Should model-based inverse inputs be used as feedforward under plant uncertainty?," IEEE Trans. Autom. Control, vol. 47, no. 11, pp. 1865–1871, Nov. 2002.
- [193] Y. Okazaki, "A micro-positioning tool post using a piezoelectric actuator for diamond turning machines", Precision Engineering, Volume 12, Issue 3, Pages 151–156, July 1990.
- [194] C. J. Li, H. S. M. Beigi, S. Li, and J. Liang, "Nonlinear piezo-actuator control by learning self tuning regulator," J. Dyn. Syst., Meas. Control, vol. 115, pp. 720–723, Dec. 1993.
- [195] Y. Li and Q. Xu, "Design and Robust Repetitive Control of a New Parallel-Kinematic XY Piezostage for Micro/Nanomanipulation," IEEE/ASME Transactions on Mechatronics, vol. 17, no. 6, pp. 1120–1132, 2012.
- [196] Y. Li and Q. Xu, "Adaptive sliding mode control with perturbation estimation and PID sliding surface for motion tracking of a piezo-driven micromanipulator," IEEE Transactions on Control Systems Technology, vol. 18, no. 4, pp. 798–810, 2010.
- [197] Q. Xu and Y. Li, "Model Predictive Discrete-Time Sliding Mode Control of a Nanopositioning Piezostage Without Modeling Hysteresis," IEEE Transactions on Control Systems Technology, vol. 20, no. 4, pp. 983–994, 2012.
- [198] Q. Xu, "Precision Position/Force Interaction Control of a Piezoelectric Multimorph Microgripper for Microassembly," IEEE Transactions on Automation Science and Engineering, vol. 10, no. 3, pp. 503–514, 2013, (SCI/EI).
- [199] Kemin Zhou, John C. Doyle and Keith Glover, "Robust and Optimal Control", Prentice Hall, ISBN-13: 978-0134565675, 1995.
- [200] K. Glover and J. C. Doyle, 'State-space formulae for all stabilizing controllers that satisfy an H_∞ -norm bound and relations to risk sensitivity', Systems Control Letters, vol.11, pp.167-172, 1988.
- [201] J. C. Doyle, K. Glover, P. K. Khargonekar and B. A. Francis, 'State-space solutions to standard H_2 and H_∞ control problems', IEEE Transactions on Automatic Control, AC 34 NA8, pp.831-846, 1989.
- [202] S. D. Eppinger and W. P. Seering, 'On dynamic models of robot force control', International Conference on Robotics and Automation, IEEE ICRA, April 1986.
- [203] J. Agnus, P. De Lit and N. Chaillet, «Micromanipulateur piézoélectrique notamment pour microrobotique», French Patent, FR0211934, 2002.
- [204] P. Apkarian and D. Noll, "Nonsmooth H_∞ synthesis", IEEE Transactions on Automatic Control, 51(1) :71–86, 2006

- [205] L. Jaulin, "Interval constraint propagation with application to bounded error estimation", *Automatica*, 36 :1547–1552, 2000.
- [206] I. Braems, N. Ramdani, M. Kieffer, L. Jaulin, E. Walter, and Y. Candau, "Guaranteed characterization of thermal conductivity and diffusivity in presence of model uncertainty," *Inverse Problems in Science and Engineering*, 15(8) :895–910, 2007.
- [207] Tarek Raïssi, Nacim Ramdani, Yves Candau, "Bounded error moving horizon state estimator for non-linear continuous-time systems: application to a bioprocess system", *Journal of Process control*, vol.15(5), 2005.
- [208] Nacim Ramdani, Nacim Meslem, Tarek Raïssi, Yves Candau, "Set-membership identification of continuous-time systems", *System Identification*, 446-451, 2006.
- [209] A.Eggers, N.Ramdani, N.S.Nedialkov, M.Fränzle, Set-Membership Estimation of Hybrid Systems via SAT Mod ODE. 16th IFAC Symposium on System Identification, pp.440-445, 2012.
- [210] V. L. Kharitonov, "Asymptotic stability of an equilibrium of a family of systems of linear differential equations", *Differential'nye Uravneniya*, Vol.14, pp.2086-2088, 1978.
- [211] V. L. Kharitonov, "The Routh-Hurwitz problem for families of polynomials and quasipolynomials", *Izvetiy Akademii Nauk Kazakhskoi SSR, Seria Fizikomatematicheskaja*, Vol.26, pp.69-79, 1979.
- [212] A.C. Bartlett, C.V. Hollot and L. Huang, "Root locations of an entire polytope of polynomials: it suffices to check the edges", *Mathematics of Control, Signals and Systems*, Vol.1, pp.61-71, 1988.
- [213] L. Wang, Z. Wang, L. Zhang and W. Yu, "Edge theorem for multivariable systems", eprint arXiv:math/0211014, 2002.
- [214] M. Dahleh, A. Tesi and A. Vicino, "On the robust Popov criterion for interval Lur's systems", *IEEE CDC*, December 1992.
- [215] H. Chapellat, M. Dahleh and S. P. Bhattacharyya, "On robust stability of interval control systems", *IEEE Transactions on Automatic Control*, Vol.36(1), pp.59-67, 1991.
- [216] E. Walter and L. Jaulin, "Guaranteed characterization of stability domains via set inversion", *IEEE Transactions on Automatic Control*, Vol.39(4), pp.886-889, 1994.
- [217] L. Wang, " H_∞ performance of interval systems", *arXiv, Optimization and Control*, 2002.
- [218] C. V. Hollot and R. Tempo, "On the Nyquist envelope of an interval plant family", *IEEE Transactions on Automatic Control*, Vol.39(2), pp.391-396, 1994.
- [219] J. Bondia, M. Kieffer, E. Walter, J. Monreal, and J. Pico, "Guaranteed tuning of pid controllers for parametric uncertain systems", *IEEE Conference on Decision and Control*, pages 2948–2953, 2004.

- [220] Y. Smaginaa and I. Brewerb, "Using interval arithmetic for robust state feedback design", *Systems and Control Letters*, 46 :187–194, 2002.
- [221] C.-T. Chen and M.-D. Wang, "A two-degrees-of-freedom design methodology for interval process systems", *Computers and Chemical Engineering*, 23 :1745-751, 2000.
- [222] K. Li and Y. Zhang, "Interval model control of consumable double-electrode gas metal arc welding process", *IEEE - Transactions on Automation Science and Engineering (T-ASE)*, 7(4) :826–839, 2009.
- [223] Sen-Jian An, Lin Huang, Enping Wang, On the parametric H-inf problems of weighted interval plants, *IEEE Transactions on Automatic Control*, Vol.45, 332-335, 2000.
- [224] Sen-Jian An, Xiheng Hu, Branka Vucetic, Wanquan Liu, "Vertex results for parametric shifted H-inf performance of weighted interval plants", *IEEE Conference on Decision and Control*, Vol.5, 4195-4196, 2000.
- [225] Wang, L., "H-inf Performance of Interval Systems", eprint arXiv:math/0211013, Vol.1, 1-8, 2002.
- [226] H. Chapellat and S. P. Bhattacharyya, "A generalization of kharitonov's theorem : robust stability of interval plants", *IEEE Transaction on Automatic Control*, 34(3) :306–311, 1989.
- [227] B. R. Barmish, "A generalization of kharitonov's four polynomial concept for robust stability problems with linearly dependent coefficient perturbations", *IEEE Transaction on Automatic Control*, 34 :157–165, 1989.
- [228] I.R. Petersen, "A new extension to kharitonov's theorem", *IEEE Transaction on Automatic Control*, 35(7) :825–528, 1990.
- [229] F. Garofalo, G. Celentano, and L. Glielmo, "Stability robustness of interval matrices via Lyapunov quadratic forms", *IEEE Transaction on Automatic Control*, 38(2) :281–284, 1993
- [230] Q. Zou and S. Devasia, "Preview-based optimal inversion for output tracking: Application to scanning tunneling microscopy" *IEEE Trans. Control Syst. Technol.*, vol. 12, no. 3, pp. 375–386, May 2004.
- [231] K. K. Leang and S. Devasia, "Feedback-linearized inverse feedforward for creep, hysteresis, and vibration compensation in AFM piezoactuators", *IEEE Trans. Control Syst. Technol.*, vol. 15, no. 5, pp. 927–935, Sep. 2007.
- [232] S. Tien and S. Devasia, "AFM imaging of large soft samples in liquid medium using iterative inverse feedforward control", in *Proc. Amer. Control Conf.*, pp. 3201–3206, 2008.
- [233] Y. Li and J. Bechhoefer, "Feedforward control of a closed-loop piezoelectric translation stage for atomic force microscope" *Rev. Sci. Instrum.*, vol. 78, pp. 1–8, Jan. 2007

- [234] D. Croft and S. Devasia, "Vibration compensation for high speed scanning tunneling microscopy", *Rev. Sci. Instr.*, vol. 70, no. 12, pp. 4600–4605, Dec. 1999.
- [235] J. A. Butterworth, L. Y. Pao, and D. Y. Abramovitch, "Architectures for tracking control in atomic force microscopes", in *Proc. IFAC World Congr.*, 2008, pp. 8236–8250.
- [236] J. A. Butterworth, L. Y. Pao, and D. Y. Abramovitch, "A comparison of control architectures for atomic force microscopes", *Asian J. Control*, vol. 11, no. 2, pp. 175–181, Mar. 2009.
- [237] Jeffrey A. Butterworth, Lucy Y. Pao, and Daniel Y. Abramovitch, "Parameter Combined Feedforward/Feedback Adaptive-Delay Algorithm With Applications to Piezo-Based Raster Tracking", *IEEE Transactions on Control Systems Technology*, Vol.20(2), March 2012.
- [238] D. Croft, S. Stilson, and S. Devasia, "Optimal tracking of piezo-based nano-positioners," *J. Nanotechnol.*, vol. 10, pp. 201–208, Jun. 1999.
- [239] Yingfeng Shan and Kam K. Leang, "Repetitive Control with Prandtl-Ishlinskii Hysteresis Inverse for Piezo-Based Nanopositioning" *American Control Conference*, pp.301-306, June 2009.
- [240] Po-Jen Koa, Yen-Po Wanga, Szu-Chi Tien, "Inverse-feedforward and robust-feedback control for high-speed operation on piezo-stages", *International Journal of Control*, Vol.86(2), 2013.
- [241] Alex Esbrook, Xiaobo Tan and Hassan K. Khalil, "Control of Systems With Hysteresis via Servocompensation and Its Application to Nanopositioning", *IEEE Trans. Control Systems Technology*, Vol.21(3), Mai 2013.
- [242] Y. Cao, S.K. Saskatoon, L. Cheng, X.B. Chen and J.Y. Peng, "An Inversion-Based Model Predictive Control With an Integral-of-Error State Variable for Piezoelectric Actuators" *IEEE/ASME Trans. on Mechatronics*, vol.18(3), 2013.
- [243] Damien De-Benedittis. *Actionneur lin aire magn tostrictif*. DEA, INPG, 1998.
- [244] Peter Cooke, "Robotics, Vision and Control", Springer, ISBN 978-3-642-20144-8, 2011.
- [245] W. Khalil, E. Dombre, "Modeling, identification and control of robots", Butterworth-Heinemann, ISBN-13: 978-1903996669, 2000.
- [246] Joel Agnus, Nicolas Chaillet, "Device for controlling a piezoelectric actuator and scanner controlled by said control device", french patent, PCT/FR2004/000026 2004.
- [247] J. Minase, T. F. Lu, B. Cazzolato, and S. Grainger, "A review, supported by experimental results, of voltage, charge and capacitor insertion method for driving piezoelectric actuators", *Precision Engineering*, vol. 34, no. 4, pp. 692–700, 2010.

- [248] L. Huang, Y. T. Ma, Z. H. Feng, and F. R. Kong, "Switched capacitor charge pump reduces hysteresis of piezoelectric actuators over a large frequency range", *Review of Scientific Instruments*, vol. 81, no. 9, Article ID 094701, 2010
- [249] Y. T. Ma, L. Huang, Y. B. Liu, and Z. H. Feng, "Note: creep character of piezoelectric actuator under switched capacitor charge pump control", *Review of Scientific Instruments*, vol. 82, no. 4, Article ID 046106, 2011.
- [250] Andrew J. Fleming, "Charge drive with active DC stabilization for linearization of piezoelectric hysteresis", *IEEE Transactions on Ultrasonics, Ferroelectrics, and Frequency Control*, Vol.60(8), 2013.
- [251] H. Jung, J.Y. Shim and D. Gweon, "New open-loop actuating method of piezoelectric actuators for removing hysteresis and creep", *Review of Scientific Instruments*, 71 (9), pp.3436-3440, 2000.
- [252] Xueliang Zhao, Chengjin Zhang, Hongbo Liu Guilin Zhang and Kang Li, "Analysis of Hysteresis-Free Creep of the Stack Piezoelectric Actuator", *Mathematical Problems in Engineering*, Volume 2013, ID-187262, 2013.
- [253] H. Jung, J. Y. Shim, and D. Gweon, "Tracking control of piezoelectric actuators", *Nanotechnology*, vol. 12, no. 1, pp. 14–20, 2001.
- [254] S. Vieira, "the behavior and calibration of some piezoelectric ceramics used in the STM", *IBM Journal of Research and Development*, vol. 30, no. 5, pp. 553–556, 1986
- [255] O. M. El-Rifai, K Youcef-Toumi, "Creep in piezoelectric scanners of atomic force microscopes", *American Control Conference*, pp.3777-3782, 2002.
- [256] B. Mokaberi and A. A. G. Requicha, "Compensation of scanner creep and hysteresis for AFM nanomanipulation", *IEEE Transactions on Automation Science and Engineering*, Vol.5, N^o2, pp.197-208, 2008.
- [257] D. Croft, G. Shed and S. Devasia, "Creep, hysteresis and vibration compensation for piezoactuators: atomic force microscopy application", *ASME Journal of Dynamic Systems, Measurement and Control*, 2001.
- [258] D. Croft, G. Shedd, and S. Devasia, "Creep, hysteresis, and vibration compensation for piezoactuators: atomic force microscopy application," in *Proceedings of the American Control Conference*, vol. 3, pp. 2123–2128, June 2000.
- [259] Yanfang Liu, Jinjun Shan, Ulrich Gabbert and Naiming Qi, "Hysteresis and creep modeling and compensation for a piezoelectric actuator using a fractional-order Maxwell resistive capacitor approach" *Smart Mater. Struct.* 22, 2013.
- [260] K. Kuhnen and H. Janocha, "Compensation of the creep and hysteresis effects of piezoelectric actuators with inverse systems", *Actuator*, pp.309-312, Bremen 1998.

- [261] H. Janocha and K. Kuhnen, "Real-time compensation of hysteresis and creep in piezo-electric actuators", *Sensors and Actuators A*, vol. 79, no. 2, pp. 83–89, 2000.
- [262] K. Kuhnen, "Modelling, identification, and compensation of complex hysteretic and log(t)-type creep nonlinearities", *Control and Intelligent Systems*, vol. 33, no. 2, pp. 134–147, 2005.
- [263] K. Kuhnen and P. Krejci, "Compensation of complex hysteresis and creep effects in piezoelectrically actuated systems a new Preisach modeling approach", *IEEE Transactions on Automatic Control*, vol. 54, no. 3, pp. 537–550, 2009.
- [264] T. Fett and G. Thun, "Determination of room-temperature tensile creep of PZT," *Journal of Materials Science Letters*, vol. 17, no. 22, pp. 1929–1931, 1998.
- [265] O. Guillon, F. Thiébaud, P. Delobelle, and D. Perreux, "Compressive creep of PZT ceramics: experiments and modelling", *Journal of the European Ceramic Society*, vol. 24, no. 9, pp. 2547–2552, 2004.
- [266] E. M. Bourim, H. Y. Kim, J. S. Yang et al., "Creep behavior of undoped and La-Nb codoped PZT based micro-piezoactuators for micro-optical modulator applications", *Sensors and Actuators A*, vol. 155, no. 2, pp. 290–298, 2009.
- [267] Eliakim Hastings Moore, "On the reciprocal of the general algebraic matrix", *Bull. AMS*, vol. 26,? 1920, p. 394-395
- [268] Saeid Bashash and Nader Jalili, "A Polynomial-Based Linear Mapping Strategy for Feedforward Compensation of Hysteresis in Piezoelectric Actuators", *ASME Journal of Dynamic Systems, Measurement and Control*, Vol.130(3), 10 pages, DOI.10.1115/1.2907372, May 2008.
- [269] Adrien Badel, Jinhao Qiu, and Tetsuaki Nakano, "A New Simple Asymmetric Hysteresis Operator and its Application to Inverse Control of Piezoelectric Actuators" *IEEE Trans Ultrason Ferroelectr Freq Control*, 55(5):1086-94, 2008.
- [270] K. Kyle Eddy, "Actuator bias prediction using lookup-table hysteresis modeling", *US Patent-08/846545*, February 1999.
- [271] Xiangjiang Wang, Gursel Alici and Xiaobo Tan, "Modeling and inverse feedforward control for conducting polymer actuators with hysteresis", *Smart Mater. Struct.*, doi:10.1088/0964-1726/23/2/025015, 2014.
- [272] F. Preisach, "Uber die magnetische Nachwirkung", *Zeitschrift fur Physik*, 94:277-302, 1935
- [273] Samir Mittal and Chia-Hsiang Menq, "Hysteresis Compensation in Electromagnetic Actuators Through Preisach Model Inversion", *IEEE/ASME Trans. on Mechatronics*, vol.5(4), december 2000.

- [274] C. Natale, F. Velardi, C. Visone, "Identification and compensation of Preisach hysteresis models for magnetostrictive actuators", *Physica B* 306, 161–165, 2001.
- [275] Martin Kozek, Bernhard Gross, "Identification and Inversion of Magnetic Hysteresis for Sinusoidal Magnetization" In *ternational Journal on Online Engineering*, 2005.
- [276] Zhi Li, Sining Liu, Chun-Yi Su, "A Novel Analytical Inverse Compensation Approach for Preisach Model", *Springer ICIRA Conference*, Volume 8103, pp 656-665, 2013.
- [277] Miklos Kuczmann, 'Vector Preisach hysteresis modeling: Measurement, identification and application', *Elsevier Physica B: Condensed Matter*, Vol.406(8), pages 1403-1409, 2011.
- [278] Miklos Kuczmann, Laurentiu Stoleriu, 'Anisotropic Vector Preisach Model', *Journal of Advanced Research in Physics*, Vol.1(1), 011009, 2010.
- [279] Declan Hughes and John T Wen, "Preisach modeling of piezoceramic and shape memory alloy hysteresis", *Smart Materials and Structures*, Issue 3, June 1997.
- [280] Robert Benjamin Gorbet, "Control of Hysteretic Systems with Preisach Representations", PhD thesis, University of Waterloo, 1997.
- [281] Yu-Feng Wang, Chun-Yi Su, H. Hong, Yue-ming Hu, "Modeling and Compensation for Hysteresis of Shape Memory Alloy Actuators with the Preisach Representation" *IEEE International Conference on Control and Automation*, 2007.
- [282] Bao Kha Nguyen, Kyoung Kwan Ahn, "Feedforward Control of Shape Memory Alloy Actuators Using Fuzzy-Based Inverse Preisach Model" *IEEE Transactions on Control Systems Technology*, Volume:17(2), 2009.
- [283] Jun Zhang, Emmanuelle Merced, Nelson Sepulveda and Xiaobo Tan, "Modeling and Inverse Compensation of Nonmonotonic Hysteresis in VO₂-Coated Microactuators", *IEEE/ASME Trans. on Mechatronics*, DOI.10.1109/TMECH.2013.2250989, 2013
- [284] G. Song, J. Q. Zhao, and X. Q. Zhou, "Tracking control of a piezoceramic actuator with hysteresis compensation using inverse Preisach model", *IEEE/ASME Transactions on Mechatronics*, 10(2):198 – 209, 2005
- [285] F. Weibel, Y. Michellod, P. Mullhaupt and D. Gillet, "Real-time compensation of hysteresis in a piezoelectric-stack actuator tracking a stochastic reference" *American Control Conference*, pp.2939-2944, Seattle WA, 2008.
- [286] K.K. Leang, Q. Zou and S. Devasia, "Feedforward Control of Piezoactuators in Atomic Force Microscope Systems", *IEEE Control Systems Magazine*, pp.70-82, february 2009.
- [287] Tan Kok Kiong, Huang Sunan, "Modeling and Control of Precision Actuators", *CRC Press*, ISBN-9781466556447, 2013.
- [288] K. Kuhnen and H. Janocha, "Inverse feedforwad controller for complex hysteretic nonlinearities in smart-materials systems", *Control of Intelligent System*, Vol.29, N o 3, 2001.

- [289] M. Al Janaideh, "about the output of the inverse compensation of the Prandtl-Ishlinskii model," ACC, pp. 247-252, Washington, DC, 2013.
- [290] Klaus Kuhnen, "Modeling, Identification and Compensation of Complex Hysteretic Non-linearities: A modified Prandtl-Ishlinskii Approach", European Journal of Control, Vol.9, No.4, pp. 407-418, 2003.
- [291] Mohammad Al Janaideh, Subhash Rakheja, Chun-Yi Su, "An analytical generalized Prandtl-Ishlinskii model inversion for hysteresis compensation in micropositioning control", IEEE/ASME Transactions on Mechatronics, vol.6(4), 2011.
- [292] U-Xuan Tan, Win Tun Latt, Cheng Yap Shee, Cameron N. Riviere and Wei Tech Ang, "Feedforward Controller of Ill-Conditioned Hysteresis using Singularity Free Prandtl-Ishlinskii", IEEE/ASME Trans. on Mechatronics, Vol.14(5), 2009.
- [293] Mohammad Al Janaideh, Pavel Krejci, "An inversion formula for a Prandtl-Ishlinskii operator with time dependent thresholds", Physica B: Condensed Matter, vol.496(8), 2011
- [294] Mohammad Al Janaideh, P Krejci, "Inverse Rate-Dependent Prandtl-Ishlinskii Model for Feedforward Compensation of Hysteresis in a Piezomicropositioning Actuator", IEEE/ASME Transactions on Mechatronics, vol.5(18), 2013.
- [295] Wei Tech Ang, Pradeep K. Khosla and Cameron N. Riviere, "Feedforward Controller With Inverse Rate-Dependent Model for Piezoelectric Actuators in Trajectory-Tracking Applications", IEEE/ASME Trans. on Mechatronics, Vol.12(2); 2007.
- [296] Omar Farhan Aljanaideh, "Modeling and Compensation of Rate-Dependent Asymmetric Hysteresis Nonlinearities of Magnetostrictive Actuators" PhD thesis, Concordia University, Montreal Quebec Canada, december 2013.
- [297] G.Y. Gu, M.J. Yang MJ, L.M. Zhu, "Real-time inverse hysteresis compensation of piezoelectric actuators with a modified Prandtl-Ishlinskii model", Rev Sci Instrum., 83(6):065106. doi: 10.1063/1.4728575, 2012.
- [298] Cao Lingzhi, Chai Yuyang, "Based on PI (Prandtl-Ishlinskii) Modeling Hysteresis in PiezoelectricActuator and FeedForward Control Compensation", International Conference on Materials, Mechatronics and Automation, 2012.
- [299] Yingfeng Shan, Kam K. Leang, "Dual-stage repetitive control with Prandtl-Ishlinskii hysteresis inversion for piezo-based nanopositioning", Mechatronics, 22, pp.271-281, 2012.
- [300] Yuansheng Chen, Jinhao Qiu, Jose Palacios, Edward C Smith, "Tracking control of piezoelectric stack actuator using modified Prandtl-Ishlinskii model", Journal of Intelligent Material Systems and Structures, vol.24(6), 7pp.53-760, 2013.
- [301] Dong Luo, Si Hai Chen, Wei Chen, Guo Hua Jiao, Yuan Fu Lu, "Inverse Hysteresis Compensation of One-Dimensional Piezoelectric Scanner with Generalized Prandtl-Ishlinskii Model", Advanced Materials Research, D.O.I.10.4028/www.scientific.net/AMR.945-949.1956, June 2014.

- [302] T. Matsuo and M. Shimasaki, 'Generalization of an isotropic vector hysteresis model represented by the superposition of stop models-Identification and rotational hysteresis loss,' IEEE Transactions on Magnetics, Vol.43, pages 1389-1392, April 2007.
- [303] J. V. Leite, N. Sadowski, P. Kuo-Peng, and J. P. A. Bastos, 'A new anisotropic vector hysteresis model based on stop hysterons,' IEEE Transactions on Magnetics, vol.41, pages 1500-1503, May 2005.
- [304] Zhi Li, Chun-Yi Su and Tianyou Chai, "Compensation of Hysteresis Nonlinearity in Magnetostrictive Actuators With Inverse Multiplicative Structure for Preisach Model", IEEE Transactions on Automation Science and Engineering, vol.11(2), pp.613-619, 2014.
- [305] R. Bouc, "Forced vibration of mechanical systems with hysteresis", Conference on Non-linear Oscillation, Prague, 1967.
- [306] Y. K. Wen, "Method for random vibration of hysteresis systems", Journal of the Engineering Mechanics Division, Vol. 102(2), pp.249-263, March/April 1976.
- [307] Y. Tang. Numerical evaluation of uniform beam modes. Journal of Engineering Mechanics, 129(12) :1475–1477, 2003.
- [308] W. Soedel. Vibrations of shells and plates. 2nd ed. Marcel Dekker, New York, 1993.
- [309] T. S. Low and W. Guo, "Modeling of a three-layer piezoelectric bimorph beam with hysteresis", Journal Microelectromechanical Systems, Vo.4(4), pp.230-237, December 1995.
- [310] M. Jouaneh and H. Tian, "Accuracy enhancement of a piezoelectric actuators with hysteresis", ASME Japan/USA Symp. Flexible Automation, pp.631-637, 1992.
- [311] C. W. Wong, Y. Q. Ni and J. M. Ko, "Steady state oscillation of hysteretic differential model. I - response analysis, II - performance analysis", Journal Engineering Mechanics, 120, 1994.
- [312] Tuma, Tomas and Lygeros, John and Sebastian, Abu and Pantazi, Angeliki, "Optimal scan trajectories for high-speed scanning probe microscopy", American Control Conference, pages 3791-3796, Montréal Canada, June 2012.
- [313] Song, Junho and Der Kiureghian, Armen," Generalized Bouc–Wen model for highly asymmetric hysteresis", Journal of engineering mechanics, pp. 610–618, 2006
- [314] Garrett M. Clayton, Szuchi Tien, Kam K. Leang, Qingze Zou and Santosh Devasia, "A Review of Feedforward Control Approaches in Nanopositioning for High-Speed SPM" J. Dyn. Sys., Meas., Control 131(6), 061101, Oct 2009.
- [315] S. Devasia, "Should model-based inverse input be used as feedforward under plant uncertainty?", IEEE Trans. Automat. Contr., vol. 47, no. 11, p.1865–1871, Nov. 2002.
- [316] Qingze Zou, Member and Santosh Devasia, "Preview-Based Optimal Inversion for Output Tracking: Application to Scanning Tunneling Microscopy", IEEE Transactions on Control Systems Technology, Vol.12(3), 2004.

- [317] Smith, O.J.M., "Feedback Control Systems", New York, McGraw-Hill Book Company, Inc., p.331-345, 1958.
- [318] Singer, N.C. and W.P. Seering, "Preshaping Command Inputs to Reduce System Vibration," ASME Journal of Dynamic Systems, Measurement, and Control, Vol. 112, p.76-82, 1990.
- [319] N. C. Singer, W. P. Seering and K. A. Pasch, "Shaping command inputs to minimize unwanted dynamics", Patent N o US-4.916.635, 1990.
- [320] Z. Lu, P. C. Y. Chen, and W. Lin, "Force sensing and control in micromanipulation", IEEE transactions on systems, man and cybernetics. Part C, Applications and reviews., vol. 36, pp. 713-724, 2006.
- [321] M. Boudaoud, S. Régnier, "An Overview on Gripping Force Measurement at the Micro and Nano-scales Using Two-fingered Microrobotic Systems", International Journal of Advanced Robotic Systems, 11:45, doi: 10.5772/57571, 2014.
- [322] F. Arai, A. Kawaji, T. Sugiyama, Y. Onomura, M. Ogawa, T. Fukuda, H. Iwata, and K. Itoigawa, "3d micromanipulation system under microscope", IEEE International Symposium on Micromechatronics and Human Science, 1998.
- [323] M. Goldfarb and N. Celanovic, "A flexure-based gripper for small-scale manipulation", Robotica, 17, 1999.
- [324] Stephan Fahlbusch, Aleksandr Shirinov, and Sergej Fatikow, "Afm-based microforce sensor and haptic interface for a nanohandling robot", IROS, EPFL, Lausanne, Switzerland, October 2002.
- [325] A. Menciassi, A. Eisinger, M. C. Carrozza, and P. Dario, "Force sensing microinstrument for measuring tissue properties and pulse in microsurgery", Mechatronics, IEEE/ASME Transactions on, 8, 2003.
- [326] F. Berkelman, L. L. Whitcomb, R. H. Taylor, and P. Jensen, "A miniature microsurgical instrument tip force sensor for enhanced force feedback during robot-assisted manipulation", IEEE Transactions on Robotics and Automation, 19, 2003.
- [327] Mokrane Boudaoud, Yassine Haddab, Yann Le Gorrec, "Modeling and optimal force control of a nonlinear electrostatic microgripper", IEEE/ASME Transactions on Mechatronics, vol.18(3), pp.1130-1139, 2013.
- [328] The Femtotools company, www.femtotools.com/.
- [329] J. Agnus, D. Hériban, M. Gauthier and V. Pétrini, "Silicon end-effectors for microgripping tasks", Precision Engineering 33, 4 (2009) 542-548.
- [330] M. A. Greminger, and B. J. Nelson, "Vision-based force measurement", IEEE Transactions on Pattern Analysis and Machine Intelligence., vol.26, pp. 290-298, 2004.

- [331] Yasser H. Anis, James K. Mills, and William L. Cleghorn, "Visual measurement of mems microassembly forces using template matching". ICRA, pages 275-280, Orlando, FL, May 2006.
- [332] G. Besançon, A. Voda, and M. Alma, "On observer-based estimation enhancement by parametric amplification in a weak force measurement device", In 47th IEEE Conf. Decision and Control, Cancun, Mexico, 2008.
- [333] G. Besançon, A. Voda, and G. Jourdan, "Kalman observer approach towards force reconstruction from experimental afm measurements", In 15th IFAC Symposium on System Identification, St Malo, France, 2009.
- [334] G. Besançon, A. Voda, and G. Jourdan, "Micro, nanosystems systems on chips - Modeling, control and estimation", chapter "Observer-based estimation of weak forces in a nanosystem measurement device", J. Wiley Sons, 2010.
- [335] G. Besançon, A. Voda-Besançon, "Observer Approach for Parameter and Force Estimation in Scanning Probe Microscopy", a chapter in "Signal measurement and estimation techniques issues in the micro/nano world", edited book by C. Clévy, M. Rakotondrabe, N. Chaillet, Springer - Verlag, New York, ISBN 978-1-4419-9945-0, August 2011.
- [336] K. S. Karvinen, M. Ruppert, K. Mahata, S. O. R. Moheimani, "Direct Tip-Sample Force Estimation for High-Speed Dynamic Mode Atomic Force Microscopy", IEEE Transactions on Nanotechnology 2015.
- [337] M. Napoli, B. Bamieh, and K. Turner, "Mathematical modeling, experimental validation and observer design for a capacitively actuated micro-cantilever", In American Control Conf., Denver, Colorado, USA, 2003.
- [338] C-S. Liu and H. Peng, "Inverse-dynamics based state and disturbance observers for linear time-invariant systems", ASME Journal of Dynamics Systems, Measurement and Control, vol.124, pp.375-381, September 2002.
- [339] J.J. Dosch, D.J. Inman and E. Garcia, "A Self-Sensing Piezoelectric Actuator for Collocated Control", Journal of Intell. Mater. Syst. and Struct., vol 3, pp. 166-185, 1992.
- [340] T. Takigami, K. Oshima, Y. Hayakawa and M. Ito, "Application of self-sensing actuator to control of a soft-handling gripper", Proc. to IEEE ICCA, pp. 902-906, Italy, 1998.
- [341] W.W. Law, W-H. Liao and J. Huang, "Vibration control of structures with self-sensing piezoelectric actuators incorporating adaptive mechanisms", Smart Mater. Struct 12, pp. 720-730, 2003.
- [342] Y. Cui, "Self-Sensing Compounding Control of Piezoceramic MicroMotion Worktable Based on Integrator", Proc. to 6th World Congress on Intell. Cont. and Autom., China, 2006.

- [343] C. K. Pang, G. Guo, B. M. Chen, T. H. Lee, " Self-sensing actuation for nan positioning and active-mode damping in dual-stage HDDs", IEEE/ASME Trans. on Mechatronics, vol. 11, no. 3, pp. 328-338, 2006.
- [344] S. O. R. Moheimani and Y. K. Yong, " Simultaneous sensing and actuation with a piezoelectric tube scanner", Rev. Sci. Instr. 79, 073702, 2008.
- [345] S. O. R. Moheimani, " Invited Review Article: Accurate and fast nan positioning with piezoelectric tube scanners: Emerging trends and future challenges", Rev. Sci. Instr. 79, 071101, 2008.
- [346] A. S. Putra, H. Sunan, T. K. Kok, S.K. Panda and T. H. Lee, "Self-sensing actuation with adaptive control in applications with switching trajectory, IEEE/ASME Trans. on Mechatronics, Vol.13(1), pp.104-110, 2008.
- [347] Jina Kim, Benjamin L. Grisso, Jeong K. Kim, Dong Sam Ha, and Daniel J. Inman, "Electrical Modeling of Piezoelectric Ceramics for Analysis and Evaluation of Sensory Systems", IEEE Sensors Applications Symposium, 2008.
- [348] A. Hammerstein, "Nichtlineare Integralgleichungen nebst Anwendungen", Acta Math, 54, pp.117-176, 1930.
- [349] N. Wiener, "Nonlinear Problems in Random Theory", New York: Wiley, 1958.
- [350] <http://www.labex-action.fr/>
- [351] Tian-Bing Xu et al, U.S. patent Publication/application, 20100096949 (Published on 4/22/2010).
- [352] Shashank Priya, Daniel J. Inman, "Energy Harvesting Technologies", Springer Verlag, ISBN: 978-0-387-76463-4, 2009.
- [353] A. Khaligh, Peng Zeng, Cong Zheng, "Kinetic Energy Harvesting Using Piezoelectric and Electromagnetic Technologies—State of the Art", IEEE Transactions on Industrial Electronics, 57(3), 850-860, 2010.
- [354] L. D'Orazio et al., Design, Automation Test in Europe Conference Exhibition (DATE), 2011
- [355] <http://www.iba-industrial.com>
- [356] <http://wardsauto.com>
- [357] C. Swedberg, "TekVet-IBM Cattle Tracker Uses Active RFID Tags", Satellite Communication, 2012.
- [358] <http://www.tekvet.com/>

- [359] Baptiste Véron, Joël Abadie, Arnaud Hubert, Nicolas Andreff, "Magnetic manipulation with several mobile coils towards gastrointestinal capsular endoscopy", *New Trends in Mechanism and Machine Science*, 681-689, 2013.
- [360] Lao-Tseu (Laozi), 'Tao Te Ching' (The way),